INFORMATION TO USERS

This manuscript has been reproduced from the microfilm master. UMI films the text directly from the original or copy submitted. Thus, some thesis and dissertation copies are in typewriter face, while others may be from any type of computer printer.

The quality of this reproduction is dependent upon the quality of the copy submitted. Broken or indistinct print, colored or poor quality illustrations and photographs, print bleedthrough, substandard margins, and improper alignment can adversely affect reproduction.

In the unlikely event that the author did not send UMI a complete manuscript and there are missing pages, these will be noted. Also, if unauthorized copyright material had to be removed, a note will indicate the deletion.

Oversize materials (e.g., maps, drawings, charts) are reproduced by sectioning the original, beginning at the upper left-hand corner and continuing from left to right in equal sections with small overlaps. Each original is also photographed in one exposure and is included in reduced form at the back of the book.

Photographs included in the original manuscript have been reproduced xerographically in this copy. Higher quality 6" x 9" black and white photographic prints are available for any photographs or illustrations appearing in this copy for an additional charge. Contact UMI directly to order.

U·M·I

University Microfilms International
A Bell & Howell Information Company
300 North Zeeb Road. Ann Arbor. MI 48106-1346 USA
313/761-4700 800/521-0600

Order Number 9509423

Debris-flow fans: Process and form

Whipple, Kelin X., Ph.D.

University of Washington, 1994

U·M·I
300 N. Zeeb Rd.
Ann Arbor, MI 48106

Debris-flow Fans: Process and Form

by

Kelin X. Whipple

A dissertation submitted in partial fulfillment of the requirements for the degree of

Doctor of Philosophy

University of Washington

1994

Approved by Thomas Dunne
(Chairperson of Supervisory Committee)
Alan Gillespie
Bernard Hallet
Richard M. Iverson

Program Authorized
to Offer Degree Geological Sciences

Date 7/11/94

In presenting this dissertation in partial fulfillment of the requirements for the Doctoral degree at the University of Washington, I agree that the Library shall make its copies freely available for inspection. I further agree that extensive copying of this dissertation is allowable only for scholarly purposes, consistent with "fair use" as prescribed in the U.S. Copyright Law. Requests for copying or reproduction of this dissertation may be referred to University Microfilms, 1490 Eisenhower Place, P.O. Box 975, Ann Arbor, MI 48106, to whom the author has granted "the right to reproduce and sell (a) copies of the manuscript in microform and/or (b) printed copies of the manuscript made from microform."

Signature ____________

Date 7-11-94

University of Washington

Abstract

Debris-Flow Fans: Process and Form

by Kelin X. Whipple

Chairperson of the Supervisory Committee: Professor Thomas Dunne
Department of Geological Sciences

Lithologic, climatic, and tectonic influences on debris-flow-dominated alluvial fan (debris-flow fan) morphology are elucidated through a combination of field mapping, map and aerial photo analysis, and a theoretical analysis of the controls on debris-flow confinement within channels. Fan size in Owens Valley, California, is controlled primarily by source drainage area and local subsidence rate, as seen elsewhere. However, spatial variability in subsidence rates is shown to be important, and may largely control fan area-drainage area relationships. Depositional patterns on debris-flow fans are governed by interactions between debris flows and channels, which are products of fluvial incision and not debris-flow scour. Channel geometry (i.e., size and gradient) is set by competition between fluvial sediment supply, stream power, and the rate of channel filling by debris flows. The channel-debris flow interaction is controlled by channel geometry, flow volume, flow hydrograph form, and flow rheology. The frequency distributions of these debris-flow properties determine fan morphology. I focus on the role of debris-flow rheology, which is sensitive to debris granulometry and water content. Abundance of boulders and debris silt-and-clay content are important, lithologically controlled properties. Hydrologic conditions associated with debris-flow initiation are hypothesized to be the most important climatically controlled variable. Numerical simulation of open-channel flow of Bingham fluids is utilized to quantify lithologically dependent differences in debris-flow rheology and to analyze the channel-debris flow interaction on fans in a range of field settings. Differences in source lithology exert the dominant influence on debris-flow fan morphology in Owens Valley. Debris-flows from the most fines-rich sources (meta-volcanic source rocks) are more viscous at the same water content (i.e., initiated under the same conditions) than granitic-source debris flows and, consequently, are poorly channelized. As a result, massive overbank deposition near the fan head is common on these fans and they develop steeper radial profiles. Similarly, enhanced overbank deposition leads to the formation of prominent channel-margin levees.

Table of Contents

List of Figures iii
List of Tables v
Introduction 1
  Problem Definition and Motivation 1
  Research Strategy 2
  Thesis Overview 3
Chapter 1 8
  Chapter Summary 8
  Introduction 9
  Basic Principles and Previous Work 12
  Study Methodology 16
  Study Site Descriptions 24
  Results 25
  Discussion 35
  Conclusions 42
  Acknowledgments 43
Chapter 2 44
  Chapter Summary 44
  Introduction 45
  Owens Valley Field Site 47
  Fan Morphology 51
  Relative Roles of Fluvial and Debris-flow Processes 56
  Debris-flow Processes and Fan Surface Morphology 61
  Discussion 75
  Conclusions 79
  Acknowledgements 80
Chapter 3 81
  Chapter Summary 81
  Introduction 81
  Approach 85
  Governing Equations for Open-Channel Flow 89
  Numerical Simulation 91

Application to Natural Debris Flows 103
Conclusions 123
Acknowledgments 124
Chapter 4 125
Introduction 125
Conceptual Framework 126
Approach 127
Descriptions of Fan Surface Morphology 130
Debris-flow Rheology 153
Analysis of Channel Conveyance Capacity 165
Discussion 173
Conclusions 179
Acknowledgments 180
Chapter 5 181
Chapter Summary 181
Introduction 181
Approach: Process and Form 182
Field Site Descriptions 183
Geologic Conditions, Fan Morphology, and Debris-flow Hazard 183
Conclusions 189
Acknowledgments 190
Bibliography 191

LIST OF FIGURES

1.1 Simplified geologic map of Owens Valley, CA 10
1.2 Schematic illustration of controls on fan area 11
1.3 Subsurface geometry of Owens Valley, CA 20
1.4 Fan area vs. Drainage area, Owens Valley 28
1.5 Fan slope vs. drainage area for debris-flow fans in Owens Valley, CA 32
1.6 Effects of spatially varying subsidence rates 37
2.1 Index map of the study site in Owens Valley, California 46
2.2 Channel network on Pinyon and Symmes Creek fans 48
2.3 Geomorphic maps of Pinyon and Symmes Creek fans 49
2.4 Debris-flow plug in a channel 52
2.5 Channel on upper Pinyon Creek fan 53
2.6 Surveys of representative channel cross sections 54
2.7 Stereo-pair of aerial photographs of Symmes Creek fan 55
2.8 Typical debris-flow deposits 57
2.9 Schematic illustration of channel modification by debris flows 59
2.10 Yield strength versus runout distance 66
2.11 Yield strength versus matrix silt-and-clay content 67
2.12 Conveyance capacities of representative channels 73
3.1 Definition sketch of the Bingham constitutive equation 86
3.2 Schematic illustration of regimes of debris-flow behavior 87
3.3 Comparison of laboratory and field estimates of debris-flow rheology 88
3.4 Schematic illustration of the bi-viscosity model 92
3.5 Comparison of model results and theory 94
3.6 Critical shear stress versus width-to-depth ratio 98
3.7 Analysis of error as a function of width-to-depth ratio 104
3.8 Map of the 1983 Black Canyon debris flow 110
3.9 Granulometry of the 1983 Black Canyon debris flow 111
3.10 Example surveys used in viscosity-calculations 113
3.11 Rheology of the 1983 and 1990 Black Canyon debris flows 116

3.12 Schematic illustration and definition of the mass balance routing scheme........120
3.13 Observed and predicted overbank deposition 122
4.1 Location map showing generalized geology of Owens Valley, CA 129
4.2 Interpretive map and aerial photograph of Symmes Creek fan 135
4.3 Topographic cross sections of Symmes Creek fan..137
4.4 Profiles of uppermost Symmes Creek and Tuttle Creek fans 138
4.5 Interpretive map and aerial photographs of Tuttle Creek fan 139
4.6 Topographic cross sections of Tuttle Creek fan 142
4.7 Comparison of average slopes of fans in Owens Valley 143
4.8 Interpretive map and aerial photograph of Rock Creek fan..............................144
4.9 Topographic cross sections of leveed channels...146
4.10 Topographic cross sections of Rock Creek fan..147
4.11 Grain-size distributions of typical debris-flow deposits in Owens Valley.........148
4.12 Interpretive map and aerial photograph of Jefferies Mine Canyon fan 150
4.13 Topographic cross sections of Jefferies Mine Canyon fan..............................152
4.14 Schematic Illustration of Rheology vs. Silt-and-Clay Content.........................157
4.15 Rheology of recent debris flows in Owens Valley..158
4.16 Photographs of large boulder wedges 161
4.17 Boulder wedge force balance definition sketch..163
4.18 Channel Area-Slope Product vs. Distance Down Fan 168
4.19 Conveyance capacities as a function of rheology 169
4.20 Idealized Debris-flow Hydrograph for Routing Analysis................................171
4.21 Predicted Debris-flow Depositional Patterns 172
5.1 Oblique aerial views of debris-flow fans..184
5.2 Transverse topographic profiles 188

LIST OF TABLES

1.1 Fan Morphometry Data 17
1.2 Regression Analysis 27
2.1 Summary of Sieving Analyses 62
2.2 Debris Flow Rheology 68
2.3 Rheologic Parameters: Black Canyon, CA 72
3.1 Results of Regression Analysis 99
3.2 Hydraulic and Rheological Parameters: Black Canyon, CA 117
4.1 Fans Studied: Location and Source Area Characteristics 131
4.2 Channel Types and Drainage Densities 132
4.3 Hydraulic and Rheologic Parameters of Debris Flows 159
5.1 Field Conditions 185
5.2 Debris-Flow Hazards 186

ACKNOWLEDGEMENTS

I owe a debt of gratitude to the great many people who contributed to the completion of this dissertation. First and foremost I wish to thank my thesis advisor, Thomas Dunne. This research would not have been possible without his guidance, unfailing optimism, and support. Each of the other members of my dissertation Committee also contributed importantly during all stages of the research and I thank them for their considerable efforts on my behalf. They are: Alan Gillespie, Bernard Hallet, Dick Iverson, and Steve Kramer. Thanks also to Professors Dave McTigue and Ron Shreve for their inputs and criticisms in the development of the analysis in Chapter 3, and to John Adams for open access to the facilities in the Remote Sensing lab. Many graduate students contributed much over the years through informal discussions and arguments. I thank in particular Daniel Miller and Ken MacLeod. Carolyn Trayler digitized all the maps and aerial photographs used in Chapter 1 and contributed significantly to the development of the ideas in that chapter. Special thanks also to the many field assistants who put in long hours surveying, point counting, and digging in the desert heat. They are, in order of appearance: Jeff Kirtland, Dan and Lynn Miller, Christie Rodgers, Peggy Shippert, Galen Whipple, and Jason Paur. Last, and not least, thanks to Katrina for her support during the trying months of writing and defending this thesis.

I dedicate this dissertation to my parents, Rich and Petey - thank you for everything.

"Every year is getting shorter, never seem to find the time
Plans that either come to naught, or half a page of scribbled lines ..."

-- Pink Floyd, "Time"

INTRODUCTION

PROBLEM DEFINITION AND MOTIVATION

Debris-flow fans are "alluvial fan" landforms on which debris flows are the dominant depositional process. Owing to the prevalence of debris flows in mountainous regions worldwide (Takahashi, 1981; Costa, 1984), the debris-flow fan is a common landform, occurring in a wide range of geologic and climatic environments (Blackwelder, 1928; Beaty, 1963; Pierson, 1980; Li, and others, 1983; Suwa and Okuda, 1983; 1990; Pierson, and others, 1990). Additionally, debris-flow dominated fans are well represented in the ancient record (e.g., Bull, 1972; Nilsen and Moore, 1984). Despite the importance of the debris-flow fan landform, and despite the early recognition of its importance (Blackwelder, 1928), few previous studies have focused specifically on the processes of debris-flow fan formation and their morphologic and stratigraphic consequences, leaving a lack of scientific knowledge about a widespread landform. This lack of knowledge is all the more disconcerting considering the potential hazard that debris flows pose to lives and structures in communities situated in mountainous environments. Most research on debris flows is motivated by practical hazards concerns and most studies have focused on either the process of debris-flow initiation or the fluid-mechanical description of the flow in an effort to predict flow occurrence and run-out distances (Takahashi, 1981; Costa, 1984). However, debris flows only pose a threat where they overlap with human activities: most commonly on active debris-flow fans. Successful prediction and mitigation of debris-flow hazard requires an understanding of the entire suite of processes active on debris-flow fans, such that both short-term and long-term patterns and frequencies of inundation and deposition can be anticipated. Thus, the dearth of studies of debris-flow behavior on fans and their interaction with the fan surface and channel system has limited rigorous, physical explanations of the landforms on fan surfaces as well as interpretations of the paleo-geographic and paleo-climatic record preserved in debris-flow fan deposits, and has frustrated attempts to predict the hazard posed to communities built on debris-flow fans (Costa, 1984). The research presented here is motivated by this combination of concerns with geomorphic understanding, stratigraphic interpretation, and engineering (understanding and predicting hazards).

Although most of the extensive literature on modern fans has focused on fluvial processes and alluvial fan sedimentation (Bull, 1977; Lecce, 1990), debris-flow fans have been identified, mapped, described, produced in laboratory-scale experiments, and even used as field laboratories for the study of debris-flow mechanics (Beaty, 1963; Hooke, 1967; Johnson, 1970; 1974; Wasson, 1977; Suwa and Okuda, 1983; 1984; 1987; Jackson, and others, 1987; 1990). Although contributing to our knowledge and awareness of debris-flow fans and providing important guides for the present study, these studies have not developed a unifying conceptual model of the formation of a debris-flow fan, nor have they sought to develop the linkages between fan morphology and stratigraphy and the environmental factors that control them. These are the goals of this dissertation.

The morphology of both alluvial and debris-flow fans is controlled by a complex suite of tectonic, lithologic, and climatic factors. On a gross scale, overall fan morphology (given by fan size and average slope) is determined by both the depositional process and the balance between source area uplift, fan aggradation, basin subsidence, and playa aggradation (Hooke, 1968; Bull, 1977; Hooke and Rohrer, 1979). On a fine scale, details of fan surface morphology are controlled by the particulars of the depositional system, with channel avulsion and lateral shifting of depositional centers across the fan playing a critical role. Although each of the tectonic, lithologic, and climatic conditions of a fan and its source basin can be expected to influence both character of the depositional system and the rate of sedimentation, it has not been established in the literature how sensitive fan morphology is to differences in each of these environmental factors. Further, as stated above, the linkages between source area characteristics and the operation of the depositional system on debris-flow fans have never before been developed.

RESEARCH STRATEGY

The wide range of variables involved in the debris-flow fan morphology problem and the wide range of scales of interest together demand a two-tiered research approach: (1) a regional study of tectonic, lithologic, and climatic controls on overall fan morphology; (2) a landform-scale study of the mechanics of the depositional process. The regional-scale study is necessary to isolate and evaluate the relative importance of tectonic, lithologic, and climatic conditions in setting overall fan morphology and is the subject of Chapter 1. Controls on overall fan slope are of particular concern to the landform-scale analysis presented in subsequent chapters. Overall fan slope varies significantly on debris-flow fans in different settings and probably depend on factors such as catchment relief and slope, catchment hydrology, debris grain-size distribution, and the sedimentation rate, which are beyond the scope of a purely landform-scale analysis. The landform-scale study is motivated by the need to understand the operation of the depositional system on debris-flow fans, and to quantify the linkages between fan morphology, hazards, stratigraphic architecture, and the environmental variables that control them. The landform-scale study consists of three parts: (1) development of a conceptual model of debris-flow fan construction; (2) development of the rheologic tools and data to quantify critical aspects of the conceptual model; and (3) an analysis of morphological differences between debris-flow fans derived under differing climatic conditions from sources of differing lithology.

THESIS OVERVIEW

The thesis is divided into five chapters. Each chapter is written as a stand-alone paper and includes a summary, introduction, and conclusion section of its own, hence, some repetition of material occurs. To improve readability of the thesis as a whole, I provide below a brief synopsis of the findings of the study, emphasizing the interconnectivity of the approaches taken in the various phases of the work.

Regional Study

Debris-flow fans occur in a wide variety of geologic and climatic environments (Blackwelder, 1928; Beaty, 1963; Pierson, 1980; Li, and others, 1983; Suwa and Okuda, 1983; 1990; Pierson, and others, 1990) and exhibit a correspondingly wide range of morphologies. Relative sizes of debris-flow fans in Owens Valley and elsewhere vary over an order of magnitude: from approximately the size of their source basins to about 10% of that value. Similarly, the overall slope of debris-flow fans varies from 4° to 20°, although the range within Owens Valley is much less (4° to 6°).

The regional-scale study presented in Chapter 1 seeks to explain these variations in overall fan morphology in the context of the physical environment of the fans, using the debris-flow fans in Owens Valley, California as an example. Fan size, as expected from previous studies (Hooke, 1968; Hooke, 1972), is controlled by drainage basin size and local tectonic setting. I emphasize the importance of spatially variable subsidence rates in determining fan area - drainage area relationships. Of more direct importance to the landform-scale study that constitutes the bulk of the thesis is the finding that overall fan slope is strongly dependent on source lithology and, within the range of conditions in Owens Valley, independent of tectonic and climatic setting. The strong dependence on source lithology suggests a rheologic control on overall fan slope because debris-flow rheology is known to be sensitive to differences in debris grain-size distributions (Fairchild, 1985; O'Brien and Julien, 1988; Phillips and Davies, 1991; Coussot, 1992; Major and Pierson, 1992).

Landform-Scale Study

I study the controls on long-term sedimentation patterns on debris-flow fans. Extensive field mapping and aerial photograph analysis are used to define conceptually the suite of processes that contribute to fan construction and the nature of their interactions. A rheologic analysis of the interaction of debris flows and the channel system is then used to quantify and generalize the qualitative findings. Fans derived under a range of geologic and climatic conditions are studied to isolate lithologic and hydrologic effects and to evaluate their relative importance.

Conceptual Model (Chapters 2 and 4)

Debris-flow fans are distinct from alluvial fans in that fluvial processes on them contribute mostly to the channelization of the fan surface and to the aggradation of only the distal margin (toe). Depositional patterns on, and therefore the morphology of, debris-flow fans are governed by interactions between debris flows and channels, that are products of fluival incision and not debris-flow scour. This is significant because detailed geomorphic maps indicate that the channels strongly influence the pattern of debris-flow deposition. The interaction of debris flows with the channel system is controlled by channel size, channel gradient, flow volume, flow hydrograph, and flow rheology. Debris-flow behavior, on any given fan, is most directly controlled by variations in bulk sediment concentration and its influence on flow rheology. Whereas low-sediment-concentration debris flows tend to smooth the surface of the lower fan, spreading into thin sheets and filling channels and surface undulations, repeated deposition of high-sediment-concentration debris flows produces the rugged topography of the upper fan. The texture of the fan surface, rough or smooth, is determined by the relative volumetric importance of these two types of debris flow. In addition, channel avulsions and the associated long-term shifting of depositional loci are driven by in-channel deposition of debris flows with the highest sediment concentrations. These debris flows, therefore, play a critical role in determining both the structure of the channel network and the long-term pattern of deposition on the fan surface as a whole. I infer that the frequency distribution of debris-flow rheologies, set by source terrain geology and hydrology, is an important control on fan morphology.

Debris-flow fan morphology can be expected to vary with geologic and climatic setting in a complex, but predictable, manner. Critical factors expected to vary with source basin lithology and climate include: (1) typical stream flow discharges; (2) the quantity and size of sediment delivered to the fluvial system; (3) the temporal frequency and volume of debris-flow events; (4) debris-flow initiation mechanisms and associated hydrologic conditions; and (5) the granulometry of the source regolith. The channels are controlled by the interplay of several factors (1-3 above). The strong dependence of debris-flow fan slope on source lithology probably reflects lithologic control of the frequency distribution of debris-flow rheologies in a given climatic setting.

Choice of a Rheologic Model (Chapter 3)

Where debris-flow runout is significantly influenced by the channel system, as documented in Chapter 2 in Owens Valley, it is useful to quantify the dependence of debris flow runout patterns on their rheology and peak discharge. These are the most relevant properties because the degree to which debris flows are confined within channels and conveyed farther down-fan depends on the relative magnitudes of the peak discharge and the conveyance capacity of the channel, which is a function of flow rheology as well as channel size and gradient. Therefore, I have analyzed the relationship between flow rheology and channel conveyance capacity, using a rheological model that: (1) is simple; (2) captures the main macroscopic flow behavior of debris flows; (3) can be related in a straightforward manner to the physical properties of the flow (i.e., water content and grain-size distribution). I use the Bingham constitutive equation (Johnson, 1965; Johnson, 1970). The criteria listed above and the choice of the Bingham model are motivated by the geomorphic applications for which the modeling is intended. For analyses requiring more precise site-specific predictions, the simplifications incorporated into the Bingham model may not be acceptable (see discussions in Iverson, 1985; Iverson and Denlinger, 1987; Iverson and LaHusen, 1993).

The Bingham model is a rheological construct, fit to field and experimental data, and as such does not rigorously account for complex grain-grain and grain-fluid interactions that underlie the physics of flowing debris. For instance, collisional and frictional interactions between gravel- and boulder-sized clasts, modulated by rapid pore pressure fluctuations, probably contribute significantly to momentum transfer in most natural debris flows (Pierson, 1986; Phillips and Davies, 1991; Iverson and LaHusen, 1993). Application of the Bingham constitutive equation to natural debris flows assumes that matrix (here defined as material < 2 mm in diameter) deformation governs the macroscopic behavior of the flow and that dynamic effects such as particle collisions and friction, pore-pressure fluctuations, and formation and destruction of grain networks are either negligible or are collectively manifested as an approximately Bingham behavior (see discussions in Iverson, 1985; Phillips and Davies, 1991; Coussot, 1992; Major and Pierson, 1992; Major, 1993). Here "approximately Bingham" is meant to include shear-thinning behavior that may be more representative of the types of dynamic effects described above, and which could be manifested in experimental and field data as an effective "yield strength". The assumptions entailed in modeling debris flows as Bingham fluids are most reasonable for muddy, matrix-rich debris flows of the type that leave matrix-supported deposits. This choice of rheologic model is discussed more fully in Chapter 3.

Application of the Rheologic Model (Chapters 3 and 4)

In Chapter 3 I present a numerical analysis of steady, uniform, open-channel flow of Bingham fluids conducted with the aim of accurately predicting the effects of channel geometry on the flow of channelized debris flows. A regression analysis of model output yields a set of non-dimensional empirical equations for predicting bankful discharges (i.e., channel conveyance capacity) as a function of channel geometry (cross-sectional shape, width, depth, slope) and material properties (yield strength, viscosity, bulk density). These equations, and the numerical model itself, are useful for deriving field-based estimates of debris-flow viscosity, motivated by the lack of agreement between previous field and laboratory estimates and the observation that laboratory measurements significantly under-predict field estimates (see discussion in Chapter 3). A new analysis of well preserved debris-flow deposits at a site in Owens Valley yields field estimates that corroborate and extend the systematic trends seen in experimental data.

In Chapters 3 and 4, field observations in Owens Valley are used to constrain debris-flow rheology (both yield strength and viscosity) as a function of debris granulometry. Debris-flow water contents can not be determined from field observations of deposits, and trends seen on plots of viscosity versus yield strength for debris flows with similar grain-size distributions are inferred to reflect differences in water content (Chapter 3). Distinct trends on plots of viscosity versus yield strength are seen for debris flows derived from different source lithologies (with differing silt and clay contents but otherwise similar grain-size distributions), consistent with laboratory observations that more fines-rich slurries have higher viscosities for the same water content. I infer that source lithology importantly influences the frequency distribution of rheologies of the debris flows delivered to the fan.

The empirical equations developed in Chapter 3 are used in Chapter 4 to explore the implications of these differences in the frequency distribution of debris-flow rheologies for the morphology of debris-flow fans derived from basins underlain by different lithologic assemblages. I show, following the principles outlined in Chapter 2, that observed differences in both overall fan slope and fan surface morphology (the "texture" or "roughness" of interfluves, the morphology of channel-margin levees, and the channel network structure) are largely attributable to differences in debris-flow rheology related to differences in the granulometry of the source regolith.

Implications for Rapid Assesment of Debris-flow Hazard (Chapter 5)

The simplified nature of the debris-flow modeling exercise incorporated into this thesis (assuming steady, uniform flow of Bingham fluids in simple, rectilinear channels) precludes direct engineering-oriented analysis of debris-flow hazards. However, successful prediction and mitigation of debris-flow hazards requires understanding of the entire suite of processes active on debris-flow fans and their mutual interactions. Thus the analysis of long-term geological controls on sedimentation patterns and fan morphology presented in this thesis does provide an important framework and context for more detailed hazards-forecasting analyses. Chapter 5 outlines briefly how a rapid assessment of the type of debris-flow hazard most prevalent on a fan can be made from observations of the morphological characteristics of the fan surface.

CHAPTER 1

Controls on fan size and slope

Chapter 1 presents the regional-scale study of tectonic, lithologic, and climatic controls on overall fan morphology. This chapter, prepared for submission to Earth Surface Processes and Landforms, provides an overview and context for the fan-scale work presented in subsequent chapters. In addition, findings of this study relevant to controls on debris-flow fan slope in Owens Valley, California, provide critical support for the analysis presented in Chapter 4.

CHAPTER SUMMARY

Study of relationships between fan morphology, basin characteristics, and tectonic setting in Owens Valley, CA, suggests that (1) local tectonic setting is the dominant control on relative fan sizes, and (2) source lithology is the dominant control on relative fan slope. Although the importance of tectonic subsidence rate in controlling the size of fans was long ago recognized in Death Valley, CA (Hunt and Mabey, 1966; Hooke, 1968), we stress the overriding importance of spatial variability in the local subsidence rate beneath fan complexes. The relationship between fan area (A_f) and drainage area (A_d) is often described by the expression $A_f = cA_d^n$, where c and n are constants. The coefficient c is generally thought to reflect differences in subsidence rates, source lithology, and climate. In the case of spatially uniform subsidence this is true. However, simple arguments, supported by the Owens Valley data, demonstrate that in settings with spatially varying subsidence rates, both c and n are set by that spatial variability and bear no direct relation to source area characteristics. Fan size data must be considered in the context of the *local* tectonic setting. In addition to this tectonic influence, a weak dependence of fan size on source lithology is supported, but not proven, by our data. Further, we find no difference in the relative sizes of fans draining heavily glaciated, slightly glaciated, and unglaciated catchments. Although this draws into question conventional wisdom about the relative efficiency of glacial and non-glacial erosion processes, enhanced production of fines which bypass the fan system due to glacial abrasion may explain the data. With the exception of those fans physically tilted and oversteepened by recent (Holocene or Late Pleistocene) tectonism, fan slope, on the other hand, is found to be independent of the tectonic setting. Fan slope is also independent of local climatic setting. Conversely, fans derived from drainages with differing lithologies have different average slope gradients. We interpret these observations as indicating that debris-flow fan slopes are controlled by depositional processes, are sensitive to differences in sediment size composition (Whipple and Dunne, 1992), and exhibit relatively short response times to tectonic disturbances (order 10^3 - 10^4 years).

INTRODUCTION

Debris-flow fans are "alluvial fan" landforms on which debris flows are the dominant mode of deposition. Debris-flow fans are typically associated with small, steep drainages, but occur in a wide range of geologic and climatic settings (Blackwelder, 1928; Beaty, 1963; Pierson, 1980; Li, and others, 1983; Suwa and Okuda, 1983; Jackson, and others, 1987). Despite their widespread occurrence and early recognition of their importance (Blackwelder, 1928), until recently little was known about the controls on debris-flow fan sedimentation, surface morphology, and how they differ from those on alluvial fans. Whipple and Dunne (1992) combined field work and theoretical considerations to build on the work of earlier investigators (Beaty, 1963; Hooke, 1967; Johnson, 1970; 1974; 1984; 1990) to develop a conceptual model of the controls on debris-flow fan surface morphology. Their analysis focused on the role of debris-flow rheology and on meso-scale landforms on debris-flow fan surfaces including: the morphology and spatial distribution of channels crossing the fan, the texture or meter-scale "roughness" of cross-fan topographic profiles, levee geometry, and cross-fan convexity. Although their conceptual model predicts a dependence of larger-scale morphological characteristics, such as fan slope, on debris-flow rheology, controls on overall fan morphology (fan size and slope) were strictly beyond the scope of that study and could not be tested with their data. In this paper we extend the earlier work of Whipple and Dunne (1992) by studying lithologic, climatic, and tectonic controls on debris-flow fan size and slope in Owens Valley, California.

Extensive bajadas (piedmonts of coalescing fans) of coalescing debris-flow fans occur in places on both sides of Owens Valley and along the full length of the valley (Fig. 1.1). Great variability in fan size with geographical position is obvious on Figure 1.1, and is matched by similar variability in fan slope. In the case of alluvial fans, fan area and slope have been shown to depend on drainage area, lithology, climate, and tectonic setting (e.g., Bull, 1964; Denny, 1965; Hooke, 1968; Hooke and Rohrer, 1977; Harvey, 1984) and the same variables can be expected to govern debris-flow fan

Figure 1.1 Simplified geologic map of Owens Valley, California. Major graben-bounding faults, inferred from gravity data, are shown as heavy dotted lines (Pakiser, and others, 1964). Surface trace of Owens Valley Fault (OVF) shown as solid, broken line. Field sites (1-4): (1) northern White Mountains group; (2) southern White Mountains group; (3) western bajada group; (4) Owens Lake group. Gravity profiles (Fig. 1.3): Labeled (A - D). Information digitized from 1:250,000-scale geologic maps of California: Mariposa and Fresno Sheets (Matthews and Burnett, 1965; Strand, 1967).

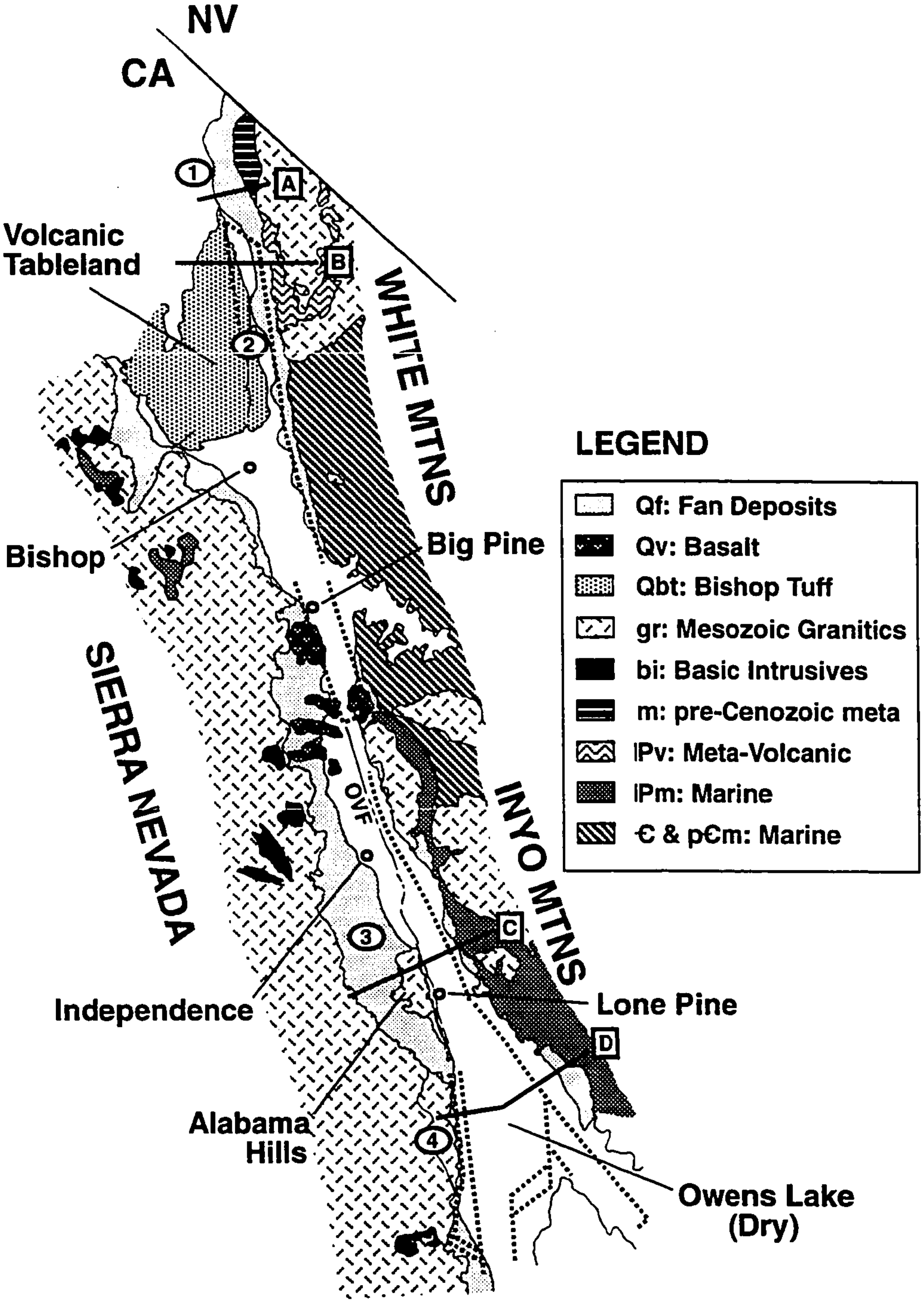
NV
CA
①
A
Volcanic Tableland
B
②
WHITE MTNS
LEGEND
Qf: Fan Deposits
Qv: Basalt
Qbt: Bishop Tuff
gr: Mesozoic Granitics
bi: Basic Intrusives
m: pre-Cenozoic meta
IPv: Meta-Volcanic
IPm: Marine
€ & p€m: Marine
Bishop
Big Pine
SIERRA NEVADA
OVF
INYO MTNS
③
C
Independence
Lone Pine
D
Alabama Hills
④
Owens Lake (Dry)

Figure 1.2 Schematic illustration of controls on fan area. Boxes indicate fundamental geologic, climatic, and physiographic controls. Diamonds indicate "filters" operating on the system. Note that the "filters" are not truly independent of geologic, climatic, and physiographic conditions, important cross correlations exist (see text).

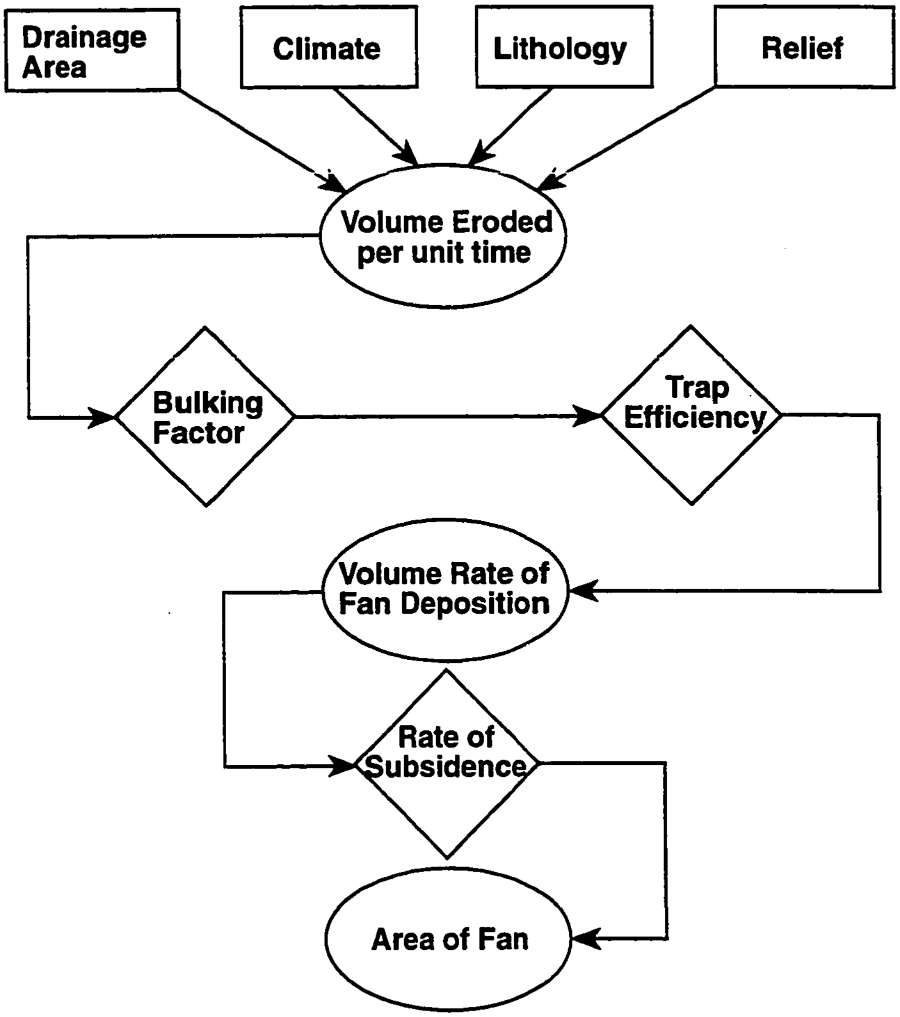
Drainage Area
Climate
Lithology
Relief
Volume Eroded per unit time
Bulking Factor
Trap Efficiency
Volume Rate of Fan Deposition
Rate of Subsidence
Area of Fan

size and slope, though the relationships may be quantitatively different, particularly in the case of fan slope. Accordingly, associated with the range of debris-flow fan properties in Owens Valley is a wide range of lithologic, climatic, and tectonic conditions including: (1) granitic, meta-sedimentary, and meta-volcanic rock types (Fig. 1.1), (2) a strong west-east climatic gradient in the Sierra Nevada rain shadow (Bierman, and others, 1991), (3) both glaciated (Late Pleistocene) and unglaciated drainages (Gillespie, 1982; Bierman, and others, 1991), and (4) spatially variable subsidence rates (Pakiser, and others, 1964). We capitalize on this diversity of field conditions to isolate and evaluate the effects of lithologic, climatic, and tectonic differences on the size and slope of debris-flow fans. For instance, the occurrence, in the same physical environment (source lithology and tectonic setting), of fans debouching from both catchments that supported large valley glaciers and those that did not provides an excellent, perhaps unique, opportunity to address the recent controversy over the relative rates of erosion in glaciated and unglaciated drainages (Hicks, and others, 1990; Harbor and Warburton, 1993).

BASIC PRINCIPLES AND PREVIOUS WORK

Fan Area - Drainage Area Relationships

The roles of physiographic, lithologic, climatic, and tectonic conditions in determining fan size can be readily deduced from simple erosion laws and the principle of conservation of mass and should be no different on debris-flow fans than they are on alluvial fans (Hooke, 1968; 1972; Jansson, and others, 1993). We briefly review these relationships to provide a conceptual framework for the current study and to motivate our approach.

Consider complex of coalescing fans building across a surface subjected to a spatially uniform subsidence rate. Fan area (A_f) is set by the net volume of sediment deposited on the fan per unit time (V_f) and the mean sedimentation rate (z_f):

$$A_f = \frac{1}{z_f} V_f \qquad (1.1)$$

(Hooke, 1968; Hooke, 1972; Jansson, and others, 1993). As first described by Hooke (1968), mean sedimentation rate should tend towards equality on all parts of a bajada subject to a uniform subsidence rate because deviations from this condition result in the growth of one fan at the expense of another until equilibrium is established. The often cited correlation between fan area and drainage area arises directly from the geometric constraint above (equation 1.1) and this tendency towards maintaining equilibrium: (1)

fan areas everywhere on a bajada (subject to a uniform subsidence rate) are directly proportional to the volume rate of sediment delivery by a constant amount, and (2) the volume rate of sediment delivery (V_f) is a function of drainage area (A_d), drainage slope (S_d), lithology, and climate. The resulting relationship between fan area and drainage area is often expressed as:

$$A_f = cA_d^n \tag{1.2}$$

where c and n are constants that vary with drainage slope, lithology, climate, and tectonic setting (Bull, 1964; Denny, 1965; Hooke, 1968; 1977; Hooke and Rohrer, 1977). For future reference, note that z_f is incorporated into the coefficient c in equation (1.2). Hooke (1968) presents evidence that n is relatively constant (n ~ .9) in the southwestern Basin and Range and argued that it ought to be independent of geologic, climatic, and tectonic conditions. However, cases where n takes values of 0.6 (Hooke, 1968) and even 0.5 (this study) exist, may be attributable to differences in tectonic setting, and are of interest.

Consideration of a simple erosion rule and mass conservation helps to illuminate the relationship between the power-law coefficients (c and n) and the controlling variables (see Fig. 1.2). In a steady-state landscape the volume rate of the removal of rock from the source drainage per unit time (V_r) is equal to the product of the rate of incision of the trunk stream (dz/dt) and the drainage area:

$$V_r = A_d\left(\frac{dz}{dt}\right) = k_e k_r A_d^{p+1} S_d^{q} \tag{1.3}$$

where p and q are constants often assumed to be equal to 1 (Seidl and Dietrich, 1992), k_e is the erodibility of the rock, k_r is the erosivity, and S_d denotes the channel slope at the drainage outlet. The exponents (p and q) are, however, poorly constrained at present are likely to vary with process (e.g., fluvial incision, glacial erosion, or debris-flow scour). Under non-steady-state conditions the exponents in equation (1.3) may take different values and A_d and S_d may be surrogates for different properties. Two limiting cases are considered. In the limiting case where incision of the trunk stream out paces the downwearing of the sideslopes such that drainage divides are not lowered, V_r is reduced to one-half the value predicted by equation (1.3) for a simple triangular valley cross section. The form of equation (1.3) is still valid and the system will tend towards steady state as valley sideslopes steepen and sediment input rates to the channel increase. In the opposite limiting condition, however, where the channel is not incising its bed and sediment delivery is limited by hillslope transport processes, equation (1.3) takes on a different meaning. Sediment yield is set by the flux of material from the hillslopes to the channel and the total length of channel (proportional to valley sideslope in a triangular valley) (Carson and Kirkby, 1972; Reneau and Dietrich, 1991). In this case A_d in equation (1.3) is a surrogate for total channel length and S_d represents valley sideslope. Given this difference in context and modeled processes, the exponents p and q have different values.

Erodibility is primarily related to lithology and erosivity to runoff, extent of glaciation, or the magnitude and frequency of debris-flow scouring events, depending on climatic and physiographic conditions. Lithology also plays a secondary role in setting the bulking factor (k_b) that determines the relationship between volume of rock eroded and total volume of sediment evacuated from the basin per unit time (V_s):

$$V_s = k_b V_r \,. \tag{1.4}$$

The volume rate of sediment delivery to the fan, finally, is related to V_s by the "trap efficiency" (t_e) of the fan system:

$$V_f = t_e V_s \,. \tag{1.5}$$

Trap efficiency is a catch-all parameter with both lithologic and climatic associations that can importantly influence the way in which differences in these environmental variables affect fan areas and fan area - drainage area relationships. Trap efficiency is largely determined by the grain-size distribution of the source regolith and fan depositional processes, which are interrelated and multivariate (lithology, climate, and tectonic setting all have important effects). Both positive and negative correlations between trap efficiency and other lithologic and climatic factors (k_e and k_r) are possible, resulting in either positive or negative feedback. For instance, enhanced erodibility is sometimes associated with increased regolith fines content (erodible volcanic terranes) and sometimes with decreased regolith fines content (weakly indurated coarse clastic sedimentary rock or highly fractured but well indurated sedimentary rocks). Further, Hooke and Rohrer (1977), citing written communication from Dr. W. Bull, argue that trap efficiency might be lower for larger drainage areas, suggesting that equation (1.5) should be replaced by

$$V_f = t_e^{'} A_d^{-r} V_s \,, \tag{1.6}$$

where r is a constant that, in principle, may vary with process. Equation (1.6) implies that the trap efficiency may affects both c and n in equation (1.2).

Combining equations (1.1) - (1.6) illustrates the manner in which the coefficients in the familiar power-law fan area - drainage area relationship are related to source-area characteristics:

$$c = \frac{1}{z_f} t_e^{\prime} k_b k_e k_r S_d^{q} \,, \qquad (1.7)$$

$$n = p + 1 - r. \qquad (1.8)$$

Although the relations between the coefficients in equations (1.7) and (1.8) and measurable physical properties have yet to be quantified, they are qualitatively known. Lithology influences t_e, k_b, and k_e. All three of these coefficients relate to similar physical properties of the source rock and both positive and negative feedbacks are possible. Similarly, climate influences t_e and k_r, which are also interrelated and important feedback mechanisms probably exist. Tectonics influences the value of c directly through control of both z_f and S_d. Tectonic control of z_f arises because of the direct link between subsidence rate and sedimentation rate, particularly where subsidence rates are spatially variable (see below). In addition, as mentioned, tectonic setting exerts a secondary influence on t_e through its long-term control of relief and erosional processes. Thus although source lithology, climate, and tectonics most directly influence c in equation (1.2), the multivariate and complex nature of the processes setting t_e, the trap efficiency, suggests that the power index (n) may also vary in different geologic, climatic, and physiographic settings. This last statement is opposed by data presented by Hooke (1968; 1972) that n is relatively constant and the dependence of the coefficient r on lithology, climate, and tectonic setting may be weak. Values of $p \sim 1$ and $r \sim 1$ may be reasonable for actively incising rugged drainages.

Fan Slope

The surface slope of fans of all types are set by the interaction channelization processes and depositional processes. Although these should vary with source lithology, climate, tectonics (drainage slope), and the sedimentation rate on both alluvial and debris-flow fans, the linkages between the physical environment, the processes, and the depositional landform are different on these two types of fan (e.g., Beaty, 1990; Whipple and Dunne, 1992). Naturally, this same set of environmental characteristics determines the type of fan. We consider only variations within the range of physical conditions that give rise to the generation of debris-flow fans.

Whipple and Dunne (1992) argue that debris-flow fan slope is controlled by catchment hydrology, debris-flow initiation mechanisms, debris-flow rheology, and sedimentation rate because these govern the interaction between the channels and the debris flows. On the basis of the conceptual model of debris-flow fan construction developed in that paper, Whipple and Dunne (1992) argue that debris-flow fan morphology can be expected to vary with geologic and climatic setting in a complex, but predictable, manner. Part of the complexity is the interaction of several multivariate and interdependent properties of the source area in determining the operation of the physical processes that control fan morphology. In this paper, we investigate the relative importance of lithologic, climatic, and tectonic (both catchment slope and local subsidence rate) differences in setting fan slope in Owens Valley by choosing field sites in which variations in each of these can be isolated.

STUDY METHODOLOGY

Data Collection

Four fan groups in Owens Valley were chosen for quantitative analysis. These include, from north to south, the northern White Mountain, southern White Mountain, western bajada, and Owens Lake fan groups (Fig. 1.1). Data used in the analysis were obtained from topographic, geologic, and gravity maps of each study site.

Morphometric parameters describing fans and their source catchments were measured on 1:24,000-scale U.S. Geological Survey topographic maps with aid of a digitizer. Aerial photographs were used to help in delimiting boundaries between coalescing fans and in locating profiles for the determination of fan slopes. Delimited fan areas include in all cases both the modern, active fan and any abandoned fan segments, in keeping with our interest in the long-term interplay of sediment supply rate and tectonic setting. Morphometric parameters obtained from the topographic map analysis and discussed below include: fan area (A_f), average fan slope (S_f), drainage area (A_d), and catchment relief (H). Melton's (Melton, 1965) ruggedness number ($R_n = HA_d^{0.5}$) was calculated as a measure of catchment steepness and. therefore, tectonic setting (Table 1.1).

An additional suite of measurements were made to characterize source basin lithology, climatic setting, and long-term sedimentation rates. Source lithology was classified on the basis of information on 1:24,000-scale and 1:250,000-scale geologic maps (Matthews and Burnett, 1965; Nelson, 1966b; Nelson, 1966a; Strand, 1967;

TABLE 1.1: Fan Morphometry Data

Sierra Nevada Fan Data

Fan Group:	Subsidence Rate	Climate	drainage area (sq km)	fan area (sq km)	average fan slope	ruggedness number
Western Bajada						
Sawmill	low	glacial	19.05	7.08	0.11	0.57
Black Canyon	low	non-glacial	6.89	4.73	0.10	0.83
Thibaut	low	glacial	4.49	8.04	0.11	0.92
North Oak	low	glacial	20.95	16.95	0.09	0.49
South Oak	low	glacial	19.30	18.50	0.08	0.51
Independence	low	glacial	24.74	16.47	0.08	0.45
Pinyon	low	glacial	12.25	13.30	0.07	0.64
Symmes	low	glacial	11.58	18.33	0.07	0.61
Shepherd	low	glacial	32.58	32.98	0.07	0.43
North Bairs	low	glacial	10.07	9.79	0.08	0.78
Bairs	low	glacial	7.74	12.13	0.08	0.75
George	low	glacial	24.54	23.77	0.07	0.50
Hogback	low	glacial	12.60	15.45	0.07	0.60
Lone Pine	low	glacial	30.57	28.67	0.08	0.41
Tuttle	low	glacial	21.32	19.60	0.08	0.49
Diaz	low	glacial	12.22	8.26	0.08	0.66
North Lubken	low	glacial	9.41	6.51	0.10	0.66
South Lubken	low	non-glacial	3.28	9.31	0.09	0.88
Carroll	low	non-glacial	9.90	13.57	0.09	0.56
Olancha	low	non-glacial	12.55	9.08	0.09	0.60
Falls/Walker	low	non-glacial	12.80	11.11	0.08	0.64
Owens Lake						
Slide Canyon	high	non-glacial	7.74	2.73	0.10	0.62
Timosea Peak	high	non-glacial	3.87	1.36	0.13	0.66
Cottonwood	high	non-glacial	35.17	4.09	0.07	0.33
Ash	high	non-glacial	38.55	2.95	0.07	0.32
Peak 8728	high	non-glacial	4.83	0.93	0.10	0.63
Braley	high	non-glacial	13.91	1.61	0.08	0.51
Cartago	high	non-glacial	24.30	3.18	0.08	0.47
Olancha-Cartago3	high	non-glacial	2.27	1.17	0.13	1.11
Olancha-Cartago2	high	non-glacial	1.43	0.69	0.16	1.22
Olancha-Cartago1	high	non-glacial	3.33	1.00	0.13	0.91

TABLE 1.1, Continued

White Mountains Fan Data

Fan Group:	Subsidence Rate	Lithology	drainage area (sq km)	fan area (sq km)	average fan slope	ruggedness number
Northern						
Montgomery	v. low	granite	13.14	24.74	0.08	0.55
Marble	v. low	granite	15.31	20.85	0.08	0.53
Queen Dicks	low	granite	8.64	6.24	0.09	0.73
Rock	low	granite	8.87	9.29	0.08	0.73
Falls Canyon	low	granite	6.89	2.38	0.08	0.78
Pellisier	low	granite	13.48	7.32	0.08	0.57
Middle Canyon	low	granite	6.64	1.18	0.10	0.79
Southern						
Birch	high	mixed	21.84	4.16	0.09	0.47
Willow	high	mixed	13.37	5.11	0.10	0.55
Cottonwood	high	mixed	12.25	4.68	0.10	0.64
Lone Tree	high	mixed	17.96	5.54	0.10	0.61
Jeffrey Mines	high	mixed	7.64	3.35	0.10	0.61
Millner	high	mixed	33.62	17.50	0.07	0.44
Sabies	high	granite	11.81	3.36	0.09	0.67
Straight	high	granite	9.95	3.19	0.12	0.70
Sacramento	high	granite	23.57	3.10	0.11	0.46
Piute	high	metased	22.96	5.00	0.12	0.44
Coldwater	high	metased	31.00	6.69	0.06	0.34
Silver	high	metased	55.89	6.76	0.04	0.28

Crowder, and others, 1972; Crowder and Sheridan, 1972; Streitz and Stinson, 1977) (Table 1.1). Differences in climatic setting were assessed on the basis of: (1) modern precipitation records (Rantz, 1969), and (2) morphological indicators of the degree of source area glaciation.

Estimating Local Long-Term Sedimentation Rate

Spatial variation in relative long-term sedimentation rate was assessed from local differences in the total depth of low density alluvial fill, as inferred from published gravity data (Pakiser, and others, 1964; Hunt and Mabey, 1966; Chapman, and others, 1973; Oliver and Robbins, 1978; Oliver and Robbins, 1982). Precise determination of fill depths is not warranted because its is not possible at present to accurately determine the timing of opening and deepening of the various structures that comprise the Owens Valley graben. We assume that the evolution of these structures has been relatively continuous and contemporaneous such that relative long-term sedimentation rates are faithfully reflected in the relative magnitudes of total fill depth. Previous studies have demonstrated that interpretations based on the regional gravity data set cited above are consistent with both newer, more densely sampled gravity data and shallow seismic data (Pakiser, and others, 1964; Serpa, and others, 1988; Keener, and others, 1993). Thus the regional gravity data should be sufficient for our needs.

Gravity models for representative cross sections through the various structural blocks that comprise the Owens Valley graben were fit with aid of a simple 2D computer algorithm (Fig. 1.3). Following Pakiser et. al. (1964) and Keener et. al. (1993) an estimated density contrast of 0.4 g/cm^3 was used in all cases. Away from the modeled cross sections, the magnitude of the local gravity anomaly and its spatial gradient were taken as a crude measure of the geometry and depth of the low-density fill.

Analysis

For analysis, fans in the four fan groups studied were classified according to geologic, climatic, and tectonic settings. The classification according to geologic and tectonic setting was performed as follows. Lithologic assemblages in each basin were classified on the basis of broadly defined lithotypes only (e.g., granitics, meta-volcanics, meta-sedimentary rocks, etc.). Fans derived from basins with more than 70% outcrop in a given rock type were considered monolithologic; others were simply considered "mixed". ("Mixed" in all cases represents a combination of granitic, meta-sedimentary, and meta-volcanic rock types). Tectonic setting was simply classified as one of either

Figure 1.3 Subsurface geometry of low-density, late Cenozoic alluvial fill in Owens Valley, California. Assumed fill and background densities are indicated. Upper plot shows both the observed (solid dots) and estimated (solid line) local Bouguer gravity anomaly (a linear regional trend has been extracted in all cases). Lower plot shows the reconstructed fill geometry shown without vertical exaggeration.
A. Bedrock bench at northern end of the White Mountains (Fig. 1.1).

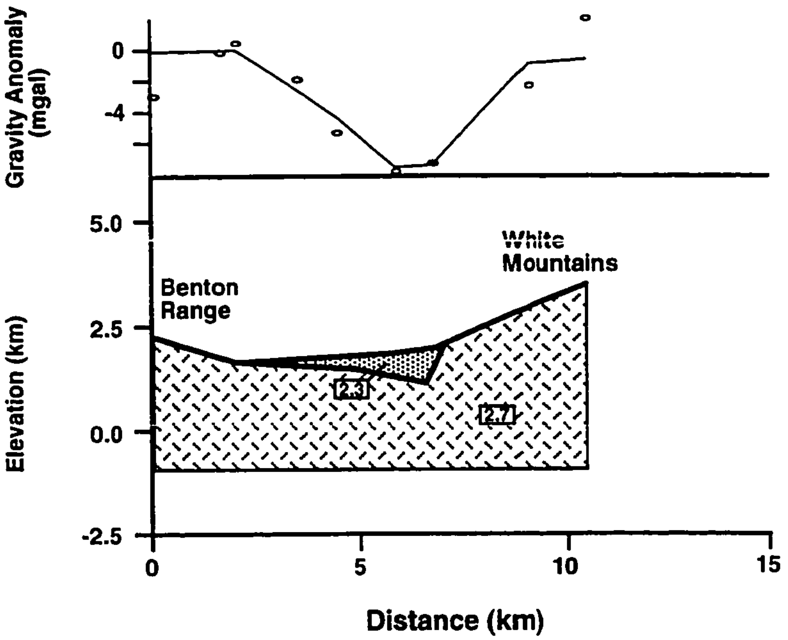
Gravity Anomaly (mgal)
0
-4
5.0
White Mountains
Benton Range
2.5
Elevation (km)
2.3
2.7
0.0
-2.5
0
5
10
15
Distance (km)

Figure 1.3
B. Narrow graben along the southern White Mountains (Fig. 1.1).

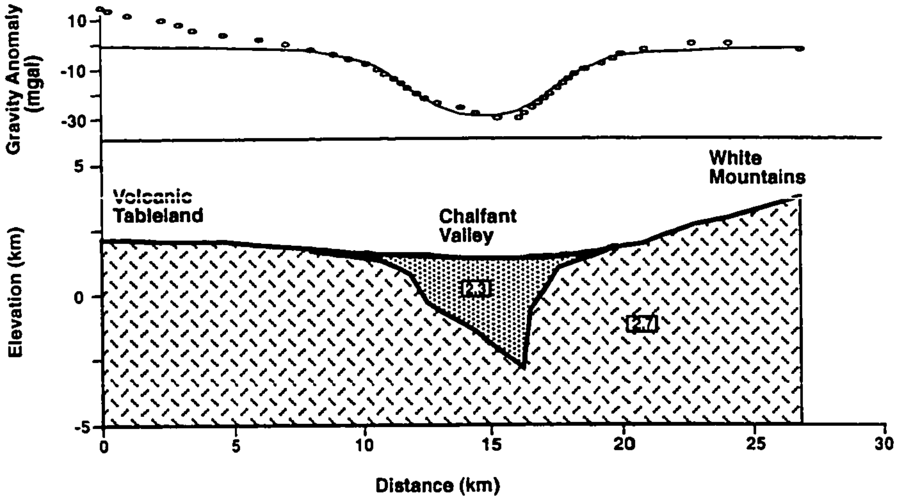
Gravity Anomaly (mgal)
10
-10
-30
5
0
-5
Elevation (km)
Volcanic Tableland
Chalfant Valley
White Mountains
2.3
2.7
0
5
10
15
20
25
30
Distance (km)

Figure 1.3
C. Extensive bedrock bench and narrow graben beneath the western bajada in the vicinity of Lone Pine and Independence (Fig. 1.1)

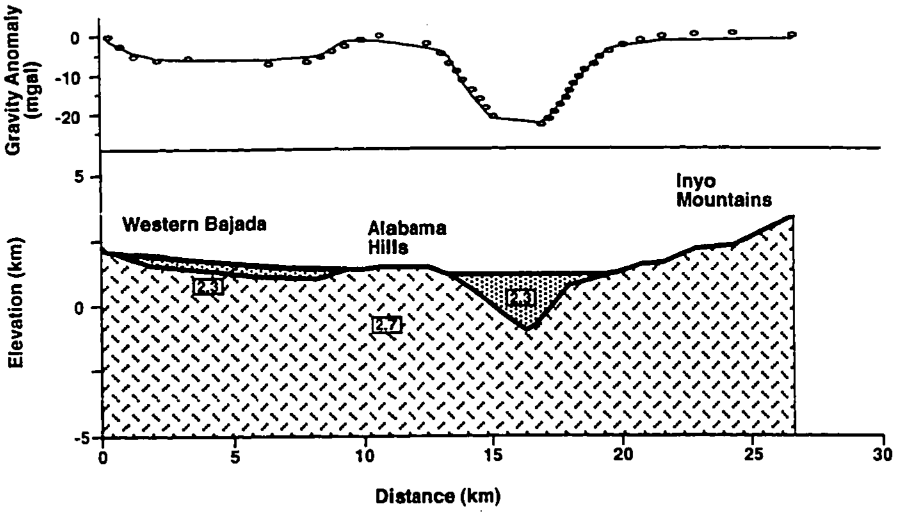
Gravity Anomaly (mgal)
0
-10
-20
5
0
-5
Elevation (km)
Western Bajada
Alabama Hills
Inyo Mountains
2.3
2.7
2.3
0
5
10
15
20
25
30
Distance (km)

Figure 1.3
D. Deep graben structure associated with Owens Lake (Fig. 1.1).

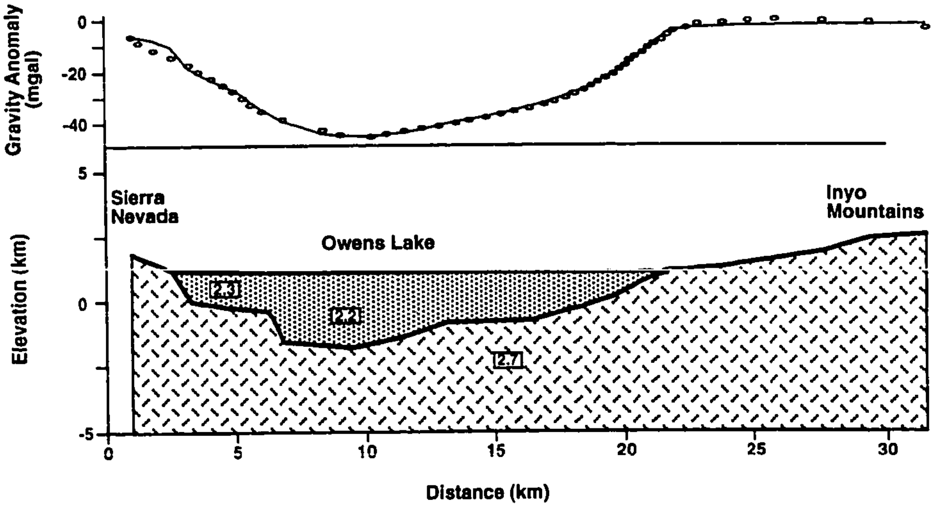
Gravity Anomaly (mgal)
0
-20
-40
5
Elevation (km)
0
-5
Sierra Nevada
Owens Lake
Inyo Mountains
2.3
2.2
2.7
0
5
10
15
20
25
30
Distance (km)

"low" or "high" subsidence rate. These two tectonic classes were defined arbitrarily on our estimates of the depth of late Cenozoic fill. Platforms supporting less than 1 km of fill are considered "low" subsidence rate environments and basins with fill depths in excess of 2 km as "high" subsidence rate environments. Climatic setting was characterized by modern mean annual precipitation data and the size of glaciers supported by the source basin.

Divisions between the fan groups studied were chosen purposefully on tectonic boundaries to facilitate study of the influence of local subsidence rate on fan size and slope. The morphometric data describing the fans and their source catchments was then subdivided according to lithologic (for the two White Mountains fan groups) and climatic setting (for the two Sierra Nevada fan groups) and plotted on scatter diagrams. Power-law regression models (equation 1.2) were computed for each fan group.

STUDY SITE DESCRIPTIONS

Geophysical Structure

Owens Valley, bounded on the west by the Sierra Nevada and on the east by the White and Inyo Ranges (Fig. 1.1), is situated at the western boundary of the Basin and Range Province. The Owens Valley graben is a complex structure that accommodates significant strike-slip as well as normal-slip displacement. The structural geology of Owens Valley has been determined by a combination of field mapping and geophysical surveys (Pakiser, and others, 1964; Hollett, and others, 1989). Owens Valley can be roughly divided into three structural units, herein referred to as the northern, central, and southern grabens.

The northern graben includes a deep half-graben (flanked by the Coyote Upwarp on the west (Pakiser, and others, 1964; Bierman, and others, 1991) and the White Mountains Fault Zone on the east) and a narrow full-graben extension north of Bishop between the Volcanic Tableland and the White Mountains. The northern extension is a deep (ca. 2.5 km), steep-sided structure that ends abruptly 40 km north of Bishop ((Pakiser, and others, 1964); Figs. 1.1 and 1.3b). Beyond the northern end of this structure, the modern fans are built onto a shallow bedrock bench. The total thickness of Cenozoic sediments on this bench does not exceed 1000 meters and probably averages about 500 meters (Fig. 1.3a).

The central graben (extending from Lone Pine to the Big Pine volcanic complex, 20 km south of Big Pine) is markedly asymmetrical, with a 10-15 km wide shallow bedrock bench to the west at the foot of the Sierra Nevada, and a deep (ca. 2 km) but narrow graben abutting the Inyo Mountains (Figs. 1.1 and 1.3c). The shallow bedrock bench illustrated in Figure 1.3c is inferred to extend north from the Alabama Hills at least as far as the town of Independence (Fig. 1.1; Pakiser, and others, 1964). In contrast, the southern graben, which includes the area around Owens Lake, is approximately symmetrical, extends the full width of the valley, and is as much as 2.5 km deep (Figs. 1.1 and 1.3d; Pakiser, and others, 1964).

Climate and Lithology

The fans of the Owens Lake group are derived from the granitic rocks of the Sierra Nevada under unglaciated conditions and are being deposited into the southern graben after bypassing a narrow bedrock bench (Figs. 1.1 and 1.3d). The western bajada group includes all fans between the southern tip of the Alabama Hills and the Big Pine volcanic complex (Fig. 1.1). These fans were derived from predominantly granitic rocks and include source basins that were variously not glaciated, slightly glaciated, and extensively glaciated. The extensive fans of the western bajada group are building out onto the shallow bedrock bench at the foot of the Sierra Nevada that separates the fans from the central graben (Figs. 1.1 and 1.3c). The southern White Mountains group includes fans derived from dominantly granitic, metasedimentary, and metavolcanic lithologies. These fans are being deposited directly into the narrow graben north of Bishop (Figs. 1.1 and 1.3b). The fourth and final group are derived from the granitic rocks of the northern White Mountains and are building out onto the bedrock bench north of the termination of the narrow graben (Figs. 1.1 and 1.3a). Both the White Mountains fan groups were derived under unglaciated conditions within the rain shadow of the Sierra Nevada.

RESULTS

As is readily visible on Figure 1.1, the spatial distribution and extent of fan deposits in Owens Valley is strongly constrained by the geophysical structure of the valley. The Owens Valley data set includes two fan groups deposited under conditions of low long-term subsidence rates (the northern White Mountain and western bajada groups) and two fan groups deposited under conditions of high long-term subsidence rates (the southern White Mountain and Owens Lake groups). Within group differences include a range of climatic and lithologic conditions and direct comparisons can be made with confidence. For instance, the extent of Late Pleistocene glaciation is the only significant difference between adjacent fans in the western bajada group and both relative fan sizes and slopes can be expected to record the climatic signal. Between group comparisons are only quantitatively useful if the tectonic setting is in all ways similar. Total fill depth in the northern and southern Owens Valley grabens is approximately equal (Figs. 1.3b and 1.3d) and it is reasonable to assume that average long-term sedimentation rates have been similar. Comparisons of relative fan sizes and slopes between these two field sites as a function of climate (non-glacial) and lithology can thus be made. However, as outlined earlier different spatial variations is subsidence rate can importantly influence relative fan sizes and care must be taken in interpreting data from different field sites.

Fan Size

Fan size is strongly correlated with both drainage area and tectonic setting (Fig. 1.4; Table 1.2). The single outliers in each of the western bajada group (Sawmill Creek) and the southern White Mountains group (Millner Creek) indicated on Figures 1.4a and 1.4b were excluded from regression analysis. The tectonic situation in each of these cases will be considered in the discussion.

The correlation with drainage area is obvious, with fan area increasing monotonically with drainage area within each fan group. The dependence on tectonic setting is clearly displayed in between-group differences in relative fan size and is particularly well illustrated in the difference between the western bajada and Owens Lake fan groups (Fig. 1.4a; Table 1.2). Here fans building into the high sedimentation rate environment of the southern graben are approximately one-tenth the size of fans on the western bajada. This difference in relative fan size is commensurate with the difference in estimated fill depths (ca. 2.5 and .25 km respectively; Fig. 1.3) and, therefore, average long-term sedimentation rates, consistent with the direct dependence anticipated in equation (1.1) (Hooke, 1968). It is important to recognize, however, that because of the difference in the fitted n-values (equation 1.2), the c-values do not reflect this ten-fold difference in relative fan size (Table 1.2). This caution regards the interpretation of this type of regression analysis and not the interpretation of the field data. The approximate quantitative correspondence between relative fan size and sedimentation rate suggests that fan areas are insensitive to the climatic differences between these two fan groups (glaciated versus non-glaciated). This possibility is

TABLE 1. 2: REGRESSION ANALYSIS

Power Law Regression Model (Af = cAd^n)

Fan Group	sample size			95% confidence band	t statistic (c)	P-value (c)	r^2
Northern Whites	7	c	0.01	0.00 - 0.07	-2.76	.033	0.757
		n	2.82	0.98 - 4.65	3.94	0.008	
Southern Whites	11	c	1.66	0.73 - 3.78	1.40	.191	0.325
		n	0.34	0.06 - 0.62	2.76	0.02	
Western Bajada	20	c	2.59	1.33 - 5.02	3.00	.007	0.609
		n	0.64	0.39 - 0.90	5.29	4.2 E-5	
(linear: n=1 forced)		c	0.94	0.84 - 1.04	19.68	1.5 E-15	0.754
		n	--	--	--	--	
Owens Lake	10	c	0.64	0.42 - 0.99	-2.36	.043	0.808
		n	0.47	0.28 - 0.66	5.81	2.6 E-4	

Figure 1.4 Fan area vs. Drainage area.
A. Fans of the western bajada and Owens Lake groups. Symbols: Owens Lake group (circles); Western bajada group (heavily glaciated catchments - open triangles; slightly glaciated catchments - open inverted triangles; unglaciated catchments - solid triangles). S indicates Sawmill Creek fan (outlier).

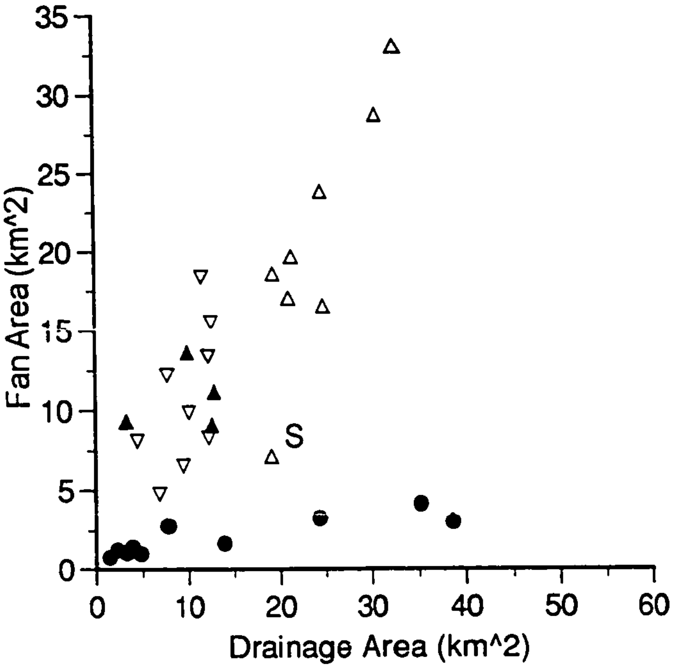
Fan Area (km^2)
0
5
10
15
20
25
30
35
Drainage Area (km^2)
0
10
20
30
40
50
60
S

Figure 1.4
B. Fans of the southern and northern White Mountains groups. Symbols: northern group (granitic source - open triangles), southern group (granitic source - solid inverted triangles; mixed source - solid squares; metasedimentary source - solid circles). Single outlier (M) is Millner Creek fan and is discussed in the text.

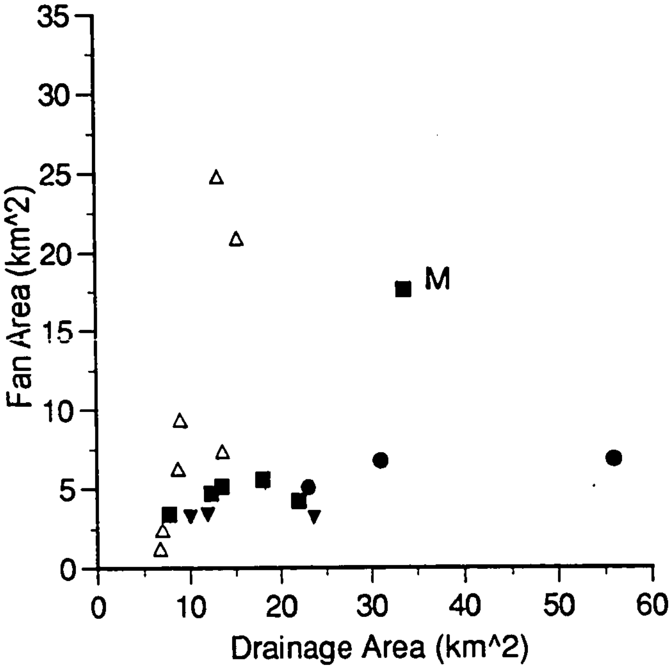
35
30
25
20
15
10
5
0
Fan Area (km^2)
M
0
10
20
30
40
50
60
Drainage Area (km^2)

Figure 1.4
C. Comparison of Owens Lake group with southern White Mountains group. Note close correspondence in relative size of granitic-source fans (symbols as in A & B, except Owens Lake group shown as open triangles).

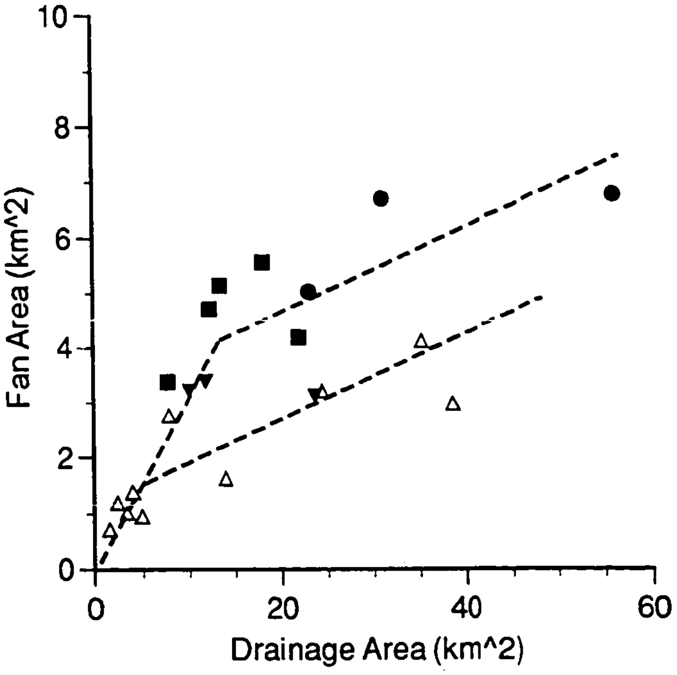
10
8
6
4
2
0
Fan Area (km^2)
0
20
40
60
Drainage Area (km^2)

strongly supported by the finding that fans derived from unglaciated, slightly glaciated, and heavily glaciated drainages on the western bajada all plot on the same trend, with no discernible differences in relative fan size (Fig. 1.4a).

Comparison between relative fan sizes in the Owens Lake group, the southern White Mountains group, and among fans derived from different source lithologies within the southern White Mountains group suggest a second-order dependence of fan size on source lithology (Fig. 1.4c). In addition, the east-west climatic gradient in the rain shadow of the Sierra Nevada (Rantz, 1969; Bierman, and others, 1991) apparently has no discernible effect on fan size: granitic-source fans in both field sites have approximately equivalent relative sizes and the fans derived from more erodible meta-sedimentary and meta-volcanic source rocks (Lecce, 1991) are slightly larger. However, although average subsidence rates in these two grabens have apparently been similar, between group differences in relative fan size could be due to differences in the spatial pattern of subsidence rates.

Fan Slope

Fan slope varies with drainage area, lithology and catchment ruggedness number, but with neither climate nor long-term subsidence rate. Despite an order of magnitude range in long-term subsidence rates (Fig. 1.3), a transition from glaciated to non-glaciated conditions, and a significant rain shadow effect, granitic-source fans throughout Owens Valley have consistent drainage area - fan slope relationships (Fig. 1.5). In contrast, the dependence on source lithology, though defined by few data, is striking (Fig. 1.5c).

Fan slope is negatively correlated with drainage area in all fan groups (Fig. 1.5; Table 1.2). Although this dependence on drainage area is presumably related to greater fluvial discharges, and hence greater fluvial "efficiency", there is no discernible difference in slope between fans derived under significantly different climatic conditions: granitic-source fans on the western bajada associated with unglaciated, slightly glaciated, and heavily glaciated drainages plot as a single trend (Fig. 1.5a). Furthermore, granitic-source fans from unglaciated catchments on both the relatively wet west side of Owens Valley (mean annual precipitation ~ 750 mm in mid-elevations) and the drier east side (mean annual precipitation ~ 300 mm in mid-elevations) (Rantz, 1969) have comparable slopes (Fig. 1.5).

Interestingly, the fans of the Owens Lake fan group display a sudden transition to steeper slopes at drainage areas less than 5 km^2 (Fig. 1.5a). Although suggestive of

Figure 1.5 Fan slope vs. drainage area for debris-flow fans in Owens Valley, California.

A. Fans of the western bajada and Owens Lake groups. Owens Lake group plotted as solid circles. Fans from the western bajada group plotted according to climate (heavily glaciated catchments - solid triangles; slightly glaciated catchments - solid inverted triangles; unglaciated catchments - open triangles). Kink in trend (at drainage area = 5 km^2) is discussed in text. S indicates Sawmill Creek fan (outlier).

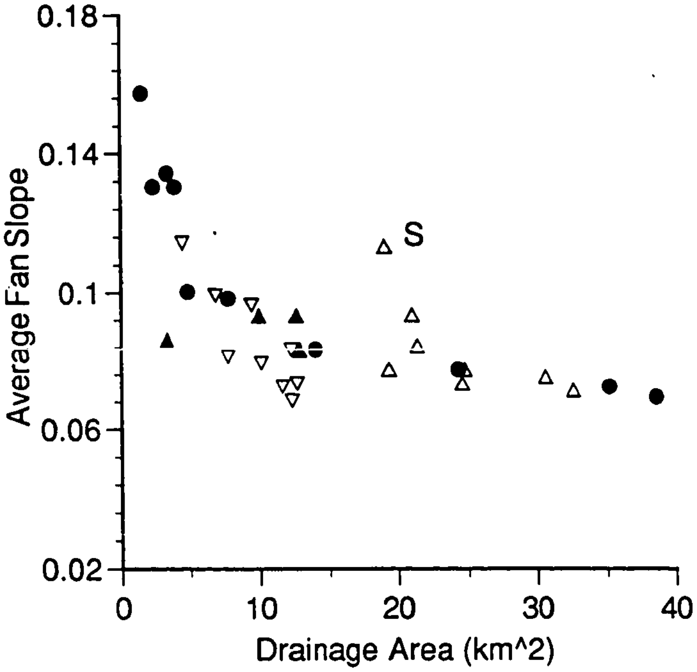
0.18
0.14
0.1
0.06
0.02
Average Fan Slope
S
0
10
20
30
40
Drainage Area (km^2)

Figure 1.5
B. Fans of the southern and northern White Mountains groups. Northern group (granitic source - open triangles). Southern group (granitic source - inverted solid triangles; mixed source - solid squares; metasedimentary source - solid circles). Tectonically oversteepened fans of the southern group are indicated (T).

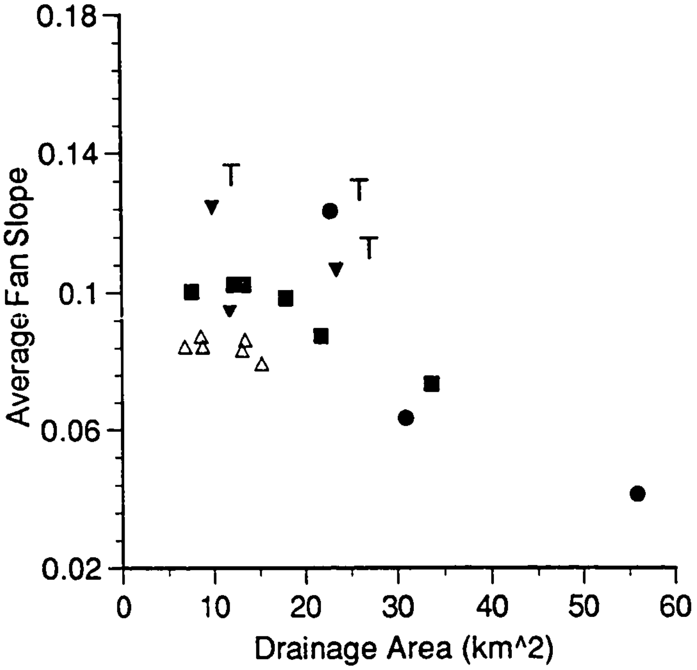
0.18
0.14
0.1
0.06
0.02
Average Fan Slope
T
T
T
0
10
20
30
40
50
60
Drainage Area (km^2)

Figure 1.5

C. Composite plot illustrating lithologic control on fan slope. Tectonically oversteepened fans and small fans restricted to the upper slopes of the bajada are excluded. Symbols: granitic-source fans of the Sierra Nevada (open squares); granitic-source fans of the White Mountains (solid circles); mixed-source fans of the southern White Mountains group (solid triangles).

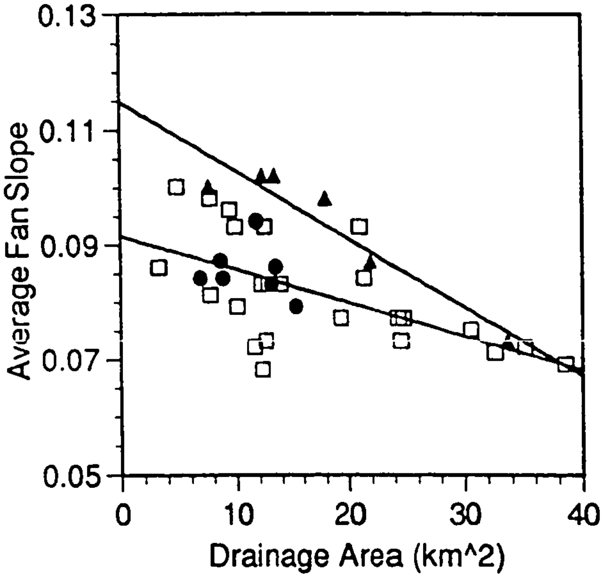
0.13
0.11
0.09
0.07
0.05
Average Fan Slope
0
10
20
30
40
Drainage Area (km^2)

a process threshold, this condition is most likely an artifact of lateral coalescence with larger fans: these small fans are restricted to the proximal reaches of the bajada as their distal portions are buried and absorbed by neighboring fans. As a result, the "average slope" of these small fans is representative of only the proximal fan slope. Similarly, the correlation with ruggedness number, which might be taken as an indication of a dependence on the amount and rate of uplift, is probably not meaningful: total catchment relief is essentially constant along both the Sierran and White Mountain fronts. Ruggedness number contains no information other than differences in drainage area. However, this direct correspondence between ruggedness number and drainage area does raise the question of whether the correlation with drainage area, in this setting, is an indication of the effects of increasing discharges or of decreasing catchment slopes.

Although fan slope is found, in general, to be independent of tectonic setting, subsidence rates, and the spatial pattern of subsidence rates, there are some instances where a direct tectonic influence on fan slope is clearly demonstrated. This influence, however, is only recognized on fans physically and recently (Late Pleistocene - Holocene) oversteepened by valley-ward tilting (Figs. 1.5b). The lack of correlation between fan slope and long-term subsidence rates indicates that such tectonic perturbations are short-lived: fans are rapidly (order 10^3 -10^4 years) re-graded to the slope dictated by depositional processes.

DISCUSSION

Controls on Fan Size

The size of fans in the closed basins of the southwestern Basin and Range is set by interplay between the rate of sediment delivery to the fan system and the rate of basin subsidence (Hooke, 1968; Hooke, 1972). Although both the sediment delivery rate and the tectonic subsidence rate must have fluctuated significantly during the past 2-5 million years, differences in relative fan size in Owens Valley are well explained by differences in local basin-fill depths, indicating that long-term average sedimentation rate is a reasonable predictor. The overriding importance of local subsidence rate over lithologic and climatic effects arises from (1) the direct dependence of fan size on sedimentation rate (equation 1.1; Hooke, 1968) and (2) the 10-fold differences in local subsidence rate.

Scatter in morphometric data (e.g., Fig. 1.4) probably reflects: (1) short-term fluctuations in fan size that occur as individual fans shift, overlap and coalesce with neighboring fans; (2) error in locating fan boundaries; and (3) minor local differences in erodibility, climate, or tectonics (Hooke, 1968). A pair of outliers, however, stand out and deserve mention. The outliers are the Millner Creek fan in the southern White Mountains group (Fig. 1.4b) and the Sawmill Creek fan in the western bajada group (Fig. 1.4a). Local differences in subsidence rates are the most plausible explanation in both cases. For instance, the Millner Creek fan is not exceptionally large, given the size of its source catchment, but stands out against the other fans depositing into the rapidly subsiding northern Owens Valley graben. This is apparently because the Millner Creek fan is supported by a relatively shallow block of the Bishop Tuff (evidence cited by Beaty (1970)). No definitive explanation can be offered at this time for the unusually small size of the Sawmill Creek fan, but it is situated at the northern margin of the western bajada fan group and may be subject to a somewhat greater rate of subsidence.

Spatially Variable Subsidence Rate

Although (Hooke, 1968; Hooke and Rohrer, 1977) have shown that power-law regressions for many fan groups in the Death Valley region have n-values near but less than unity ($n \sim 0.9$), we find significant differences in n-values amongst the fan groups studied here (Table 1.2) and similar values were reported in two cases by Hooke (1968). Exponents (in equation 1.2) slightly less than unity have been explained previously in terms of specific sediment yield (e.g., Hooke, 1968). This explanation, however, is untenable for n-values much less than unity.

Specific sediment yield is generally found to decrease with drainage area in response to declining valley side-slope gradients and increasing proportions of sediment storage in floodplains and valley floors (Church, and others, 1988). The steep, mountainous basins considered in this study, however, have negligible amounts of valley-floor storage and Hooke (1968) has shown that valley side-slope gradient declines only slightly with increasing drainage area in much of the Owens Valley - Death Valley region. Exponent values on the order of 0.9 might be attributable to declining specific sediment yields or diminishing trap efficiency with increasing drainage area, but neither effect can explain the low exponent values obtained in parts of Owens Valley. We suggest that low exponent values are an artifact of spatially non-uniform subsidence rates.

Figure 1.6 Effects of spatially varying subsidence rates. A. Schematic illustration of a simple, asymmetric valley. Symbols defined in text. B. Schematic illustration of fan area - volume rate of deposition relationships. Power-law fits to upper curve (fan complexes where the larger fans bypass the shallow bedrock bench) will give low n-values and correspondingly high c-values.

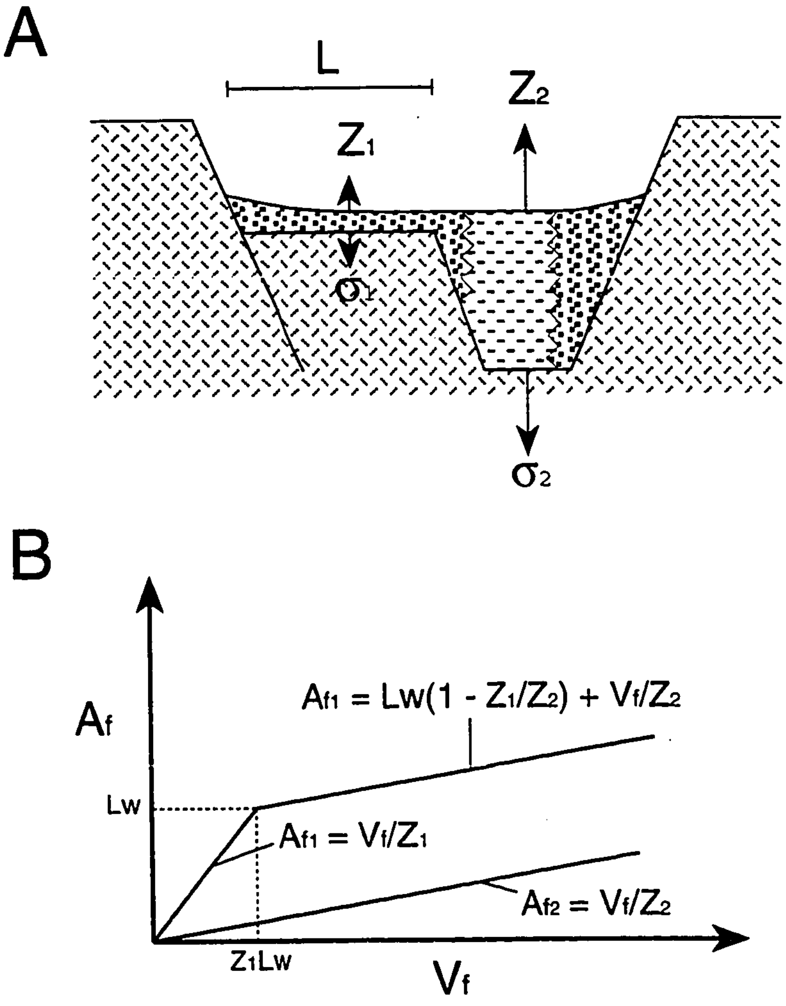
A
L
Z_2
Z_1
σ_1
σ_2
B
A_f
$A_{f1} = Lw(1 - Z_1/Z_2) + V_f/Z_2$
Lw
$A_{f1} = V_f/Z_1$
$A_{f2} = V_f/Z_2$
Z_1Lw
V_f

Spatially variable subsidence rates are an ubiquitous property of tectonically active depositional basins. As first recognized in Death Valley, differences in local subsidence rate can have a dramatic influence on fan size relative to drainage area (Hunt and Mabey, 1966; Hooke, 1968; 1972). In Death Valley, as in Owens Valley, local subsidence rate is the primary control on relative fan sizes, with lithologic variability playing a secondary role, at least in Death Valley (Hooke and Rohrer, 1977). Although in the particular instance of Death Valley Hooke (1968) and later Hooke and Rohrer (1977) found the power-law index (n) in equation (1.2) to be independent of local subsidence rate, or "tectonic setting", simple geometrical arguments are used below to show that both c and n in equation (1.2), as determined by regression of field data, are sensitive to spatial variation in local subsidence rate, independent of any lithologic, climatic, or physiographic differences in the source terrane.

The importance of spatially variable subsidence rate arises from the condition of equilibrium between adjacent fans and between the fans and the valley floor described by Hooke (1968; 1972). The requirement of a tendency towards equilibrium imposes the condition that the mean rate of net surface aggradation relative to a fixed horizontal datum must everywhere be approximately equal:

$$z(x1,x2)-\sigma(x1,x2)\approx k\ , \qquad (1.9)$$

where k is a constant equal to zero in a steady-state landscape. Regardless of whether the valley floor is experiencing net subsidence or net aggradation ($k \neq 0$) local sedimentation rate varies with local subsidence rate. Figure 1.6 highlights the dependence of relative fan sizes on spatial variations in subsidence rates using as an example a simple structural configuration characteristic of the Owens Valley grabens and common in the Basin and Range Province in general. Source areas on either side of the hypothetical valley illustrated in Figure 1.6a are presumed to be identical. In the case where the rate of sediment delivery to all fans is small, such that the condition

$$V_f < z_1 Lw\ , \qquad (1.10)$$

(where L is the length of the bedrock bench and w is the mean fan width) holds, then n in equation (1.2) is independent of subsidence rate ($n_1 = n_2$) and c is directly dependent on sedimentation rate ($c_1 = V_f/z_1 > c_2 = V_f/z_2$), analogous to the condition found in Death Valley by Hooke (1968). However, in the case where sediment delivery to some fans is large,

$$V_f > z_1 L w \, , \tag{1.11}$$

then both c_1 and n_1 (assuming an equation of the form of (1.2) is fit to the field data) are dependent on L, z_1, and z_2 (Fig. 1.6b). In this scenario, for smaller ratios of fan to valley floor sedimentation rate (z_1/z_2), n decreases and c increases. Similarly, it is easily demonstrated that if sedimentation rate increases linearly with distance from the range front (as might occur in simple tilting) then A_f varies with V_f to the one-half power. A power-law equation fit to fan size - drainage area data in such a setting would discover an n-value one-half of that in an otherwise similar setting with spatially uniform subsidence rates. An implication is that in either of these common settings the values of both c and n are set by the spatial distribution of subsidence rates and bear little direct relation to the physical characteristics of the source area or the theoretical relationships developed in equations (1.7) and (1.8); fan area - drainage area relationships of the form ($A_f = cA_d^n$) must be considered in the context of local tectonic setting.

Subsidence rates that increase with distance from the range front probably explain the low exponents obtained for the southern White Mountains (n = .34; Table 1.2) and the Owens Lake (n = .47; Table 1.2) fan groups. In both cases, the n-value is significantly less than unity at the 95% confidence level (Table 1.2). The n-value for the western bajada fan group is surprisingly low (n = .64) considering the extent of the shallow bench underlying these fans (Fig. 1.3c) and the linear appearance of the scatter plot of these data (Fig. 1.4a). Correspondingly, the 95% confidence band includes near-unity values (.39 < n < .90) and a linear regression fits the data well (Table 1.2). These results are consistent with relatively uniform subsidence rates. The case of the northern White Mountains group is different. The unusually high n-value (2.82) is an artifact of two things: (1) there are very few data points; and (2) the two largest fans are laterally unconstrained (see Fig. 1.1) and are building out beyond the northern limit of the valley-floor alluvium. These two fans are effectively in a different tectonic environment than their neighbors to the south are not in direct competition with them.

Although the association between the power-law exponent and tectonic environment apparently has remained unrecognized until now, the general conclusion that fan area - drainage area relationships are controlled to first order by tectonic setting is not new (e.g., Denny, 1965; Hunt and Mabey, 1966; Hooke and Rohrer, 1977). However, although Hooke (1977) clearly relegates lithologic differences to second-order importance, the relative importance of tectonic, lithologic, and climatic factors has not been clearly established in the literature. For instance, (Lecce, 1991) argues that differences in fan size along the western flank of the White Mountains in Owens Valley California, here attributed to differences in graben structure, are primarily due to differences in lithologic erodibility, catchment physiography, and sediment storage on hillslopes. An unfortunate geographical coincidence is apparently responsible for the confusion: the termination of the deep, narrow graben that runs along the flank of the White Mountains approximately coincides with the transition to more resistant granitic rocks in the northern White Mountains (Fig. 1.3). This is not to say that the effects described by Leece (1991) do not operate, only that they are of second-order importance to tectonic differences along the White Mountains.

Lithology

As mentioned, the relative sizes of granitic-source and mixed-source fans in the Owens Lake group and the southern White Mountains group are suggestive of a second-order lithologic influence (Fig. 1.7). Two objections might be raised, however, and the data are inconclusive. First, the difference in the relative sizes of the granitic and mixed-source fans in the southern White Mountains group is small and scatter on this order is seen in fan size data in monolithologic terranes (ie., Fig. 1.7a). Second, these data are a case in point for the argument above concerning spatially variable subsidence rates. As illustrated in Figure 1.7c, the difference between the sizes of the Owens Lake and southern White Mountains fans could simply reflect difference in the size and relative subsidence rates of the shallow bedrock benches underlying the fans (see **Fig. 1.n**). This same complication makes it impossible for us to say anything definitive about the influence of the east-west climatic gradient on the sizes of fans derived from unglaciated basins.

Climate

Climate is expected to influence fan area - drainage area relationships in much the same manner as lithologic erodibility and basin slope: directly influencing the sediment yield. However, as was the case with lithologic erodibility, our study of relative fan sizes in Owens Valley found no convincing evidence that fan area - drainage area relationships carry a climatic signal. As a case in point, heavily glaciated, lightly glaciated, and unglaciated basins of the eastern Sierra Nevada associated with a single tectonic setting plot as a single line in fan area - drainage area space (Fig. 1.7a). Basins more extensively modified by glacial scour (e.g., Lone Pine, Shepherd, and

Independence Creeks) have both the largest drainage areas and the largest fans, but the apparently enhanced sediment production is not reflected in fan area - drainage area relationships. This implies that either: (1) glaciation did not increase the long-term sediment yield from these basins, or (2) the processes of glacial erosion produce a greater percentage of fines that can be delivered as suspended and wash load, thus effectively reducing the trap efficiency of the fans and masking the glacial signal. Determining which factors predominate would be an important step forward in our understanding of glacial processes and their impact on landscape evolution.

Controls on Fan Slope

Drainage area affects both the magnitude of fluvial discharges and typical sediment:water ratios generated during debris-flow events (Wells and Harvey, 1987). Drainage area thus influences both the size and continuity of channels on the fan surface and the rheology of the debris flow, both of which importantly constrain the operation of debris-flow fan depositional processes, and thus the slope of the depositional surface (Whipple and Dunne, 1992). Similarly, source lithology is known to be an important control on fan slope because it governs, to first order, the regolith granulometry (climatic variables that influence hillslope weathering environments should play an important, but apparently secondary, role), which in turn critically controls debris-flow rheology (Phillips and Davies, 1991; Major and Pierson, 1992). All else being equal (which is rarely the case -- complex inter-dependencies exist between regolith granulometry, near surface hydrology, debris-flow initiation mechanisms, resulting sediment:water ratios, and debris-flow rheology), a source regolith with a higher fines (silt and clay) content will produce debris flows with higher effective viscosities, result in more extensive overbank deposition, and generate steeper fan profiles (Whipple and Dunne, 1992).

The difference between granitic-source and mixed-source fans along the White Mountains is a clear example of this effect: adjacent granitic and mixed-source basins have similar physiographic and hydrologic characteristics (here all else is equal) and yet fans derived from these basins have markedly different surface morphologies and slopes (Fig. 1.9c; Bierman, and others, 1991; Whipple, 1991; Whipple, 1993). The fact that fan slope is independent of both tectonic and climatic setting, but sensitive to source lithology, indicates that the rheological controls on fan slope discussed by Whipple and Dunne (1992) are dominant, at least within the range of conditions found in Owens Valley.

CONCLUSIONS

The size of fans in Owens Valley, California, is directly related to catchment area and the details of the local tectonic setting. Differences in tectonic setting account for the full range of variability in relative fan sizes in Owens Valley and there is no conclusive evidence in our data that either source lithology or climate importantly influence either fan sizes or the coefficients in the familiar power law relationship ($A_f = cA_d^n$) used to describe them. Indeed, in settings with spatially varying subsidence rates, both c and n are set by that spatial variability and bear no direct relation to source area characteristics; fan size data must be considered in the context of the local tectonic setting. Interestingly, relative fan sizes in the same tectonic environment do not vary with the degree of Late Pleistocene glaciation in their source catchments. An implication is that glaciation did not significantly affect the long-term average sediment yields from these drainages. An alternative explanation may lie in the enhanced production of fines in a glacial environment, effectively, and significantly, reducing the trap efficiency of the fan system. This issue merits further study.

Unlike fan size, fan slope is in general found to be independent of tectonic setting. Although fan slope is subject to significant, short term, perturbation by tectonic disturbance, the slope of debris-flow fans is determined over the long term by depositional processes alone. Fan slope is therefore dependent on both drainage basin size and source lithology (Whipple and Dunne, 1992; Whipple, 1993). In general, steeper fans are associated with smaller basins and basins cut into lithologic assemblages supporting fines-rich regoliths. This follows because: (1) smaller basins are associated with smaller flood discharges and hence less efficient channelization of fan surfaces; (2) flood/debris-flow events in smaller basins typically have higher sediment:water ratios, which is conducive of more overbank deposition and the aggradation of steeper fan slopes; (3) fines-rich source regoliths generate debris flows with higher effective viscosities for a given sediment:water ratio. Surprisingly, despite a strong cross-valley precipitation gradient in the rain shadow of the Sierra Nevada and a cross-valley transition from primarily glaciated to unglaciated conditions during the late Pleistocene, there is no indication of a climatic control on the slope of debris-flow fans in Owens Valley, California. Presumably the climatic signal is simply overwhelmed by the sensitivity of debris flow rheology to differences in source lithology, and the direct influence debris-flow rheology exerts on fan depositional processes and, hence, fan slope (Whipple and Dunne, 1992).

ACKNOWLEDGMENTS

This research was supported by the National Science Foundation, Grant EAR-9004843, awarded to the first author and T. Dunne. Critical reviews of an early draft by R. LeB. Hooke and T. Dunne greatly improved the manuscript. The authors also wish to acknowledge insightful discussions with Daniel Miller. The authors are grateful to the White Mountain Research Station and the staff at the Bishop Laboratory for providing accomodation.

CHAPTER 2

Conceptual Model: The influence of debris-flow rheology on fan morphology, Owens Valley, California

Chapter 2 presents the conceptual model of fan processes developed on the basis of detailed field and aerial photographic work in Owens Valley. This chapter has already been published in the Geological Society of America Bulletin under the title: "The influence of debris-flow rheology on fan morphology, Owens Valley, California" (v. 104, p. 887-900, 1992) by K. Whipple and T. Dunne. It includes a preliminary analysis of the rheologic controls on channel conveyance capacity (explained in text) that has since been updated and is supplanted by the analysis presented in Chapter 3.

CHAPTER SUMMARY

We have investigated factors controlling the surface morphology of debris-flow fans comprising the bajada along the western slope of Owens Valley, California. These fans have average slopes of 4°, an extensive network of abandoned, boulder-lined channels, rough, undulatory surfaces near the range front, and smooth distal surfaces. Field relationships and mechanical considerations indicate that the channels of the bajada are products of fluvial incision and not debris-flow scour. This is significant because detailed geomorphic maps indicate that the channels strongly influence the pattern of debris-flow deposition. The locus of debris-flow deposition on a channelized fan surface is set by the interaction of debris flows with the channel system, and is controlled by channel size, channel gradient, flow volume, flow hydrograph, and flow rheology. Debris-flow behavior is most directly controlled by variations in bulk sediment concentration and its influence on flow rheology. Whereas low-sediment-concentration debris flows tend to smooth the surface of the lower fan, spreading into thin sheets and filling channels and surface undulations, repeated deposition of high-sediment-concentration debris flows produces the rugged topography of the upper fan. The texture of the fan surface, rough or smooth, is determined by the relative volumetric importance of these two types of debris flow. In addition, channel avulsions and the associated long-term shifting of depositional loci are driven by in-channel deposition of debris flows with the highest sediment concentrations. These debris flows, therefore, play a critical role in determining both the structure of the channel network and the long-term pattern of deposition on the fan surface as a whole. We

infer that the frequency distribution of debris-flow rheologies, set by source terrain geology and hydrology, is an important control on fan morphology.

INTRODUCTION

Debris-flow fans occur in a range of environments and show great variability in size, slope, and surface morphology (e.g., Blissenbach, 1954; Beaty, 1963; Ryder, 1971; Suwa and Okuda, 1983; Harvey, 1984; Johnson, 1984). The present study analyzes the process of debris-flow fan construction on a bajada along the western slope of Owens Valley, California (Fig. 2.1) to explain the physical controls on fan morphology. We discuss controls on the original, depositional morphology exclusively. We avoid a discussion of tectonic or climatic factors, in order to study the operation of the fan depositional system in isolation. In addition, controls on the overall properties of fan size and slope are only discussed qualitatively; we focus on fan surface morphology, i.e. the combination of surface texture, textural patterns, and the morphology and spatial distribution of channels crossing the fan. Field mapping indicates that the Owens Valley bajada consists almost entirely of debris-flow deposits (see later), and our interpretations in their strictest form should only be extended to similar depositional systems, although certain generalizations may be made from our results.

The surface morphology of debris-flow fans is set by: the nature of the channel system; the spatial distribution of debris-flow deposits on the fan surface; and the interaction between the debris flows and the channels. Johnson (1970; 1984) and Hooke (1967; 1987) have established that the locus of debris-flow deposition is controlled by debris-flow volume and yield strength and the degree of flow confinement within channels. The present study builds on their work by: 1) documenting the interplay between channels and debris flows in the formation of the Owens Valley bajada; 2) evaluating the "degree of flow confinement" through an analysis of the factors controlling channel conveyance capacity (defined as the discharge of the bankfull flow); and 3) considering the long-term morphological consequences of deposition by debris flows with variable volumes, peak discharges, and rheologies. Our approach is first to define the interplay of debris-flow and fluvial processes in fan formation on the basis of field observations in Owens Valley, and then to draw upon current understanding of debris-flow rheology (e.g., Johnson, 1970; Major and Pierson,

Figure 2.1. Index map of the study site in Owens Valley, California. The bajada, consisting of coalescing fans, is delineated approximately by the trace of the Sierran range front (dashed line) to the west and the Los Angeles Aqueduct to the east.

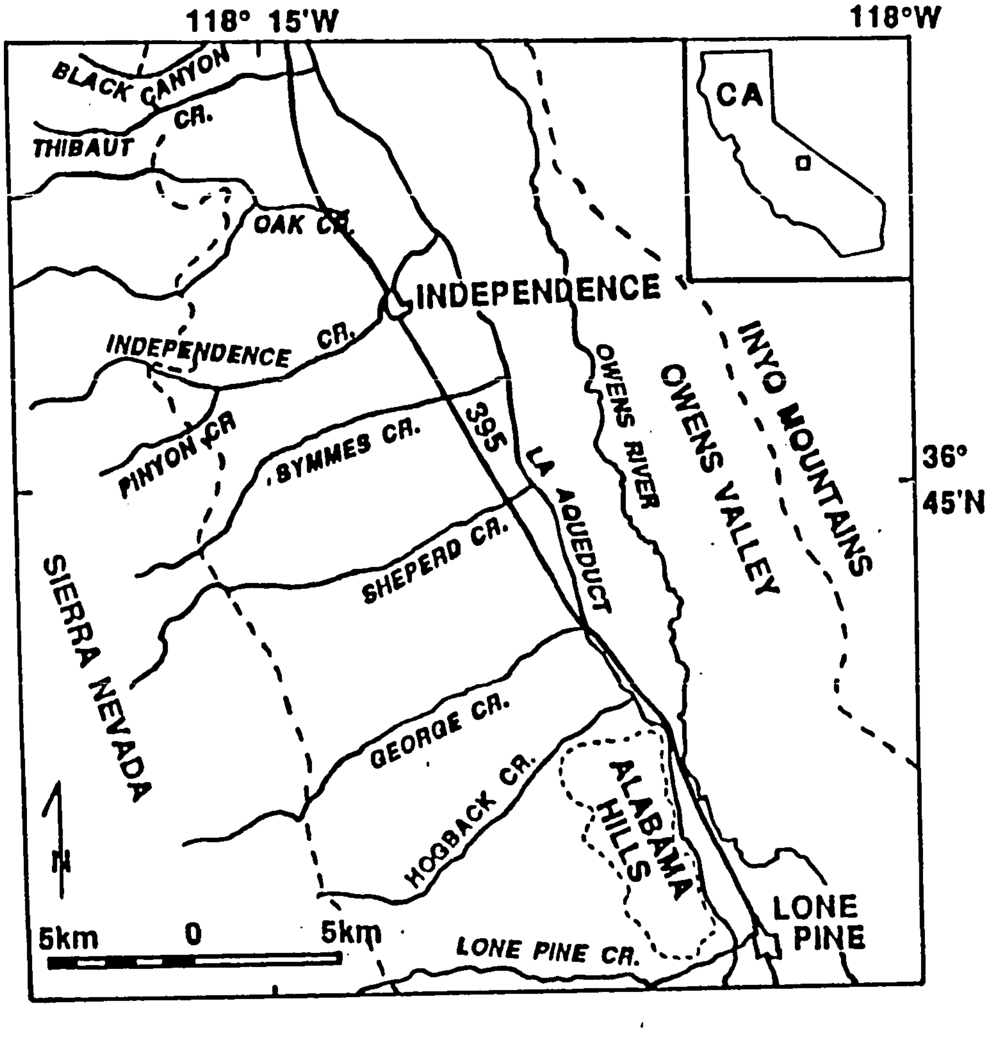

118° 15'W
118°W
36°
45'N
BLACK CANYON
THIBAUT
CR.
OAK CR.
INDEPENDENCE
INDEPENDENCE CR.
PINYON CR
SYMMES CR.
SHEPERD CR.
GEORGE CR.
HOGBACK CR.
LONE PINE CR.
395
LA AQUEDUCT
OWENS RIVER
OWENS VALLEY
INYO MOUNTAINS
SIERRA NEVADA
ALABAMA HILLS
LONE PINE
CA
N
5km
0
5km

1990; Whipple, in press) to explore the interaction of debris flows with the fan surface and the sensitivity of this interaction to rheological variability.

This paper presents: (1) a description of the Owens Valley field site; (2) a description of fan morphology; (3) a discussion of the relative roles of fluvial and debris-flow processes in fan aggradation and in the channelization of the bajada surface; (3) an analysis of debris-flow processes and their role in setting the surface morphology of the fans; and (4) a general discussion of the physical controls on the depositional morphology of debris-flow fans.

OWENS VALLEY FIELD SITE

Owens Valley is a graben bounded on the west by the Sierra Nevada and on the east by the White-Inyo Range (Fig. 2.1). Sediment shed from the rugged highlands, mostly as debris flows, has contributed to broad piedmonts of coalescing fans (bajadas) at the foot of both the White Mountains (Beaty, 1963) and the Sierra Nevada (Trowbridge, 1911; Blackwelder, 1928), and to a deep valley fill (Knopf, 1918; Pakiser and others, 1964). The eastern escarpment of the Sierra Nevada is flanked by an extensive, uninterrupted bajada between the towns of Independence and Lone Pine (Fig. 2.1). Drainage basins supplying debris to the bajada extend 5-8 km from the fan heads to the range crest, cover 12-32 km^2, have total relief of 2-2.5 km, and stream gradients that increase from about 6° at the mountain front to greater than 30° in the headwaters. The bajada itself extends 10-12 km from the range-front and has a slightly concave upward longitudinal profile: surface gradients decrease linearly with distance from the range front but average about 4°. Transverse profiles are convex upward near the range front but are nearly flat farther downslope where adjacent fans have coalesced.

The bajada surface between Independence and Lone Pine (Fig. 2.1) was chosen for study because (1) this stretch of the piedmont is particularly well developed and fan morphology is not complicated by bedrock constrictions, volcanic activity, or complex foothill tectonics, and (2) the Quaternary history of fan aggradation on this part of the bajada is known (Gillespie, 1982; Bierman and others, 1991). Our field mapping was restricted to Late Wisconsin (Tioga, 15-18 ka) age surfaces (Gillespie, 1982) on two adjacent fans (Fig. 2.2). The Tioga surface is the youngest extensive surface on the bajada and offers the best preservation of the original depositional morphology.

Figure 2.2. Channel network on Pinyon and Symmes Creek fans. Channel patterns were traced from 1:24,000-scale aerial photographs and the distribution of major debris-flow snouts transferred from geomorphic maps prepared at a 1:3,000-scale. Insets show the locations of Figures 2.3a, 2.3b, and 2.7.

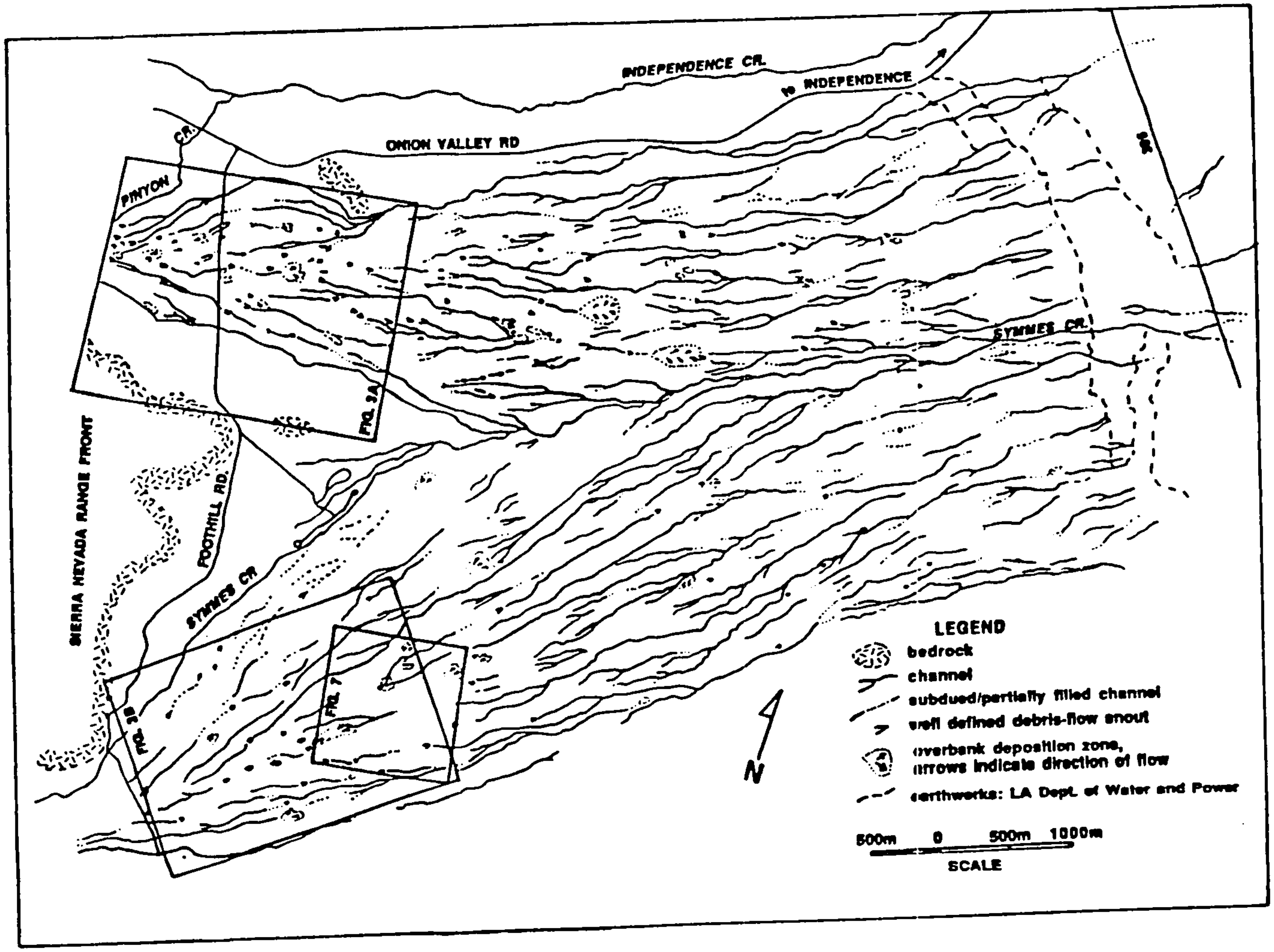
INDEPENDENCE CR.
to INDEPENDENCE
ONION VALLEY RD
395
PINYON CR.
SYMMES CR.
FIG. 3A
SIERRA NEVADA RANGE FRONT
FOOTHILL RD.
SYMMES CR
FIG. 3B
FIG. 7
N
LEGEND
bedrock
channel
subdued/partially filled channel
well defined debris-flow snout
overbank deposition zone, arrows indicate direction of flow
earthworks: LA Dept. of Water and Power
500m 0 500m 1000m
SCALE

Figure 2.3. (A) Geomorphic map of part of upper Pinyon Creek fan, showing the distribution of debris-flow snouts and levees, boulders, and channels on the fan surface.

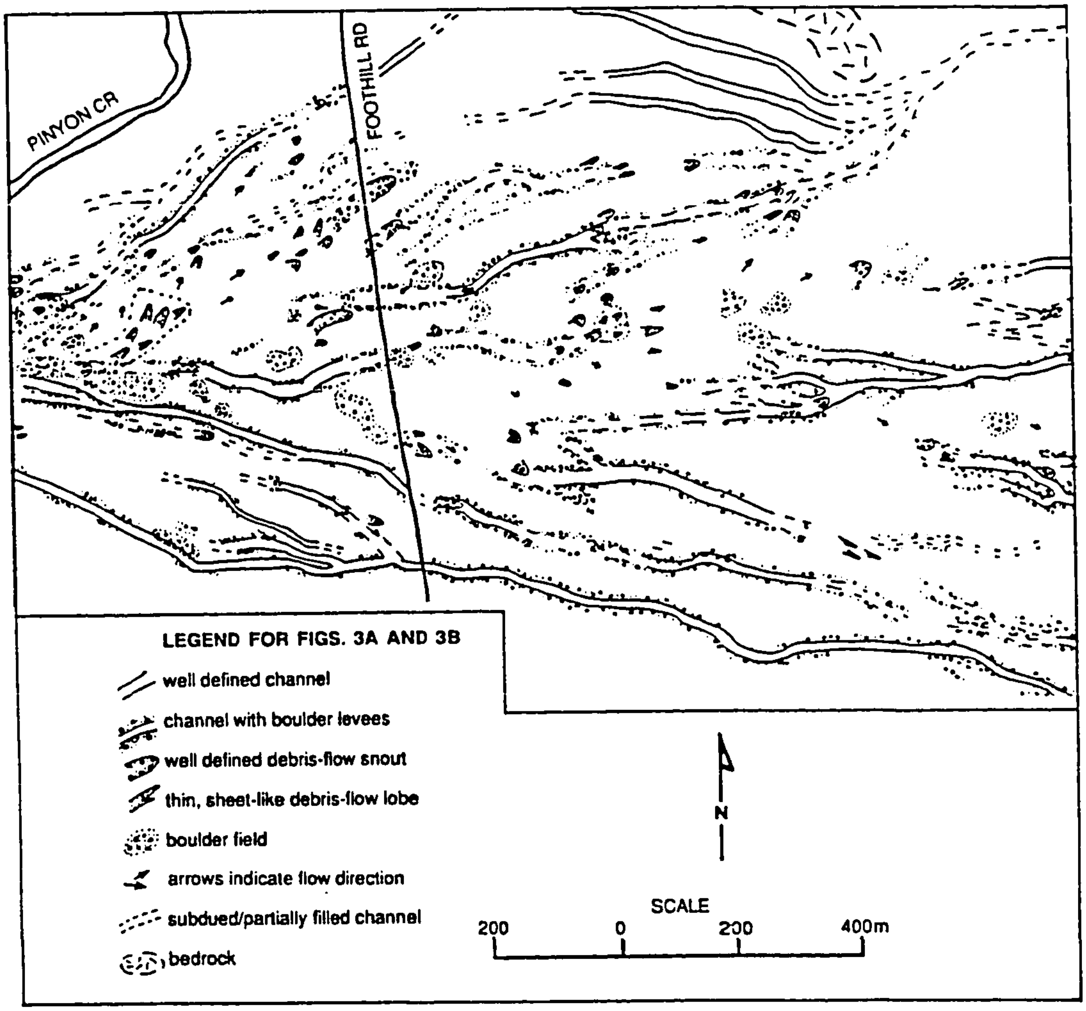
PINYON CR
FOOTHILL RD
LEGEND FOR FIGS. 3A AND 3B
well defined channel
channel with boulder levees
well defined debris-flow snout
thin, sheet-like debris-flow lobe
boulder field
arrows indicate flow direction
subdued/partially filled channel
bedrock
N
SCALE
200
0
200
400m

Figure 2.3. (B) Geomorphic map of part of upper Symmes Creek fan. The repeated pattern of channel blockage, up-fan aggradation and channel infilling, followed by channel diversion is seen on both maps and is characteristic of the upper two thirds of the bajada. The lower left portion of this map is covered by the stereo-pair of aerial photographs in Figure 2.7.

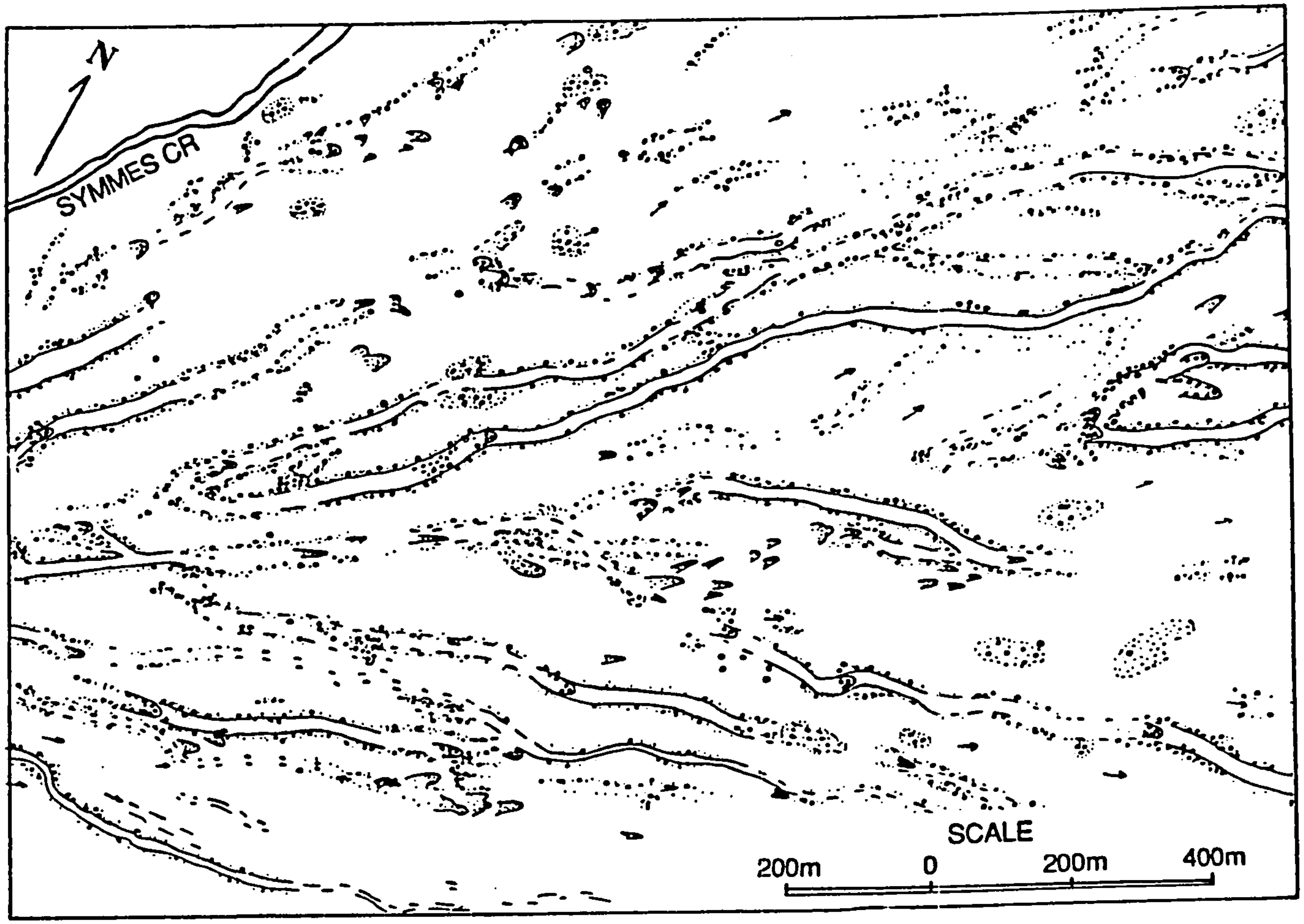
N
SYMMES CR
SCALE
200m
0
200m
400m

FAN MORPHOLOGY

The spatial distributions of channels, bouldery levees, boulder fields, and boulder-laced snouts or terraces were mapped in the field using aerial photographs, enlarged to 1:3000-scale, as base maps. The bajada surface has been smoothed on a centimeter-to-decimeter scale by the processes of soil creep, biogenic transport, slope wash, and rainsplash and thus some of the finer details of the original surface morphology have been degraded.

The bajada, which from a distance appears to have a smooth, unbroken surface, is found upon closer inspection to have an intricate, undulating surface marked by boulder-laced, lobate snouts or terraces and by channels lined with paired, narrow boulder levees formed by trains of boulders along the channel edge. The distribution, pattern, and spatial density of boulders, snout-nosed terraces, channels, and boulder levees all vary with distance from the range front. The upper reaches of the bajada (0-3 km from the range front), where surface gradients average about 5°, have a rough, boulder-strewn surface with overlapping bouldery terraces and many boulder-lined channels (Fig. 2.3). Local relief is typically 2-3 meters. The mid-fan reaches (3-7 km from the range front) have gradients of about 3°, smoother surfaces, fewer overbank debris-flow lobes, and a lower density of boulders; here, broad, smooth interfluves are cut by 1.5-2.5 m-deep channels with patchy boulder levees. Farther from the range front, distinct debris-flow lobes are less common and boulders are sparse on a very smooth, low-relief surface, interrupted only by subdued channels, often less than 1 m deep.

Individual debris-flow deposits on the upper and mid-fan portions of the bajada occur both on the open fan surface and in channels. Diffusive degradation of the fan surface may have obliterated the margins of thin, boulder-free overbank debris-flow deposits. Few of these could be mapped (Fig. 2.3). Mappable overbank deposits are preserved as flat-topped terraces or lobes which are commonly 20-30 m wide, 50-100 m long, and 1-2 m thick (Fig. 2.3), and are usually found immediately upslope of discontinuous channel segments. Boulder-rich deposits without distinct margins were mapped simply as "boulder fields" (Fig. 2.3) and may represent either partially buried or morphologically degraded overbank debris-flow lobes or boulders stranded in zones of decreasing flow depth (i.e., unconfined flow of mobile debris flows). Debris flows that

Figure 2.4. Debris-flow plug in a channel; photograph taken from the left bank of the channel, just downstream of the plug (figure to left of debris snout for scale).

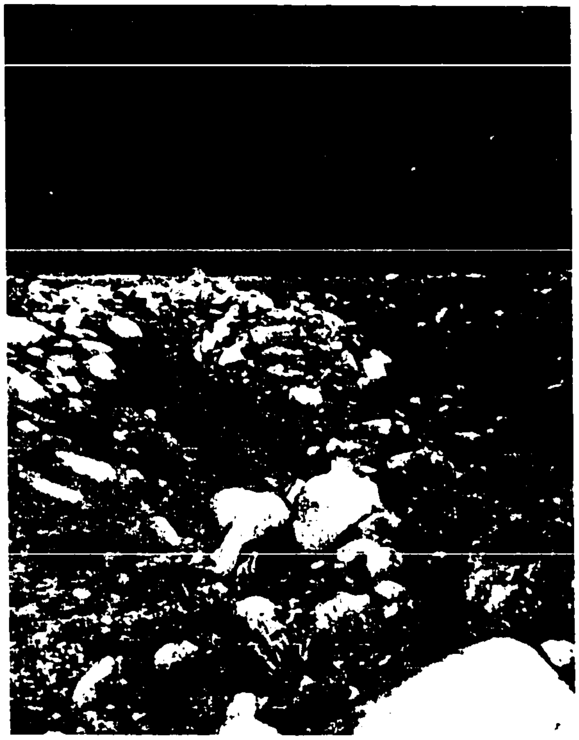

Figure 2.5. Channel on upper Pinyon Creek fan, typical of the bajada's abandoned channels and illustrating their broadly U-shaped cross-sectional morphology, the well developed paired boulder levees, and the smooth convergence of the levees with the adjacent fan surface. Channel is 20 m wide and 2 m deep. See figure 2.6B for a surveyed cross section.

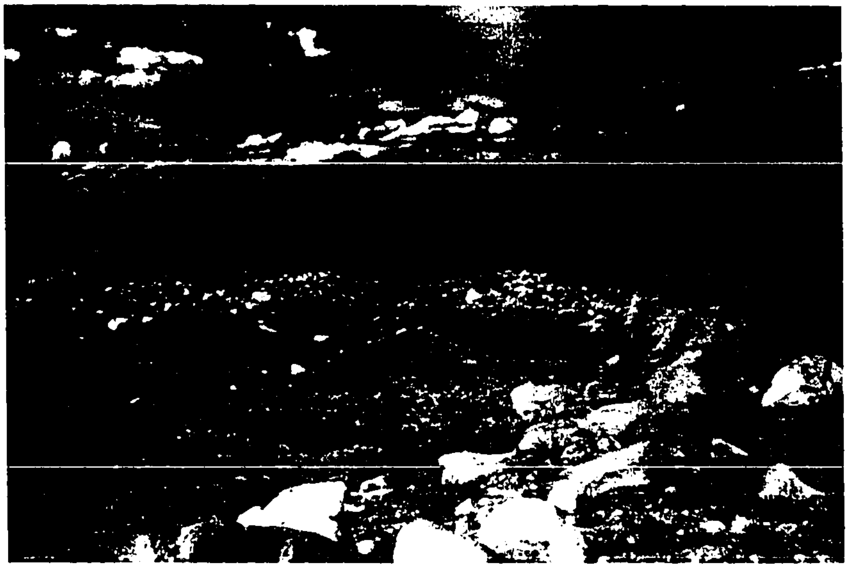

Figure 2.6. Surveys of representative channel cross sections, plotted at a 4x vertical exaggeration. For each channel, a survey immediately upstream of a debris-flow plug (triangles) is compared with a survey immediately downstream of that plug (squares). Width-to-depth ratios are indicated for each channel section. The steep-sided, flat-floored channel cross sections shown for comparison (dotted lines) are referred to in the discussion of channel formation (see also Fig. 2.9). (A) Deeply incised channel on upper Pinyon Creek fan. (B) Typical channel on upper Pinyon Creek fan. (C) Channel typical of the lower bajada (located 6 km from the range front).

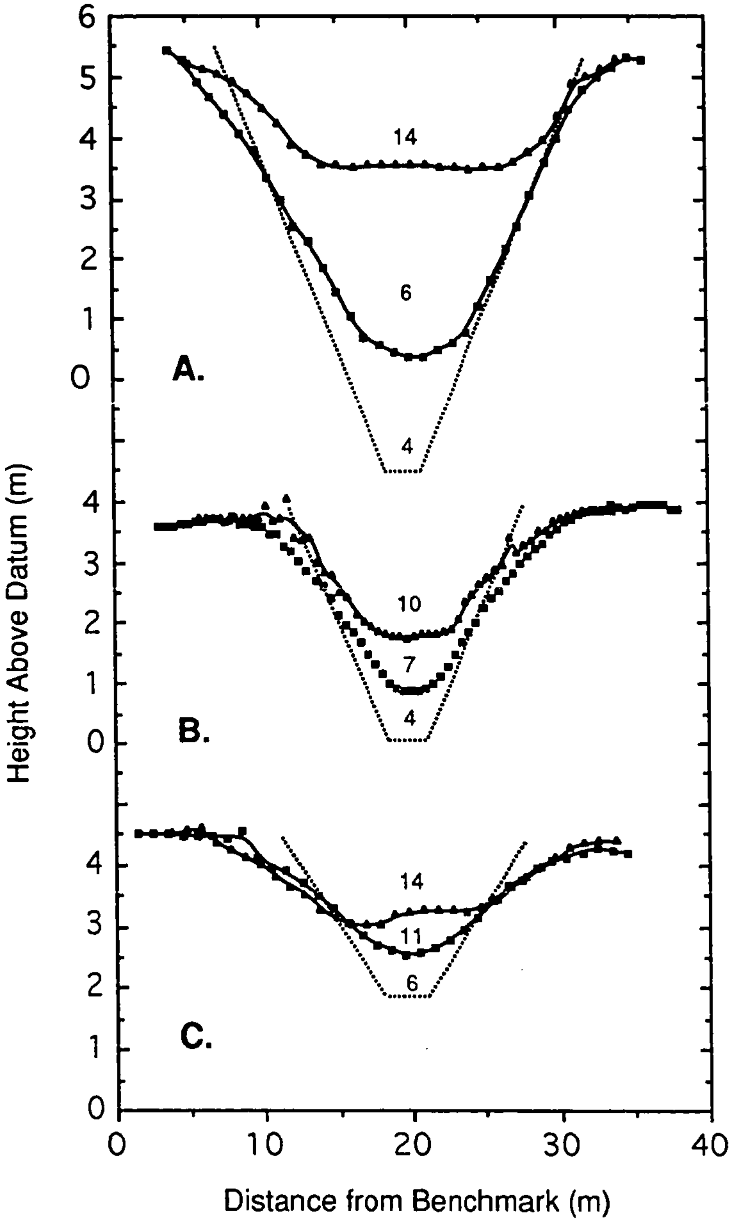

Height Above Datum (m)
6
5
4
3
2
1
0
14
6
4
A.
4
3
2
1
0
10
7
4
B.
4
3
2
1
0
14
11
6
C.
0
10
20
30
40
Distance from Benchmark (m)

Figure 2.7. Stereo-pair of aerial photographs of part of Symmes Creek fan (BLM Project CA01-77, Frames 1-35-7 and -8), illustrating the relationship between channels and the adjacent fan surface. Field of view is 1 km^2. North is to the right and flow from top to bottom. Orientation relative to field maps is shown on Figure 2.2. Several well defined debris-flow plugs are visible and can be seen to have blocked the channels. The topographic high upstream of the right-most channel is a direct result of channel blockage: local aggradation in the interim between channel blockage and the excavation of a new channel obliterates channel courses and adds to the topographic complexity of the upper slopes of the bajada.

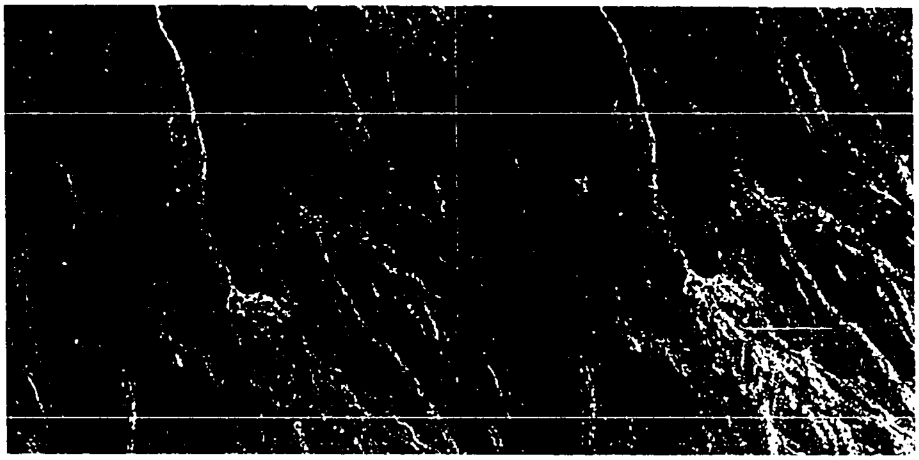

came to rest in channels are preserved as elongate plugs (Fig. 2.4) which block channels (Figs. 2.2 and 2.3).

Channels that cross the bajada are relatively straight, have broadly U-shaped cross sections, smooth floors, width-to-depth ratios ranging from 7 to 12, and gradually decrease in cross-sectional area down the fan (Figs. 2.5 and 2.6). Since their abandonment in late Wisconsin time, channel walls have been slightly degraded by slope processes and channel floors smoothed by the accumulation of a thin layer of colluvium, but, in essence, the channels preserve their original morphology (see below). The drainage system as a whole consists of a subparallel to dendritic network of discontinuous channels (Fig. 2.2) rather than the branching distributary network usually associated with alluvial fans (Denny, 1965; Bull, 1977). Although few channels can at present be traced to the fan apex, they do not head as gullies on the fan surface; the discontinuous channels have been buried from up-fan and abandoned (see Fig. 2.7). The distinctive network of discontinuous channels on the bajada reflects a suite of channel-shifting and fan-building processes which are different from those operating on alluvial fans, as recognized by Beaty (1970).

RELATIVE ROLES OF FLUVIAL AND DEBRIS-FLOW PROCESSES

The relative importance of fluvial and debris-flow deposition was determined on the basis of examination of surficial deposits and exposures of the fanglomerate over much of the bajada surface between Thibaut Creek and George Creek, and along Lone Pine Creek (Fig. 2.1) where channel incision has exposed extensive sections. Criteria used to distinguish debris-flow from fluvial deposits included: the presence of boulder-laced snouts and levees on the surface; matrix-supported structure of exposed sediments; poorly sorted textures, including a minimum of 5-10% silt and clay by weight; and the absence of stratification, rounding, or sorting of clasts (Sharp and Nobles, 1953; Bull, 1977). The fanglomerate is predominantly a matrix-supported diamicton with a gravelly, silty-sand matrix (Fig. 2.8) and we found no distinctively fluviatile sediments except along the eastern margin of the bajada (Fig. 2.8c) and in exposures along Lone Pine Creek where it crosses the Alabama Hills (see Trowbridge, 1911). Boulders with median diameters in excess of 1 meter are common within the diamicton, those larger than 5 meters across are rare. Although fluvial sedimentation has contributed little to the aggradation of most of the bajada, fluvial processes have

Figure 2.8. (A) Debris-flow deposit along the upper reaches of Symmes Creek, person for scale. Note the lack of sorting and stratification and the matrix-supported structure. (B) Debris-flow sediments exposed in a gully wall (1.5 m high for scale) on the lower portion of Symmes Creek fan.

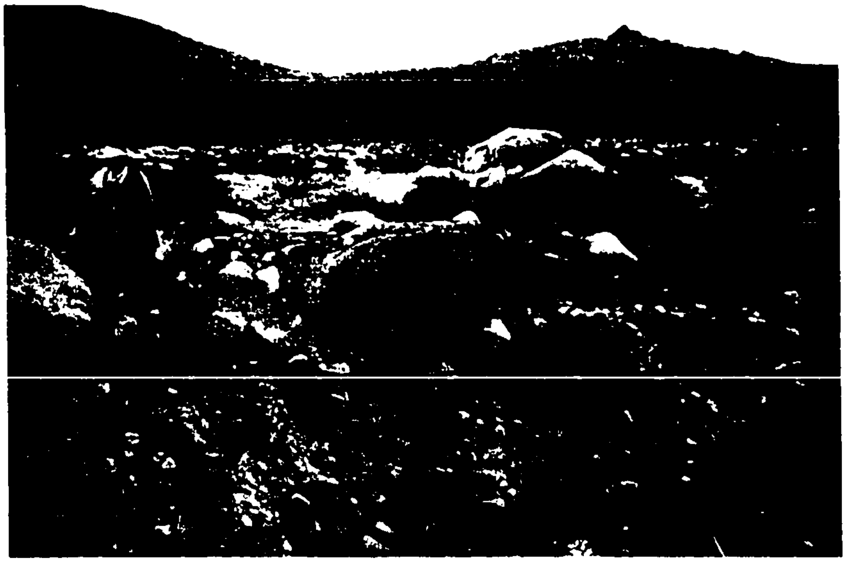

Figure 2.8. (C) Debris-flow overlying stratified fluvial sand and fine gravel in a gully immediately east of Highway 395 on Pinyon Creek fan (scale marked in decimeters).

Figure 2.9. Schematic illustration of channel modification by debris flows. Vertical exaggeration is 4x. (A) This sketch depicts a fluvial channel (w/d = 4) with an armored floor which has been exploited by one or more debris flows -- resulting in minor axial deposition (as explained by Johnson, 1970) -- but no significant in-channel deposition. Since abandonment, colluvium derived from the adjacent sidewalls has accumulated on the channel floor. Modified width-to-depth ratio is 6. (B) This sketch depicts the same channel, but this time partially filled by a debris-flow plug before abandonment. Modified width-to-depth ratio is 12.

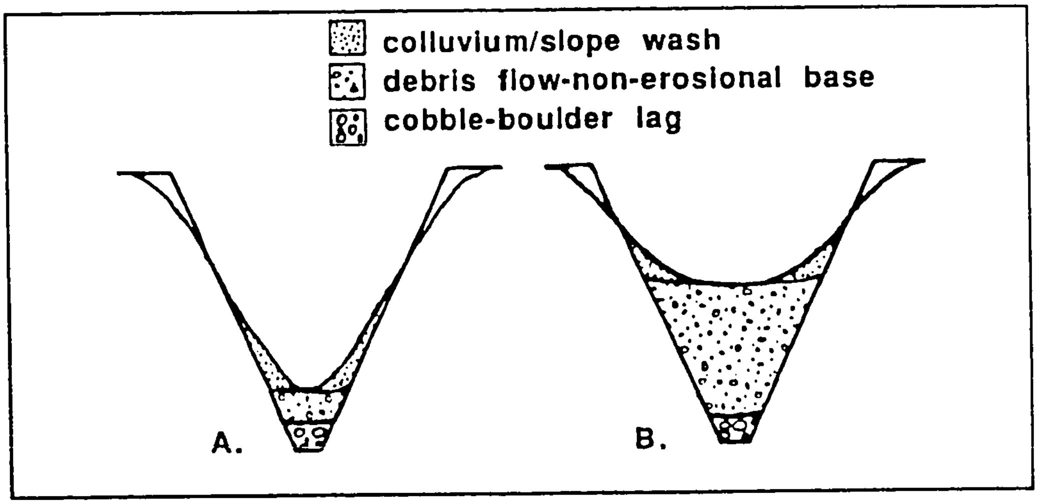
colluvium/slope wash
debris flow-non-erosional base
cobble-boulder lag
A.
B.

played a critical role in the construction of the fans by eroding channels through the debris-flow deposits (see below).

Channels on a debris-flow fan can be built by either (1) self-confinement of debris flows between their own levees or (2) channel scour by floodwaters or debris flows. The degree to which pronounced levee aggradation occurs varies between debris-flow fans (see Beaty, 1963; Whipple, 1991) and is controlled at least in part by the physical properties of the debris flows (see below; Whipple, in press). The relative importance of self-confinement of debris flows and channel scour, however, is easily discerned on the basis of cross-sectional morphology: self-confinement of debris-flows between steep-sided levees produces channels whose beds lie above the general elevation of the fan surface (Sharp, 1942, Fig. 2.2, p. 224).

The abandoned channels on the Owens Valley bajada (in contrast to those described by Sharp) are inset into the fan surface (Fig.s 2.5 and 2.6) and only short reaches of a few channels exhibit sharply defined levees. In some cases, as seen in Figure 2.7, channels on the upper slopes of the bajada run down the axes of broad topographic highs, indicating that overbank deposition has aggraded the adjacent fan surface and contributed to apparent channel entrenchment, in the manner described by Hooke (1967, p. 457-458). However, most of the channels have been produced dominantly by erosional processes and not by levee aggradation; channel morphology is everywhere consistent with partial infilling of originally steep-sided, V-shaped or flat-floored channels (Figs. 2.6 and 2.9). In addition, the general structure of the channel network is diagnostic of an erosional, rather than depositional, system: the network forms a sub-parallel to dendritic pattern (Fig. 2.2). Whether channels were excavated by debris-flow or fluvial scour, however, can not be determined on the basis of cross-sectional morphology. Observations of the erosional potential of modern debris flows must be used to address this important issue.

Field observations in Owens Valley and elsewhere indicate that debris flows can not have contributed significantly to channel scour on the moderate slopes of the bajada. Channels exploited by debris flows within the past decade (three on the western and two on the eastern slopes of Owens Valley) show no sign of scour by the debris flows. Vegetation is flattened and stripped of bark, but channel bed elevation is unchanged except where incised by subsequent stream flows. Similar conclusions about the geomorphic role of debris flows on fans have been reached by many investigators (e.g., Blackwelder, 1928; Beaty, 1963; Hooke, 1987). Moreover, Pierson

(1980), Okuda and others (1980), and Suwa and Okuda (1980) have documented that scour gives way to deposition on slopes of 6-8° for debris flows with flow depths, and thus basal shear stresses, comparable to those in Owens Valley. Thus we conclude that the channels of the Owens Valley bajada were cut by streams and not by the debris flows themselves.

DEBRIS-FLOW PROCESSES AND FAN SURFACE MORPHOLOGY

Some debris flows come to rest after only a short transport distance, freezing on the relatively steep slopes (4-6°) of the fan head as sharply defined lobes and channel plugs. Other debris flows traverse the entire length of the fan, eventually spreading as thin, tabular deposits on the gentle slopes (1-2°) of the bajada margin. Similar observations have been made on many debris-flow fans (e.g., Blackwelder, 1928; Sharp and Nobles, 1953; Beaty, 1963; Johnson, 1984). Because the spatial pattern of debris-flow deposition in part controls the morphology of the fan surface, it is useful to explain the down-fan segregation of these two types of debris flows.

Textural Analysis of Debris-flow Deposits

Textural analyses were conducted to determine whether sedimentological variability is an important factor in the mobility of the Owens Valley debris flows. Clasts in exposures were point-counted to characterize the coarse fraction (clasts coarser than 32 mm) of the deposits. Samples (2-3 kg each) of the matrix (defined as material finer than 32 mm) were sieved to characterize the finer fraction.

The results of point counting, augmented by visual estimates of the percentage of cobbles and boulders in many additional exposures, indicate that the Owens Valley debris-flow deposits are matrix-rich, with clasts in excess of 32 mm in diameter comprising 30-40% of the volume of the proximal and mid-fan deposits (Fig. 2.8a), and 10-20% of the finer-grained distal deposits (Fig. 2.8c). Concentrations of up to 60-80% coarse clastic material occur locally in levees and on the margins of debris-flow snouts (see Fig. 2.4).

Sieve analyses show that there is little variability in the matrix portion of different debris-flow deposits (Table 2.1). The matrices of all debris-flow deposits sampled are very poorly sorted (σ_ϕ = 2.1 - 3.3), and are comprised of 30-55% angular gravel, 40-60% sand, and 7-12% silt-and-clay by weight. The consistent composition of the matrix fraction of debris-flow deposits from all parts of the fan, particularly in

Table 2.1. Summary of Sieving Analyses

	Runout distance (km)	Mean grain size (mm)	Sorting (phi)	Silt-and-clay (%)
Debris flows				
	0.9	1.1	3.0	8.8
	1.0	1.0	3.0	11.1
	1.3	0.9	2.9	7.5
	1.3	0.8	2.9	10.3
	1.7	0.5	2.8	12.2
	2.1	0.5	3.3	18.8
	2.1	0.7	2.7	11.5
	2.4	1.3	2.7	5.3
	2.5	0.8	2.8	10.7
	2.7	1.1	2.7	7.9
	2.9	1.0	2.8	9.1
	4.4	1.4	2.1	4.2
	8.5	1.0	2.7	7.9
	8.5	1.0	2.6	8.7
	8.5	0.8	2.5	9.2
	8.5	0.9	2.5	7.2
	8.5	0.7	2.9	14.0
	8.9	1.2	2.7	8.3
Fluvial Samples				
	--	1.1	1.3	1.5
	--	1.1	1.7	1.4

terms of their silt-clay content (Table 2.1) implies that textural variability has not strongly influenced depositional patterns on the Owens Valley bajada.

Rheological Analysis of Debris-Flow Deposits

Motivation

The rheology of debris flows has received much attention (see reviews by Takahashi, 1981; Costa, 1984; and Iverson and Denlinger, 1987), and a wealth of estimates of rheological parameters has been published (e.g., Pierson, 1980, Table 2, p. 244; Fink and others, 1981; Costa, 1984, Table 1, p. 272; Johnson, 1984, Table 8.1, p. 294; Major and Voight, 1986). However, with the exception of work by Suwa and Okuda (1983) in Japan, previous studies have not attempted to use the study of debris-flow rheology to address the formation of debris-flow landforms. In this study, we draw upon current understanding of debris-flow rheology (e.g., Johnson, 1970; Fairchild, 1985; Major and Pierson, 1990; in press; Phillips and Davies, 1991; Whipple, in press) to elucidate quantitatively the controls on (a) debris-flow deposition and (b) the confinement of debris flows within channels. Both aspects of the debris-flow runout problem (controls on deposition and confinement) are important because a debris-flow entering a channel from the mountain front will remain mobile until the combination of its depth and the channel gradient require the cessation of flow (see below). The depth of a given flow is maintained by flow confinement between channel banks, and therefore an important control on runout distance is the degree to which a debris flow is confined within the channel and the degree to which it is allowed to spread overbank, thin, and deposit (Johnson, 1984; Hooke, 1987).

Theory

Debris flows involve the rapid downslope translation of poorly sorted debris admixed with a small amount of water, typically 10-25 % by weight (Pierson, 1986). Debris flows like those in Owens Valley are matrix-rich, with a dominantly granular matrix containing about 10% silt and clay by weight. The silt-clay fraction is critical to retention of water within the slurry and, hence, is the most important textural control on flow mobility.

Deformation of debris slurries under shear involves a complex suite of grain-grain and grain-fluid interactions and is governed by both frictional and viscous forces (Savage and Sayed, 1984; Iverson and Denlinger, 1987; Iverson and LaHusen, 1989). However, on a macroscopic scale the dynamic response of debris slurries to an applied shear stress can be modeled as that of a non-Newtonian continuum with the properties of yield strength and viscosity. Although both the yield strength and viscosity may vary with sediment concentration (C_S), grain-size distribution (GSD), clast angularity and roughness, clay mineralogy, effective normal stress, strain rate, and strain history, to a first order approximation C_S and GSD are the dominant variables (see below). Consequently, many hydrodynamic attributes of debris slurries and some important characteristics of their deposits can be accounted for with relatively simple constitutive equations.

For the purpose of this study, the visco-plastic, or Bingham, flow law proposed by Johnson (1970) is taken as an adequate description of debris-flow dynamics. In one-dimensional form, the visco-plastic flow law is:

$$\tau_{zx} - \tau_o = \mu \frac{du}{dz}\ ; \qquad \tau_{zx} > \tau_o \tag{2.1a}$$

$$\frac{du}{dz} = 0 \qquad ; \qquad \tau_{zx} \leq \tau_o \tag{2.1b}$$

where (τ_{zx}) is the driving stress, (τ_o) is the yield strength, (μ_B) is the viscosity, and (du/dz) is the velocity gradient. In the discussion below we constrain yield strength and viscosity to be constant in any given debris flow, but to vary with the physical composition of the debris-flow, as observed in laboratory and field studies.

Laboratory studies have documented a dependence of yield strength and viscosity on debris-flow texture and sediment concentration (Fairchild, 1985; O'Brien and Julien, 1988; Phillips and Davies, 1991; Major and Pierson, 1990; in press). In general these studies have shown that: 1) for a given grain-size distribution, yield strength and viscosity are correlated with one another and with sediment concentration; 2) both yield strength and viscosity increase by over an order of magnitude over a narrow range of sediment concentration; 3) for a given water content, flows with a larger proportion of fines have higher yield strengths and apparent viscosities. The latter statement is a little misleading, however, because slurries of finer-grained material typically hold more water than more granular slurries. As a consequence, slurries with the greatest proportions of silt and clay usually have the lowest yield strengths and viscosities and are generally more mobile.

Methods

Prediction of debris-flow runout patterns requires that the yield strenghts and viscosities of the debris flows be known. The late Wisconsin age of the fan surfaces studied precludes detailed rheological analyses of the debris-flow deposits: the degree of deposit preservation on these surfaces permits estimation of flow yield strengths but not viscosities. As this is not sufficient to fully develop the rheological controls on fan surface morphology, Whipple (1992) conducted a companion study of well-preserved modern debris-flow deposits on the Black Canyon fan just north of Independence (Fig. 2.1), and documented a correlation between yield strength and viscosity. The reported correlation is used here to complement field estimates of yield strength in a quantitative description of the rheological variability recorded in the fan deposits.

Johnson (1970; 1984) outlined field methods for estimating the yield strength of debris flows from their deposits. At the instant of deposition, the yield strength of a visco-plastic material must be equal to the basal shear stress ($\tau_o = \tau_b$). Assuming conditions of steady, uniform, gravity-driven flow, the basal shear stress is given by:

$$\tau_b = \rho_b g h \sin\theta = \tau_o \ , \qquad (2.2)$$

where ρ_b is the bulk density, h is flow depth, θ is the surface slope of the flow, and the equivalence on the right-hand side indicates the condition for deposition. Equation (2.2) is best applied to debris deposits on planar surfaces and Johnson (1984) has derived another relationship for channelized flows:

$$\tau_o = \frac{\rho_b g d_c \sin\theta}{(2d_c/w_c)^2 + 1} \qquad (3.2)$$

where w_c and d_c are the critical width and depth at which channelized flow ceases, and where the magnitude of the denominator scales with the relative importance of sidewall to channel floor drag. Thus an estimate of yield strength can be derived from field surveys of deposit geometry and an estimate of bulk density.

Thickness and surface slope were measured for all well-preserved overbank debris flow lobes, as were depth, width and surface slope for all well-preserved channel plugs. Bulk density was estimated following a procedure outlined by Johnson (1984) in which debris is reconstituted in the laboratory to its approximate original water content. The bulk density estimate depends partly on estimates of the volumetric concentration of coarse debris (V_C) (< 32 mm) obtained by point counting. However, the density of the reconstituted matrix (~ 2.1 g/cm^3) is close enough to that of granitic

Figure 2.10. Yield strength estimates from debris-flow deposits on Pinyon and Symmes Creek fans plotted as a function of runout distance, measured in km radially from the apex. The upper envelope of yield strength estimates represents the rheological limitation on flow runout distance.

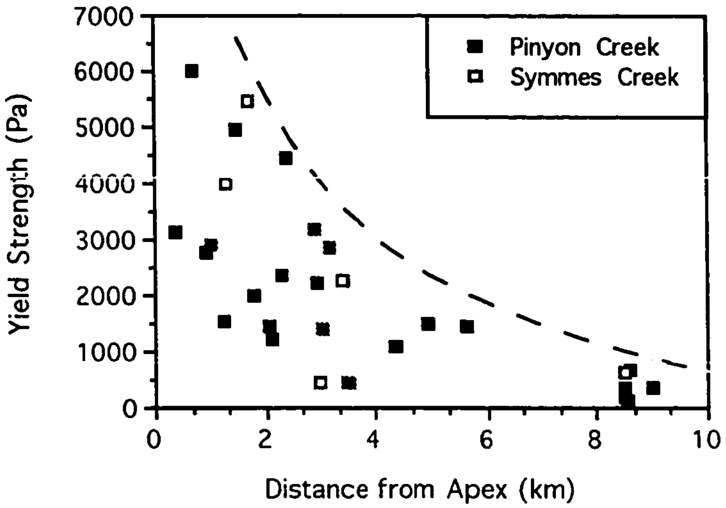

Yield Strength (Pa)
7000
6000
5000
4000
3000
2000
1000
0
0
2
4
6
8
10
Distance from Apex (km)
■ Pinyon Creek
□ Symmes Creek

Figure 2.11. Estimated yield strength plotted against percentage of silt-and-clay in the matrix for all debris-flow deposits for which sieve analyses are available. No overall correlation is evident. Triangles represent debris-flow deposits at the distal margin of the bajada and suggest a second-order correlation with silt-clay content.

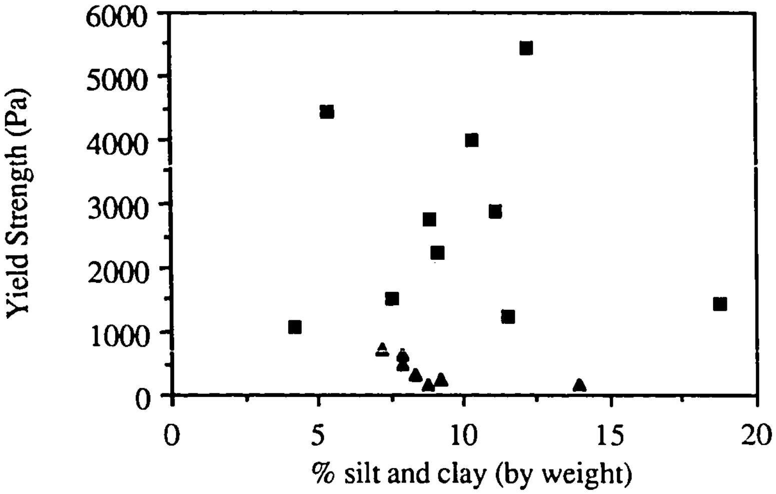
Yield Strength (Pa)
6000
5000
4000
3000
2000
1000
0
0
5
10
15
20
% silt and clay (by weight)

Table 2.2. Debris Flow Rheology

Runout (km)	Slope (%)	Thickness (m)	Width/Depth (m)	Yield Strength (Pa)
0.36	7.9	1.5 - 2.0	--	3120
0.67	9.4	--	32 / 3.0	6000
0.90	10.5	1.2 - 1.3	--	2900
0.94	7.0 - 7.7	--	13 / 1.5 - 2.3	2770
1.25	7.9	0.8 - 1.0	--	1530
1.30	9.0	--	30 / 2.0 - 2.2	4000
1.46	9.5	--	14 / 2.8	4940
1.70	8.0	--	30 / 3.0 - 3.6	5450
1.78	7.3 - 8.7	1.2	--	1980
2.06	7.0 - 8.7	0.9	--	1450
2.11	8.0	0.5 - 1.0	--	1240
2.28	11.4	1	--	2350
2.40	9.6	2.2	--	4450
2.88	8.0	2.0 - 2.2	--	3180
2.93	7.0	--	13 / 1.5 - 1.8	2230
3.05	8.0	0.8 - 1.2	--	1400
3.15	8.0		10 / 1.9	2850
3.40	6.0 - 12.0	1.0 - 1.3	--	2260
3.48	7.0	0.3	--	450
4.00	4.5	0.5	--	460
4.37	6.6	0.7 - 1.0	--	1090
4.97	6.5	--	9 / 1.2	1500
5.66	5.2	--	9 / 1.5	1440
8.50	1.9	0.45	--	180
8.50	1.8	0.6	--	220
8.50	1.8 - 2.6	0.2 - 1.0	--	350
8.50	4.9 - 5.2	0.6	--	625
8.52	1.8 - 2.1	0.35	--	140
8.60	3.5	0.75 - 1.2	--	700
8.90	2.1-2.6	0.6	--	300

boulders (~ 2.7 g/cm^3) that the total bulk density is not sensitive to errors in V_c; it was taken as 2.1 g/cm^3 for boulder-poor deposits and 2.3 g/cm^3 for boulder-rich deposits.

Results

Equations (2.2) and (2.3) were used to estimate yield strength for 38 well-defined debris-flow lobes on Pinyon Creek and Symmes Creek fans. The results of the analysis are compiled in Table 2.2. Sources of error include estimation of bulk density (±10%), measurement of deposit thickness (±5%), measurement of surface slope (±10%), and deviations from the ideal conditions assumed in equations (2.2) and (2.3). Measurement uncertainties alone are responsibe for a possible ± 15% error in yield strength estimates.

Runout distances of debris flows on the bajada are roughly correlated with estimated yield strength (Fig. 2.10). Debris flows with the highest yield strengths are limited to the upper reaches of the bajada and only the low-yield-strength debris flows are capable of reaching the bajada margin, as anticipated by Johnson (1984) and Hooke (1987). However, a low-yield strength debris flow which encounters a channel blocked by previous in-channel deposition is forced overbank where it spreads laterally, thins, and halts, regardless of position on the fan. Overbank flow and deposition also occur wherever peak discharge exceeds the conveyance capacity of unblocked channels. Thus, depending on the peak flow rate and the geometry of the fan surface, a low-yield-strength debris flow may deposit on any part of the fan; the greater scatter amongst the short-run debris flows in Figure 2.10 is a result of these factors. On the other hand, the upper envelope defined by the data in Figure 2.10 represents the maximum potential run-out distance of a flow with a given yield strength, as constrained by the gradual downfan decrease in fan slope and channel depths.

Interpretation

The rheological variability documented in Table 2.2 is interpreted to result dominantly from variations in sediment concentration. The observed variability in silt and clay content is of sufficient magnitude to influence flow mobility (Fairchild, 1985; O'Brien and Julien, 1988; Phillips and Davies, 1991; Major and Pierson, 1990; in press), but there is no systematic or fan-wide correlation between percentage of fines and either flow runout distance or estimated yield strength (Table 2.2, Fig. 2.11). Data on a suite of debris-flow deposits at the bajada margin (triangles in Fig. 2.11) suggest a second-order dependence of flow mobility on matrix GSD. This second-order effect, however, apparently has had little influence on the general pattern of debris-flow deposition. Thus, in so far as the mobility of a debris flow is governed by the properties of its matrix, it may be inferred that variable sediment concentration and therefore water content, rather than grain-size composition, has been the most important (first-order) control on flow mobility.

The mobility of matrix-supported debris flows is controlled dominantly by matrix properties and differences in the precentage of coarse material are almost certainly less important than variations in sediment concentration. Although a greater percentage of large clasts (< 32 mm) was observed in deposits on the upper fan, those deposits are matrix-supported (Fig. 2.8) and interlocking of the larger clasts is unlikely to have greatly influenced flow mobility, except perhaps at bouldery fronts and margins (Pierson, 1986). Even so, frictional resistance at the flow front is unlikely to influence the mobility of the main body of a debris flow unless it is already moving slowly and decelerating (see footage in Costa and Williams, 1984). Thus, only in the final stages of debris-flow deposition is a concentration of boulders at the flow front likely to enhance the effective yield strength and viscosity of the flow. In this paper, we ignore this late-stage effect and concentrate only on the dominating influence of the sediment concentration in the main body of the debris flow. In general, our arguments about the controls on debris-flow deposition are not significantly affected by this simplification, only the specific details of the frequency distribution of debris-flow rheologies delivered to any fan (see later) will be altered by considering the secondary influence of the presence or absence of a bouldery frontal bore.

Rheological Constraints on Channel Conveyance Capacity

Motivation

Where debris-flow runout is significantly influenced by the channel system, as documented earlier for the Owens Valley bajada (Fig. 2.3), it is useful to quantify the influence of the channels on debris flow runout patterns in terms of the physical properties of the debris flows, such as their rheology and peak discharge. These are the most relevant properties because the degree to which debris flows are confined within channels and conveyed farther down-fan depends on the relative magnitudes of the peak discharge and the conveyance capacity of the channel, which is a function of flow rheology as well as channel size and gradient. Therefore, we have analyzed the relationship between flow rheology and channel conveyance capacity.

Methods

We use the visco-plastic model (equation 2.1) to calculate channel conveyance capacity as a function of flow rheology and distance down-fan. The analytical approach is simple but results in a reasonable approximation of the relationship between channel conveyance capacity and debris flow rheology (see below). The size and geometry of the channels as a function of distance down-fan is constrained by field surveys of representative channel cross sections. The rheology of the debris flows, as a function of sediment concentration, is constrained by data on modern debris flows in Owens Valley (Table 2.3; Whipple, 1992) which document a correlation between yield strength and viscosity for a series of flows with similar grain-size distributions. Coupled with the range of yield strengths estimated on the basis of field measurements (Table 2.2), this correlation is taken to describe, to first order, the rheological variation characteristic of the debris flows of the Owens Valley bajada.

Bankfull discharges of debris flows with a range of yield strengths and viscosities were calculated for channel cross sections and gradients characteristic of the upper, middle, and lower reaches of the bajada (see Fig. 2.6). Steady uniform flow through straight channels was assumed. The channel cross-section was divided into a series of 1m-wide vertical sections and independent one-dimensional solutions were obtained for each section. The discharge through each meter-wide increment of the channel cross section (q_i) is obtained by solving the visco-plastic constitutive equation (1) for the velocity gradient (du/dz) and twice intergating over the flow depth (h) (see Johnson, 1970, p. 503):

$$q_i = \frac{1}{2}\left\{\frac{1}{\mu_B}\rho_b g \sin\theta\left[0.67 h_d^3 + h_d^2(h - h_d)\right]\right\} \qquad (2.4)$$

where h_d is the thickness of the deforming region, which is a function of the yield strength and is determined by application of equation (2.2) ($h_d = h - \tau_o/\rho_b g \sin\theta$). Discharges determined with equation (2.4) were summed across the channel to estimate the total bankfull discharge, which is taken as an estimate of the channel conveyance capacity.

This method of calculation ignores the lateral stresses between adjacent sections and therefore creates an artificial condition in which the non-deforming "plug" deforms in the cross-stream direction (only), greatly simplifying the calculations but surpressing the importance of sidewall drag. As a result, the estimates of bankfull discharge presented below are somewhat overestimated. However, debris flows have some

Table 2.3. Rheologic Parameters: Black Canyon, California

Debris-Flow Surge	Cross-sectional Area (m^2)	Average Velocity ($m\ s^{-1}$)	Peak Discharge ($m^3\ s^{-1}$)	Yield Strength (Pa)	Bingham Viscosity (Pa s)	Newtonian Viscosity (Pa s)
83-II*	56	7.8	435 ± 15	2150 ± 150	430 ± 50	1000
83-IIIa'	19	5.2	95 ± 15	540 ± 30	380 ± 70	550
83-IIIb'	13	6.0	75 ± 12	540 ± 30	180 ± 45	290
83-IV	6	4.8	22 ± 8	300 ± 45	30 ± 15	60
90-I	13	5.2	68 ± 10	340 ± 80	225 ± 75	280
90-II	2	4.5	8 ± 1	80 ± 35	18 ± 3	22

* No estimates available for pulse 83-I.

' Estimates a & b for pulse 83-III taken at different locations.

Figure 2.12. Conveyance capacities calculated for channels representative of the uppermost (ca. 1 km down-fan), middle (ca. 3 km), and lower fan (ca. 6 km) are shown in (A) as functions of rheology (sediment concentration). Yield strength and viscosity are correlated as constrained by data in Table 2.3 (Whipple, 1992), and are related to "relative sediment concentration" as follows: "low" = $\tau_0 < 1000$ Pa, $\mu_B < 300$ Pa-s; "high" = $\tau_0 > 3000$ Pa, $\mu_B > 500$ Pa-s. Channels used in the calculations have cross-sectional areas of 31, 24, and 20 m^2, and gradients of 0.087, 0.070, and 0.052, for the upper, middle, and lower fan respectively. (B) Results of calculations from (A) re-scaled to emphasize the gradual down-fan decrease in channel capacity for debris flows with "low" and "intermediate" sediment concentrations.

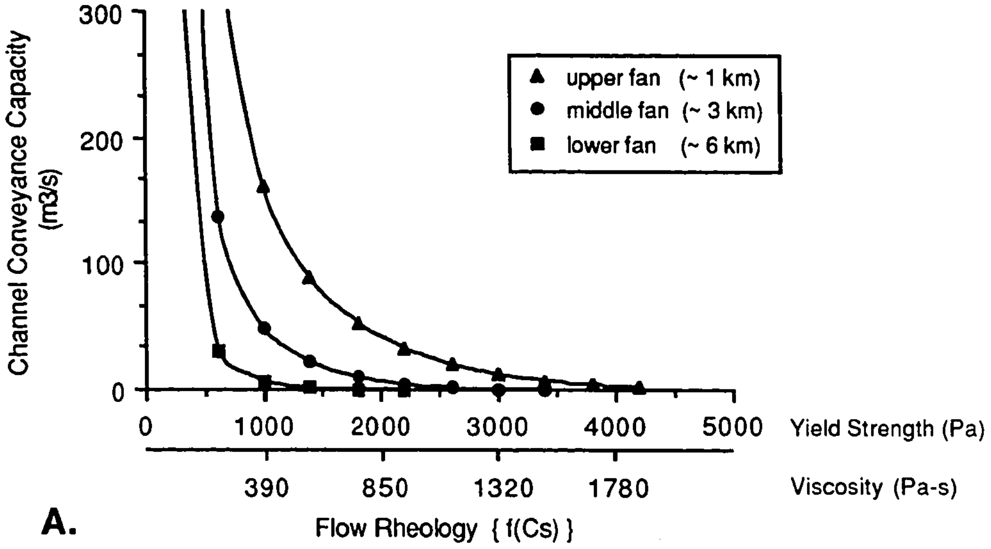
Channel Conveyance Capacity (m3/s)
300
200
100
0
upper fan (~ 1 km)
middle fan (~ 3 km)
lower fan (~ 6 km)
0
1000
2000
3000
4000
5000
Yield Strength (Pa)
390
850
1320
1780
Viscosity (Pa-s)
Flow Rheology { f(Cs) }

A.

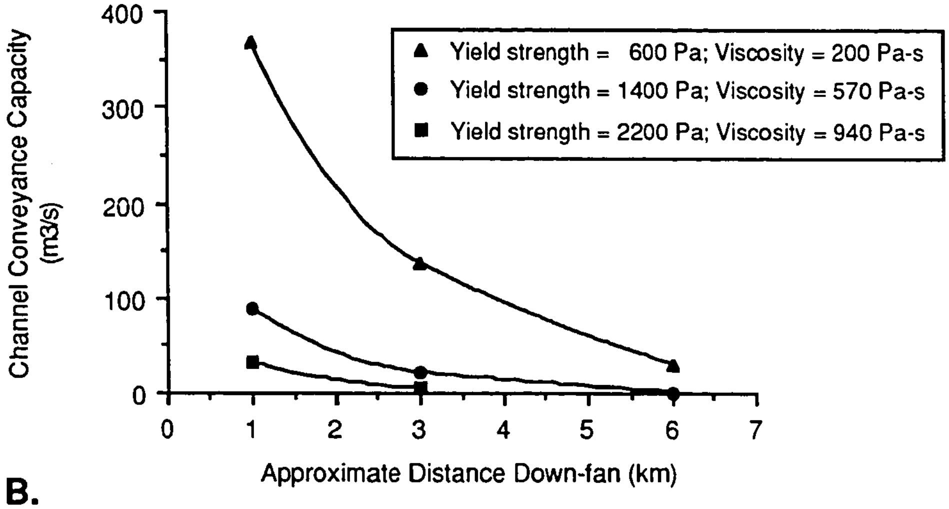
Channel Conveyance Capacity (m3/s)
400
300
200
100
0
Yield strength = 600 Pa; Viscosity = 200 Pa-s
Yield strength = 1400 Pa; Viscosity = 570 Pa-s
Yield strength = 2200 Pa; Viscosity = 940 Pa-s
0
1
2
3
4
5
6
7
Approximate Distance Down-fan (km)

B.

capacity for self-confinement (Sharp, 1942) and bankfull discharge is in fact a minimum estimate of the true conveyance capacity of a channel. Furthermore, from a more sophisticated analysis presented by Whipple (1992), it is known that for the broad channels of the bajada the one-dimensional analysis only overestimates the discharge by 15 - 50 %, with the greater errors occurring for higher values of the yield strength. The weak dependence on flow yield strength implies that channel conveyance capacity will be slightly more sensitive to changes in flow rheology than indicated in the calculations presented below. However, this effect is minimal and the predicted sensitivity of channel conveyance capacity to variations in flow rheology or to changes in channel size and slope is not significantly affected by the above simplification of the open-channel flow problem.

Results

Channel conveyance capacity varies non-linearly with flow rheology (Fig. 2.12a), and declines steadily down-fan as channel gradient and size diminish (Fig. 2.12b). Low-sediment-concentration debris flows travel farther downfan than high-sediment-concentration flows because (a) the have lower yield strengths, and (b) their lower yield strengths and viscosities allow them to remain confined within channels for a greater distance down-fan. This interaction causes a greater down-fan segregation of debris-flows according to rheology than anticipated on the basis of yield strength alone. However, because channel size and gradient decline with distance down-fan, unless flow volume is consumed by deposition on channel floors, even the most mobile debris flows eventually spill overbank and spread on the fan surface.

According to Figure 2.12, flows with peak discharges less than or equal to the conveyance capacity of a channel remain fully confined and are translated farther down-fan without significant flood-peak attenuation. Flows with peak discharges in excess of channel conveyance capacity lose part of their volume overbank with consequent flood-peak attenuation. That portion of a debris flow which is forced overbank spreads laterally, thins, and deposits. Near-zero values (< 25 m^3/s on Fig. 2.12) of the calculated bankfull discharge, therefore, indicate imminent deposition of all debris flows, regardless of peak discharge. This follows because flows with peak discharges upto the bankfull value are approaching the critical flow depth and will soon freeze as channel plugs, and flows with greater peak discharges will be forced overbank where deposition will likewise occur. The very low conveyance capacities of channels for high-sediment-concentration debris flows therefore anticipates their propensity for blocking channel courses.

DISCUSSION

Patterns of deposition by debris flows with variable rheologies, volumes, and hydrographs produce the surface morphology of debris-flow fans. Variations in the physical properties of the debris flows delivered to any given fan arise from a combination of (1) differing initiation mechanisms (Fairchild, 1987), (2) differences in water content at time of failure, (3) differences in the GSD of the source regolith, and (4) varying degrees of dilution of the debris flows by incorporation of floodwaters while in transit to the fan head (see Pierson and Scott, 1985). These variations can be described statistically as a frequency distribution of debris-flow rheologies, volumes, and hydrographs at the fan head. The rheological analysis presented above allows us to describe, albeit qualitatively, the dependence of depositional morphology on the frequency distribution of debris-flow properties. In order to facilitate this discussion, we consider the morphological consequences of deposition by the two endmembers of the possible suite of debris-flow rheologies: "high-sediment-concentration" debris flows (high-C_S flows) and "low-sediment-concentration" debris flows (low-C_S flows). Although many debris flows exhibit surging behavior characterized by spatially variable sediment concentrations (highest at the flow front and progressively lower towards the tail) (Pierson, 1984; 1986), in the discussion that follows we treat the high-C_S and low-C_S surges conceptually as separate events.

High-Sediment-Concentration Debris Flows

High-C_S debris flows are only mobile on relatively steep slopes. They overtax the conveyance capacity of even steep channels on the upper part of the fan (Fig. 2.12), and either freeze as lobate snouts a short distance after overtopping channels or freeze within channels as elongate plugs, depending on whether their peak discharge exceeds the conveyance capacity of the channel or not. Their deposits are generally limited to the upper reaches of the bajada where slopes exceed 4.5°. The rough, undulating surface of the upper reaches of the bajada results from repeated and overlapping deposition of such flows. High-yield-strength flows have great boulder-transporting competences (Rodine and Johnson, 1976) and the boulder-laced character of their deposits augments the rough appearance of the upper reaches of the bajada. Many of the "boulder fields" mapped on the upper reaches of the fans represent degraded or partially buried accumulations of high-C_S debris-flow deposits within which individual flow boundaries could not be reliably demarcated in the field.

Mappable overbank lobes of high-C_S flows are rare except near the fan head and debris-flow deposition is largely directed by the channels (Fig. 2.3). The channels themselves, however, are often blocked by deposition of high-C_S debris flows, which plays an important role in the long-term evolution of the channel system and in the dispersal of debris-flow sediments across the fan. In many cases the upstream ends of discontinuous channel segments are marked by well-defined debris-flow lobes (Figs. 2.2, 2.3 and 2.7). In other cases, abandoned channels have been buried from up-fan but no distinct debris-flow snout could be identified in the field and thus does not appear on the geomorphic maps. We infer that new channels are cut in response to channel blockage by high-C_S debris flows; floodwaters are diverted around recently deposited debris-flow plugs and avulsion of the channel results. Thus, the network of sub-parallel abandoned channels arises from repeated avulsions of a single channel, driven by deposition of high-C_S debris flows. Typically, however, final diversion of flow to a new channel course is not accomplished instantaneously and the upper portion of the plugged channel is usually obliterated by deposition of debris flows during the interval between channel blockage and the excavation of a new channel. Localized deposition during this interval builds up a local topographic high which adds to the relief or roughness of the fan surface. As a result, new channel courses rarely diverge immediately behind the channel plugging debris flow, but rather some distance up-fan (Fig. 2.3).

Low-Sediment-Concentration Debris Flows

Debris flows with relatively low sediment concentrations have low yield strengths and viscosities (Fairchild, 1985; O'Brien and Julien, 1988; Phillips and Davies, 1991; Major and Pierson, 1990; Whipple, 1992). They can traverse slopes as gentle as 1-2°, are capable of spreading laterally into thin sheets, have limited boulder-transporting capabilities, and can attain high velocities, particularly where confined in channels. On the upper reaches of the bajada large discharges of such flows remain within the channel (Fig. 2.12). As a result, the fate of a low-C_S flow is dictated largely by the condition of the channel system it encounters. When an unblocked channel presents an open transport corridor, one of these flows typically: 1) moves rapidly down-fan through the channel, leaving behind thin sheets of mud and rocks on interfluves wherever peak discharge exceeds channel conveyance capacity; 2) deposits boulders on channel margins during overbank flow; and 3) spreads laterally into a wide, smooth lobe, usually devoid of boulders, at the point down-fan where flow discharge greatly exceeds channel conveyance capacity. Selective deposition of boulders occurs not only along channel margins but also in zones of expanding or unconfined flow, such as where channels are partially infilled but not blocked. This selective deposition process has been recognized elsewhere (Okuda and Suwa, 1983; Fairchild, 1985; Suwa, 1988) and contributes the formation of "boulder fields" and to the relative depletion of boulders in the distal fan deposits. If the channel has actually been blocked, rather than just partially infilled, by a preceding high-C_S debris flow, wholesale deposition of even the most mobile debris flows may occur on the upper slopes of the bajada. In this case, the low-C_S flows are trapped behind the intervening channel-plug and contribute to the rapid in-filling and obliteration of the up-fan reach of the recently plugged channel. Thus, low-C_S debris flows are responsible for (in part) the rapid in-filling of the upper reaches of blocked channels, the aggradation of the interfluves of the middle and upper fan, and the aggradation of the lower fan. As a result, the distal portion of the fan develops a smooth, low-relief surface and the interfluves on the middle fan are likewise smooth.

Controls on Depositional Morphology

Rheological controls on depositional patterns in combination with fluvial controls on the erosion of channels determine the morphology of an aggrading fan surface. The depositional morphology of debris-flow fan surfaces is most directly affected by the efficiency or vigor of the fluvial system and the frequency distribution of debris-flow rheologies, volumes, and hydrographs (here represented by the peak discharge). Fluvial processes control: (1) channel size and down-fan extent; (2) the likelihood that a recently deposited channel plug will be scoured away; and (3) the duration of the interval between channel blockage and the establishment of a new, continuous channel course. For a given fluvial system, the frequency distribution of debris-flow rheologies, volumes, and hydrographs sets: (1) the slope of the fan surface (depending on the volumes of overbank flows and their yield strengths); (2) the proportion of the surface which is rough (characteristic of high-C_S flows) and smooth (characteristic of low-C_S flows); (3) whether debris-flow deposition characteristically produces wide overbank lobes or is restricted to narrow strips along channels (the former circumstance leads to steeper fan slopes and is favored by debris flows with high peak discharges and volumes); (4) the temporal frequency and spatial pattern of channel blockages. The latter is particularly important because it controls the frequency of channel-shifting events. This determines both the extent and structure of the network of abandoned channels and the longevity of any given channel course, which importantly constrains the height that can be attained by aggrading levees and, therefore, limits the convexity of cross-fan profiles.

With the controls on the depositional morphology of debris-flow fans thus delimited, the morphological expression of different frequency distributions of debris-flow properties can be predicted in a qualitative manner. For instance, if built exclusively by high-C_S debris flows, the entire fan would resemble the steeper proximal reaches of the Owens Valley bajada. Slopes would be steep. The surface would have a rough texture, lacking the broad interfluves of the lower portions of the bajada. If the fluvial system were strong, the surface would exhibit many well-defined abandoned channels. A fan built exclusively by low-C_S debris flows would, on the other hand, have a gentler slope and smoother surface with few well-preserved channels. The latter follows because channel avulsion would be less frequent and shifting would more likely be driven by gradual up-fan migration of depositional centers. Furthermore, any abandoned channels would tend to be filled in by subsequent overbank spreading of the low-C_S debris flows. Finally, a fan built by a strongly bimodal population of high- and low-C_S debris flows would likely exhibit a steep proximal portion with surface features characteristic of high-C_S flows separated by a distinct break in slope from a smoother, more gently sloping lower fan.

In a less hypothetical application, the characteristics of the Late Pleistocene depositional system preserved on the Owens Valley bajada can be constrained qualitatively. Channel longevity and channel-shifting intervals were apparently short: surface convexity is minimal, little levee aggradation has occurred (Fig.s 2.5, 2.6 and 2.7), and an extensive network of abandoned channels is preserved on much of the bajada (see Fig. 2.2). High-C_S channel-plugging debris flows must have occurred frequently. However, the general paucity of overbank lobes of high-yield-strength debris flows (Fig. 2.3) implies that (1) the high-C_S debris flows generally did not involve great volumes and peak discharges of material, and (2) the fluvial system was vigorous and managed to maintain relatively deep, continuous channels despite the frequent channel-blockage events. Further, the predominance of low-relief surfaces on the bajada (e.g., the lower fan and the broad, smooth interfluves of the midfan) suggests that the greatest proportion of sediment was delivered to the fans as low-C_S debris flows.

CONCLUSIONS

A model has been presented which relates the morphology of an aggrading debris-flow fan to the physical properties of the debris flows (temporal frequency, rheology, volume, peak discharge) and the "strength" of the fluvial system. The conceptual framework for the model was based on field mapping on a bajada in Owens Valley, California, and the model is strictly applicable only to similar depositional systems. On the Owens Valley bajada, fluvial processes are dominantly erosional and the active channel system has at all times consisted of a single, or few, active channel(s). Debris-flow depositional patterns are controlled by the channels and the physical properties of the debris flows; channel avulsion, and hence the shifting of depositional loci, is driven by in-channel deposition of relatively immobile debris flows. Fans of the type described in our model are common in mountainous regions in both semi-arid (e.g., Basin and Range Province, USA) and humid-temperate (e.g., Japanese Alps) climatic zones, and our model is applicable in a wide range of environments. However, fans frequently inundated by huge debris flows which massively overwhelm their channels, such as those situated below active stratovolcanoes, are not well described by our model.

In our model, the morphology of an aggrading debris-flow fan is related to debris flow properties via a rheological analysis of debris-flow confinement (in channels) and runout. The rheological analysis assumes that: (1) the visco-plastic rheological model adequately describes debris-flow behavior; (2) debris-flow mobility is sensitive to the water content of the slurry (sediment concentration); and (3) variations in matrix grain-size distribution and the concentration of large boulders in the flow are less important to flow mobility than differences in the bulk sediment concentration. The latter assertion is valid for the Owens Valley field setting, but may break down in field areas where textural variability is greater. In such cases, the model must be augmented to consider variations in both texture and sediment concentration. With these assumptions, we show that channel capacity, and hence the degree of flow confinement, is very sensitive to changes in debris-flow sediment concentration, with important consequences for fan morphology. The model predicts that fan slope, roughness patterns, channel network structure, levee heights, and the convexity of cross-fan profiles are strongly influenced by the frequency distribution of debris-flow rheologies, volumes, and hydrographs delivered to the fan. The model provides a framework for the study of how and why morphological differences arise between debris-flow fans derived from different source areas or under different climates.

ACKNOWLEDGEMENTS

This research was supported in early stages by grants from the Department of Geological Sciences at the University of Washington, the Geological Society of America, and Sigma Xi. Later stages were supported primarily by the National Science Foundation (Grant EAR-9004843 to T. Dunne). Additional support was provided by NASA (Grant NAGW-1317 to A.R. Gillespie and J. Harden, and Grant NAGW-85 to J.B. Adams) and the National Science Foundation (Grant EAR-8518058 to T. Dunne). Discussions with A.R. Gillespie, R. Anderson, and S. Anderson contributed importantly to the formulation of ideas presented in this paper. The authors are grateful to the White Mountain Research Station and the staff at the Bishop Laboratory for providing accomodation, and to J. Kirtland, P. Shippert, and G. Whipple for field work. Thoughtful reviews by S. Reneau and an anonymous reviewer improved an earlier draft of the manuscript.

CHAPTER 3

Open-Channel Flow of Bingham Fluids: Applications in Debris-Flow Research

Chapter 3 develops the numerical tools for analyzing debris-flow deposits necessary for refining the analysis presented in Chapter 2 and provides field estimates of the rheology of granitic-source debris flows in Owens Valley. In addition, this chapter provides a more extensive review of the current understanding of debris-flow mechanics than was provided in Chapter 2. This chapter has been prepared for submission to the Journal of Geology.

CHAPTER SUMMARY

The results of a numerical simulation of open-channel flow of Bingham fluids provide improved capabilities for analyzing debris flows and their deposits, and for routing debris flows. Most published field estimates of debris-flow rheological properties depend on application to natural channels of analytical solutions for flow through channels with either circular or very wide channel cross sections. Lack of a general solution for flow of Bingham fluids in channels with realistic shapes has restricted capabilities in debris-flow modeling and field data analysis. Numerical solutions permit generalization and extension of analytical solutions to channels of arbitrary cross-sectional form without loss of accuracy. The numerical model (FIDAP) utilizes a well established finite-element formulation of the non-Newtonian fluid flow problem and reproduces available analytical solutions nearly exactly. A regression analysis of model results constrains general, easily applied equations that give discharge and plug velocity as functions of channel geometry, channel slope, debris total bulk density, viscosity, and yield strength. These empirical equations are suitable for back-calculation of debris-flow viscosity from field data, engineering analysis, and for incorporation into one- and two-dimensional debris-flow routing models. An analysis of debris-flow rheology on the basis of field observations in Owens Valley, California, utilizing this method yields the most reliable field estimates of debris-flow yield strengths and viscosities to date. These new field estimates corroborate the findings of recent laboratory studies and provide the first evidence that these findings can be extrapolated to field scale.

INTRODUCTION

I study steady, uniform open-channel flow of Bingham fluids. Specifically, I address the influence of channel cross-sectional geometry and width-to-depth ratio on the relationships between driving stress, material properties (yield strength and viscosity) and the discharge and velocity of bankfull flows. The analysis is motivated by the need to develop predictive capabilities in the modeling of debris-flow runout and deposition on fans, where debris-flow hazard is most serious (Costa and Williams, 1984; Jackson, and others, 1987; Whipple, 1993).

The Bingham constitutive equation is, in one-dimensional form (Johnson, 1970):

$$\tau_{zx} - \tau_o = \mu \frac{du}{dz} \; ; \qquad \tau_{zx} > \tau_o \qquad (3.1a)$$

$$\frac{du}{dz} = 0 \qquad ; \qquad \tau_{zx} \leq \tau_o \qquad (3.1b)$$

where τ_{zx} is the driving shear stress, τ_0 is the yield strength in shear, μ is the Bingham viscosity, and du/dz is the velocity gradient normal to the bed (Fig. 3.1). The applicability of the Bingham model to natural debris flows has been questioned (e.g., Iverson and Denlinger, 1987). However, the mechanical behavior of natural debris flows is still poorly understood (Iverson and Denlinger, 1987; Savage, 1993) and no rigorous, physically satisfying and universally applicable constitutive model has been developed. The Bingham model is a rheological construct, fit to field and experimental data, and as such does not rigorously account for complex grain-grain and grain-fluid interactions that dictate the mechanics of flowing debris. For instance, collisional and frictional interactions between gravel- and boulder-sized clasts, modulated by pore pressures, probably contribute significantly to momentum transfer in most natural debris flows (Johnson, 1970; Pierson, 1986; Phillips and Davies, 1991; Iverson and LaHusen, 1993). Work specifically addressing the role of friction and dynamic pore pressure fluctuations in debris flows is currently underway (Iverson and LaHusen, 1993), but many issues remain unresolved.

Despite its limitations the Bingham model has considerable merit. There is considerable experimental evidence that mud-rich sandy slurries behave as approximately Bingham fluids (Fairchild, 1985; O'Brien and Julien, 1988; Phillips and Davies, 1991; Coussot, 1992; Major and Pierson, 1992; Coussot and Piau, in press). Although these experimental results are not directly applicable to natural debris flows because of differences in particle sizes (Phillips and Davies, 1991; Iverson and

LaHusen, 1993), a clear understanding of the relative importance of matrix deformation and clast-to-clast interactions (either frictional or collisional) in natural debris flows is still lacking. Differences in the total grain-size distribution, that probably govern the relative importance of these two modes of momentum transfer, may explain geographical differences in debris flow behavior (i.e., Johnson, 1970; Takahashi, 1978; Okuda, and others, 1980; Lawson, 1982; 1984). For instance, Coussot (1992) suggests on the basis of his work with both small and larger rheometers that the clay content (amount and mineralogy) determines the global behavior of the mixture: he concludes that beyond a critical clay content (as yet not rigorously constrained, but thought to be in the range of 4-10% by weight), a poorly sorted mixture behaves as a simple visco-plastic fluid regardless of the maximum particle size. Coussot's (1992) findings are preliminary, and have yet to be reproduced, but they do indicate that some types of debris flow may be reasonably modeled as Bingham fluids as suggested by Johnson (1965; 1970).

To help clarify which "types" of debris flow do and do not exhibit approximately Bingham behavior, it is useful to consider the three main modes of shear resistance and momentum transport in most debris flows: inelastic collisions, enduring frictional contacts, and viscous deformation of the "fluid". In this usage the term "fluid" may take on different meanings in different debris flows, depending on grain-size distribution, water content, and strain rate: "fluid" includes whatever fraction of the material acts in a simple viscous or visco-plastic manner. For instance, in silt-and-clay (fines) poor flows the "fluid" is the interstitial water, in fines-rich debris flows the "fluid" includes at least the silt-clay-water slurry, and may include the suspended sandy fraction, if the sandy slurry behaves in a viscous manner over the range of strain rates of interest. Different modes of momentum transport can be expected to dominate under differing circumstances, depending on the strain rate and debris granulometry (Fig. 3.2).

Iverson and LaHusen (1993) have shown that the boundaries between the inertial, frictional, and macroviscous regimes can be qualitatively determined through evaluation of non-dimensional numbers developed in the work of Bagnold (1954) and Savage and Hutter (1989). Their analysis, and a similar application by Major and Pierson (1992), shows that mud-rich debris flows of the type studied here fall into either the frictional or macroviscous regime: low strain rates, fluid pore pressures, expanded grain-size distributions, and high viscosity interstitial fluids (silt-clay-water slurries) combine to reduce the importance of inertial collisions. The popular inertial-regime model advocated by Takahashi (1978; 1980; 1991) is therefore considered inappropriate for the type of debris flow studied here. Determination of the relative importance of frictional and viscous effects is more problematical and the necessary experimental work has not been completed (Iverson and LaHusen, 1993). As indicated by the curvature of the boundary between the frictional and macroviscous domains on Figure 3.2, the transition between viscous and frictional behavior may lie within the range of grain-size distributions and strain rates of interest for many debris flows, including the type studied here. For instance, Major and Pierson (1992) found that sand-silt-clay-water slurries behaved in an essentially viscous manner for sand concentrations of less than 20% and strain rates greater than 5 s^{-1}. At higher sand contents and lower strain rates, frictional interactions became important in their experiments. However, it remains unclear exactly where this transition in flow behavior takes places (e.g., the work of Coussot (1992) discussed above) and therefore how much error is entailed in the application of the Bingham model to mud-rich debris flows.

One clear drawback of the Bingham model is the assumption of a constant (plastic) yield strength. This assumption is untenable. Barnes and Walters (1985) have questioned the existence of a true yield strength in even the most fine-grained slurries, and the strength of more granular slurries must be in part frictional and therefore depth-dependent, sensitive to pore pressures, and probably strain-rate dependent (frictional interactions must dominate at the lowest strain rates and in the final moments of flow cessation and deposition) (Johnson, 1970; Iverson and Denlinger, 1987; Iverson and LaHusen, 1989; Phillips and Davies, 1991). The assumption of a constant yield strength is retained here for simplicity, and because the role of dynamic pore pressures in modulating the effective frictional strength is not yet quantitatively understood. I assume that the effective yield strength associated with ultimate flow cessation is the appropriate "strength" to use in application of the Bingham model.

Application of the Bingham constitutive equation to natural debris flows assumes that matrix (defined here as material < 2 mm in diameter) deformation governs the macroscopic behavior of the flow and that dynamic effects such as grain collisions, fricition, pore-pressure fluctuations, and formation and destruction of grain networks are either negligible or are collectively manifested as an approximately Bingham behavior (see discussions in Iverson, 1985; Phillips and Davies, 1991; Coussot, 1992;

Major and Pierson, 1992; Major, 1993). Here "approximately Bingham" is meant to include shear-thinning behavior that may be more representative of the types of dynamic effects described above, and that could be manifested in experimental and field data as an effective "yield strength" (Fig. 3.1). Deformation of the matrix is assumed to govern the *constitutive behavior* of the total mixture (i.e., approximately Bingham), not the magnitudes of effective global viscosity and yield strength -- these are clearly influenced by the presence of abundant (> 20% by volume) gravel and boulder-sized clasts (Johnson, 1970; Pierson, 1980; Pierson, 1986; Phillips and Davies, 1991).

The assumptions entailed in modeling debris flows as Bingham fluids are most reasonable for muddy, matrix-rich debris flows of the type that leave matrix-supported deposits. Both the viscosity and yield strength of mud-rich sandy slurries vary systematically with water content and debris granulometry (Fairchild, 1985; O'Brien and Julien, 1988; Phillips and Davies, 1991; Coussot, 1992; Major and Pierson, 1992; Coussot and Piau, in press). The same may be expected of natural debris flows. The experimental studies cited above, however, have been unable to reproduce the range of yield strengths and viscosities estimated in the field (Costa, 1984). Indeed, there is a general lack of accordance between laboratory and field estimates where both are available (Fig. 3.3). Although the disagreement between laboratory and field data could be due to inadequacies of the Bingham model, I demonstrate in this paper that carefully obtained field estimates in fact corroborate and extend the systematic trends seen in laboratory analyses.

APPROACH

I model mud-rich debris flows as Bingham materials. The application considered is that of steady uniform flow in rectilinear, prismatic channels. A primary goal is quantification of the influence of channel cross-sectional geometry and width-to-depth ratio on bankful flow discharge. As noted by Johnson (1984) his approximate solutions for flow through semi-elliptical channels (Johnson, 1970) are in error. In addition, published analytical solutions of two-dimensional flow of Bingham materials (Oldroyd, 1947) are too restrictive for application to open-channel flow. A commercially available finite-element code is used instead. The goal of the analysis is the development of accurate, easily applied equations for discharge and plug velocity of open-channel flows for use in back-calculation of debris-flow viscosity from field data or for computing the conveyance capacity of debris-flow channels. Model results are

Figure 3.1 Definition sketch of the Bingham constitutive equation (dashed line). Shear-thinning power law constitutive equation (solid line) is shown for comparison (discussed in text).

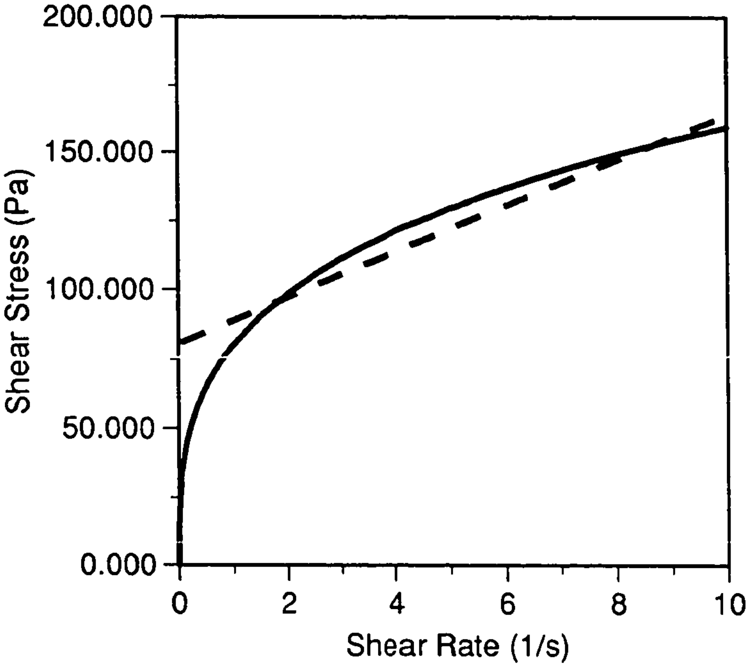
200.000
150.000
100.000
50.000
0.000
Shear Stress (Pa)
0
2
4
6
8
10
Shear Rate (1/s)

Figure 3.2 Schematic illustration of regimes of debris-flow behavior. The dominant mode of shear resistance and momentum transport in debris flows is hypothesized to be a function of strain rate and debris silt-and-clay content, as indicated by experimental work on a wide of debris-water mixtures (cited in text). Poorly sorted debris and water contents in the range consistent with the debris flow process are assumed (see classification in Pierson and Costa (1987)).

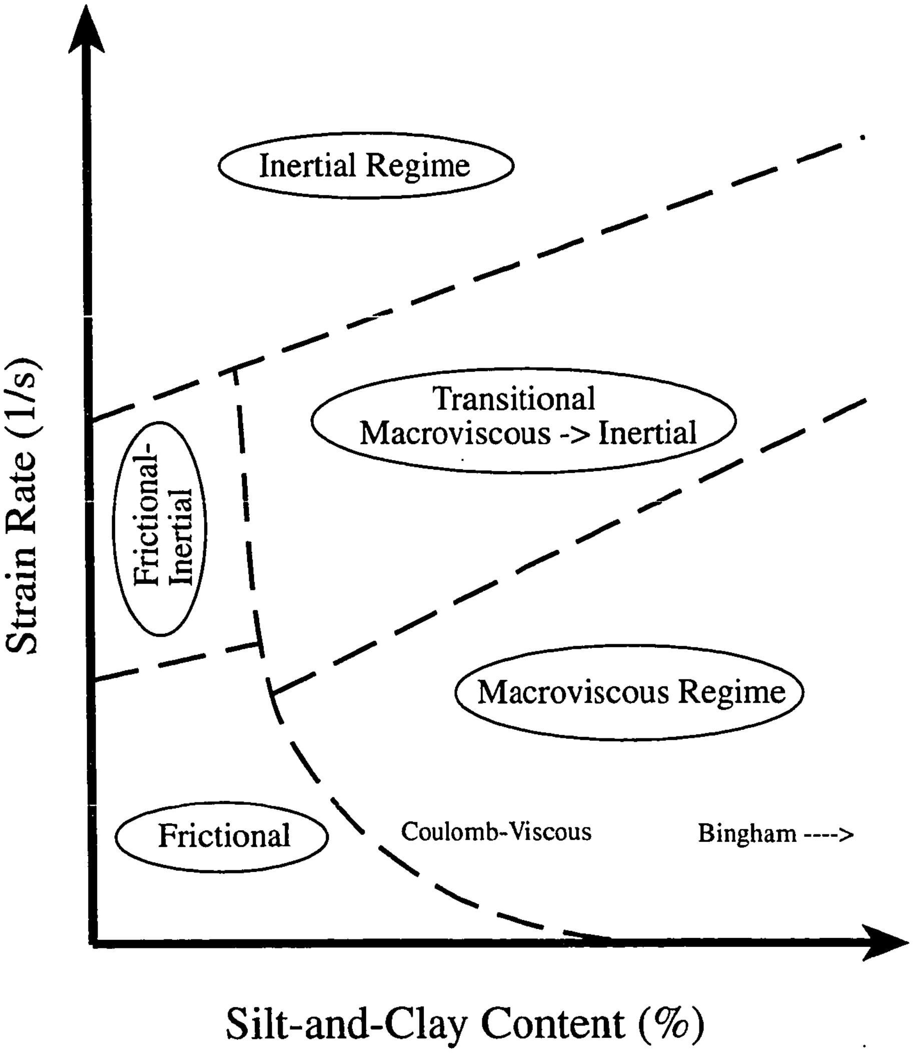
Inertial Regime
Transitional
Macroviscous -> Inertial
Frictional-
Inertial
Macroviscous Regime
Frictional
Coulomb-Viscous
Bingham ---->
Strain Rate (1/s)
Silt-and-Clay Content (%)

Figure 3.3 Comparison of laboratory and field estimates of debris-flow rheology. Experimental data sources: Jiangjia Gully (JG, Lab: Li, and others, 1983); 1980 North Fork Toutle River lahar (NF, Lab (1985): Fairchild, 1985; NF, Lab (1992): Major and Pierson, 1992); Mount Thomas, New Zealand (MT, Lab: Phillips and Davies, 1991). Field data sources: Jiangjia Gully (JG, Field: Li, and others, 1983); 1980 North Fork Toutle River lahar (NF, Field: Wigmosta, 1983); Mount Thomas, New Zealand (MT, Field: Pierson, 1980). Error bars represent the reported uncertainties for all data expect Fairchild's (1985). In this case the shaded region was digitized from the cloud of experimental data.

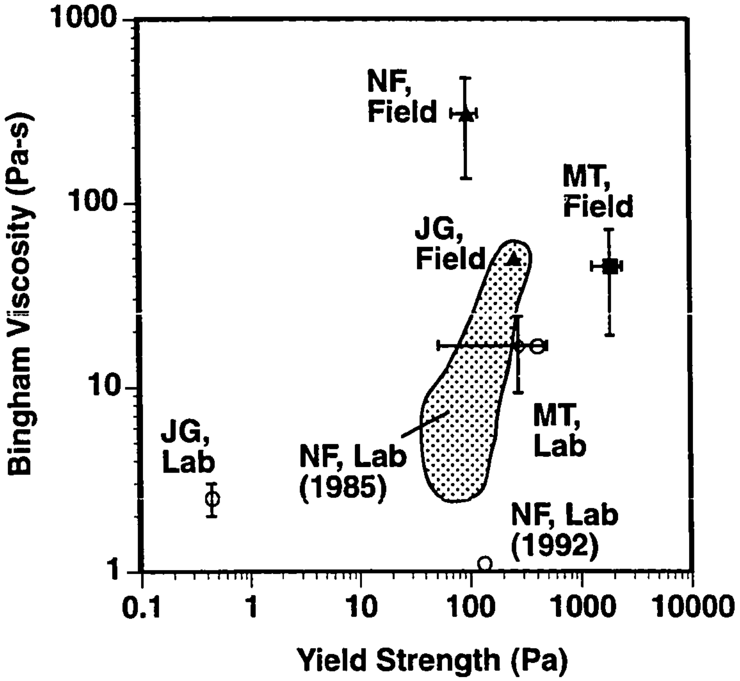

1000
100
10
1
Bingham Viscosity (Pa-s)
0.1
1
10
100
1000
10000
Yield Strength (Pa)
NF, Field
MT, Field
JG, Field
MT, Lab
JG, Lab
NF, Lab (1985)
NF, Lab (1992)

readily summarized by a generalized non-dimensionalized form of the analytical solution for flow through infinitely wide channels given by Johnson (1970). Regression analysis is used to determine the values of coefficients that vary with channel form and width-to-depth ratio. In addition, the numerical model is used to derive estimates of debris-flow rheological properties from observations at a field site in Owens Valley, California. These new estimates are consistent with laboratory data on debris flows with similar granulometries.

In the modeling exercise the following additional assumptions are made: the debris-flow material is homogeneous, isotropic, and incompressible, and a no-slip condition holds at the bed. These assumptions are restrictive but not unreasonable, particularly considering the simplifications already incorporated into the Bingham model. Debris flows are characteristically well mixed, and inhomogeneities such as vertical stratification in either mean particle size or water content are of secondary importance although longitudinal differences in both granulometry and water content are conspicuous (e.g., Okuda, and others, 1980; 1984; Pierson, 1986). Debris flows are not strictly incompressible, but the wide distribution of grain-sizes and generally low strain rates in the field settings of interest (i.e., on debris-flow fans) combine to minimize dilation and consolidation. Also, the question of compressibility is most important in terms of the physical processes that govern slurry viscosity. Given that I use the simple Bingham model, the further assumption of incompressibility is not problematic. Finally, although slip at the bed has been witnessed in some field settings, for some (generally fines-poor and boulder- and gravel-rich) types of debris flow (Okuda, and others, 1980; Costa and Williams, 1984; Iverson and LaHusen, 1993), it is less likely to occur in mud-rich debris-flows flowing on gentle gradients such as those modeled here.

GOVERNING EQUATIONS FOR OPEN-CHANNEL FLOW

The problem of open-channel flow of Bingham materials is fully described by the set of equations for the conservation of mass, the conservation of momentum, the Bingham constitutive relation and appropriate boundary conditions. Conservation of mass for incompressible materials is given by

$$\nabla \cdot u = 0, \tag{3.2}$$

which is identically satisfied in the case of steady uniform rectilinear flow considered here. In this case, the conservation of linear momentum reduces to the quasi-static force balance given by

$$\nabla \cdot \tau = \rho g, \tag{3.3}$$

where τ is the total stress tensor, ρ is the total bulk density and g is the acceleration due to gravity.

For consideration of complex channel geometries, the Bingham constitutive law, given in its familiar one-dimensional form in equation 3.1, must be generalized (Prager, 1961; Bird, and others, 1982), and can be written as

$$\tau_{ij} = 2\lambda\dot{\varepsilon}_{ij} \qquad \text{for } T > \tau_o, \tag{3.4a}$$
$$\dot{\varepsilon}_{ij} = 0 \qquad \text{for } T \le \tau_o, \tag{3.4b}$$

where the effective viscosity, λ, is defined by

$$\lambda = \mu + \frac{\tau_o}{2D}, \tag{3.4c}$$

τ_{ij} is the deviatoric stress tensor, $\dot{\varepsilon}_{ij}$ is the rate-of-strain tensor, given by

$$\dot{\varepsilon}_{ij} = \frac{1}{2}\left[\left(\frac{du_i}{dx_j}\right) + \left(\frac{du_j}{dx_i}\right)\right], \tag{3.4d}$$

τ_o is the yield strength, μ is the Bingham viscosity, and T and D are the second invariants of the stress and strain-rate tensors, respectively, defined by

$$T^2 = \frac{1}{2}\tau_{ij}\tau_{ij}, \tag{3.4e}$$
$$D^2 = \frac{1}{2}\dot{\varepsilon}_{ij}\dot{\varepsilon}_{ij}. \tag{3.4f}$$

The surface defined by the locus of points where T = τ_o marks the boundary between shearing fluid and fluid that is either at rest (so-called "dead zones") or moving at a uniform velocity (the so-called "non-deforming plug").

A fundamental difficulty in obtaining numerical solutions for the flow of Bingham fluids in complex geometries is the fact that the location of the plug boundary is not known *a priori* and that different differential equations apply on either side of this internal boundary (i.e., equations 3.4a and 3.4b). The situation is further complicated by the appearance of a singularity at the plug boundary, where the condition D = 0 holds (equation 3.4c). Fortunately, finite-element methods have been developed that are able to overcome these difficulties in a reliable, straightforward and numerically efficient manner (e.g., Bercovier and Engleman, 1980; Gartling and Phan-Thien, 1984; Walton and Bittleston, 1991; Szabo and Hassager, 1992).

NUMERICAL SIMULATION

Finite-Element Formulation

Gartling and Phan-Thien (1984), O'Donovan and Tanner (1984), Beverly and Tanner (1992), and Wilson (1993) have shown that a so-called bi-viscosity model in which strain continues within the "plug", but at a greatly reduced rate, closely approximates the numerically more complex Bingham model for values of μ/μ_r less than 10^{-2}, where μ_r is the viscosity within the plug region (Fig. 3.4). Beverly and Tanner (1992) refined the above condition to one where the magnitude of μ_r must be greater than 10^3 times the magnitude of the yield strength (τ_o). Each of these studies independently developed finite-element solution schemes and showed that both numerically computed plug-region geometries and velocity profiles closely matched analytical solutions for Bingham fluids in simple geometries, and approximate variational solutions in slightly more complex geometries. Several other authors (Bercovier and Engleman, 1980; Beris, and others, 1985; Walton and Bittleston, 1991; Szabo and Hassager, 1992) have successfully modeled the flow of Bingham fluids by employing a similar construct in which D in equation (3.4c) is replaced by D + ε, where ε is a small parameter (typically order 10^{-8} s^{-1}). This device allows the entire flow field to be modeled with a single constitutive relation (equation 3.4a), eliminating the need to solve simultaneously for both the location of the yield surface and the velocity field, and avoids the numerical difficulty associated with the singularity at the yield surface. This approach is philosophically the same as that employed by Gartling and Phan-Thien (1984), and is the solution method employed here. The small value of the parameter ε guarantees that both conditions for convergence with the Bingham solution, $\mu/\mu_r < 10^{-2}$ and $|\mu_r| > 10^3(|\tau_o|)$, are satisfied.

The finite-element method is particularly well suited to the solution of flow fields of Bingham fluids in complex geometries (Walton and Bittleston, 1991; Szabo

Figure 3.4 Schematic illustration of the bi-viscosity approximation to the Bingham model used in the numerical simulation. Variables are defined in the text.

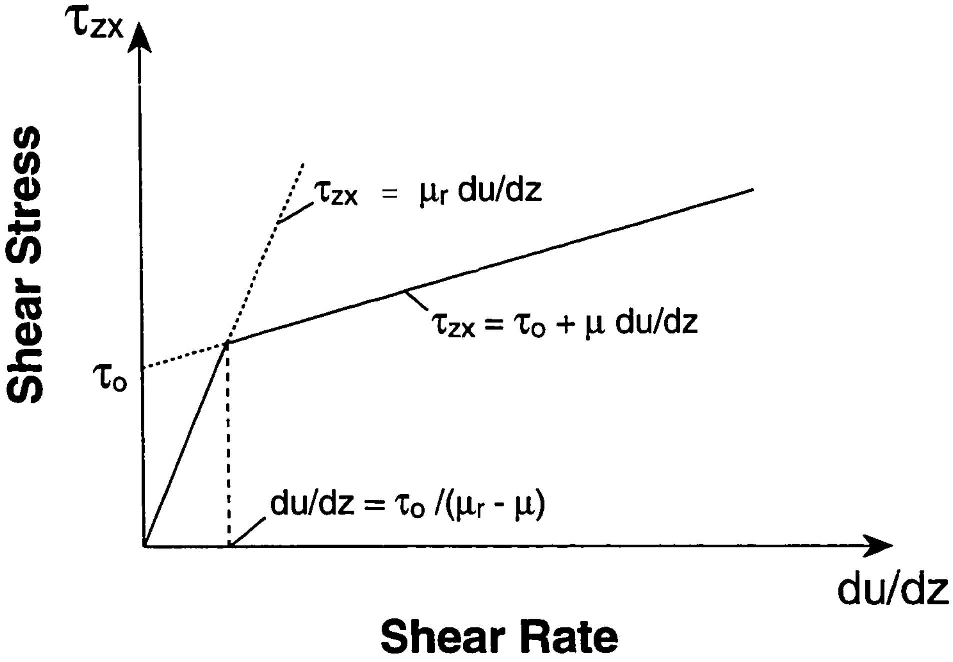

τ_{zx}
Shear Stress
$\tau_{zx} = \mu_r \, du/dz$
$\tau_{zx} = \tau_o + \mu \, du/dz$
τ_o
$du/dz = \tau_o / (\mu_r - \mu)$
du/dz
Shear Rate

and Hassager, 1992) and an existing general-purpose finite element code (FIDAP) was chosen for use in the analysis presented here. FIDAP (Fluid Dynamics Analysis Package) is a widely used computational fluid dynamics program capable of modeling a wide variety of non-Newtonian fluids, including Bingham fluids (e.g., Lee and Tucker, 1987; Bay and Tucker, 1992). FIDAP uses the solution technique described above, offers the advantage of being entirely menu-driven, and is supported by pre- and post-processing modules. Details of the finite-element formulation and the specifics of the FIDAP code were described by Engleman (1980).

The problem of steady uniform rectilinear, gravity-driven flow through channels of constant cross-sectional form is formulated as a three-dimensional problem, with an element array that is only one element thick in the down-stream direction. Elements are of the 27-node quadrilateral brick type. This choice permits 4th-order Gaussian integration for improved numerical accuracy, particularly in the vicinity of the yield surface, and the use of quadratic basis functions, which greatly improves the accuracy of the solution and reduces the required mesh density as the laminar velocity field is naturally quadratic in form. Picard iteration (successive substitution) is employed because of its large radius of convergence; iteration schemes designed to accelerate convergence (e.g., Newton-Raphson) generally fail in the case of non-Newtonian flow problems (Walton and Bittleston, 1991). Using this approach, equations (3.2-3.4) are solved with FIDAP, subject to the appropriate boundary conditions: a stress-free surface and no slip along the channel walls.

Model Confirmation

Simulations using FIDAP, configured as described above, match the analytical solutions for both plug velocity and discharge through a circular channel or on an infinitely wide planar surface almost exactly, for all values of the yield strength (Fig. 3.5). Dimensions of the non-deforming plug are also predicted accurately. Unfortunately, it is impossible to test rigorously the performance of the model in more challenging, complex situations (see discussion by Oreskes, and others, 1994). However, several authors have reported unqualified successes in extensive testing of similar finite element formulations of the Bingham flow problem (Beverly and Tanner, 1992; Szabo and Hassager, 1992; Wilson, 1993). In addition to tests against approximate analytical variational solutions in geometries where such solutions can be obtained, Szabo and Hassager (1992) tested the bi-viscosity formulation against a computationally more expensive finite-element formulation of the exact Bingham model

Figure 3.5 Comparison of model results and theory for flow through a circular channel. Non-dimensional discharge (Q_N) (squares) and non-dimensional velocity (U_N) (circles) are shown as a function of non-dimensional yield strength (τ_o/τ^*). Smooth curves are the analytical solutions. Note that solutions for all values of the driving stress collapse to these curves when non-dimensionalized.

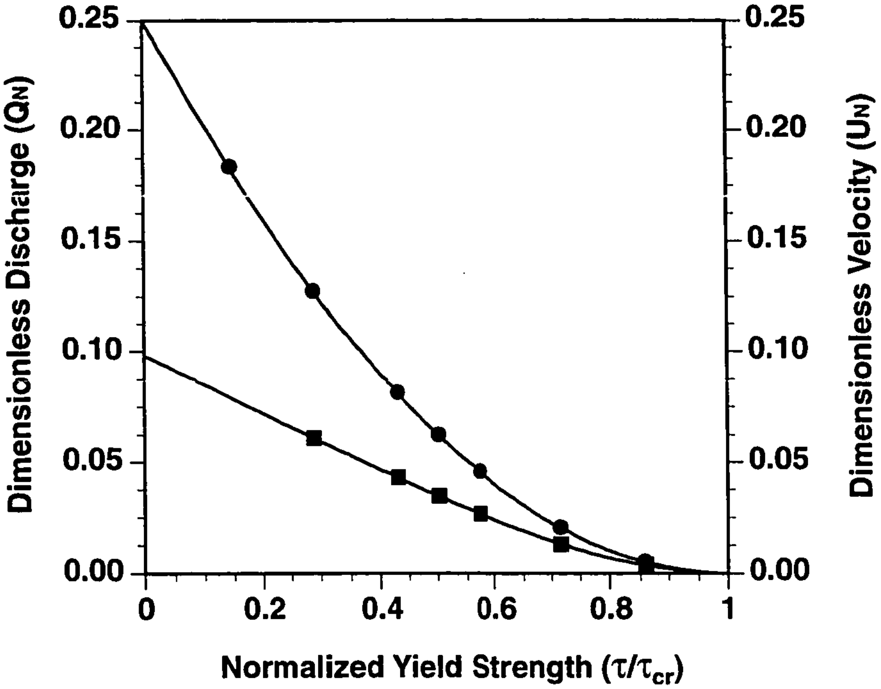

0.25
0.20
0.15
0.10
0.05
0.00
Dimensionless Discharge (Q_N)
0.25
0.20
0.15
0.10
0.05
0.00
Dimensionless Velocity (U_N)
0
0.2
0.4
0.6
0.8
1
Normalized Yield Strength (τ/τ_{cr})

in more complex geometries. Solutions with the approximate bi-viscosity formulation matched those of the exact Bingham model closely, with the limitation that the exact geometry of yield surfaces were less well defined (iterative mesh refinement would be required to determine the geometry of complex yield surfaces precisely). This limitation is important in some industrial problems involving the flow of Bingham plastics (e.g., Walton and Bittleston, 1991; Szabo and Hassager, 1992), but has little relevance in the debris-flow routing problem considered here because flow discharges are insensitive to the exact geometry of the "non-deforming plug" (Szabo and Hassager, 1992). Finally, in cases where rigorous testing is not possible, the validity of finite-element models is usually tested by comparing solutions as a function of element size: if the solution converges below some critical nodal spacing, the solution is considered valid (Zienkiewicz and Taylor, 1991).

For the steady, uniform open-channel problems analyzed here, solutions converged rapidly as the number of elements in the mesh was increased from 24 to 96, with only minor differences in velocities even over this range. However, as reasonably accurate determination of plug dimensions was also desired as model output, runs were generally configured with over 100 elements. Therefore, in the terminology of Oreskes (1994), the model can be said to have been "confirmed" and model predictions should accurately capture the influence of channel geometry on plug dimensions, plug velocities, and channel discharges, assuming the Bingham model is reasonable.

Results and Analysis

A series of model runs in which fluid density, channel slope, channel centerline depth, Bingham viscosity, and yield strength were varied systematically in channels with fixed geometries showed that, when appropriately non-dimensionalized, all solutions collapse to single, monotonic relationships between flow variables and material yield strength. Variables used in the analysis are: non-dimensional discharge, Q_N, defined as

$$Q_N = \frac{Q\mu}{\rho g S W H^3}\ , \tag{3.5}$$

where Q is the discharge, W is channel width and H is channel centerline depth; non-dimensional plug velocity, U_N, defined as

$$U_N = \frac{U_p\mu}{\rho g S H^2}\ , \tag{3.6}$$

where U_p is the plug velocity; and non-dimensional yield strength (τ_o/τ^*), defined as

$$\frac{\tau_o}{\tau^*}=\frac{\tau_o}{\rho g H S}\ . \qquad (3.7)$$

Because all solutions collapse to simple relationships between these non-dimensional variables, the effects of varying channel form and width-to-depth ratio could be investigated independently of variations in fluid density, flow depth, channel slope, and Bingham viscosity.

Several terms related to the material yield strength and the stress state in the fluid are used in the discussion below. In the interest of clarity, these are defined here and consistent usage is maintained throughout the discussion. Yield *strength* (τ_o) in all cases refers to a property of the material. Critical shear *stress* (τ_{cr}) refers to the maximum yield *strength* at which flow is possible in that channel - a property of channel geometry and the driving stress. Three non-dimensional terms related to the yield strength and the critical shear stress are used in the analysis: (1) the ratio of yield strength to a reference shear stress (τ_o/τ^*), defined above (equation 3.7); (2) the ratio of the critical shear stress to this reference shear stress (τ_{cr}/τ^*); and (3) the ratio of the yield strength to the critical shear stress (τ_o/τ_{cr}). The first of these (τ_o/τ^*) is used to collapse model output to manageable form, and to derive an estimate of the second (τ_{cr}/τ^*). The last (τ_o/τ_{cr}) is used in empirical equations relating discharge and plug velocity to channel geometry, driving stress, and material properties.

Flow of Bingham Fluids as a Function of Channel Geometry

A series of model runs was performed on channels with rectangular, elliptical, and trapezoidal cross-sectional forms. The trapezoidal channels are chosen to have 33° sideslopes and flat bottoms. For each channel form, runs were made for channel width-to-depth ratios (Θ) of 1, 2, 5, 10, 20, and 50 (3, 5, 10, 20, and 50 for the trapezoidal channels). Each "run" consisted of 6-12 solutions of the velocity field, each for different values of the yield strength as it varied between zero and the critical shear stress (τ_{cr}) for flow through that channel. Note that the actual value of the critical shear stress was not known *a priori*, and yield strength was simply increased incrementally until the computed discharge approached zero.

Critical shear stress

Critical shear stress was determined via regressions of discharge and velocity data against yield strength (τ_o/τ^*) (described below): the non-dimensional critical shear stress (τ_{cr}/τ^*) is given by the non-dimensional yield strength (τ_o/τ^*) at which both discharge and plug velocity go to zero. Model output also included estimates of plug centerline thickness (h_o) and surface width (w_o) that could be used to estimate the critical shear stress. However, as mentioned in the description of the numerical solution scheme, the determination of flow velocity is more accurate than the determination of the plug boundary. Critical shear stress was determined for each of the rectangular, elliptical, and trapezoidal channels as a function of width-to-depth ratio (Θ). The results are reported in non-dimensional form (τ_{cr}/τ^*) in Table 3.1 and illustrated on Figure 3.6.

Bankfull Discharge

To derive an empirical equation for predicting flow discharges, non-dimensionalized model output was regressed against a generalized form of the analytical solution for the discharge of a Bingham fluid flowing through an infinitely wide channel:

$$Q_N = K\left[a\left(\frac{\tau_o}{\tau_{cr}}\right)^3 - b\left(\frac{\tau_o}{\tau_{cr}}\right) + c\right] \qquad (3.8)$$

where K, a, b, and c are constants. In the case of model output, these coefficients vary with channel form and width-to-depth ratio only - the non-dimensionalization is robust. For an infinitely wide channel, K, a, b, and c are known analytically and take values of 1.0, 0.167, 0.5, and 0.333, respectively (Johnson, 1970). For a circular channel the analytical solution for the discharge can be written in a similar form in which the exponent on the first term on the right hand side of equation (3.8) is 4 rather than 3, K is 0.5, and a, b, and c are 0.0327, 0.131, and 0.0982, respectively (Johnson, 1970). Despite the theoretical difference in exponents, discharge through a circular channel can be represented satisfactorily by equation (3.8). In this case, the coefficients a, b, and c can be determined through regression and take values of 0.0823, 0.284, and 0.20 ($r^2 = .99$; Table 3.1).

In the analysis of model output, estimates of the non-dimensional discharge number (Q_N) were plotted and regressed against the yield strength normalized by the critical shear stress (τ_o/τ_{cr}). Equation (3.8) was used as the regression model and was

Figure 3.6 Critical shear stress (τ_a/τ^*) versus width-to-depth ratio for elliptical (squares), rectangular (circles) and trapezoidal channels (triangles). Also shown is the approximate solution given by Johnson (1970, eqn. 14.15) (diamonds).

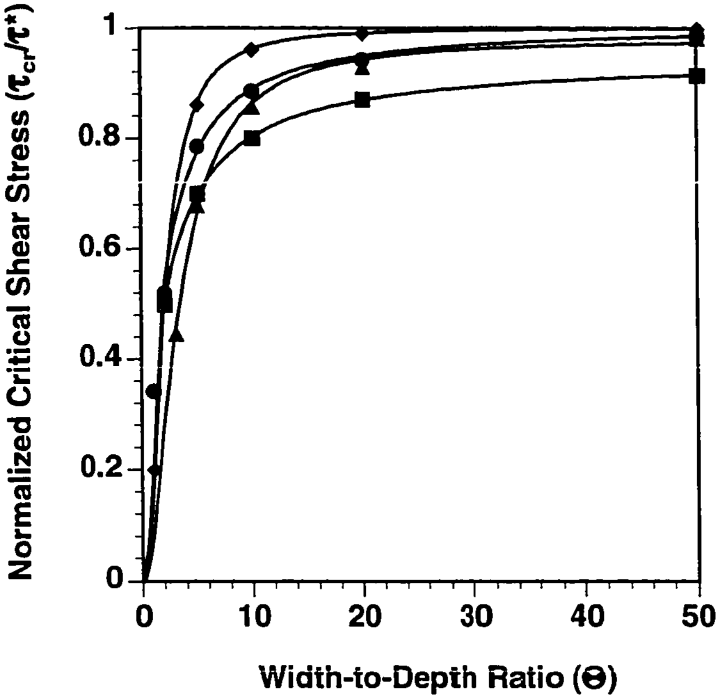
Normalized Critical Shear Stress (τ_{cr}/τ^*)
1
0.8
0.6
0.4
0.2
0
0
10
20
30
40
50
Width-to-Depth Ratio (Θ)

Table 3.1. Results of Regression Analysis

Critical Yield Strength	τ_{cr}/τ^*	$\tau^* = \rho g H S$	r²
Elliptical Channels	$0.95 \Big/ \left[(1.8/\Theta)^{1} + 1\right]$		.999
Rectangular Channels	$1.00 \Big/ \left[(1.8/\Theta)^{1.2} + 1\right]$		.999
Trapezoidal Channels	$0.98 \Big/ \left[(3.3/\Theta)^{1.8} + 1\right]$		.997

Discharge

$$Q_N = \frac{Q\mu}{\rho g S W H^3} = K(\Theta)\left[a\left(\frac{\tau_o}{\tau_{cr}}\right)^3 - b\left(\frac{\tau_o}{\tau_{cr}}\right) + c\right]$$

	K(Θ)	**a**	**b**	**c**	**r²**
Circular Channels	0.5 (fit to analytic)	0.0823	0.284	0.20	.999
Infinitely Wide Channels	1.0	0.167	0.5	0.333	analytic
Elliptical Channels	$1 \Big/ \left[(2/\Theta)^2 + 1\right]$	0.0971	0.296	0.198	.961
Rectangular Channels	$1 \Big/ \left[(2.5/\Theta)^{1.7} + 1\right]$	0.156	0.482	0.326	.991
Trapezoidal Channels	$1 \Big/ \left[(4/(\Theta - 2))^{1.2} + 1\right]$	0.159	0.491	0.332	.994

Table 3.1, Continued.

Plug Velocity

$$U_N = \frac{U_p \mu}{\rho g S H^2} = K(\Theta)\left[a\left(\frac{\tau_o}{\tau_{cr}}\right)^2 - b\left(\frac{\tau_o}{\tau_{cr}}\right) + c\right]$$

	K(Θ)	a	b	c	r^2
Circular Channels	0.5	0.5	1.0	0.5	analytic
Infinitely Wide Channels	1.0	0.5	1.0	0.5	analytic
Elliptical Channels	$1/\left[(2/\Theta)^2+1\right]$	0.503	1.01	0.502	.999
Rectangular Channels	$1/\left[(1.7/\Theta)^{2.4}+1\right]$	0.505	1.01	0.508	.988
Trapezoidal Channels	$1/\left[(3.3/\Theta)^4+1\right]$	0.496	1.00	0.505	.995

found to hold for channels of any of the three geometries and with any width-to-depth ratio (Θ): r^2 values for the regressions equaled or exceeded 0.99 in all cases (Table 3.1). The coefficients (a,b, and c) vary with channel form (i.e., rectangular, elliptical, or trapezoidal) and K is a function of width-to-depth ratio, but equation (3.8) can be taken as the general equation for the discharge of steady, uniform rectilinear flows of Bingham fluids through open channels with simple geometries. The values of K, a, b, and c were determined from model output as a function of channel form and width-to-depth ratio by first regressing discharge number against the non-dimensionalized yield strength (equation 3.8) and then regressing the coefficients obtained against width-to-depth ratio (Table 3.1). The regression model for this part of the analysis was taken from the analytical solution for laminar flow of a Newtonian fluid through an elliptical channel (Batchelor, 1967):

$$Q_N = \frac{\pi}{16} K(\Theta), \qquad (3.9a)$$

$$K(\Theta) = 1 \Big/ \left[(2/\Theta)^2 + 1\right]. \qquad (3.9b)$$

The basic form of equation (3.9b) was retained in all regressions, but the coefficient and exponent in the term involving Θ were allowed to vary. Again, this regression model proved to be of general applicability, with r^2 values in excess of 0.92 in all cases (Table 3.1).

Plug Velocity

A similar procedure was followed to derive analogous equations for plug velocity (U_P). In the case of plug velocity, the analytical solutions for flow through both infinitely wide and circular channels reduce to:

$$U_N = K\left[a\left(\frac{\tau_o}{\tau_{cr}}\right)^2 - b\left(\frac{\tau_o}{\tau_{cr}}\right) + c\right] \qquad (3.10)$$

a, b, and c are 0.5, 1.0, and 0.5 for both circular and infinitely wide channels (Johnson, 1970). The constant K, again a function of width-to-depth ratio, is 0.5 for circular channels and 1.0 for infinitely wide channels. As with regressions for non-dimensional discharge, equation (3.10) holds for plug velocities in channels of all width-to-depth ratios: r^2 values exceed 0.99 in all cases (Table 3.1). Equation (3.9b) was again used as the regression model in the regressions against width-to-depth ratio, with r^2 values exceeding 0.96 in all cases (Table 3.1). Regression models for both plug velocity and channel discharge match known analytical solutions nearly exactly.

Discussion of Model Results

Johnson's (1970) analytical solutions for flow through infinitely wide and circular channels, together with his approximate solutions for flow through elliptical channels, form the basis for most published field estimates of debris-flow rheological properties. Unfortunately, the solutions presented for elliptical channels are in error ((Johnson and Rodine, 1984), p. 304) and the errors involved in application of the idealized circular and infinitely wide channel solutions to field problems can be serious. Researchers have either used the elliptical-channel solution (e.g., (Johnson, 1970; Pierson, 1980), or have been forced to make untested approximations to account for sidewall drag in the plane-flow equation (e.g., Jeyapalan et. al. (1983) substituted hydraulic radius for depth), or to "fit" circular geometries to natural channels (e.g., Fink et. al. (1981) chose an 'effective' channel radius that gave the correct cross-sectional area). The results of the current modeling exercise are used below to evaluate the accuracy of these approximation schemes.

Plug Dimensions

Model results show that in all but the narrowest channels ($\Theta < 2$ for rectangular and elliptical channels, $\Theta < 5$ for trapezoidal channels), centerline plug thickness (h_o) increases linearly with yield strength and can be predicted from the relation:

$$h_o = \frac{\tau_o}{\rho g S(\tau_{cr}/\tau^*)}, \tag{3.11}$$

where τ_{cr}/τ^* is given by equations in Table 3.1. Unfortunately, the relationship between plug width, yield strength, and channel geometry is not as simple, and does not hold much promise for deriving estimates of debris-flow yield strength from easily-obtained measurements of plug width (Johnson, 1970; Pierson, 1984; Pierson, 1986). Model results show that for trapezoidal and rectangular channels plug width increases non-linearly with yield strength, and is an insensitive measure of yield strength, particularly for wide channels ($\Theta > 10$) and high yield strengths ($\tau_o/\tau_{cr} > 0.5$). Moreover, the relationship between plug width and yield strength is particularly sensitive to cross-sectional channel geometry: even slight deviations from the idealized channel forms modeled here can significantly alter plug widths. It appears that field estimation of debris-flow yield strengths is only feasible from measurements of deposit thickness as discussed below.

Plug Velocity and Channel Discharge

Significant errors can be anticipated in the application of common approximations to natural channels because they: 1) do not properly account for the variation of critical shear stress with channel geometry; and 2) involve arbitrary adjustments of the effective channel depth, to which discharge is very sensitive (see equation 3.8). I evaluated the error incurred in adopting each of these approximations for predicting the discharge of Bingham fluids through simple trapezoidal channels with width-to-depth ratios from 3 to 50. This analysis shows that the error involved is non-linearly related to the yield strength, reaching maximum values as yield strength approaches the critical value.

The circular approximation is accurate for narrow channels ($\Theta = 3$), but drastically overestimates discharge for wide channels (Fig. 3.7a). Similarly, the wide-channel approximation breaks down at width-to-depth ratios less than 10, yielding a five- to sixty-fold overestimation of discharge for high-yield-strength flows through narrow channels ($\Theta = 3$, Fig. 3.7b). The wide-channel approximation does work well for wide channels ($\Theta \geq 10$) and for low yield strengths ($\tau_o/\tau_{cr} < 0.5$). Somewhat surprising, however, is the finding that errors remain large for high yield strength debris-flows ($\tau_o/\tau_{cr} > 0.7$) in all but the widest channels (Fig 3.7b). The error at high yield strengths stems from the overestimation of the critical shear stress under the plane-flow approximation (Fig. 3.7); if the equations given in Table 3.1 are used to define critical shear stress, the wide-channel approximation works satisfactorily for channels with width-to-depth ratios greater than or equal to ten.

The most consistent results over a wide range of width-to-depth ratios are obtained with the hydraulic radius approximation (Fig. 3.7c). The hydraulic radius method, however, overestimates sidewall drag. As a result, channel discharges are consistently under predicted by 50% to 100%, depending on the yield strength (Fig. 3.7c).

APPLICATION TO NATURAL DEBRIS FLOWS

The equations for discharge and plug velocity presented in Table 3.1 cover a wide range of simple channel geometries and therefore are suitable for application to many natural channels. The equations have been reduced to a consistent, convenient

Figure 3.7 Analysis of the error in calculating discharge incurred through application of standard geometric approximations to trapezoidal channels as a function of width-to-depth ratio (reported as percent error relative to the numerical simulation results). Numbers above curves indicate width-to-depth ratio (Θ).

A) Circular channel approximation.

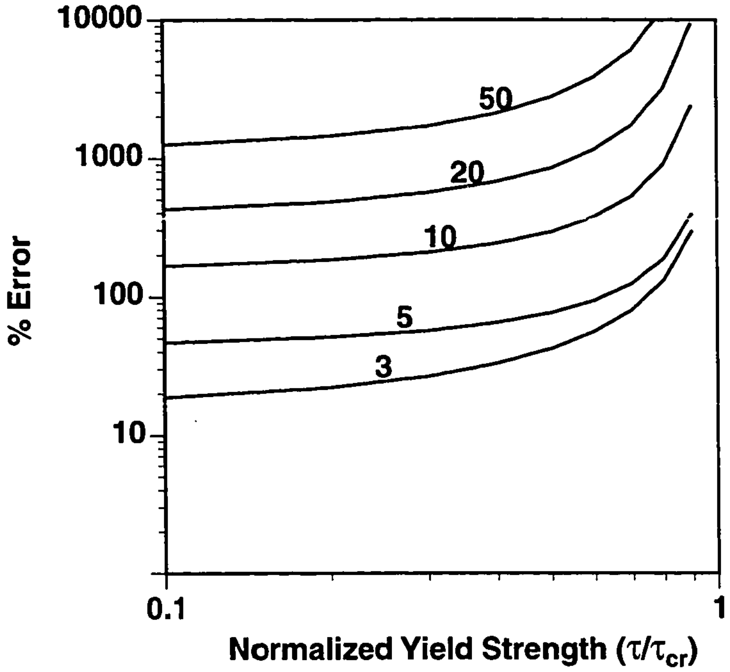
10000
1000
100
10
% Error
0.1
1
Normalized Yield Strength (τ/τ_{cr})
50
20
10
5
3

Figure 3.7 **B**) Infinitely-wide channel approximation.

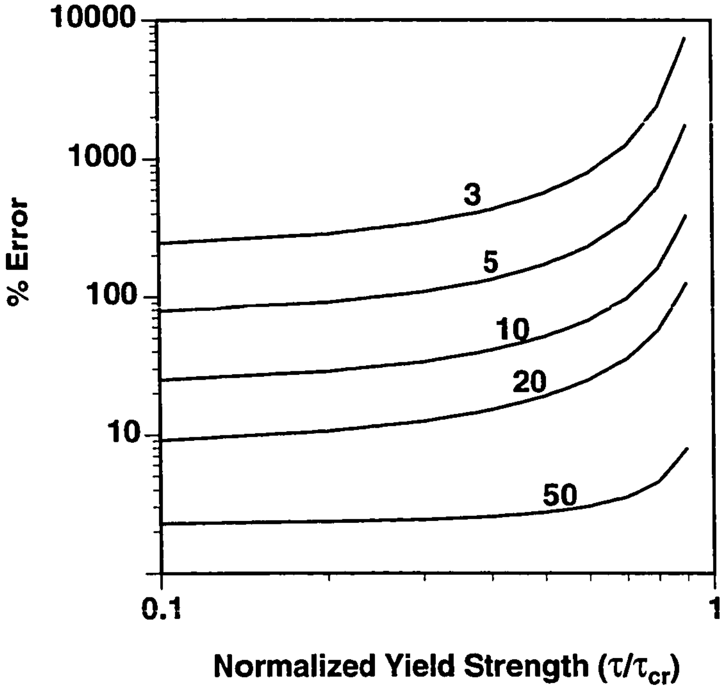
10000
1000
100
10
% Error
3
5
10
20
50
0.1
1
Normalized Yield Strength (τ/τ_{cr})

Figure 3.7 C) Infinitely-wide channel approximation using hydraulic radius for depth.

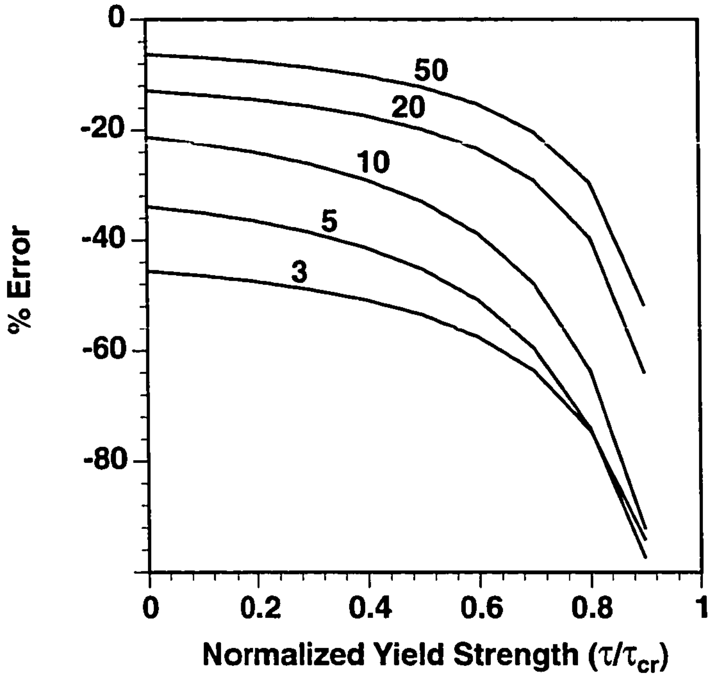

0
-20
-40
-60
-80
% Error
50
20
10
5
3
0
0.2
0.4
0.6
0.8
1
Normalized Yield Strength (τ/τ_{cr})

and easily used form. These equations upgrade the previously available analytical solutions for channels with idealized cross-sectional geometries. Applications for which these equations are best suited include: (1) accurate back-calculation of debris-flow viscosity from field data; (2) estimation of debris-flow conveyance capacity of both natural and design channels as a function of debris-flow yield strength and viscosity (Whipple, 1992; Whipple and Dunne, 1992); and (3) simple debris-flow routing schemes (Whipple, 1992). Each of these applications is illustrated below in a specific field example.

Field Estimation of Debris-Flow Yield Strength and Viscosity

In addition to applying the equations in Table 3.1 to field analysis of debris-flow deposits, the numerical code (FIDAP), or a similar finite-element formulation, can be used to back-calculate debris-flow viscosity directly for flows through arbitrary cross-sections, given field estimates of yield strength, channel slope, bulk density, and either plug velocity or discharge. This important application is illustrated first.

Methods

Although the Bingham model approximately captures the main macroscopic behavior of fines-rich, matrix-supported debris flows (i.e., it deviates only slightly from a shear-thinning rheology; Fig. 3.1), the apparently strain-rate and strain-history dependence of the "yield strength" complicates efforts to asses debris-flow yield strength in the field. First and foremost, the complex nature of a debris flow's "strength" invalidates field-estimation techniques that rely on the existence of a true plastic strength. A commonly used example is Johnson's (1970; 1984) boulder-immersion method (Pierson, 1980; Fink, and others, 1981; Pierson, 1984). Similarly, the size and shape of the "non-deforming plug" predicted in the Bingham velocity solutions may have little relationship to the size and shape of a "plug", if any exists, in a natural debris flow in shear. If the Bingham constitutive equation is used to model the flow of a dynamic, shear-thinning material (e.g., Fig. 3.1), the appropriate value of the "strength" is that related to the ultimate cessation of flow because correct prediction of runout distances and deposit thickness are common goals of such an analysis. Consequently, a reasonable method of field estimation is that based on deposit thickness (h) and surface slope (S). This method states simply that at time of deposition the mean basal shear stress was approximately equal to the yield strength:

$$\tau_o \approx \tau_b = \rho g h S, \qquad (3.12)$$

that strictly only applies to uniform slabs of infinite extent. However, equation (3.12) is reasonably accurate for lobes with width-to-depth ratios in excess of 10 and the relationship between normalized critical yield stress (τ_{cr}/τ^*) and width-to-depth ratio (Θ) (Table 3.1) may be used to approximate the effects of sidewalls in the case of debris flows deposited within channels. For a dynamic yield strength, this method estimates the effective strength at time of deposition (presumably a maximal value) and is, in principle, equivalent to the yield strength that would be determined in a laboratory analysis.

The snouts of wide overbank lobes deposited on relatively planar surfaces are the most suitable for estimation of yield strength because surface slope and thickness of the deposit can be determined most accurately here and the infinite slope approximation in most closely satisfied. Suitable locations are not difficult to find and consistent estimates of yield strength (+/- 15%) are easily obtained. Care must be taken, however, to avoid localities where debris could be ponded, or where the infinite slope approximation (equation 3.12) is invalid (i.e., on levees deposited at channel bends). Yield strength will typically be overestimated in such localities.

Flow viscosity is more difficult to constrain. Wherever flow discharges can be estimated either from direct observation or from reconstruction of mudlines preserved along channel courses, numerical simulation can be used to calculate the flow viscosity, provided the yield strength is known. Peak discharge (Q_p) can be estimated from measurements of flow super-elevation (Δh), flow width (w), and cross-sectional area (A) at bends by applying Chow's formula for steady, uniform flow through a bend with radius of curvature (r_c):

$$\langle u \rangle = \left(\frac{\Delta h}{w} r_c g \right)^{\frac{1}{2}} \tag{3.13a}$$

$$Q_p = \langle u \rangle A \tag{3.13b}$$

where $\langle u \rangle$ is the cross-sectionally averaged velocity. Wigmosta (1983) analyzed the error involved in the application of equation (3.13) to debris flows and reports an approximate 10-15% expected error. Major and Iverson (1993) found larger errors in controlled experiments designed to test equation (3.13). Wigmosta's analysis did not account for the passage of the frontal bore of a debris-flow surge through the bend, which may explain the discrepancy. Here, the conditions of steady, radial flow are violated, particularly at sharp bends where peak super-elevations can greatly exceed that predicted by equation (3.13). This phenomenon is readily observed in footage of debris flows rounding sudden bends at the Dongchuan Debris Flow Observatory in China (Costa and Williams, 1984). Unfortunately, the passage of the frontal bore is typically responsible for the peak mudlines and care must be taken in the application of equation (3.13). Where possible, multiple bends should be surveyed to reduce measurement error and sharp bends should be avoided. At present it is not possible to accurately correct for bore effects and further experimental and analytical work on this problem is warranted.

Analysis of Deposits on the Black Canyon Fan, California

Two recent debris-flow deposits (dating from 1983 and 1990) on the Black Canyon Fan near Independence, California, were studied. Neither flow was witnessed by the author and flow hydraulics had to be reconstructed from mudlines. The field methodology included: (a) mapping of the internal stratigraphy of the deposits to determine the extent and chronological sequence of individual debris-flow surges; (b) determination of the granulometry of the deposits of each surge; (c) measurement of the thickness and surface slope of overbank deposits of each surge; and (d) measurement of super-elevation of mudlines, channel centerline curvature, and channel cross-sectional geometry at bends.

Mapping established a sequence of six distinct surges, four in 1983 and two in 1990 (Fig. 3.8). Surveys of the 1983 deposits and mudlines were completed before the occurrence of the 1990 flows and all except the first surge of the 1983 flow (83-I) were sufficiently well preserved to allow a detailed reconstruction of flow hydraulics. Inter-surge differences in deposit granulometry are restricted to the coarse tail of the total grain-size distribution (Fig. 3.9). The granulometry of the < 32 mm fraction varies only slightly and coarser clasts comprise a maximum of 22% of the deposit by weight (surge 2) (Figs. 3.9a and 3.9b): the coarse clasts are well dispersed in the matrix plus fine gravels mixture. The sand-to-clay fraction (the "matrix") is identical (Fig. 3.9c). Yield strength estimates were derived from measurements of deposit thickness and slope, as described above. Multiple estimates of yield strength were made for each surge and the range of values are reported in Table 3.2. Peak discharge was estimated at 2-3 closely spaced bends for each surge using equation (3.13).

Where possible, a representative cross section of a nearby straight channel reach (typically located between two of the surveyed bends), was surveyed for use in the

Figure 3.8 Map of the 1983 Black Canyon debris flow. Locations of mudline and cross section surveys are indicated, as are locations where yield strength estimates were made. The 1990 debris flow deposits are not shown but followed the channel course abandoned during the 1983 event (indicated on map).

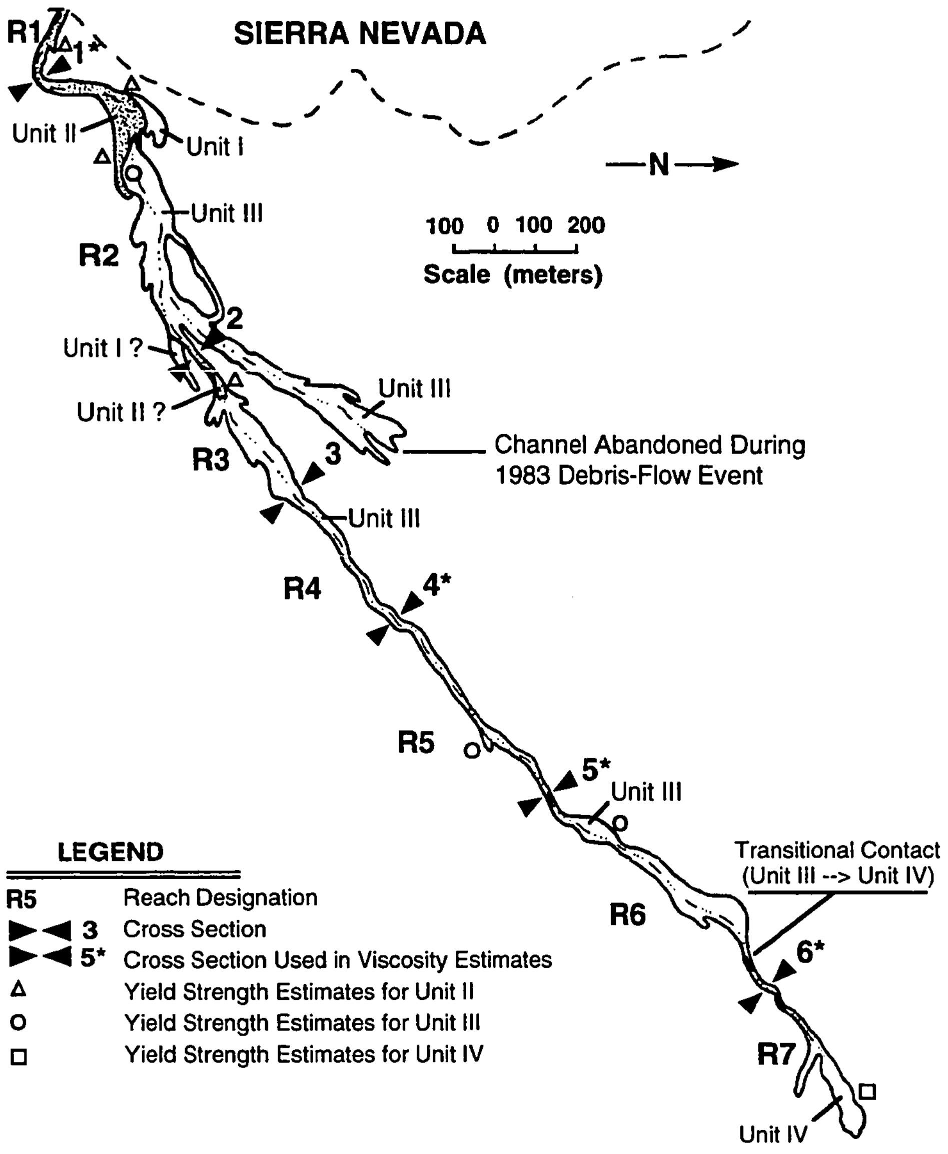
SIERRA NEVADA
R1
1*
Unit II
Unit I
Unit III
R2
2
Unit I ?
Unit II ?
Unit III
Channel Abandoned During
1983 Debris-Flow Event
R3
3
Unit III
R4
4*
R5
5*
Unit III
R6
Transitional Contact
(Unit III --> Unit IV)
6*
R7
Unit IV
—N→
100 0 100 200
Scale (meters)
LEGEND
R5 Reach Designation
▶◀ 3 Cross Section
▶◀ 5* Cross Section Used in Viscosity Estimates
△ Yield Strength Estimates for Unit II
○ Yield Strength Estimates for Unit III
□ Yield Strength Estimates for Unit IV

Figure 3.9 Granulometry of the 1983 Black Canyon debris flow.
A. Total grain-size distribution. Symbols: surge 1 (solid circles); surge 2 (open triangles); surge 3 (open circles); surge 4 (solid squares).
B. Grain-size distribution of the < 32 mm fraction. Symbols as in A.

A

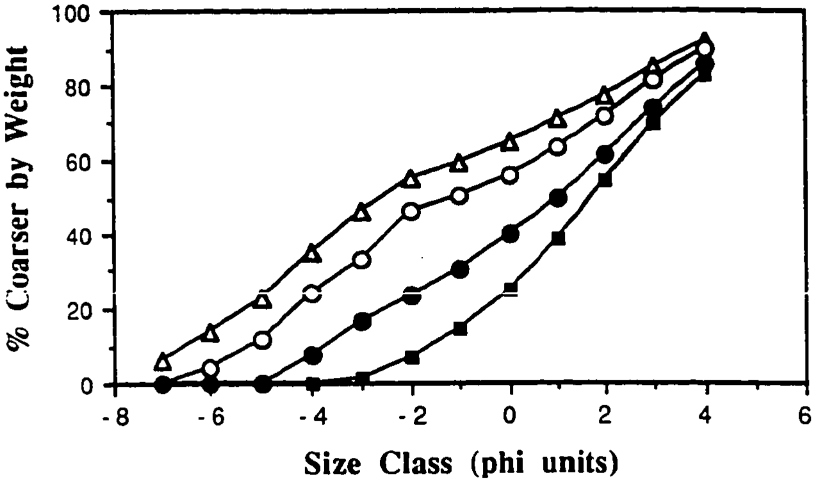

100
80
60
40
20
0
% Coarser by Weight
-8
-6
-4
-2
0
2
4
6
Size Class (phi units)

B

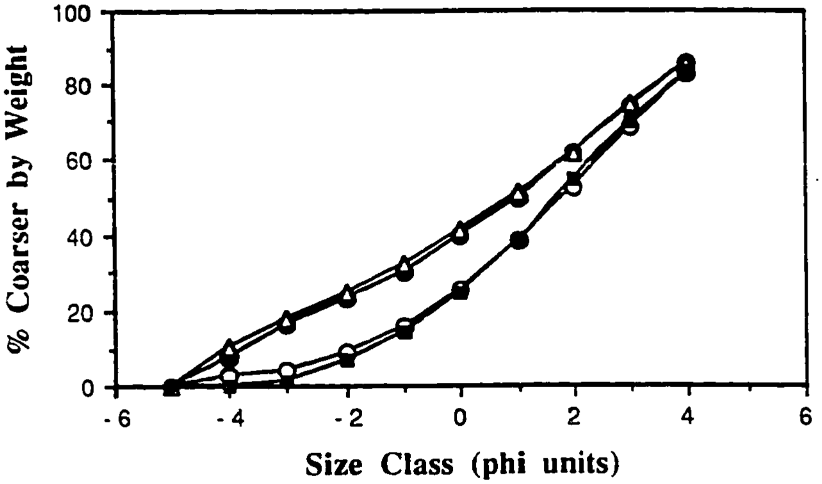

100
80
60
40
20
0
% Coarser by Weight
-6
-4
-2
0
2
4
6
Size Class (phi units)

Figure 3.9

C. Grain-size distribution of the < 2 mm fraction. Symbols as in A.

D. Comparison with grain-size distribution of the 1980 North Fork Toutle River Lahar (data from Scott (1988)). Symbols: dashed lines are total Black Canyon grain-size distributions; North Fork Lahar at 14.7 km (squares), 47.8 km (triangles), and 97.7 km (circles) (distances from Mt. St. Helens crater).

C

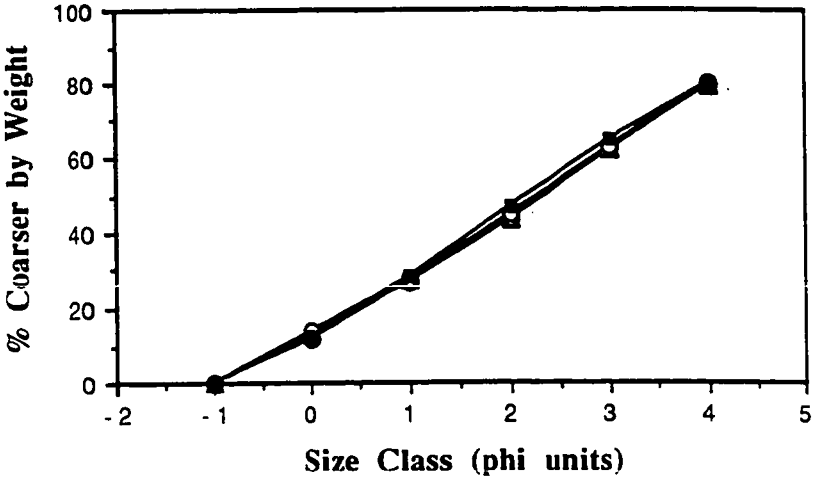
% Coarser by Weight
100
80
60
40
20
0
-2
-1
0
1
2
3
4
5
Size Class (phi units)

D

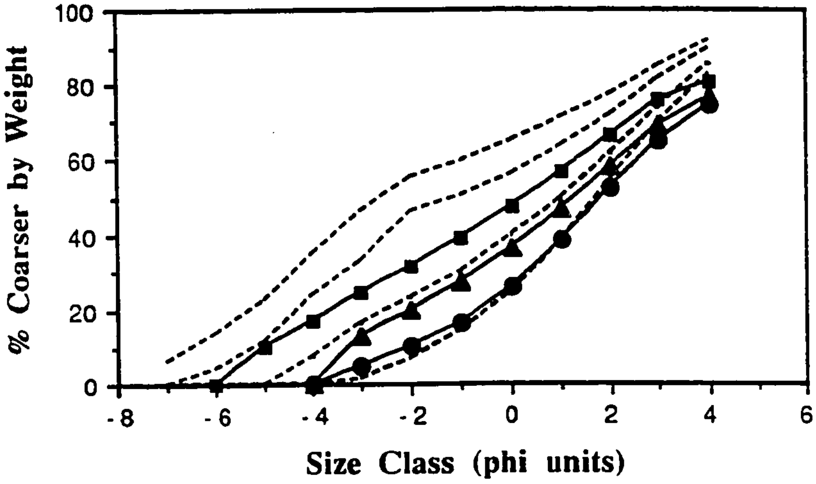
% Coarser by Weight
100
80
60
40
20
0
-8
-6
-4
-2
0
2
4
6
Size Class (phi units)

Figure 3.10. Example channel centerline curvature and cross section surveys used in the back-calculation of debris-flow viscosity. The range of acceptible discharge estimates (Table 3.2) for each cross-section was determined from the range of mean velocity estimates (equation 3.13a) and the range of plausible flow cross-sectional areas accounting for possible non-linearity of the flow surface profile (concave upward).

A. Upper plot: Centerline curvature survey indicating locations of cross-sections A, B, and C. Radius of curvature fit by eye to both curves also indicated. Lower plot: Cross-section and flow surface profile reconstructed from mudlines at section A ($r_c = 58.5$ m).

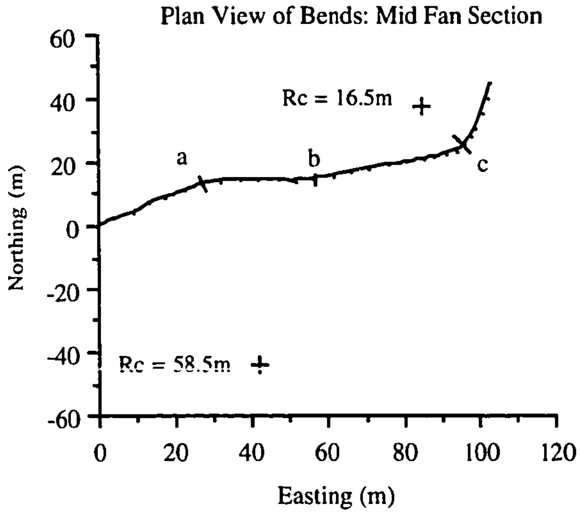
Plan View of Bends: Mid Fan Section
Rc = 16.5m
Rc = 58.5m
a
b
c
Northing (m)
60
40
20
0
-20
-40
-60
Easting (m)
0
20
40
60
80
100
120

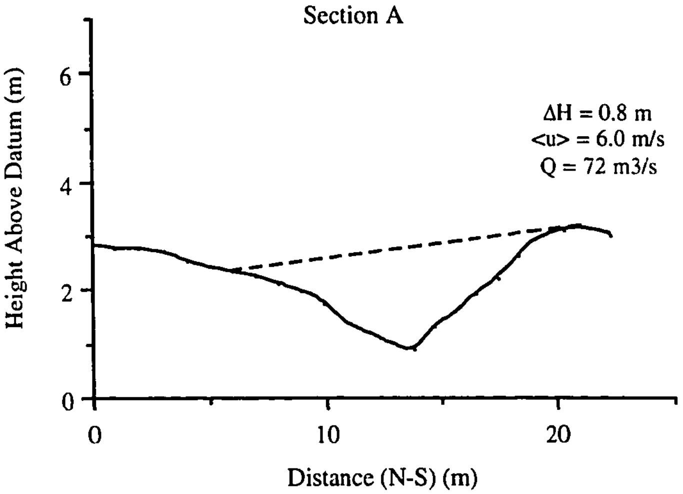
Section A
ΔH = 0.8 m
<u> = 6.0 m/s
Q = 72 m3/s
Height Above Datum (m)
6
4
2
0
Distance (N-S) (m)
0
10
20

Figure 3.10. B. Upper plot: Cross-section and flow surface profile reconstructed for the straight reach, section B. Back calculation for viscosity was done using this section and discharge estimates from the two curves (sections A and C). Lower plot: Cross-section and flow surface profile reconstructed from mudlines survey at section C ($r_c = 16.5$ m)

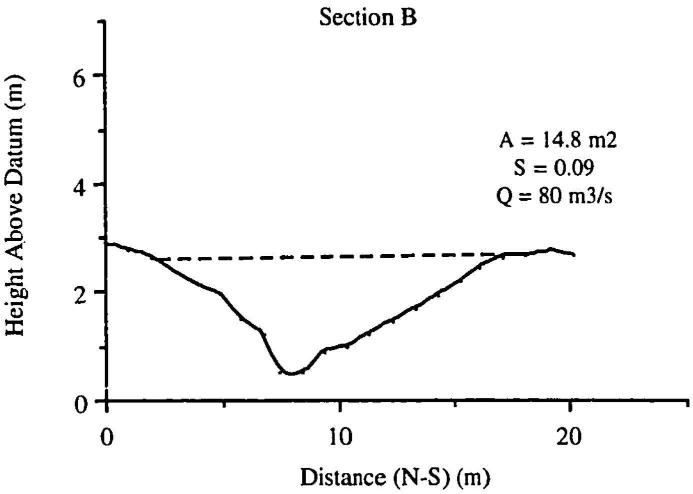
Section B
Height Above Datum (m)
0
2
4
6
0
10
20
Distance (N-S) (m)
A = 14.8 m2
S = 0.09
Q = 80 m3/s

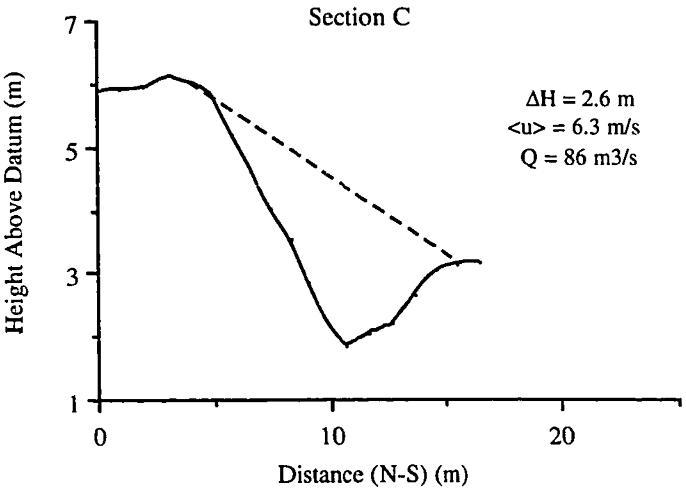
Section C
Height Above Datum (m)
1
3
5
7
0
10
20
Distance (N-S) (m)
ΔH = 2.6 m
<u> = 6.3 m/s
Q = 86 m3/s

back-calculation procedure (Figs. 3.8 and 3.10). These straight channel reaches were selected for back-calculation of flow viscosity because they provide the closest approximation to the conditions of steady, rectilinear flow assumed in the calculations. Cross sections were surveyed at locations where no super-elevation of mudlines could be detected and where the channel bed had either not been significantly lowered by post-debris-flow fluvial erosion or the former channel bed could be reconstructed. Viscosity was then back-calculated for each surge from the discharge and yield strength estimates.

The back-calculation procedure involved calculating the discharge (Q_{calc}) of a flow with the yield strength determined in the field and a reference viscosity (μ_o). Since discharge is inversely proportional to viscosity, the actual viscosity (μ) of the flow can be determined directly from the relation:

$$\mu = \mu_o \left(\frac{Q_{calc}}{Q_p} \right). \tag{3.14}$$

No iteration is required. Viscosities estimated in this manner are subject to the errors in the yield strength estimate, the average velocity estimate, and the reconstructed estimate of flow cross-sectional area. Therefore, viscosity estimates are reported as the plausible range allowed by field data (Table 3.2). Estimates of the effective Newtonian viscosity were also obtained for each surge by repeating the viscosity calculation for the case of a zero yield strength.

These results (Table 3.2) document a well-defined correlation between yield strength and viscosity. Inter-surge differences in yield strength and viscosity may be attributable to differences in grain-size distribution, water content, or both. Water contents of the Black Canyon debris flows are unknown and it is not possible to make a definitive statement about the relative contribution of grain-size effects to the differences in rheology. However, observed differences in debris granulometry are minimal, and the inter-surge differences in yield strength and viscosity are consistent with a progressive dilution of successive surges of the Black Canyon debris flows -- a phenomenon commonly observed in debris flows elsewhere (Okuda, and others, 1980; Pierson, 1984; Pierson, 1986).

Discussion of Field and Laboratory Estimates of Rheological Parameters

The field estimates for the Black Canyon debris flows overlap with, and follow the same trend as, laboratory estimates for deposits of the 1980 North Fork Toutle

Figure 3.11 Rheology of the 1983 and 1990 Black Canyon debris flows. Laboratory estimates for the granulometrically similar North Fork Toutle lahar obtained in two independent studies are shown for comparison. Symbols: Black Canyon field data (solid squares with error bars); experimental data of Major and Pierson (1992) (open triangles); experimental data of Fairchild (1985) (shaded region). Both laboratory studies show systematic increases in both yield strength and viscosity with decreasing water content (i.e., water content decreases from lower left to upper right in this plot).

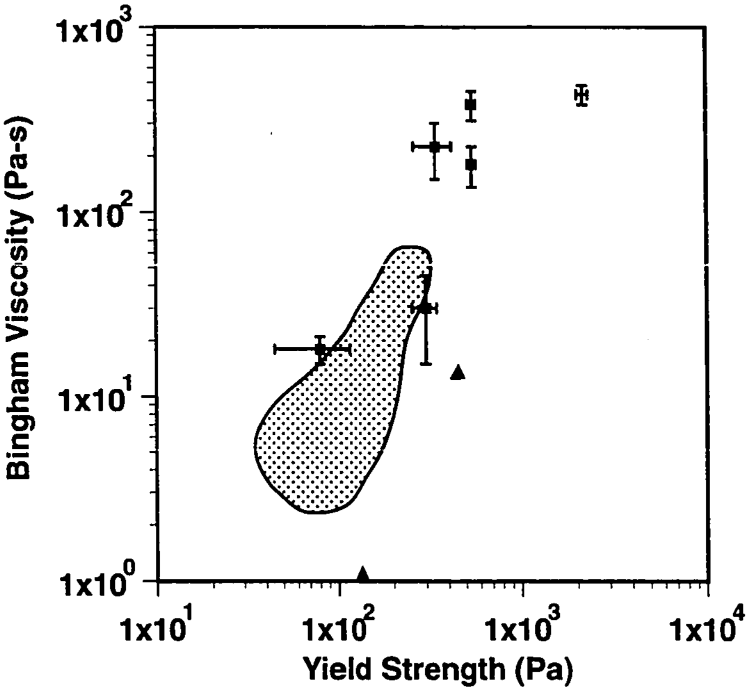
1x10^3
1x10^2
1x10^1
1x10^0
Bingham Viscosity (Pa-s)
1x10^1
1x10^2
1x10^3
1x10^4
Yield Strength (Pa)

Table 3.2. Hydraulic and Rheological Parameters: Black Canyon, California.

Debris-Flow Surge	Cross-sectional Area (m^2)	Average Velocity ($m\ s^{-1}$)	Peak Discharge ($m^3\ s^{-1}$)	Yield Strength (Pa)	Bingham Viscosity (Pa s)	Newtonian Viscosity (Pa s)
83-II*	56	7.8	435 ± 15	2150 ± 150	430 ± 50	1000
83-IIIa'	19	5.2	95 ± 15	540 ± 30	380 ± 70	550
83-IIIb'	13	6.0	75 ± 12	540 ± 30	180 ± 45	290
83-IV	6	4.8	22 ± 8	300 ± 45	30 ± 15	60
90-I	13	5.2	68 ± 10	340 ± 80	225 ± 75	280
90-II	2	4.5	8 ± 1	80 ± 35	18 ± 3	22

* No estimates available for pulse 83-I.

' Estimates a & b for pulse 83-III taken at different locations.

River lahar at Mt. St. Helens (Fairchild, 1985; Major and Pierson, 1992) (Figs. 3.9 and 3.11). Grain-size distributions in these deposits are similar (Fig. 3.9d). In fact, the experimental mixture used by Major and Pierson (1992) is nearly identical to the <2 mm fraction of the Black Canyon deposits (22% in the experiments as compared to 18-20% silt-and-clay in the field case). Substantial differences in flow behavior might be expected, however, because of the presence of gravel in the field. Interestingly, the flume experiments of Fairchild (1985) excluded only the coarse gravel fraction (> 22 mm). Comparison of the there data sets suggests, but does not prove, that the presence of the gravel fraction did not play a dominant role in setting the rheology of the Black Canyon debris flows.

To interpret the Black Canyon data in the context of previously published rheological analyses, it is important to understand why field and laboratory estimates of rheological parameters generally do not overlap (e.g., Fig. 3.3). First, a common problem in laboratory analyses of debris slurries (particularly those including coarse materials) is slippage between the slurry and the walls of the apparatus (e.g., O'Brien and Julien, 1988). If this occurs and goes undetected, viscosities may be grossly underestimated. Second, in the field, any accelerations felt by the debris flow will be incorporated into the viscosity estimate, which is derived under the assumption of steady, uniform laminar flow: conditions in which flow is not yet fully developed, or in which roughness elements and/or channel curvature retard the flow of the debris, will result in overestimation of the viscosity (e.g., Johnson and Rodine, 1984; Pierson, 1985; Macedonio and Pareschi, 1992). However, unless such effects are modeled explicitly, it is appropriate to incorporate them into the viscosity parameter, so long as their effect is averaged over some appropriate distance or number of irregularities. Only data from similar settings should be used. Finally, as described earlier, the presence of coarse clasts in field-scale debris flows may importantly influence the mechanical behavior of the debris, affecting the effective yield strength in particular.

Based on these general considerations, I speculate on the lack of accordance between field and laboratory estimates (Fig. 3.3). In the case of the Bolluck Creek debris flows at Mt. Thomas, New Zealand, the major difference between field and laboratory measurements appears to be related to the role the coarse clastic fraction (> 32 mm) plays in the effective yield strength of debris flows (Pierson, 1980; Phillips and Davies, 1991). The importance of this effect was highlighted in Phillips' and Davies' large rheometer experiments and Pierson's field observations of the thicknesses of clast-poor lobes suggest yield strengths that overlap with the laboratory estimates for clast-free (> 32 mm removed) samples. Conversely, in the case of the debris flows of China's Jiang Jia Gully (Li, and others, 1983), field estimates appear to be fairly well constrained, and laboratory estimates may be affected by slip between the slurry and the smooth-walled viscometer used in that study (Coussot, personal communication, 1992).

The differences in viscosity estimates by Fairchild (1985) and Major (1992) for the North Fork lahar may reflect differences in either debris granulometry (see above) or experimental design. Fairchild (1985) analyzed flume data assuming that the flow was steady, fully developed and one-dimensional. Any sidewall drag and/or down-flume acceleration was therefore incorporated into the effective viscosity; the reported viscosities are limiting maximum values. Conversely, the coaxial rotating cylinder rheometer used by Major and Pierson (1992) can be expected to yield minimum estimates of the viscosity for several reasons: (1) the vertical orientation of the cylinders (parallel to the action of the gravitational body force) will minimize frictional contributions to the effective viscosity (Iverson, pers. comm., 1993); (2) segregation of material and non-uniform sediment concentrations within the annulus can be a problem in these devices; and (3) shear was only observed in a narrow band adjacent to the inner cylinder, suggesting, in reference to (2) above, that only the viscosity of a relatively dilute boundary layer was measured with this device.

Debris-Flow Routing

Simple Mass Balance Routing

A simple mass balance routing scheme is illustrated in Figure 3.12. Input for the mass balance routing scheme includes: (1) a series of surveyed channel cross sections that divide the channel into study reaches; (2) measurement of channel bed slope at each cross section; (3) an input hydrograph, including stage and water content as a function of time; and (4) information on yield strength and viscosity as a function of water content. Steady, uniform laminar flow is assumed and all accelerations (unsteady flow, convective acceleration around bends, exchange of momentum between the channel and overbank flows, backwater effects) are ignored. Using the equations in Table 3.1, the conveyance capacity (i.e., the bankfull discharge) of each cross section is calculated as a function of water content and the input hydrograph is routed down-channel according to the rules illustrated in Figure 3.12.

Figure 3.12 Schematic illustration and definition of the mass balance routing scheme.

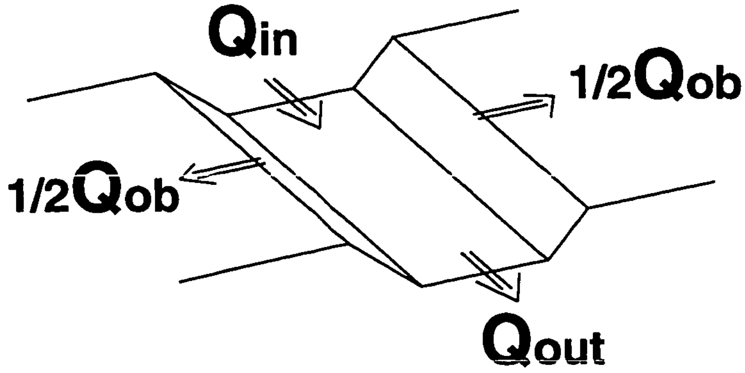
Qin
1/2Qob
1/2Qob
Qout

C_c = Conveyance Capacity
V = Volume Deposited Overbank
L = Length of Reach
W = Half-Width of Inundation

$Q_{out} = MAX\ (Q_{in}, C_c)$
$Q_{ob} = Q_{in} - Q_{out}$
$V = Q_{ob} * Duration$
$W = 0.5 V_r g S / (L \tau_o)$

Application of this simple routing scheme to the 1983 Black Canyon debris flow is illustrated in Figure 3.13, which demonstrates that the gross pattern of overbank deposition of well channelized debris flows can be captured with the simple mass balance routing scheme. Cross sections 2 and 3 are the only sections not used in the 'calibration' of the Bingham model to the Black Canyon flows, and depositional patterns on either side of these sections constitute the only real test presented by the analysis (only one of the four surges was 'calibrated' at each of the other sections); Figure 3.13 is offered as a general proof of concept rather than a rigorous test of the mass balance routing scheme. Mass balance routing is appropriate for addressing geological questions of a heuristic nature relating to either fan morphology or stratigraphy, but is too crude to be useful in site-specific engineering analyses. For such studies, more advanced hydrodyamic models, at least, are required.

Hydraulic Routing Models

Results of the numerical simulations reported here have important potential applications in both one- and two-dimensional hydraulic models of debris-flow runout and deposition. In hydraulic routing models, the internal mechanics of the flow process, and the influence of boundary roughness and channel geometry are all represented by the friction slope term, which relates the total boundary shear stress to the average velocity of the flow (French, 1985). If they are to predict accurately debris-flow runout, it is imperative that correctly formulated friction slope terms be incorporated into hydraulic models. This condition has generally not been met in existing debris-flow routing models (Takahashi and Tsujimoto, 1985; MacArthur and Schamber, 1986; Mizuyama, and others, 1987; Takahashi, 1991; O'Brien, 1993). For instance, the formulation used by both MacArthur and Schamber (1986) and O'Brien (1993), purportedly for Bingham fluids, fails to predict the correct relationship between channel slope and average velocity in the simple case of steady uniform flow in an infinitely wide channel.

Insofar as the Bingham model is appropriate for the type of debris flow to be modeled, accurate friction slope estimates can be derived directly from the model results presented in Table 3.1. FIDAP was used to solve for the flow field under conditions of steady, rectilinear flow. Under these conditions, the energy grade line, the flow surface and the channel bed are all parallel; the friction slope and the bed slope are equal. Determining average velocity ($\overline{U}$) from equation (3.8) ($\overline{U}$ = Q/WH, for

Figure 3.13 Observed and predicted overbank deposition volumes per reach for the 1983 Black Canyon debris flow using the mass balance routing scheme. Reach definition and cross section locations are shown on Figure 3.8. A). Deposit volumes estimated from field data. B). Overbank deposit volumes predicted in the calculation.

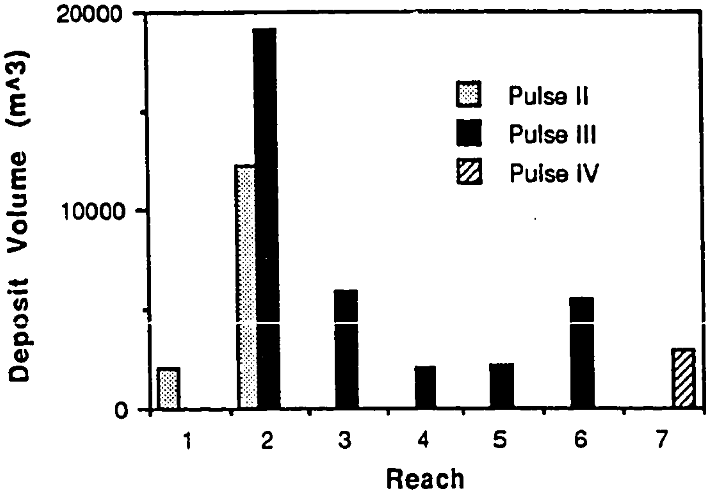

Estimated Deposit Volume

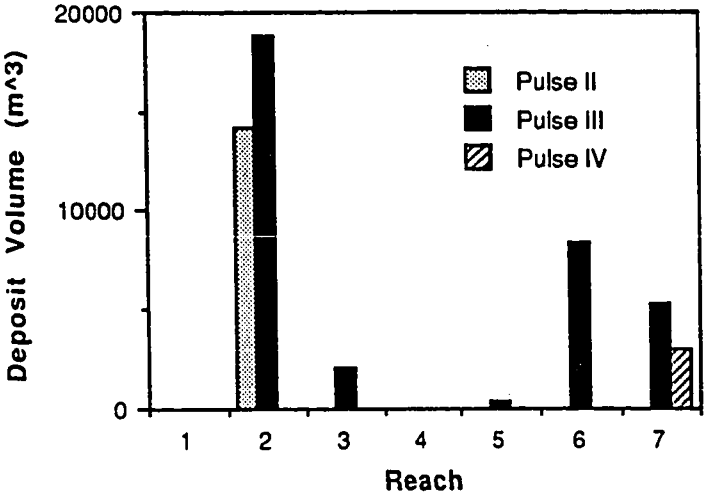

Predicted Overbank Deposition

rectangular channels) and solving for slope therefore yields an expression for the friction slope (S_f) for flow through rectangular channels:

$$S_f = \frac{\overline{U}\mu}{\rho g H^2 K(\Theta)\left[a\left(\frac{\tau_o}{\tau_{cr}}\right)^3 - b\left(\frac{\tau_o}{\tau_{cr}}\right) + c\right]}\,, \qquad (3.15)$$

where K(Θ), a, b, and c are given in Table 3.1 and τ_{cr} is assumed to be a function of bedslope only. Equation (3.15) provides an estimate of the friction slope that accurately accounts for sidewall drag in rectangular channels with a wide range width-to-depth ratios. The formulation used by MacArthur and Schamber (1986) and O'Brien (1993) drops important terms from equation (3.15) and takes no account of cross-sectional channel geometry. Similar expressions are easily derived for elliptical and trapezoidal channels: equation (3.15) must simply be adjusted for differences in cross-sectional area. The assumption that τ_{cr} is a function of bed slope alone is generally acceptable, but could result in significant error in places where bed slope changes abruptly, resulting in a strong divergence between the bed slope and the energy grade line. Even granted this limitation, incorporation of equation (3.15) as the friction slope term in existing Bingham debris-flow routing models is recommended.

CONCLUSIONS

Numerical solution of steady, uniform, rectilinear open-channel flows of Bingham fluids was undertaken, motivated by the need to develop predictive capabilities in the modeling of debris-flow runout and deposition. The solutions were obtained with commerically available finite-element code that uses well established solution scheme for non-Newtonian flows (Bercovier and Engleman, 1980; Gartling and Phan-Thien, 1984; Walton and Bittleston, 1991; Szabo and Hassager, 1992) and were used to constrain, via a regression analysis, a set of empirical equations that give discharge and plug velocity as functions of channel geometry, channel slope, and material properties.

Although the applicability of the Bingham model to natural debris flows has been questioned (e.g., Iverson and Denlinger, 1987), there is experimental evidence that mud-rich sandy slurries behave approximately as Bingham fluids (Fairchild, 1985; O'Brien and Julien, 1988; Phillips and Davies, 1991; Coussot, 1992; Major and Pierson, 1992; Coussot and Piau, in press). Application of the Bingham constitutive equation to debris flows assumes that matrix deformation governs the macroscopic behavior of the flow and that dynamic effects such as particle collisions and friction, pore fluid migration or escape, and formation and destruction of grain networks are either negligible or are collectively manifested as an approximately Bingham behavior (Phillips and Davies, 1991; Coussot, 1992; Major and Pierson, 1992; Major, 1993), assumptions that are most reasonable for muddy, matrix-rich debris flows. The numerical model is used to analyze a well preserved mud-rich debris- flow deposit on the Black Canyon fan in Owens Valley, California. The resulting yield strength and viscosity estimates corroborate and extend the systematic trends seen in laboratory analyses (Fairchild, 1985; O'Brien and Julien, 1988; Coussot, 1992; Major and Pierson, 1992) into the range of commonly observed field values (Costa, 1984). The close correspondence of field and laboratory data lends credence to the application of the simple Bingham equation to mud-rich debris flows. Although similar data are lacking for debris flows with a range of different granulometries, these results are a first step towards developing predictive capabilities in debris-flow modeling with the Bingham model.

ACKNOWLEDGMENTS

This research was funded by the National Science Foundation, Grant EAR-9004843, awarded to the author and T. Dunne. Critical reviews of an early draft by R. Shreve, B. Hallet, and R. Iverson signficantly improved the manuscript. The author is indebted to D. McTigue and D. Gartling for suggesting the FIDAP program. The author is also grateful to the White Mountain Research Station, Bishop Laboratory, for providing accomodation. Galen Whipple, Jason Paur, and Peggy Shippert are acknowledged for their enthusiastic and able assistance in the field.

CHAPTER 4

Lithologic and climatic control of sedimentation patterns on debris-flow fans: implications for fan surface morphology

Chapter 4 integrates the findings of Chapters 1-3 in an analysis of morphological differences between fans derived under a range of lithologic and climatic conditions. Chapter 4 extends and refines the conceptual framework presented in Chapter 2 and the numerous citations of the work of Whipple and Dunne (1992) are simply references to material presented there. The numerical methods developed in Chapter 3 are utilized to obtain field estimates of the rheological behavior of debris flows derived from different lithologic assemblages and then to analyze the controls on channel conveyance capacity to explore the rheologic, and therefore lithologic, controls on fan morphology. The findings of Chapter 1 are utilized to help isolate the contributions of lithologic, tectonic, and climatic controls on fan slope.

INTRODUCTION

Understanding the operation of channels in an aggrading depositional environment has long been recognized as a key to understanding fan sedimentation and morphology (Bull, 1977). This statement is true for all types of fan, regardless of whether the dominant depositional process is stream flow, debris flow, or turbidity current. On alluvial fans characterized by a distributary network of shallow, rapidly aggrading and shifting, braided channels, surface aggradation and channel formation are intimately coupled. The mechanics of a braided channel system governs fan sedimentation patterns and their response to environmental variables. Most of the extensive literature on modern fans has concentrated on fluvial processes and the controls on alluvial fan sedimentation (Bull, 1977; Lecce, 1990). However, debris-flow fans, defined as "alluvial fan" landforms on which debris flows are the dominant depositional process, are common in mountainous environments worldwide (Blackwelder, 1928; Beaty, 1963; Pierson, 1980; Li, and others, 1983; Suwa and Okuda, 1983). Quite unlike conditions on their fluvial counterparts, channel formation (by fluvial incision) and surface aggradation (by debris-flow deposition) are largely uncoupled on debris-flow fans. Moreover, Whipple and Dunne (1992) have shown that on these fans the evolution of the channel network, the lateral shifting of depositional centers, and the operation of the sediment dispersal system in general are largely controlled by debris-flow rather than fluvial processes. An implication is that the linkages between fan morphology, hazards, stratigraphic architecture, and environmental variables such as lithology, climate, and tectonics must be entirely different on these two types of fan. Prediction of debris-flow hazards, anticipation of the effects of climate change, and the interpretation of both modern and ancient debris-flow fan bodies in terms of their environment all demand an understanding of these linkages.

The morphology of a debris-flow fan is set by the physiographic, hydrologic, and lithologic characteristics of its source area that dictate the size and down-fan extent of channels on the fan surface, the frequency distribution of debris-flow hydrographs and rheologies, and the sedimentation rate, because these factors govern the interaction of the channels and debris flows. Consequently, the morphology of debris-flow fans in different settings varies widely on a gross scale (average fan slope, cross-fan convexity) and a fine scale (channel density, channel network structure, surface texture, levee heights and widths). Whipple and Dunne (1992) developed a conceptual model of debris-flow fan construction and outlined the role of debris-flow rheology in establishing fan sedimentation patterns, and, consequently, surface morphology. However, they considered fans in only one geologic setting and could not address the relative roles of lithologic, climatic, and tectonic conditions in determining fan morphology. Tectonic control of overall fan morphology (size, average slope) was discussed in Chapter 1. Here I address lithologic and climatic controls on: the size and down-fan extent of channels, the frequency distribution of debris-flow rheologies, and the style and frequency of channel avulsions. Specifically, I focus on the role of three factors in controlling the debris flow-channel interaction: (1) boulder abundance, (2) debris fines content, and (3) the hydrologic conditions associated with debris-flow initiation.

CONCEPTUAL FRAMEWORK

Factors critical to fan morphology that can be expected to vary with source basin lithology and climate include: (1) typical stream flow discharges; (2) the quantity and size of sediment delivered to the fluvial system; (3) the temporal frequency of debris flows; (4) debris-flow initiation mechanisms, initiation site geometries, failure volumes, and water contents at failure; (5) source regolith granulometry; (6) amount of flow bulking by channel scour; (7) amount of dilution by mainstem and tributary stream-flow discharges; and (8) the magnitude of subsequent stream-flow discharges.

Factors (1), (2), (3) and (8) determine the "efficiency" of the fluvial system and factors (4) through (7) the frequency distribution of debris-flow hydrographs and rheologies. The linkages between these variables and debris-flow fan morphology are outlined below in a qualitative manner.

Whipple and Dunne (1992) established that the depositional morphology of an aggrading debris-flow fan surface is most directly controlled by the combination of the "efficiency" of the fluvial system and the frequency distributions of the rheologies and hydrographs of the debris flows delivered to the fan. The "efficiency" of the fluvial system refers to the stream's ability to maintain deep channels on the fan surface. Fluvial channels strongly influence debris-flow depositional patterns by directing the dispersal of debris-flow sediments to all parts of the fan. Therefore the size, slope, and down-fan extent of the fluvial channels are important variables. For channels of a given geometry the rheology and hydrographs of the debris flows govern the debris flow-channel interaction. Debris flows may be confined within channels and conveyed efficiently down fan, may overwhelm channel banks and deposit overbank, contributing to levee aggradation, or may come to rest in channels, potentially blocking the channel. Thus, the frequency distribution of debris-flow rheologies and hydrographs importantly influences the locus and extent of overbank deposition, the morphology of depositional landforms, and the temporal frequency and spatial pattern of channel blockages.

Channel-blocking events are most often associated with deposition of the driest and most boulder-rich flows and may cause sudden avulsions, depending on the hydrologic conditions associated with debris-flow initiation (i.e., the magnitude of subsequent stream flow discharges) and the erodibility of the freshly emplaced deposit. The spatial and temporal pattern of channel avulsions is crucial in the evolution of fan surface morphology because it sets the channel network structure, the longevity of individual channel courses, and limits the accumulation of channel-margin levees and the development of cross-fan convexity (Whipple and Dunne, 1992). Therefore, elucidation of lithologic and climatic control of the style and frequency of channel avulsion events is a primary goal of this chapter.

APPROACH

Field Site

I study morphological differences between debris-flow fans derived under diverse lithologic and climatic conditions in Owens Valley, California (Fig. 4.1; Chapter

1). The approach is general, but the specific application is somewhat restricted by the range of conditions in Owens Valley. Fan types studied include: (1) fans derived from glaciated basins underlain by granitic rocks (between Independence and Lone Pine at the foot of the Sierra Nevada; locations 4, 5, and 6 on Figure 4.1); (2) fans derived from unglaciated basins underlain by granitic rocks on both the west side (locations 4 and 7 on Figure 4.1) and the east side (locations 1 and 2 on Figure 4.1) of the valley; and (3) fans derived from unglaciated basins underlain by mixed assemblages of metasedimentary, metavolcanic, and granitic rocks (henceforth "mixed-source" fans) on the east side of the valley (location 3 on Figure 4.1). Fans below glaciated basins were aggraded primarily during glacial times (Gillespie, 1982; Bierman, and others, 1991) and their morphologies therefore reflect glacial conditions. Unglaciated basins on the east side of the valley stand in the rain shadow of the Sierra Nevada and currently receive approximately one third the annual precipitation characteristic of the west side of the valley (4-6 cm/yr compared to 10-15 cm/yr; Rantz, 1969). Because granitic-source fans occur in the full range of climatic conditions, and because climate is invariant between the closely spaced White Mountain field sites, lithologic and climatic influences can be studied in isolation.

Research Strategy

Preliminary investigation of fan morphology from aerial photographs and field reconnaissance identified field sites representative of each of the three fan types listed above: (1) the Symmes and Pinyon Creek fans; (2) the Olancha fan on the west side and the Rock Creek fan on the east; and (3) the Jefferies Mine Canyon and Lone Tree Creek fans, respectively. In addition to the three basic fan types listed above, variable boulder abundance was identified as an important secondary lithologic variable within the group of granitic-source fans. Tuttle Creek fan (location 6 on Figure 4.1) was chosen as representative of the boulder-rich variety. These sites are listed in Table 4.1 and are the focus of this chapter.

For each of the chosen field study sites, high-resolution low-sun-angle aerial photographs were obtained to facilitate both remote interpretation and field mapping. Differences in fan surface morphology were documented through a combination of map analysis, interpretation of aerial photographs, field mapping, and topographic surveys. Associated differences in debris-flow sedimentology were documented through a combination of point counting and sieving of sediment samples. Differences in debris-flow rheology associated with different source lithologies (i.e., different debris grain-

Figure 4.1. Location map showing generalized geology of the Sierra Nevada and the White Mountains. Field sites are indicated by number: (1) Montgomery Creek, (2) Rock Creek, (3) Lone Tree Creek and Jefferies Mine Canyon, (4) Black Canyon, (5) Pinyon and Symmes Creeks, (6) Tuttle Creek, and (7) Olancha Creek.

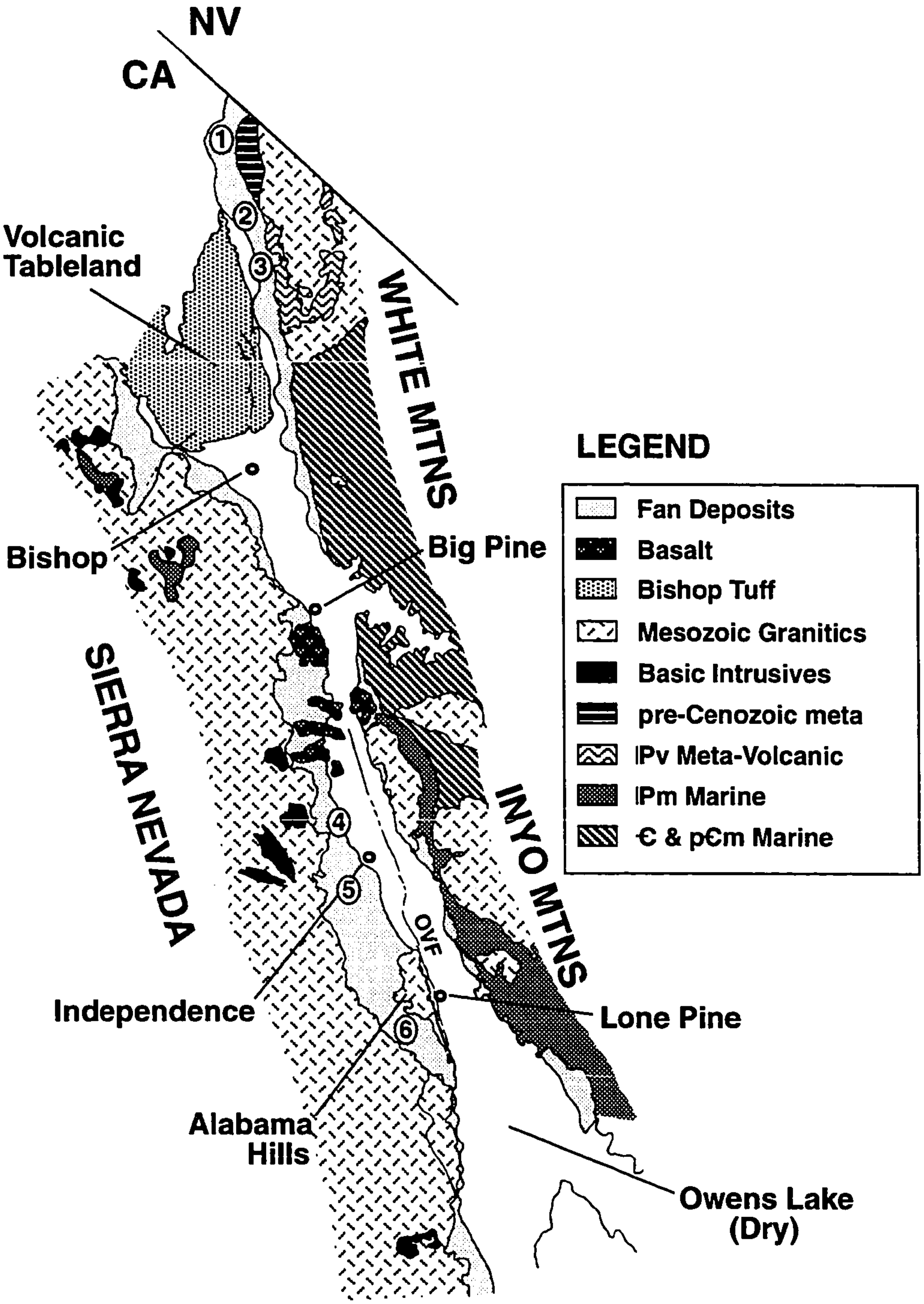
NV
CA
①
②
③
Volcanic Tableland
WHITE MTNS
LEGEND
Fan Deposits
Basalt
Bishop Tuff
Mesozoic Granitics
Basic Intrusives
pre-Cenozoic meta
IPv Meta-Volcanic
IPm Marine
€ & p€m Marine
Bishop
Big Pine
SIERRA NEVADA
INYO MTNS
④
⑤
OVF
Independence
Lone Pine
⑥
Alabama Hills
Owens Lake (Dry)

size distributions) were assessed via a rheological analysis of well preserved modern debris-flow deposits using the methodology and equations developed in Chapter 3. The sedimentology and rheology of granitic-source debris flows on the west side of Owens Valley have already been described Chapters 2 and 3.

Using this basic data set I evaluate the relative morphological influences of the climatic and lithologic differences between the various field sites. Surveys of channel cross sections are used to evaluate climatic control of channel size and slope (reported as the product of channel cross-sectional area and gradient, and henceforth referred to as "channel slope-area product") as a reflection of fluvial "efficiency". Inter-fan differences in the mechanism(s) of channel avulsion and relative channel longevity are inferred qualitatively from the maps and topographic profiles, according to the principles outlined above and in Chapter 2. Owing to the complexity of the process, the discussion of channel avulsion mechanisms and the controls on channel longevity is qualitative in nature. Similarly, data on climatic control of the frequency distributions of debris-flow rheologies and hydrographs are lacking and climatic influences on debris-flow sedimentation can be assessed in qualitative terms only. However, the rheologic and channel cross-section data permit a quantitative analysis of the lithologic influence on debris-flow runout and, hence, the evolution of debris-flow fan morphology. Lithologic effects related to both the boulder abundance and the fines content of debris flows with otherwise similar grain-size distributions are evaluated. The former is assessed through a simple force-balance analysis of the influence of bouldery snouts that form at the front of some debris flows (Takahashi, 1981; Costa and Williams, 1984; Pierson, 1986; Suwa, 1988), and the latter through an analysis of rheologic control of channel conveyance capacity.

DESCRIPTIONS OF FAN SURFACE MORPHOLOGY

Granitic-Source Fans from Glaciated Basins, "Average" Boulder Abundance

The surfaces of these fans, typified by the Symmes Creek fan, are characterized by many well preserved abandoned, boulder-lined channels with little relief on levees, narrow bouldery debris-flow snouts, and generally smooth, low-relief interfluves (Figs. 4.2 and 4.3). The most distinctive feature of these fans is the dense network of abandoned channels. Typically only the most distal 10% of these fans is unchannelized. Average channel density is about 4.5 km^{-1}, equating to a typical channel spacing of about 220 meters (Table 4.2). Channels are arranged in a sub-parallel to dendritic

Table 4.1. Fans Studied: Location and Source Area Characteristics

Fan**	Location*	Drainage Area (km^2)	Lithology	Late Pleistocene Climate	Modern Precipitation#
Symmes	5	11.58	Granitic	Glacial	10-15 cm/yr
Pinyon	5	12.25	Granitic	Glacial	10-15 cm/yr
Tuttle	6	21.32	Granitic	Glacial	10-15 cm/yr
Black Canyon	4	6.89	Granitic	Non-glacial	10-15 cm/yr
Olancha	7	12.55	Granitic	Non-glacial	10-15 cm/yr
Rock	2	8.87	Granitic	Non-glacial	4-6 cm/yr
Falls	2	6.89	Granitic	Non-glacial	4-6 cm/yr
Jefferies Mine	3	7.64	Mixed	Non-glacial	4-6 cm/yr
Lone Tree	3	17.96	Mixed	Non-glacial	4-6 cm/yr

* Location reference numbers keyed to Figure 4.1

** Detailed maps and surveys reported for fans in **bold**.

# Data generalized from (Rantz, 1969)

Table 4.2. Channel Types and Drainage Densities.

Fan	Drainage Density (km^-1)	% Unchannelized (area)	Channel Types % Incised	% Raised	% Bldr-levee*
Pinyon Creek	4.26	7	99	1	0
Symmes Creek	4.76	13	99	1	0
Rock Creek	4.4	23	80	12	8
Falls Canyon	5.7	0	73	24	3
Lone Tree Creek	1.01	45	30	70	0
Jefferies Mine Canyon	2.64	37	36	64	0

* denotes shallow channels created by self-confinement of flows between bouldery levees

network, are approximately trapezoidal in cross section with 30-33° side slopes (for more detail see Whipple and Dunne (1992)), and have channel slope-area products ranging from about 10 m^2 at the fan head to less than 1 m^2 on the lower fan. Channel-margin levees are poorly developed and rarely exhibiting relief in excess of 10% of channel depth. Very few channels have been raised above the general level of the fan surface by repeated in-channel and overbank deposition (Table 4.2).

Mappable debris-flow deposits are most common on the upper fan and are usually narrow bouldery snouts, typically 25-40 meters wide and perhaps 100 meters long (Fig. 4.2). On the lower fan, thin, wide overbank deposits of low-sediment-concentration debris flows are dominant on a smooth, low relief surface.

Granitic-Source Fans from Glaciated Basins, "High" Boulder Abundance

Boulder abundance, particularly near the fan head, varies considerably between fans on the Sierran bajada. The abundance of boulders may be controlled by the jointing characteristics of the source pluton, but this hypothesis has not been tested. Fans with the greatest boulder abundances exhibit a suite of distinct morphological characteristics, most noticeably a steeper fan head, which may be attributable to the mechanical behavior debris flows heavily freighted with large boulders, as demonstrated in the simple force-balance analysis presented below. The Tuttle Creek fan, derived from the Whitney Pluton, is a good example of these boulder-rich fans.

Unlike most of the Sierran fans, the Tuttle Creek fan has a segmented profile, with an uppermost reach that is significantly steeper (9.0°) than the upper reaches of less bouldery fans (5.5° - 6.0°), such as the Symmes Creek and Pinyon Creek fans described above (Fig. 4.4). The upper segment ends at an abrupt break-in-slope about 0.6 km downfan, where the fan surface attains a slope (6.6°) more in accord with the other granitic-source fans on the bajada. The uppermost segment of the Tuttle Creek fan is significantly less well channelized than less bouldery fans and the lower reaches of Tuttle Creek fan itself (Figs. 4.5 and 4.6). Shallow, leveed channels raised above the general fan surface are more common, as are massive, bouldery overbank debris-flow snouts and channel plugs (Figs. 4.5 and 4.6). In addition, overbank debris-flow deposits often appear as large topographic highs consisting of many over-lapping, coalesced debris-flow lobes (Fig. 4.5). The middle and lower reaches of Tuttle Creek fan are indistinguishable from those of the less bouldery granitic-source debris-flow fans studied here and by Whipple and Dunne (1992) and channel sizes are similar (see Figs. 4.2-4.6).

Granitic-Source Fans from Unglaciated Basins of the Sierra Nevada

Along the Sierran front, a number of granitic-source fans derived from basins that were either unglaciated or that supported only small headwaters glaciers were studied during the preliminary aerial photograph and field reconnaissance, including the Olancha Creek and the Black Canyon fans (Table 4.1; Fig. 4.1). Black Canyon may have supported a small glacier in its upper basin (Gillespie, 1982), but most of the basin was effectively unglacierized. Stream hydrology and the conditions of debris-flow initiation in this basin were probably little different from comparable unglaciated basins. I assume that this was the case. The Olancha Creek basin was not glaciated. No detailed maps or topographic surveys of these fans are reported here, but it is worth noting that they are in most ways difficult to distinguish morphologically from granitic-source fans below glaciated basins. The one distinguishing characteristic of many, but not all, of these fans is a tendency towards fewer well preserved abandoned channels and a greater percentage of "raised" channels -- channels running down axial highs, presumably accumulated through repeated overbank deposition over a prolonged period of time. The Black Canyon fan exhibits perhaps the most striking example of this morphological characteristic. Channel sizes are similar to those of fans below glaciated basins with similar drainage areas.

Granitic-Source Fans from Unglaciated Basins of the White Mountains

The average slope of these fans is comparable to that of granitic-source fans with similar drainage areas on the western slope of Owens Valley derived from both glaciated and unglaciated basins (Fig. 4.7). The surface morphology of these fans, typified by the Rock Creek fan, is similar to that described above for the granitic-source fans derived from unglaciated basins of the Sierra Nevada.

The upper 20% of Rock Creek fan has a rough surface, is steep (> 7°), and is characterized by many boulder-rich debris-flow snouts and numerous small boulder-lined channels (Fig. 4.8). The surface morphology of upper Rock Creek fan is most similar to the upper reaches of the boulder-rich Tuttle Creek fan, although the channels are smaller. The channels on this upper surface are often shallow with well-defined, bouldery narrow levees and have channel area-slope products of only 2.5 - 3.2 m^2 (Table 4.2; Fig. 4.9).

The surface morphology of the middle and distal reaches of Rock Creek fan is similar to other granitic-source fans in Owens Valley. Channel density is similar (~ 4.4 km^{-1}) to that on the Sierran fans (Table 4.2). However, with exception of a few major

Figure 4.2. **A**. Interpretive map of Symmes Creek fan.

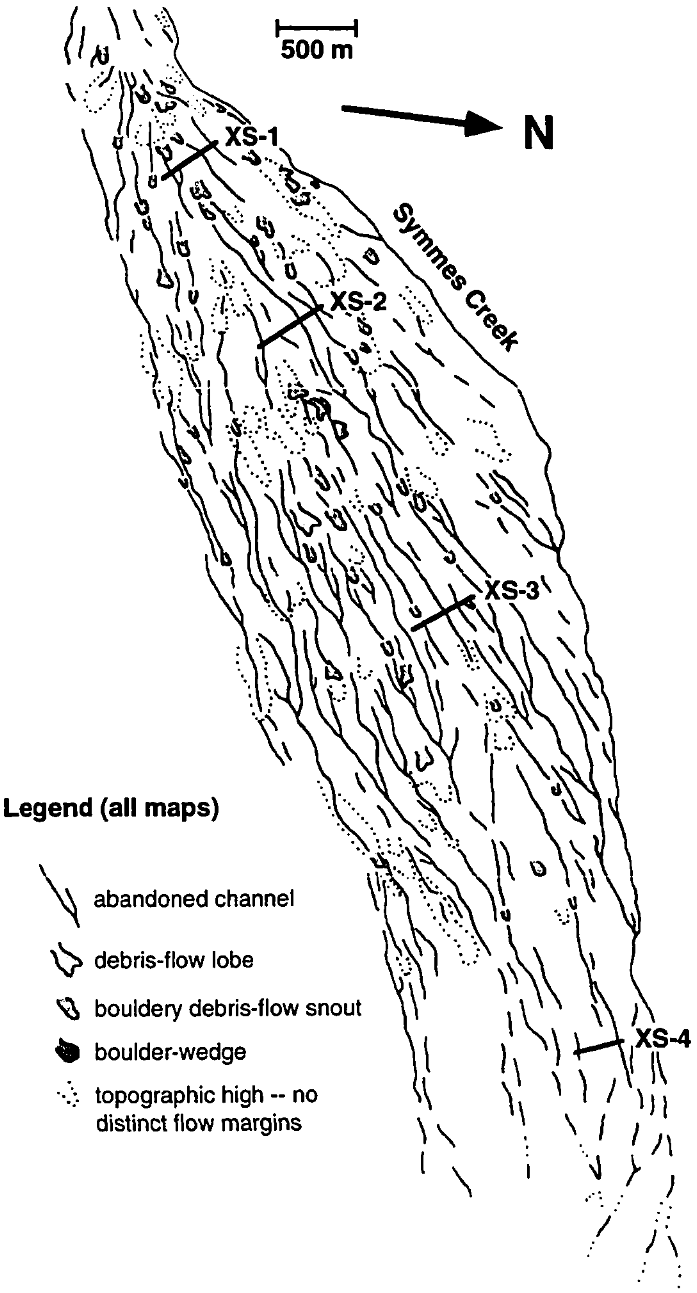
500 m
N
XS-1
XS-2
XS-3
XS-4
Symmes Creek
Legend (all maps)
abandoned channel
debris-flow lobe
bouldery debris-flow snout
boulder-wedge
topographic high -- no distinct flow margins

Figure 4.2. **B**. Aerial photograph of upper Symmes Creek fan.

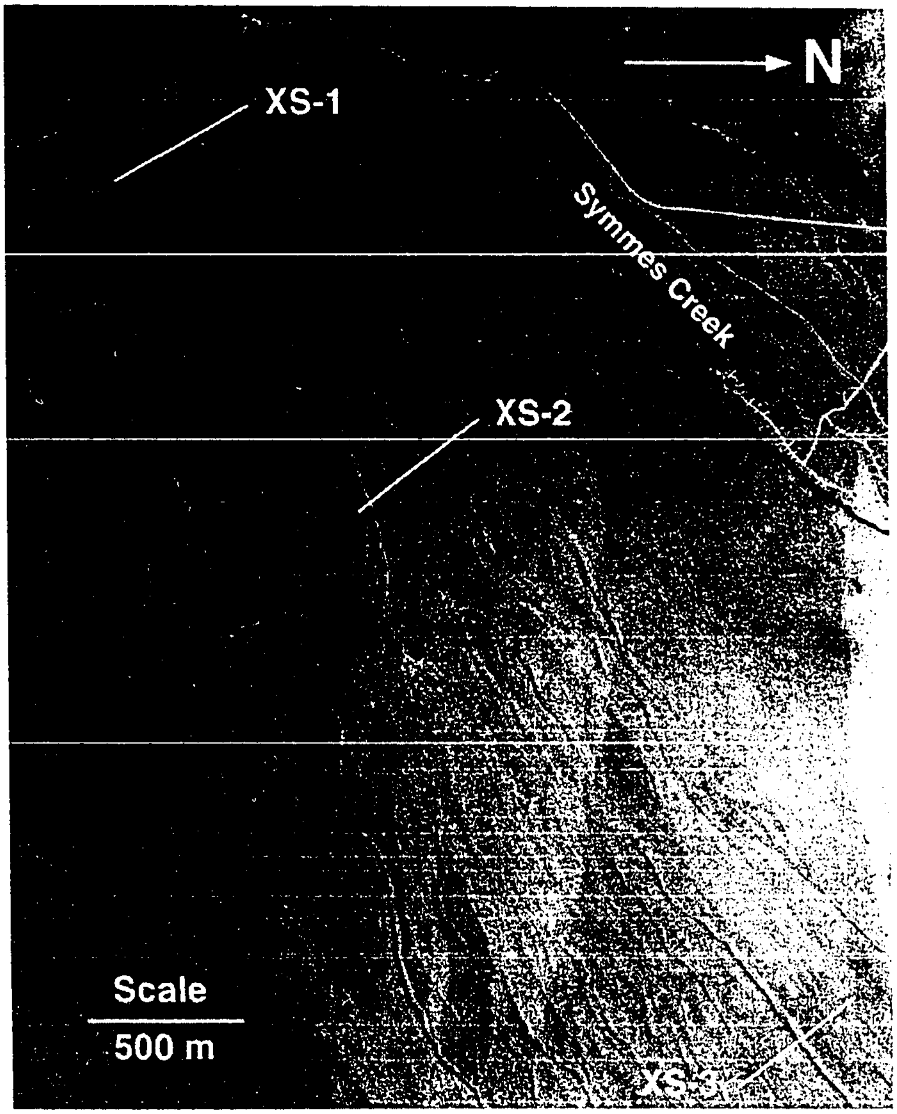
N
XS-1
Symmes Creek
XS-2
Scale
500 m
XS-3

Figure 4.3. Topographic cross sections of Symmes Creek fan (located on Fig. 4.2a).

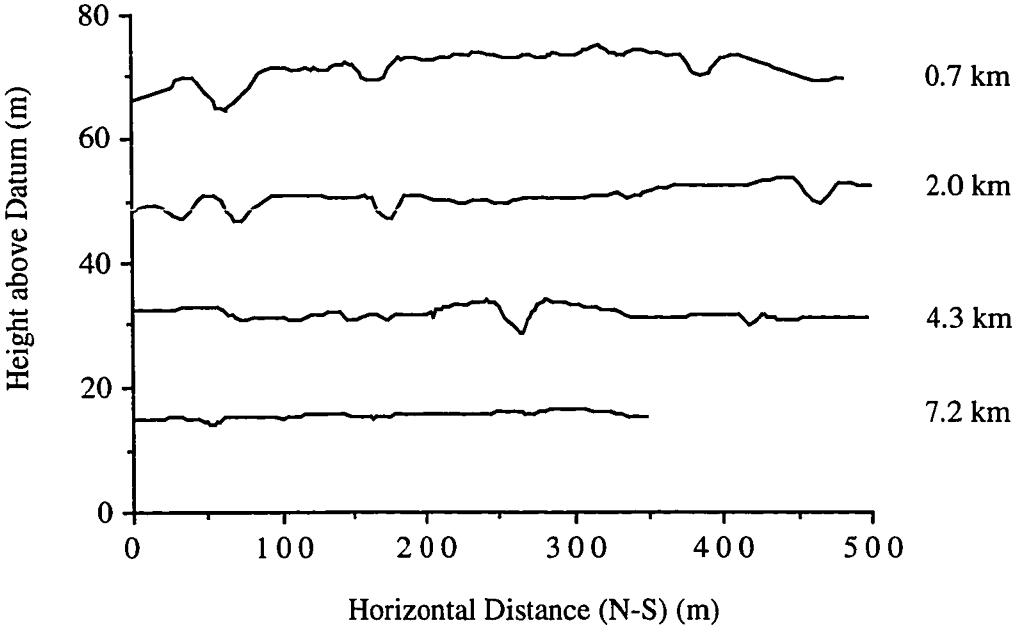
80
60
40
20
0
Height above Datum (m)
0
100
200
300
400
500
Horizontal Distance (N-S) (m)
0.7 km
2.0 km
4.3 km
7.2 km

Figure 4.4. Longitudinal Profiles of uppermost Symmes Creek (dashed line) and Tuttle Creek (solid line) fans. Dotted vertical line marks the sudden break in slope at the base of the steep uppermost "segment".

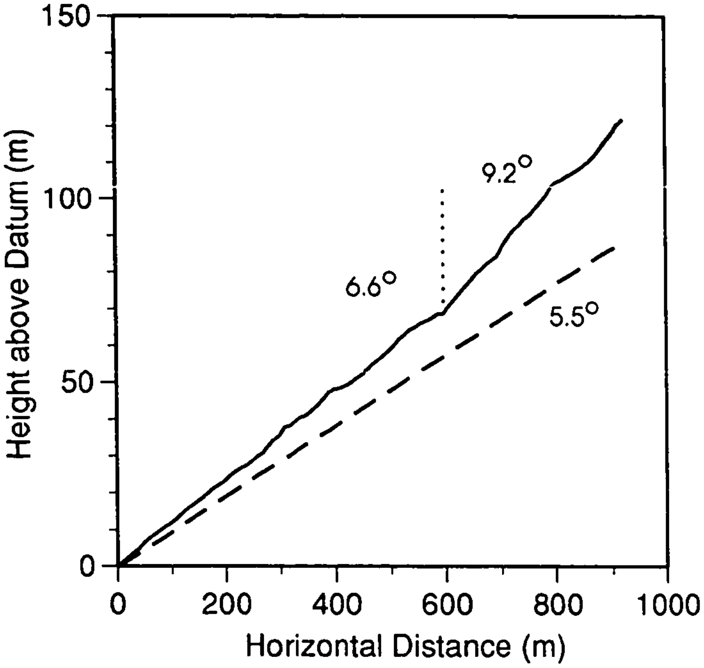
150
100
50
0
Height above Datum (m)
0
200
400
600
800
1000
Horizontal Distance (m)
9.2°
6.6°
5.5°

Figure 4.5. **A**. Interpretive map of upper Tuttle Creek fan.

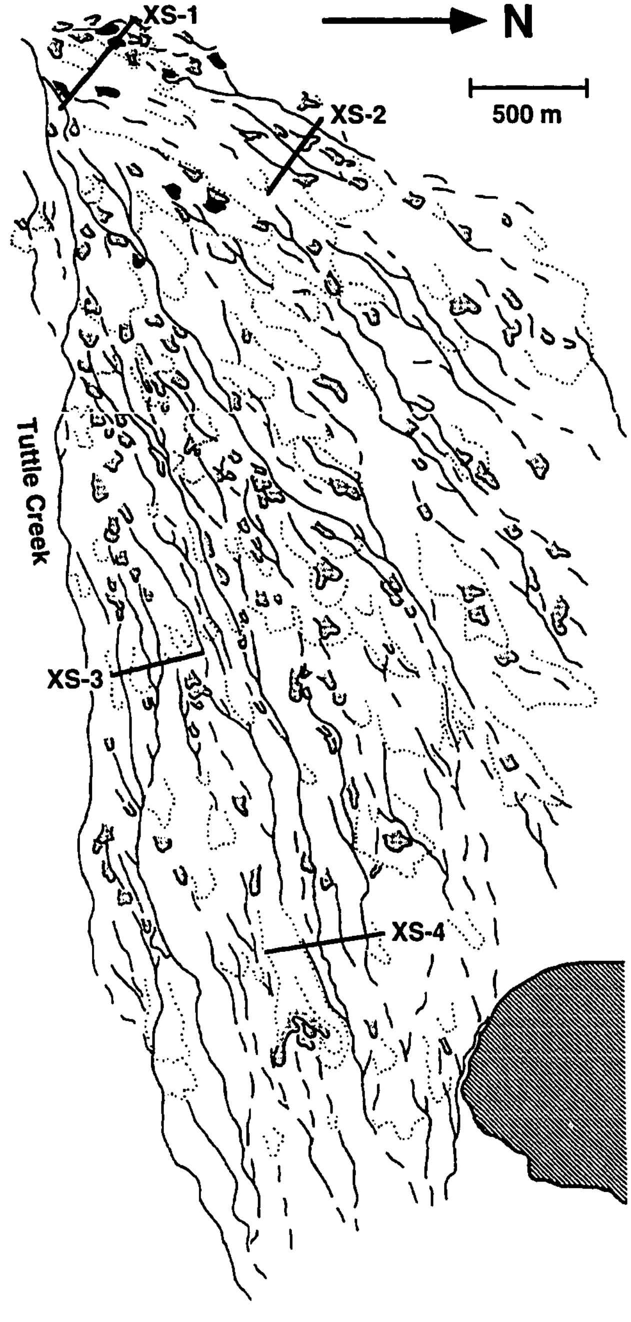
XS-1
N
XS-2
500 m
Tuttle Creek
XS-3
XS-4

Figure 4.5. **B**. Aerial photograph of upper Tuttle Creek fan.

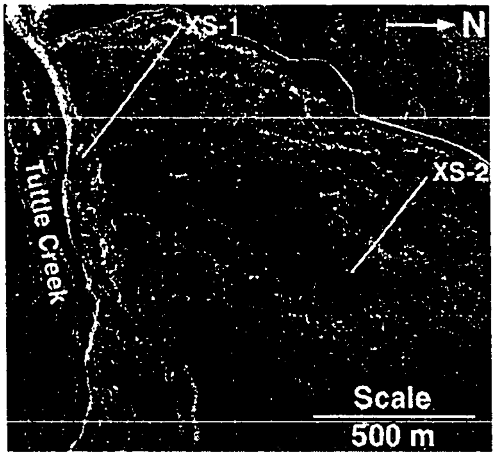
XS-1
N
XS-2
Tuttle Creek
Scale
500 m

Figure 4.5. C. Aerial photograph of the middle section of Tuttle Creek fan.

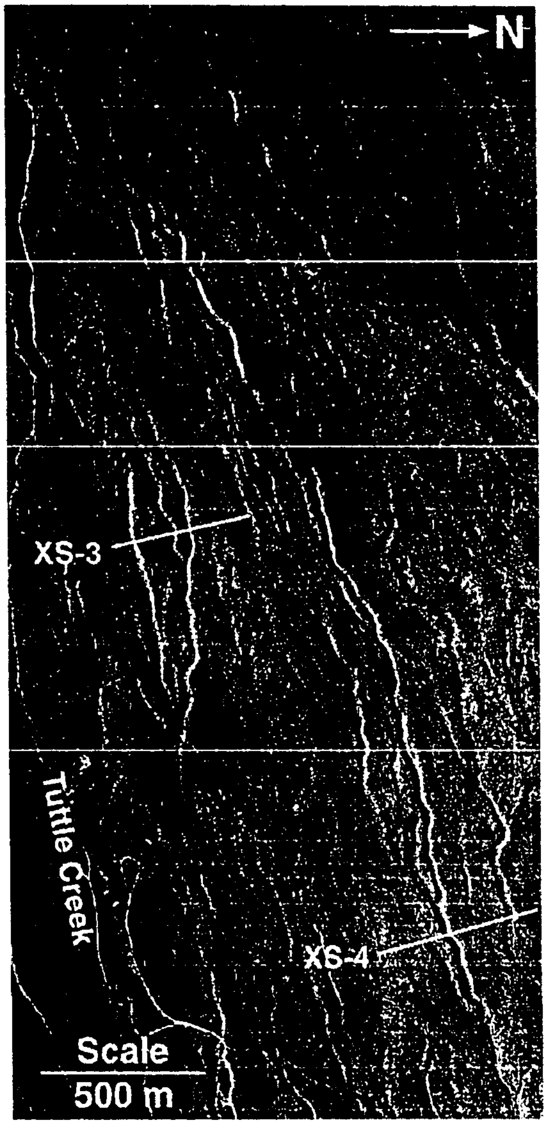
N
XS-3
Tuttle Creek
XS-4
Scale
500 m

Figure 4.6. Topographic cross sections of Tuttle Creek fan (locations shown on Figs. 4.5b and c).

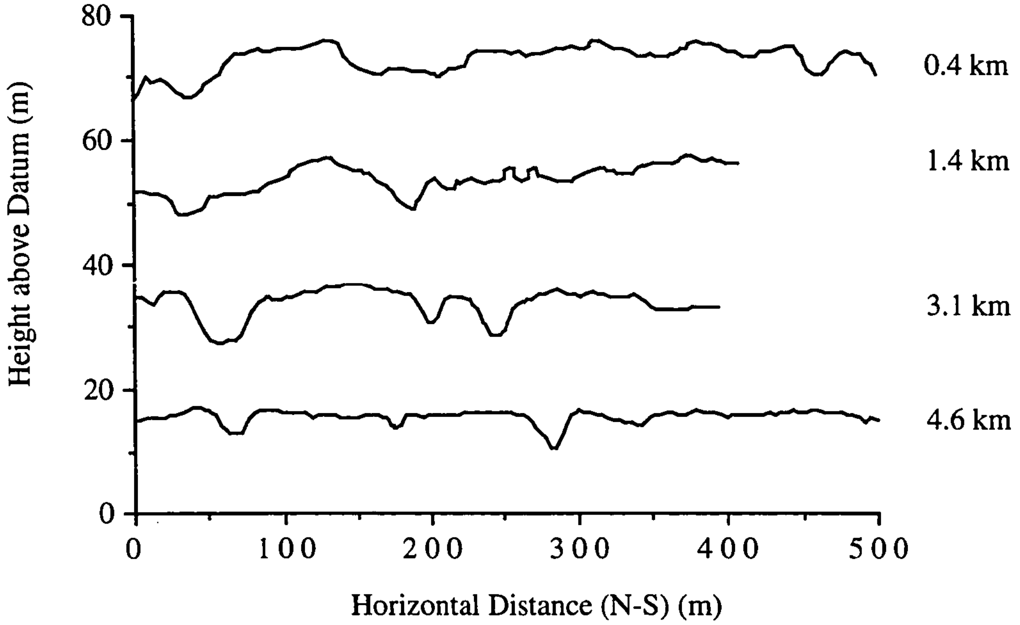

80
60
40
20
0
Height above Datum (m)
0.4 km
1.4 km
3.1 km
4.6 km
0
100
200
300
400
500
Horizontal Distance (N-S) (m)

Figure 4.7. Comparison of average slopes of fans in Owens Valley. Solid triangles: mixed-source fans of the White Mountains. Open squares: granitic-source fans of the Sierra Nevada, including fans from both glaciated and unglaciated basins. Solid circles: granitic-source fans of the White Mountains.

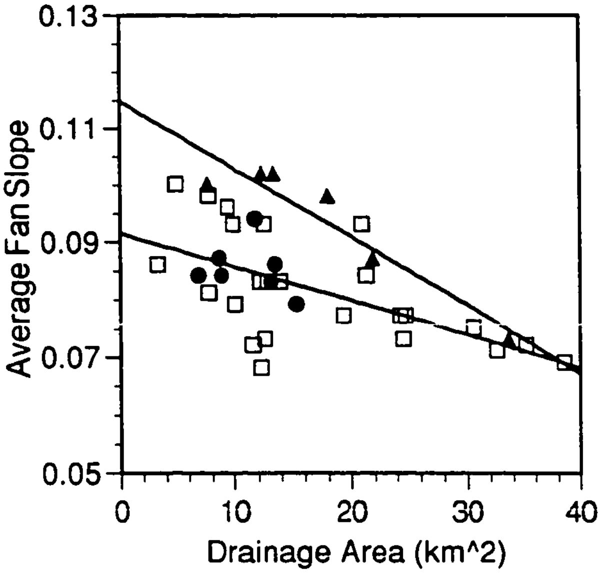
0.13
0.11
0.09
0.07
0.05
Average Fan Slope
0
10
20
30
40
Drainage Area (km^2)

Figure 4.8. A. Interpretive map of Rock Creek fan.

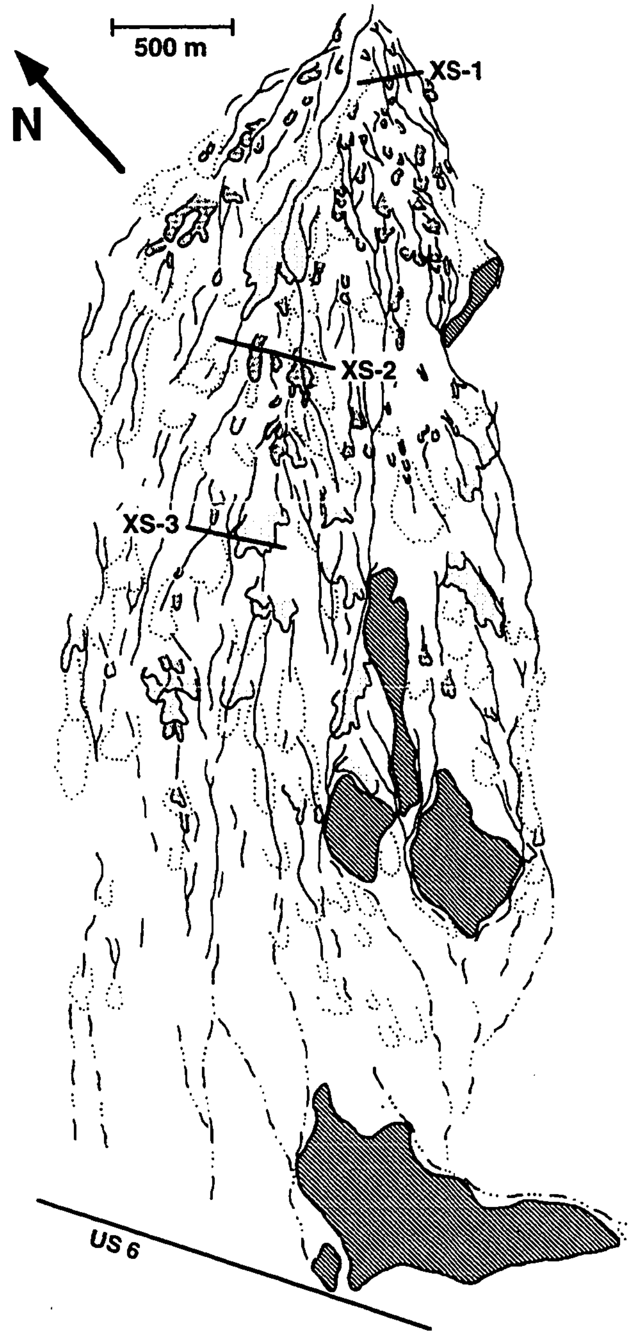
500 m
N
XS-1
XS-2
XS-3
US 6

Figure 4.8. **B**. Aerial photograph of upper and middle Rock Creek fan.

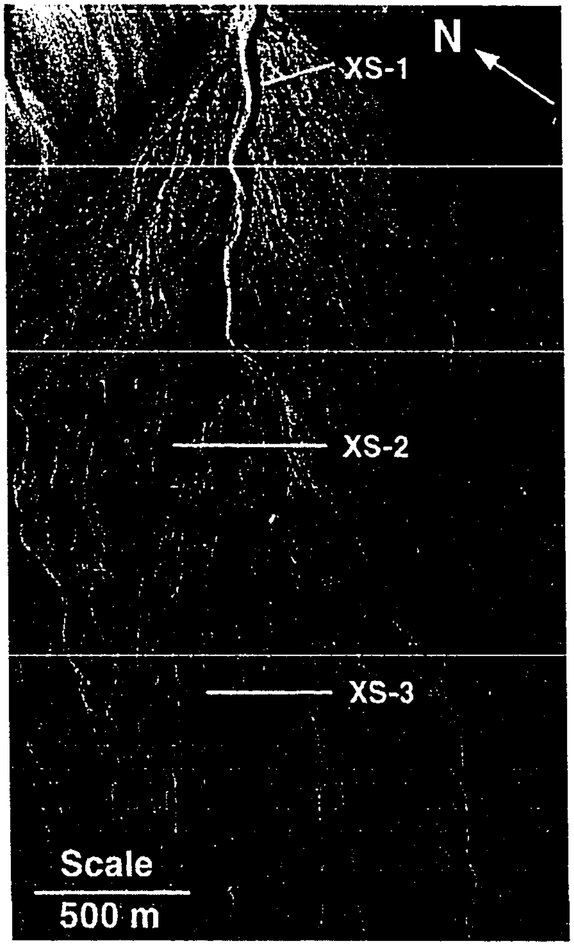
N
XS-1
XS-2
XS-3
Scale
500 m

Figure 4.9. Topographic cross sections of leveed channels on upper Rock Creek fan.

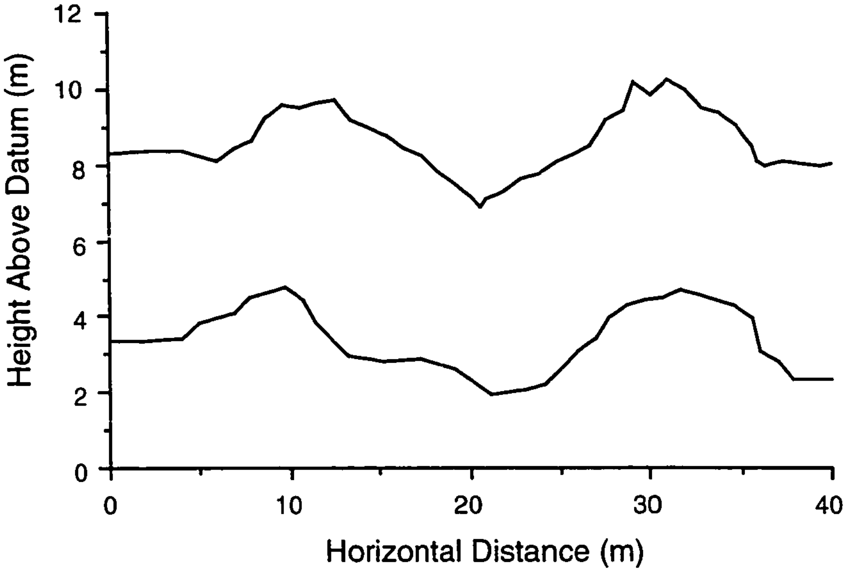
12
10
8
6
4
2
0
Height Above Datum (m)
0
10
20
30
40
Horizontal Distance (m)

Figure 4.10. Topographic cross sections of Rock Creek fan (locations shown on Fig. 4.8b).

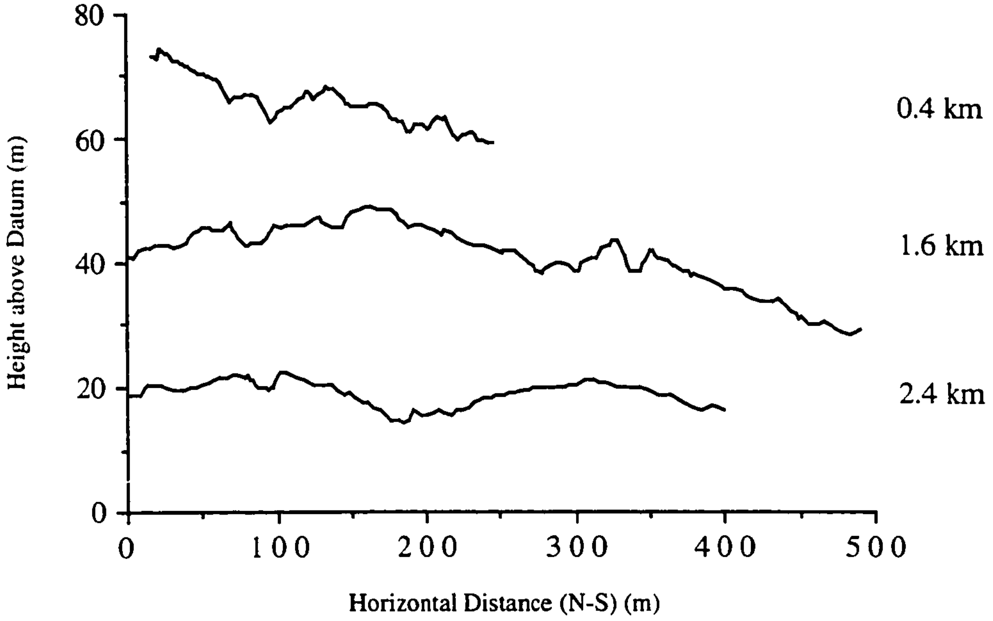

80
60
40
20
0
Height above Datum (m)
0
100
200
300
400
500
Horizontal Distance (N-S) (m)
0.4 km
1.6 km
2.4 km

Figure 4.11. A. Ternary diagram showing total grain-size distributions of typical debris-flow deposits in Owens Valley. Here "gravel" includes all sizes greater than 2 mm. Open squares: granitic-source, Sierra Nevada (glaciated). Solid triangles: granitic-source, Rock Creek fan. Open circles: mixed-source, White Mountains. Dashed triangle indicates the range of grain-size distributions reported by Li et. al. (1983) for the debris flows at Jiangjia Gully.

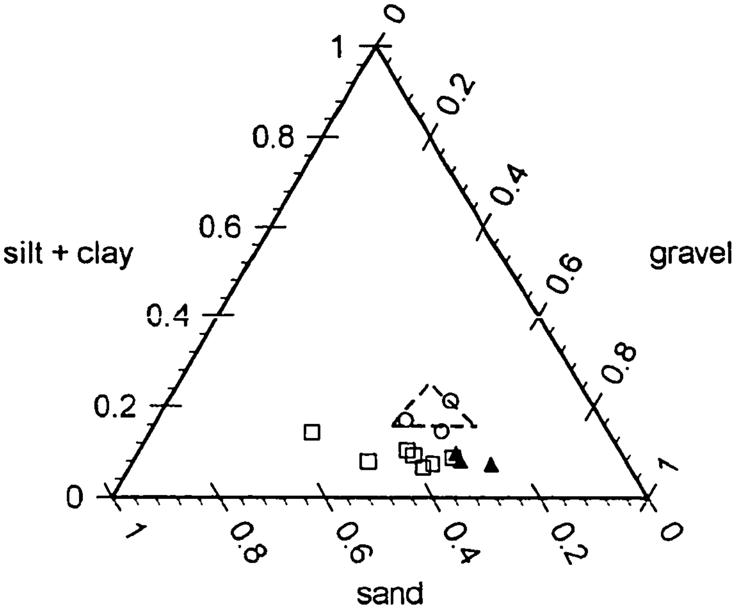

silt + clay
gravel
sand
0
0.2
0.4
0.6
0.8
1

Figure 4.11. **B**. Ternary diagram showing grain-size distributions of the < 32 mm fraction of debris-flow deposits in Owens Valley. Open circles: mixed-source, White Mountains. Solid stars: recent debris-flow deposits on the Black Canyon fan. Solid diamonds: granitic-source, Rock Creek fan. Open diamonds: granitic-source, Sierra Nevada (glaciated).

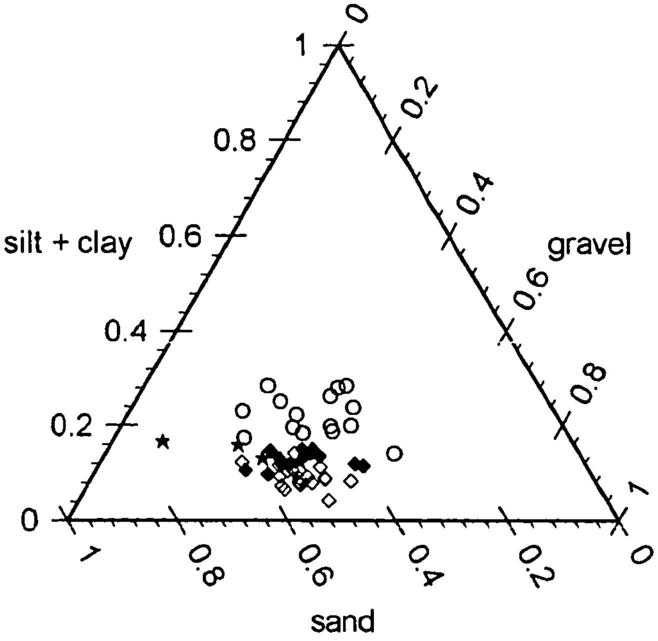
0
1
0.2
0.8
0.4
silt + clay
0.6
gravel
0.6
0.4
0.8
0.2
0
1
1
0.8
0.6
0.4
0.2
0
sand

Figure 4.12. A. Interpretive map of Jefferies Mine Canyon fan.

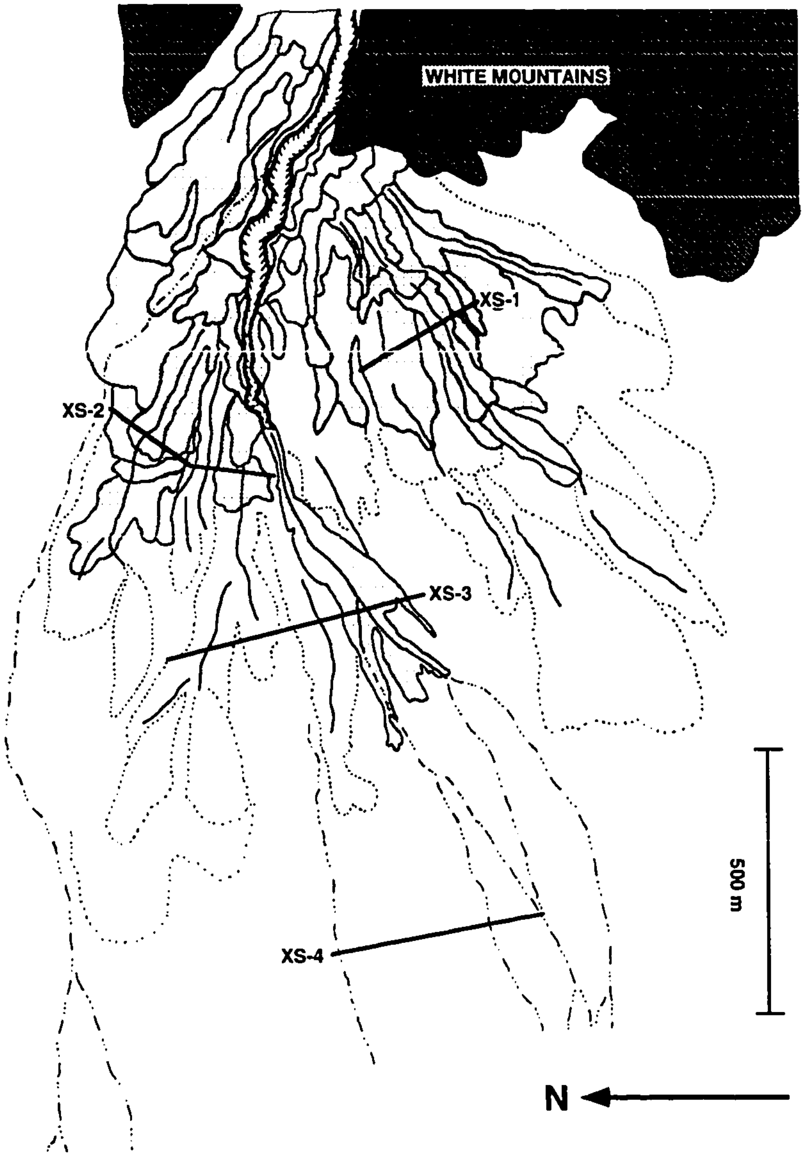
WHITE MOUNTAINS
XS-1
XS-2
XS-3
XS-4
500 m
N

Figure 4.12. **B**. Aerial photograph of Jefferies Mine Canyon fan. Light-colored patch is the deposit of the 1958 debris flow.

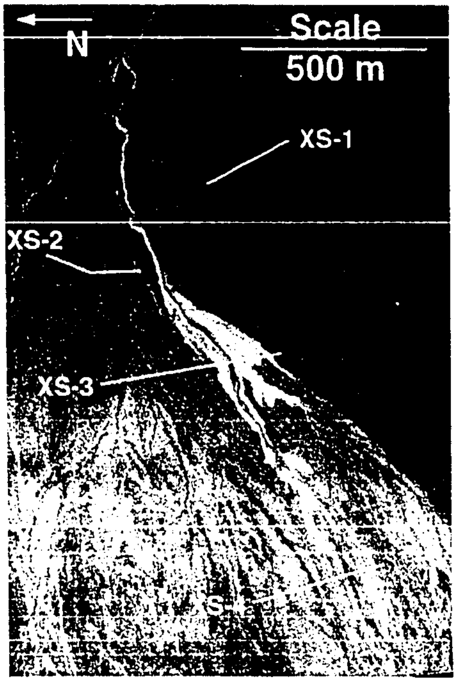
N
Scale
500 m
XS-1
XS-2
XS-3
S-

Figure 4.13. Topographic cross sections of Jefferies Mine Canyon fan.

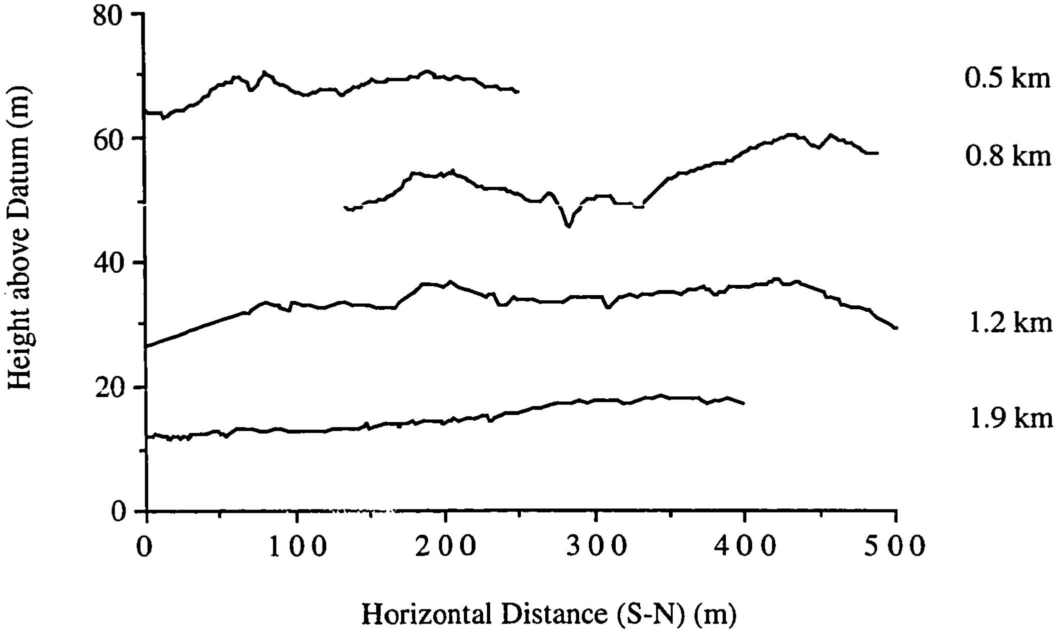
80
60
40
20
0
Height above Datum (m)
0
100
200
300
400
500
Horizontal Distance (S-N) (m)
0.5 km
0.8 km
1.2 km
1.9 km

paleo-channel courses, most of the channels are small, like those of the upper fan, and the dendritic aspect of the channel network structure characteristic of the glaciated Sierran fans is absent (Figs. 4.8 and 4.10). The four or five major paleo-channels run along well developed, 200 m-wide axial highs with 5-10 m of relief (Fig. 4.10), as was the case with many of the granitic-source fans from unglaciated basins of the Sierra Nevada. In addition, the mid-fan reach includes a number of wide (> 100 m), boulder-depleted overbank debris-flow lobes with about 1m relief at lobe margins -- a landform not seen on granitic-source fans on the west side of the valley.

Mixed-Source Fans of the Southern White Mountains

Unlike their granitic counterparts, the mixed-source fans, typified by the Jefferies Mine Canyon fan, have surfaces dominated by on-lapping wide terraces defined by broad overbank debris-flow lobes that add relief to interfluves, broad channel-margin levees built up to levels well above the general elevation of the surrounding fan surface, fewer abandoned channels, and fewer large boulders (Table 4.2; Figs. 4.12 and 4.13). Abandoned channels form a sparse sub-parallel to radial network without a dendritic aspect. Fan heads are typically incised to a depth of 5 m or more. Channel densities are significantly lower than on the Sierra fans, averaging about 1.8 km^{-1}. Further, as much as the lower 30-45% of these fans can be virtually unchannelized (Fig. 4.12). Beyond the fan-head trench, channel area-slope products range from 0.5 to 3.8 m^2, diminishing rapidly towards zero on the lower fan.

Cross-fan profiles show both greater convexity and greater relief on channel-margin levees than seen on any other fans. Nearly all abandoned channels have levees with significant relief and are situated atop linear highs (100-200 m wide, 5-10 m of relief) that give the fans a corrugated appearance and contribute to the overall cross-fan convexity (Figs. 4.12 and 4.13). Narrow debris-flow snouts and channel plugs are rare or absent and wide (> 100 m) overbank debris-flow lobes are the most characteristic landforms on these fans (Fig. 4.12).

DEBRIS-FLOW RHEOLOGY

A brief review of the mechanics of debris flows follows as a basis for the rheological analysis presented in the next section. The mechanical behavior of matrix-supported, muddy (> 10% silt-and-clay in the matrix, where matrix is defined as material < 2 mm in diameter) debris flows can be approximated as a Bingham fluid that is a simple fluid in which there is no flow below a critical stress (the yield strength), but that flows in a linear viscous manner in response to stresses in excess of this critical stress (Johnson, 1970; Coussot, 1992; Major and Pierson, 1992).:

$$\tau_{zx} = \tau_o + \mu\left(\frac{du}{dz}\right)^n, \quad \text{for}\, \tau_{zx} \geq \tau_o \qquad (4.1a)$$

$$\frac{du}{dz} = 0, \qquad \text{for}\, \tau_{zx} < \tau_o \qquad (4.1b)$$

where z is oriented perpendicular to the bed, n = 1, τ_{zx} is the shear stress, τ_0 is the yield strength, μ is the viscosity, and u is the velocity. A non-linear shear-thinning Herschel-Bulkley model (n < 1 in equation 1a) is preferred by some authors (e.g., Coussot, 1992) but the divergence of laboratory data from the simpler Bingham model is minimal, particularly in the context of realistic field applications. However, most laboratory studies have investigated only the behavior of the matrix fraction of the debris (sand size and smaller); a drawback of the Bingham model is that it does not explicitly account for frictional and collisional interactions between gravel- and boulder-sized clasts that probably contribute significantly to both the apparent viscosity and yield strength of most natural debris flows (Iverson and LaHusen, 1993). Recognizing this, Johnson (1970) advocated use of the Coulomb-viscous model, which explicitly incorporates the frictional component of the yield strength. Application of the Coulomb-viscous model, however, requires explicit incorporation of complex, dynamic pore pressure effects (Johnson and Rodine, 1984; Iverson and Denlinger, 1987; Iverson and LaHusen, 1993) that are as yet not quantitatively understood. Work specifically addressing the role of friction and dynamic pore pressure fluctuations is currently underway (Iverson and LaHusen, 1989; Iverson, 1993; Iverson and LaHusen, 1993), but many issues remain unresolved and the Bingham model remains a useful construct for geomorphological analyses of debris-flow processes. For analyses requiring more precise site-specific predictions, the simplifications incorporated into the Bingham model may not be acceptable (see discussions in Iverson, 1985; Iverson and Denlinger, 1987; Iverson and LaHusen, 1993).

Application of the Bingham constitutive equation to natural debris flows assumes that the matrix deformation governs the macroscopic behavior of the flow and that dynamic effects such as grain collisions, friction, pore-pressure fluctuations, and formation and destruction of structural grain networks are negligible or are collectively manifested as an approximately Bingham behavior (see discussions in (Pierson, 1980;

Pierson, 1986; Phillips and Davies, 1991). Deformation of the matrix is assumed to govern the constitutive behavior of the total mixture (i.e., approximately Bingham), not the magnitudes of the effective global viscosity and yield strength -- these are clearly influenced by the presence of abundant (> 20% by volume) gravel- and boulder-sized clasts [Johnson, 1970 #64; Coussot, 1992; Major and Pierson, 1992; Major, 1993). These assumptions are most reasonable for muddy, matrix-rich debris flows of the type that leave matrix-supported deposits. In other, fines-poor debris flows they are not. The Bingham model should only be used to describe matrix-rich muddy debris flows in which boulders appear to play a minor role in macroscopic flow behavior.

Laboratory studies have shown that both the yield strength and viscosity of mud-rich sandy slurries vary systematically with bulk slurry water content and debris granulometry (Fairchild, 1985; O'Brien and Julien, 1988; Phillips and Davies, 1991; Coussot, 1992; Major and Pierson, 1992). These findings have been corroborated in the field for natural debris flows (Chapter 3). Both debris-flow yield strength and viscosity are sensitive to the fines (silt and clay) content of the debris. For the same bulk water content, more fines-rich debris slurries exhibit higher strengths and higher viscosities (Fairchild, 1985; Major and Pierson, 1992). This result is not surprising -- clearly a suspension of sand in a dense silt-clay-water slurry must be more viscous than the same suspension of sands in a dilute slurry. However, the increase in viscosity and strength with increasing fines content only holds for relatively fines-rich debris flows that behave in an approximately Bingham or macroviscous manner (see Chapter 3): fines-poor, friction-dominated flows should become more mobile with increasing fines content (Fig. 4.14). Furthermore, although a clear understanding is still lacking, the role of clay-sized particles appears to be critical (Coussot, 1992; Coussot and Piau, in press) and debris-flow rheology should be sensitive to both clay content and mineralogy as well as total fines content.

Field Estimation of Debris-Flow Rheology

For debris flows in which massive bouldery fronts do not control flow behavior, viscosity and yield strength can be estimated in the field from well-preserved deposits (Johnson and Rodine, 1984). In Chapter 3 I outlined the field and analytical techniques necessary to derive accurate field estimates and presented data representative of the granitic-source debris flows of the Sierran fans (data from deposits on the Black Canyon fan). Here I present comparable data for the mixed-source and granitic-source flows of the White Mountain fans, derived using the field and analytical methods described in Chapter 3.

A number of debris flows have occurred on the White Mountain fans within the past 40 years (e.g., Beaty, 1963; Beaty, 1974) and four of them are sufficiently well preserved to allow reconstruction of peak flow hydraulics and rheology. These recent flows include three from mixed-source basins (Willow Creek and Lone Tree Creek, 1952; Jefferies Mine Canyon, 1958) and one from a granitic source (Montgomery Creek, 1989). The mixed-source debris-flow deposits studied are fines-rich (silt-and-clay ~ 15-20% of the total distribution and ~ 30-40% of the < 2 mm fraction) and the granitic-source deposit is more granular (silt-and-clay ~ 7-10% of the total distribution and ~ 18-22% of the < 2 mm fraction). Both are representative of the sediments that compose the bulk of the stratigraphy on their respective fans (Fig. 4.11; Hubert and Filipov, 1989). Further, the granitic-source debris-flow deposit is sedimentologically similar to the granitic-source debris-flow deposits on the western slope of the valley (Fig. 4.11; Whipple and Dunne, 1992). Moreover, despite differences in source lithology and climatic history, clay mineralogy in the debris-flow deposits is dominated by smectites and illites on both sides of the valley (Hubert and Filipov, 1989; K. Menking, UCSC, pers. communication).

None of the debris-flow deposits along the White Mountain front record the remarkable level of detail preserved in the Black Canyon debris-flow deposits studied in Chapter 3. In each case the hydraulics of only the peak flow surge could be reconstructed (Table 4.3). Figure 4.15 plots the yield strength and viscosity estimates on the White Mountain debris flows together with the Black Canyon data presented in Chapter 3. Also included on Figure 4.15 are published field rheology estimates from JiangJia Gully in China (Li, and others, 1983), shown because the JiangJia Gully debris flows have grain-size distributions that are similar to the mixed-source debris flows in Owens Valley (Fig. 4.11). There is significant overlap in the estimates of the rheology of the two types of debris-flow (granitic- and mixed-source flows), but the data diverge dramatically at higher yield strengths and viscosities (Fig. 4.15). This finding is in accordance with laboratory observations that, at the same water content, fines-rich debris flows have higher viscosities than fines-poor debris flows, and that viscosity is more sensitive to differences in fines content that is yield strength (See Fig. 4.14; Fairchild, 1985; Major and Pierson, 1992). The observed difference in rheology can be expected to have a dramatic influence on the effective conveyance capacities of

Figure 4.14. Schematic Illustration of Rheology vs. Silt-and-Clay Content. Generalized trends in yield strength and viscosity for poorly sorted debris mixtures as a function of silt-and-clay content for a constant sediment concentration. The transition between frictional and macroviscous behavior is discussed in Chapter 3. The Bingham model is not applicable within the frictional domain and the trends in yield strength and viscosity are drawn to reflect the anticipated decrease in "mobility" at lower fines contents and higher hydraulic conductivities. Curves are generalized in a schematic fashion from data presented by Fairchild (1985) and Major and Pierson (1992).

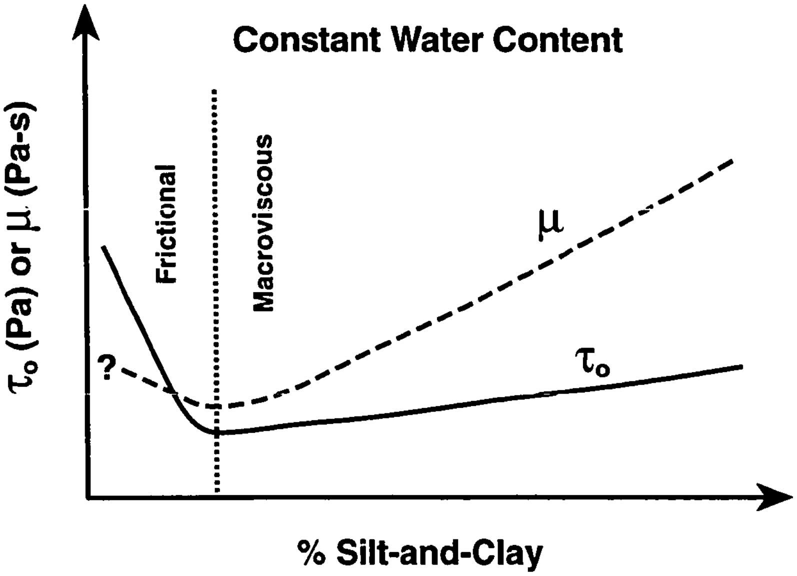
Constant Water Content
τ_o (Pa) or μ (Pa-s)
Frictional
Macroviscous
μ
?
τ_o
% Silt-and-Clay

Figure 4.15. Estimates of rheological parameters for recent debris flows in Owens Valley, California. A Bingham constitutive model is assumed.

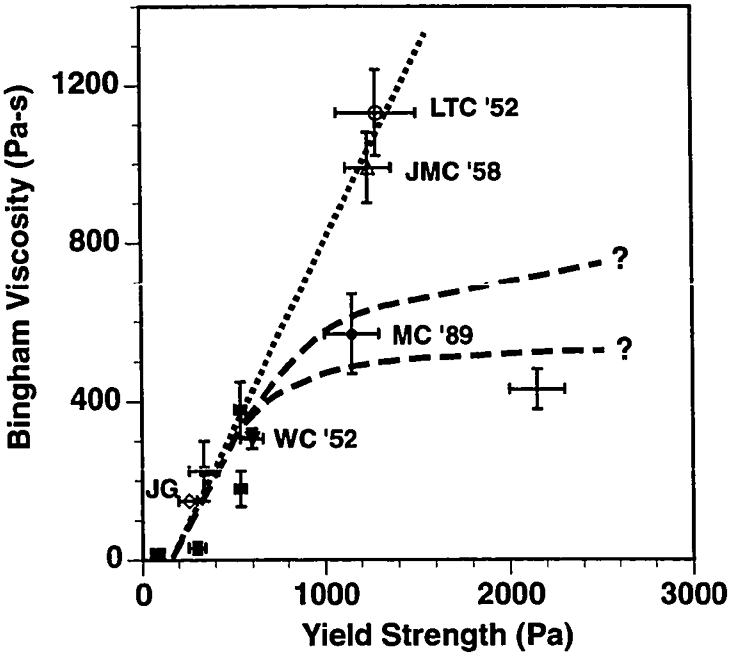

Bingham Viscosity (Pa-s)
1200
800
400
0
LTC '52
JMC '58
MC '89
WC '52
JG
?
?
0
1000
2000
3000
Yield Strength (Pa)

Table 4.3. Hydraulic and Rheologic Parameters of Debris Flows

Debris Flow	Channel Geometry					Flow Hydraulics			Rheologic Parameters		
	W (m)	D (m)	A (m^2)	S	Rc (m)	Uave (m/s)	Qp (m^3/s)	Uave/D	To (Pa)	Ub (Pa-s)	Un (Pa-s)
LTC '52	56	5.2	150	0.11	144	6.2	920 - 942	1.2	1285 + 215	1130 + 110	1565 + 25
WC '52	9.5	1.8	10.6	0.14	78	4.3 - 5.0	45.6 - 53.8	2.6	600 + 60	307 + 25	400 + 35
JMC '58	19	3	38	0.1	20 - 26	2.3 - 2.6	83.7 - 100	0.8	1240 + 124	990 + 90	1660 + 180
MC '89											
Site 1	14.7	5.9	53.3	0.08	86.5	8	425	1.4	1150 + 50	580 + 32	830 + 30
Site 2a	10.5	4.7	31	0.1	77.5	4.1 - 4.25	126 - 132				
Site 2b	12.5	4.3	25.5	0.1	50	4.25 - 4.6	109 - 117	1	1150 + 50	570 + 100	900 + 100

LTC - Lone Tree Creek
WC - Willow Creek
JMC - Jefferies Mine Canyon
MC - Montgomery Creek

channels, and may explain many of the morphological differences between fans derived from different source terrains.

Mechanics and Sedimentation of Boulder-Rich Debris Flows

Bouldery flow fronts are a common feature of many debris flows (Okuda, and others, 1980; Costa, 1984; Costa and Williams, 1984; Pierson, 1986). Often such bouldery fronts are small, extending no more than a few particle diameters and appear to be easily shoved aside by the body of the flow (Costa and Williams, 1984). In this case, bouldery fronts should exert at most a secondary influence on debris-flow runout and deposition patterns. Whipple and Dunne (1992) used this argument in their discussion of rheological controls on fan morphology on relatively boulder-poor fans. However, yield strengths in excess of about 4 kPa reported by Whipple and Dunne (1992) are associated with the most bouldery debris-flow snouts and probably reflect some contribution from frictional interactions at the flow front. Furthermore, in debris flows derived from very boulder-rich source materials these bouldery flow fronts can be massive. Deposits of this type of debris flow often preserve a large boulder wedge at the leading edge of an otherwise matrix-rich debris flow (Fig. 4.16a). The boulder wedge can be as much as 50 m long and typically is an open-work gravel-boulder deposit virtually devoid of matrix (Fig. 4.16b). Apparent yield strengths estimated from the debris behind such wedges in Owens Valley range from 8.7 - 12.4 kPa, corresponding to surface slopes of 6-9° and deposit thicknesses of 3-5 meters.

Frictional interactions between boulders must dominate the mechanical behavior of these massive wedges, particularly at the slow strain rates characteristic of flow on fan surfaces; their strength is probably better considered in terms of an effective angle of internal friction than a (constant) "yield strength". Further, the effective yield strength of this type of debris flow (i.e. the conditions under which they deposit) may not correlate strongly with either the fines content of the matrix nor the bulk water content of the flowing mass. Massive boulder wedges probably act as moving frictional dams at the flow front (Coleman, 1993) and, in some circumstances, runout may be limited by the debris flow's ability to propel this dam across the gentle slope of a fan, rather than the rheology of the bulk of the debris flow itself. In this case, the Bingham constitutive equation is not well suited to modeling the runout process. Rather, a mechanical treatment of the moving dam and its influence on the global behavior of the debris flow is required.

Figure 4.16. **A.** Photograph of large boulder wedge on upper Tuttle Creek fan. Pinyon pines provide scale.

Figure 4.16. **B**. Close up photograph of a boulder wedge on upper Rock Creek fan. Note the open-work structure. Deposits are typically matrix-free near the surface, as shown here.

Figure 4.17. Boulder wedge force balance definition sketch. Variables defined in text.

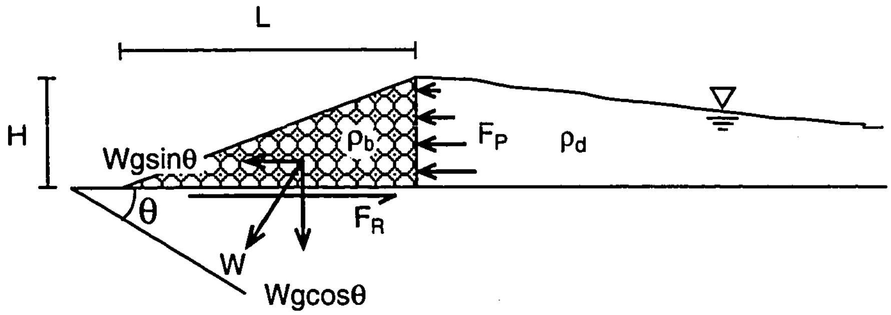
L
H
Wgsinθ
ρb
FP
ρd
θ
FR
W
Wgcosθ

A simple force-balance analysis illustrates that the global influence of a frontal boulder wedge is dictated by its volume (V) and effective bed friction angle (ϕ_b'). Consider a steady rectilinear shear flow of debris on an inclined plane. Let the debris flow consist of a triangular shaped wedge of boulders and gravel of density ρ_b riding at the front of a simple fluid of density ρ_d (Fig. 4.17). Assume the fluid has negligible strength and that the boulder wedge slips at the base and deforms internally but maintains a constant shape. Four forces act on the boulder wedge (Fig. 4.17): (1) the downslope component of its weight (Fg); (2) frictional resistance at the bed (Fr); (3) the pressure force exerted on the back of the wedge by the fluid (Fp); and (4) the seepage force arising from fluid through-flow, if any (Fs). At equilibrium the frictional resistance (Fr) exactly balances the sum of the three driving forces (Fg + Fp + Fs). Assuming minimal through-flow and negligible seepage force (i.e., that the boulder wedge is impermeable to the viscous debris-flow slurry) and that the pressure at the fluid-dam interface is hydrostatic, the force balance reduces to:

$$\tan\theta = \tan\phi_b' - \left(\frac{\rho_d}{\rho_b}\right)\left(\frac{H}{L}\right), \tag{4.2}$$

where θ is the bed slope, H is the height of the wedge, L is its length, and the effective bed friction angle incorporates all effects due to pore fluid pressures and lubrication of frictional contacts between mud coated boulders. Video footage of boulder-rich debris flows obtained by Dr. H. Suwa of Kyoto University, Japan, clearly demonstrates that pore-fluid pressures play an important role in governing bed friction: debris-flow snouts rapidly grind to a halt when traversing a grate that allows rapid pore-fluid escape. Effective bed friction angles, however, can not at this time be predicted theoretically because pore-fluid behavior in these coarse-grained, shearing mobile dams is not well understood. Coleman (1993) has looked at this problem qualitatively in an idealized laboratory setting but many questions remain unanswered.

On slopes less than that predicted by equation (4.2), steady flow is not possible and frictional resistance at the flow front will cause the debris flow to decelerate, effectively limiting flow mobility and down fan translation. Since the relative densities of fluid and boulder bore probably vary only slightly between debris flows, effective bed friction and wedge aspect ratio (H/L) emerge as the critical variables.

If forward motion of the debris flow is retarded by the boulder wedge, the resulting back-water effect causes stage to rise and the flow may bypass or overtop the bouldery dam. In response, the wedge grows in height as more boulders reach the front or are mined from depth and deposited at the top of the dam (as observed by Coleman (1993) in his experiments with clear-water bores and PVC "boulders"). In addition, the dam may steepen in response to mounting longitudinal compressive stresses, as is seen in the critical taper theory for accretionary prisms (Dahlen, 1984). The increasing height of the dam is accompanied by an increase in the total pressure force on the back of the dam and the force balance shifts towards equilibrium so long as the wedge continues to steepen. Dam height is limited by the height of confining channel walls because beyond this limit the flow will simply bypass the dam. Wedge aspect ratio, and hence the critical bed slope for steady flow (equation 4.2) is therefore limited by channel depth and the volume of the wedge. For large boulder-wedge volumes and correspondingly small aspect ratios the critical angle for steady flow approaches the effective bed frictional angle and the presence of the boulder wedge may strongly influence global flow mobility. Conversely, for small boulder-wedge volumes, the boulder wedge is easily oversteepened, the critical angle for steady flow is much less than the effective bed friction angle and the presence of the boulder wedge does not limit flow runout.

ANALYSIS OF CHANNEL CONVEYANCE CAPACITY

Given the small size of frontal boulder accumulations on most of the Owens Valley debris-flow deposits (only a few particle diameters long), the Bingham model is useful for analyzing the controls on their confinement in channels and down fan translation. The boulders and gravels in these flows surely contribute to their effective viscosity and yield strength, but the moving dam analysis does not apply. Only the most boulder-rich of the granitic-source debris flows supported boulder wedges of sufficient size to act as effective impediments to flow (Fig. 4.16). Among the fans studied, deposits of this type of debris flow occur exclusively on the upper reaches of the Tuttle Creek and Rock Creek fans (Figs. 4.5a and 4.8a). In this section I consider the rheologic or mechanical controls on down-fan translation of both boulder-rich and boulder-poor debris flows through channels of a given geometry. Climatic controls on channel size are discussed separately.

Boulder-rich debris flows

Where frontal boulder accumulations are of sufficient size to limit global flow mobility, the conveyance capacity of channels will be limited by the critical slope given by equation (4.2). Therefore, effective confinement and down fan translation of this type of debris flow is unlikely, except in deeply incised channels in which flow depths may be sufficient for the flow to oversteepen, override, and possibly re-entrain the boulder wedge. Although quantitative predictions are currently precluded by the lack of a theoretical understanding of effective bed friction angles, it is possible to estimate bed friction angles from field data, given certain assumptions. Equation (4.2) can be used to estimate limiting values of the effective bed friction angle in places where massive boulder wedges *appear* to have limited the down-fan translation of the debris flows.

The apex of the Tuttle Creek fan is one such field locality -- its steep slope (ca. 8-9°) is associated with massive boulder wedges, up to 50 m long and 5 m high, that are absent on less steep fans. Assuming that the steep slope of the Tuttle Creek fan-head is representative of the critical slope for translation of these massive boulder dams, the plausible range of effective bed friction angles can be determined from the geometry of the boulder deposits, given an estimate of the fluid-dam density contrast. For θ equal to 8°, (H/L) between 0.1 and 0.2, ρ_d between 1.8 and 2.1 g/cm^3, and ρ_b between 2.4 and 2.5 g/cm^3, plausible values of ϕ_b' range from 12° to 18°, reflecting the importance of basal pore-fluid pressure. Further experimental and observational work on the runout process of debris flows with large frontal boulder accumulations (e.g., Suwa, 1988; Coleman, 1993) is required before further progress can be made on this problem.

Boulder-poor debris flows

Where debris flows do not support massive frontal boulder wedges, the down fan translation of the debris flows is governed by the geometry of the channels and the rheology of the debris flows. Channel geometry and flow rheology in combination set the conveyance capacity of a channel, defined as the discharge at bankfull stage, which can be calculated using the equations developed in Chapter 3. Down-fan translation of debris flows can be assessed though an analysis of the rheologic controls on channel conveyance capacity according to the following set of rules: (1) debris flows with peak discharges less than the channel conveyance capacity are translated rapidly down fan without suffering significant attenuation; (2) debris flows with peak discharges in excess of the conveyance capacity overtop channel banks and deposit after thinning to a critical thickness determined by yield strength, material density, and surface slope (Johnson, 1970); and (3) debris flows for which conveyance capacities are near zero freeze within channels, block the channel, and may cause the channel to avulse. These simple rules were incorporated into the simple "mass-balance" routing scheme described in Chapter 3. This routing scheme is used here to illustrate the manner in which source lithology influences debris-flow sedimentation patterns and, hence, fan surface morphology. This application is intended to illustrate generalized rheologic controls on broad sedimentation patterns only. Accurate routing of debris flows requires a more sophisticated approach (see discussion in Chapter 3).

The conveyance capacity and debris-flow routing analysis was carried out as follows. (1) Representative cross sections of well preserved abandoned channels along the full length of the Symmes Creek, Rock Creek, Jefferies Mine Canyon and Lone Tree Creek fans were surveyed in the field. (2) Smooth curves were fit to cross section data, giving channel size and slope as a function of distance down fan (Fig 4.18). (3) Synthetic channel cross sections were generated at regular intervals down fan using these generalized curves and a simple trapezoidal channel geometry. (4) Channel conveyance capacity as a function of rheology was calculated for each of the synthetic channel cross sections using the equations given in Chapter 3 and the rheological data presented above (Fig. 4.15) for the mixed-source and granitic-source debris flows of Owens Valley (Fig. 4.19). (5) An idealized hypothetical debris-flow hydrograph (Fig. 4.20) was routed down each of the synthetic channel courses according to the rules of the mass-balance routing scheme.

The discharges and durations of the three surges of the hypothetical hydrograph (Fig. 4.20) are arbitrary. The same hydrograph is routed down each channel system to study the influence of debris-flow rheology in isolation. The intention is to model rheological differences in debris flows generated from identical initiation sites under identical hydrologic conditions, and therefore with identical water contents, but with different grain-size distributions (i.e., from each of the relatively fines-poor granitic sources and relatively fines-rich mixed-lithology sources). Although both viscosity *and* yield strength vary with fines content for a given sediment concentration, viscosity is far more sensitive to small changes in granulometry (Fig. 4.14; Fairchild, 1985; Major and Pierson, 1992). For the purpose of argument, I assign identical yield strengths to all hypothetical hydrographs, regardless of source lithology, as a crude proxy for holding water content constant ($(\tau_o)_{S1} = 2200$ Pa; $(\tau_o)_{S2} = 1200$ Pa; $(\tau_o)_{S3} = 200$ Pa). Viscosities, on the other hand, are assigned to each surge according to the assigned yield strength and the data in Figure 4.15 (granitic source: $(\mu)_{S1} = 600$ Pa-s; $(\mu)_{S2} = 500$

Figure 4.18. Channel Area-Slope Product vs. Distance Down Fan. Channel area-slope product per unit drainage area (m2/km2) is shown as a function of position down fan for Jefferies Mine Canyon fan (solid squares), Lone Tree Creek fan (solid circles), Rock Creek fan (open triangles), and Symmes Creek fan (open diamonds). Line is an exponential curve fit to the Symmes Creek data.

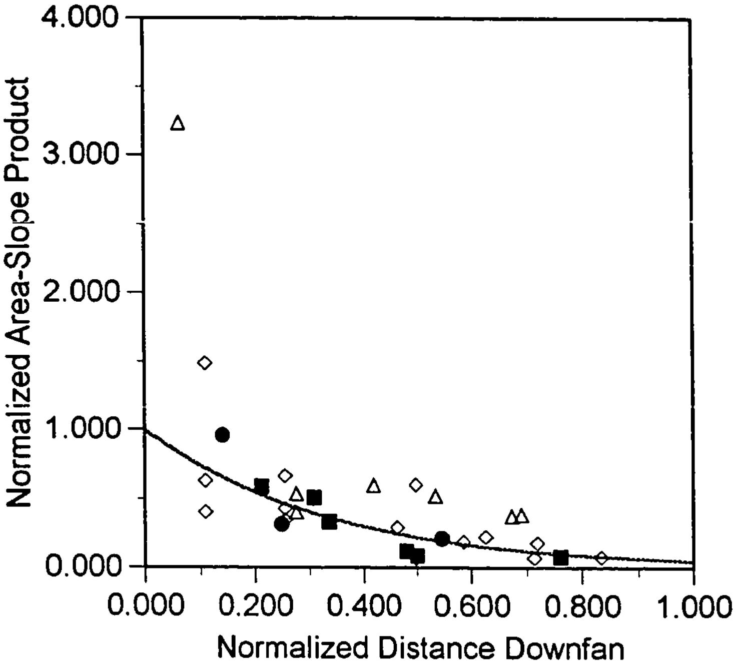
4.000
3.000
2.000
1.000
0.000
Normalized Area-Slope Product
0.000
0.200
0.400
0.600
0.800
1.000
Normalized Distance Downfan

Figure 4.19. Conveyance capacities as a function of rheology.
A. Conveyance capacity of the composite Rock Creek channel for Surge S1 (open diamonds) and S2 (open triangles), and the composite Jefferies Mine Canyon channel, also for Surge S1 (solid circles) and S2 (solid squares).

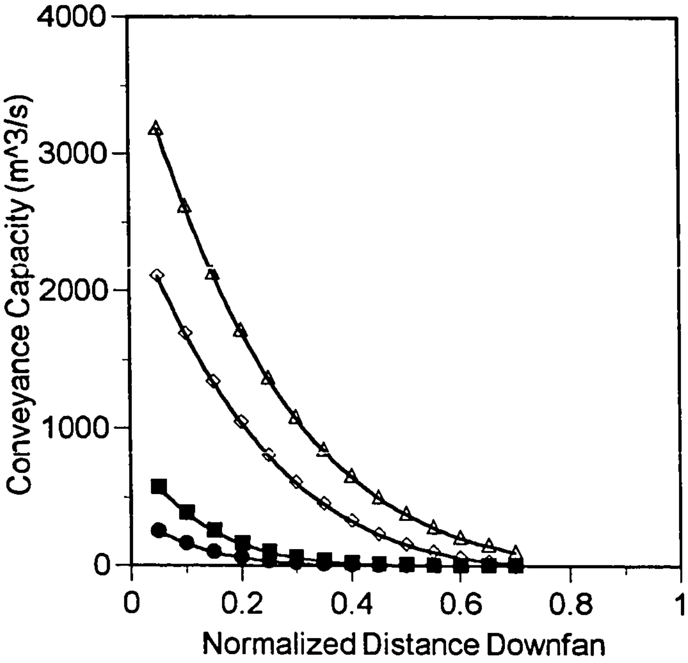

4000
3000
2000
1000
0
Conveyance Capacity (m^3/s)
0
0.2
0.4
0.6
0.8
1
Normalized Distance Downfan

Figure 4.19. **B**. Conveyance capacity of the composite Symmes Creek channel for Surge S1 (open diamonds) and S2 (open triangles), and the composite Jefferies Mine Canyon channel, also for Surge S1 (solid circles) and S2 (solid squares).

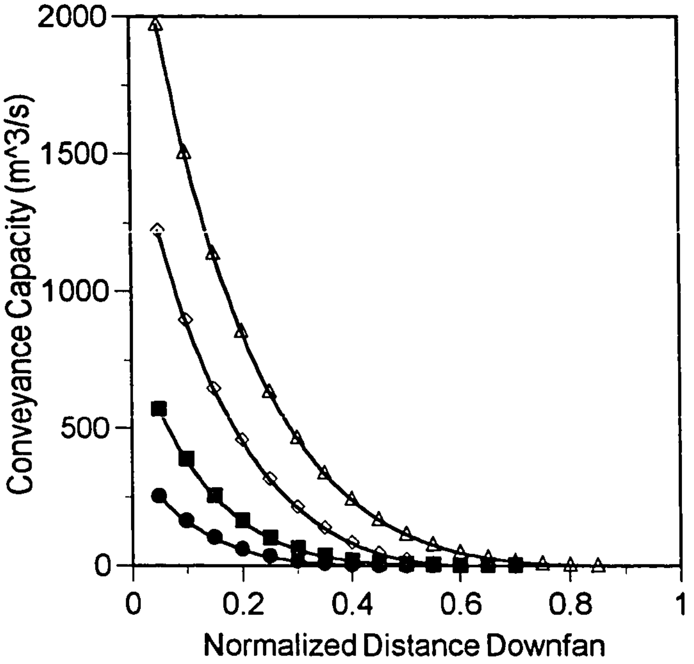
2000
1500
1000
500
0
Conveyance Capacity (m^3/s)
0
0.2
0.4
0.6
0.8
1
Normalized Distance Downfan

Figure 4.20. Idealized Debris-flow Hydrograph for Routing Analysis. Yield strength and viscosity of surges S1, S2, and S3 assigned in text according to data in Fig. 4.15.

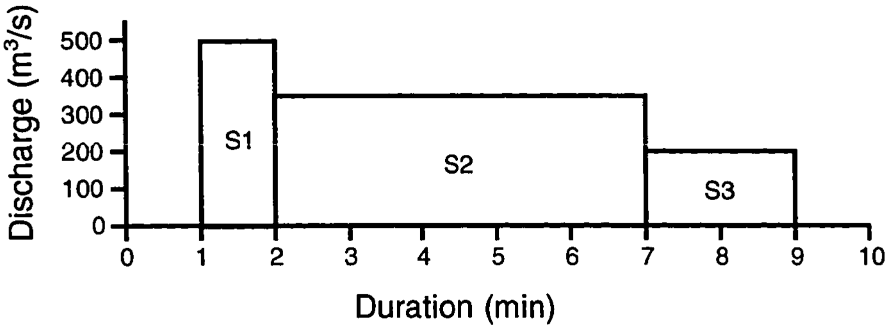
Discharge (m³/s)
500
400
300
200
100
0
S1
S2
S3
0
1
2
3
4
5
6
7
8
9
10
Duration (min)

Figure 4.21. Predicted Debris-flow Depositional Patterns. Results shown for the idealized channel systems of Jefferies Mine Canyon fan (gray), Symmes Creek fan (ruled), and Rock Creek fan (Black). % volume deposited is given by the volume of debris forced overbank per reach, during passage of the three surges of the hypothetical hydrograph illustrated in Fig. 4.20.

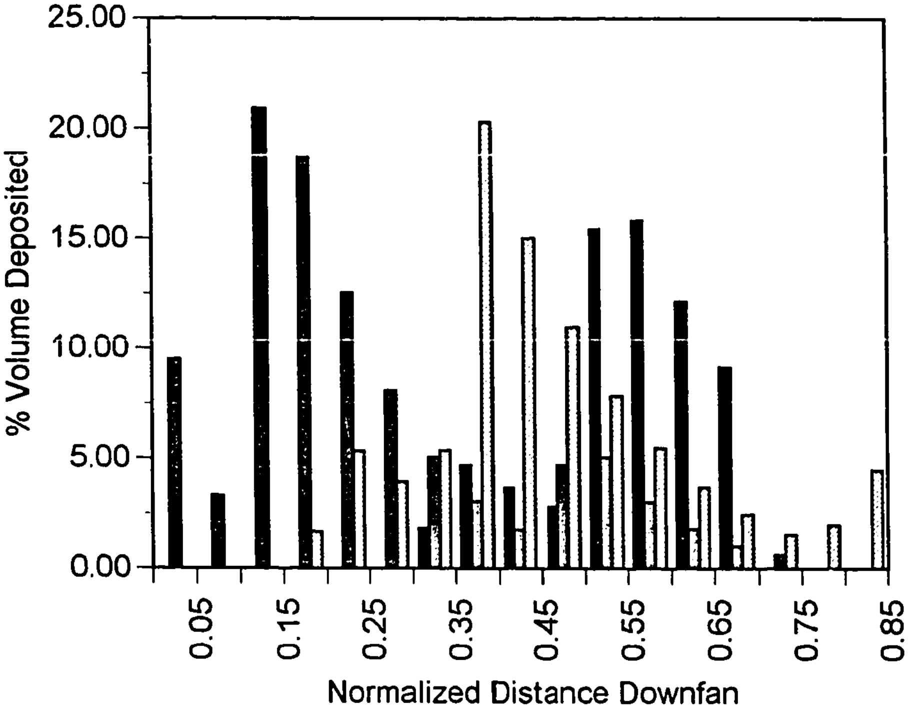
25.00
20.00
15.00
10.00
5.00
0.00
% Volume Deposited
0.05
0.15
0.25
0.35
0.45
0.55
0.65
0.75
0.85
Normalized Distance Downfan

Pa-s; $(\mu)_{S3}$ = 100 Pa-s; mixed-lithology source: $(\mu)_{S1}$ = 1800 Pa-s; $(\mu)_{S2}$ = 1050 Pa-s; $(\mu)_{S3}$ = 100 Pa-s). Negligible water loss from debris flows during runout across the fans is assumed. This assumption is justified by the low hydraulic conductivities of the debris and the relatively short travel times, as discussed by (Whipple and Dunne, 1992).

Figure 4.21 shows the generalized depositional patterns predicted by routing the hypothetical debris-flow hydrographs described above down the channel systems of each of the Symmes Creek, Rock Creek, and Jefferies Mine Canyon fans (representing respectively: granitic-source fans from glaciated basins; granitic-source fans from unglaciated basins of the semi-arid White Mountains; and mixed-source fans from the White Mountains). In each case down-fan distance is normalized by fan length and predictions are only made down to the position of the most distal measured channel section. Depositional patterns associated with individual surges of the hypothetical hydrograph are not shown. The simple routing analysis (Fig. 4.21) predicts that debris flows will be less well channelized on mixed-source fans than on granitic-source fans in the same climatic setting (i.e., on the Jefferies Mine Canyon fan as compared to the Rock Creek fan), suggesting a strong lithologic influence on debris-fan morphology.

DISCUSSION

Lithologic Control of Fan Morphology

For a given climate, lithology can influence debris-flow fan morphology both directly and indirectly. Indirect influences include possible impacts on stream hydrology and the size and quantity of material delivered to channels for fluvial transport. Direct influences stem from lithologic control of: (1) sedimentation rate (by limiting the rate of colluvium production); and (2) the granulometry of the colluvium (both in terms of boulder abundance and fines content). As discussed below, both of these factors are also influenced by the climate and long-term climatic history.

The sensitivity of debris-flow rheology to minor changes in debris grain-size distributions (Fairchild, 1985; Major and Pierson, 1992) and the importance of debris-flow rheology in fan sedimentation (Whipple and Dunne, 1992) argue that control of regolith granulometry should be the dominant lithologic effect. Possible lithologic control of channel size and down fan extent (a function of both hydrology and the size and quantity of sediment) is discussed together with the climatic controls on channel geometry. Here I consider the effects of differing boulder abundance and fines content in otherwise similar debris flows.

Boulder Abundance

The role that boulder abundance plays in debris-flow fan sedimentation is straightforward and easily appreciated, although not rigorously quantifiable at present. It indirectly controls fan morphology on all debris-flow fans by affecting the erodibility of freshly emplaced channel plugs. Boulder-rich debris-flow snouts are less easily eroded and are more likely to drive frequent channel avulsions, leading to reduced channel longevity, reduced levee aggradation, an increased density of abandoned channels, and reduced cross-fan convexity. However, as demonstrated above, when the bouldery wedge at the front of a flow attains a certain critical size, such that it is massive enough to retard the advance of the entire debris flow, boulders play an important and direct role in determining debris-flow depositional patterns and, hence, fan morphology.

If the boulder wedge is too massive to be pushed aside and deposited as narrow boulder levees along the flow path, it will be deposited within the channel, usually not far from the fan apex, depending on fan slope, channel depths, and the effective bed friction angle. Once the boulder wedge has come to rest, the body of the debris flow will flow around the obstruction or will be ponded behind the boulder dam, filling in much of the pre-existing channel. Whether the body of the debris flow is ponded behind the boulder dam or flows around it, a massive deposit of boulders is left on the upper reaches of the fan in either case. Thus, where debris flows with massive boulder wedges are common, channel avulsions on the upper fan will be frequent. With the frequent avulsions, there may not be sufficient time for the fluvial system to establish new channel courses between debris-flow events -- channel sizes will be small and overbank deposition will be enhanced correspondingly. Rapid aggradation of the fan head will ensue. As evidenced on the upper slopes of the Tuttle Creek and Rock Creek fans, eventually the uppermost fan surface will be graded to a slope of 7-9° to accommodate some down slope transport of the boulder-rich debris flows.

Debris Fines Content

The fines (silt and clay) content of the source regolith is crucial because it governs debris-flow viscosity and, secondarily, yield strength (Fairchild, 1985; O'Brien and Julien, 1988; Coussot, 1992; Major and Pierson, 1992). Neighboring source areas, with similar physiographic and hydrologic properties, but distinct regolith fines contents (but where the bulk porosity and strength of the regolith are similar, as should be the case in adjacent basins in the White Mountains) will produce debris flows with similar volumes and water contents but markedly different rheologies, with important consequences for fan morphology, as reflected in the channel conveyance capacity analysis above. Where regolith granulometry is radically different (e.g., dominantly silt and clay) debris-flow water contents (or, more precisely, the frequency distribution of debris-flow water contents) will be different and the arguments given below, which pertain specifically to field conditions in Owens Valley, do not apply.

For clarity I reiterate the specifics of the sedimentological variability of debris-flow deposits in the various field sites. Sieving of 1-2 kg samples from debris-flow deposits in Owens Valley shows that debris fines content (reported here as % silt-and-clay in the < 32 mm size fraction) clusters into three overlapping but separable groups (Fig. 4.11b): (1) granitic-source debris flows from glaciated basins of the Sierra Nevada (data from the Symmes and Pinyon Creek fans) contain 7-12% fines; (2) granitic-source debris flows from unglaciated basins on both sides of the valley (data from the Black Canyon and Rock Creek fans) contain 10-16% fines; and (3) mixed-lithology-source debris flows from unglaciated basins of the White Mountains (data from the Lone Tree Creek and Jefferies Mine Canyon fans) contain 17-28% fines. Debris-flow deposits on all fans studied have a similar range of gravel and sand contents (Fig. 4.11b).

The overall similarity of the Rock Creek and both the glacial- and nonglacial-source fans of the Sierra Nevada (average slopes are similar; narrow, bouldery debris-flow lobes and channel plugs are common; abandoned channels are common and closely spaced; and mappable, wide overbank debris lobes are rare) suggests that direct lithologic control of debris granulometry is, at least in Owens Valley, more important than any climatic influence on fan morphology. Moreover, the one distinctive morphological feature common to many, but not all, of the fans from unglaciated basins (a higher percentage of "raised" channels with significant relief on levees -- see Figs. 4.8 and 4.10) is most strongly developed on the Rock Creek and Black Canyon fans, which have the highest debris fines contents (10-16% silt-and-clay in the < 32 mm fraction) of the granitic-source fans studied. As discussed below for the fines-rich mixed-source fans, a tendency to build more substantial levees is expected where debris-flow viscosities are higher and overbank deposition more common.

In contrast to the situation on the granitic-source fans (Whipple and Dunne, 1992), debris flows on mixed-source fans are poorly channelized and massive overbank deposition, particularly near the fan head, is predicted by the channel conveyance capacity analysis (Figs. 4.19 and 4.21). This circumstance leads to rapid fan-head aggradation and anticipates a steepening of the fan surface. Both a prevalence of landforms associated with unconfined spreading of debris flows and steeper profiles are diagnostic characteristics of fans derived from basins underlain by mixed lithologic assemblages (Figs. 4.7, 4.11 and 4.12). Despite the frequent and massive overbank deposition, individual channel courses on the mixed-source fans appear to be longer lived because abandoned channels and paleo-channel traces are less common and channel-margin levees are prominently developed (i.e., there are many "raised" channels) (Table 4.2, Fig. 4.13). Channel avulsions are apparently less frequent. One plausible explanation lies in the absence of bouldery snouts on these debris flows: channel-filling debris-flow deposits lacking boulders are easily eroded by the clear-water floods that commonly follow thunderstorm-generated debris flows (Hooke, 1987). The presence of well developed raised channels on the bouldery granitic-source Rock Creek fan, however, suggests either that (1) the higher-viscosity of the more fines-rich debris flows is more important to the aggradation of prominent levees and the formation of "raised" channels than is channel longevity, or that (2) the timing and magnitude of post-debris-flow floods is more important to the likelihood of channel avulsion than is the erodibility of the deposits. Thus, either lithologic or hydrologic factors, or both, may be responsible for the morphological differences between granitic-source fans derived from unglaciated as opposed to glaciated basins in Owens Valley. The two effects are not clearly separable at present.

Climatic Control of Fan Morphology

Fans derived under a range of climatic settings were studied (Table 4.1). As indicated in the discussion above, despite the broad range of climates (glaciated; unglaciated with 10-15 cm annual precipitation; and unglaciated with only 4-6 cm annual precipitation) distinctive morphological indicators clearly related to the climatic differences are difficult to define.

Climatic differences between sites in Owens Valley that are relevant to debris-flow sedimentation patterns include: (1) differing stream discharges; (2) differing debris-flow initiation environments; and (3) differing weathering environments. The first of these factors should affect channel size and (coupled with lithologic controls) down-fan extent. The second factor may influence channel longevity, as discussed in the previous section, and in combination with the third factor influences the frequency distribution of debris-flow rheologies. I consider separately the controls on channel form and debris-flow rheologies.

Channel Size, Down-fan Extent, and Longevity

Channels on debris-flow fans are not self-formed alluvial channels -- they are more akin to gullies (Whipple and Dunne, 1992). Therefore, channel width and depth both increase with time during prolonged occupation of a given channel course, limited by stream-flow discharge, fan slope, sediment supply and caliber, amounts of levee aggradation by overbank debris-flow deposition, and position relative to base level. Thus, channel cross-sectional area is correlated with drainage area and annual precipitation and decreases with distance from the apex as (1) discharges diminish due to infiltration loses, (2) slope declines, and (3) local base level (effectively the valley floor) is approached. In addition to this gradual down-fan decline in channel size, the distal most portions of most of the fans studied are virtually unchannelized -- a situation that arises because the fluvial system eventually shifts from an erosional to a depositional regime (i.e., the down-fan divergence of fluvial sediment flux is negative). Sediment supply and caliber (controlled by both lithology and climate) strongly influence the down-fan divergence of sediment flux and, therefore, limit the down-fan extent of channels.

Modern stream discharges are greatest on fans below large basins on the west side of the valley. Annual precipitation in the basins of the eastern Sierra Nevada is roughly 300% of that in basins draining the White Mountains (10-15 cm/yr as opposed to 4-6 cm/yr). Symmes Creek, Pinyon Creek, Black Canyon creek, and Olancha Creek are perennial streams. Rock Creek, Lone Tree Creek, and Jefferies Mine Canyon creek are ephemeral, flowing only during the Spring melt and briefly after isolated rainfall events. A similar precipitation gradient presumably prevailed during the late Pleistocene as well. As a result, channels on the White Mountain fans are generally smaller than those on the Sierran fans (Figs. 4.2b, 4.4c, 4.8b, and 4.12b). However, if channel area-slope product per unit drainage area is considered, there is no clear climatic signal in the "effective" channel size (Fig. 4.18). This close effective match in channel size and slope probably reflects a combination of the higher rates of overbank deposition and levee aggradation associated with the more viscous mixed-source debris flows and the greater longevity of channels on boulder-poor fans and fans below unglaciated basins in thunderstorm-dominated climates.

The down-fan extent of channels is more variable and appears to lithologically controlled. Granitic-source fans are well channelized, regardless of climatic setting, and mixed-source fans have the largest unchannelized distal areas (Table 4.2). The lower reaches of many channels on the mixed-source fans are choked with fluvial sediment and a greater supply of gravel-sized sediment is probably responsible for the restricted down-fan extent of these channels. Similarly, Hubert and Filipov (1989) report a greater percentage of fluvial material in measured sections on the distal parts of the mixed-source fans than Whipple and Dunne (1992) found on the granitic-source Sierran fans.

The channels of the Rock Creek fan are an interesting case and point to the importance of channel longevity in setting channel size. The distribution of channels on the Rock Creek fan is bimodal: most of the abundant channels are small with narrow bouldery levees (Fig. 4.8b), but there are also a few prominent, relatively large channels that run along well developed axial highs (Figs. 4.8b and 4.10). Both sets of channels fall, however, within the scatter of channel sizes seen on fans below glaciated basins on the wetter west side of the valley, particularly if the small size of the Rock Creek drainage is considered (Table 4.1, Fig. 4.18). Why should such a bimodal distribution of channel sizes arise? One plausible explanation lies in the incision of the apex of the Rock Creek fan, which is apparent on Figure 4.8a. Whereas the reason for the fan-head incision is not known (and may be related to either climatic or tectonic effects, or both), it is interesting to note that the small channels are generally associated with the older part of the fan (tracing back to the now-abandoned fan apex) and the large "raised" channels with the younger, post-incision part of the fan (Fig. 4.8b). The small channels are also associated with the abundant boulder-rich deposits of the upper fan (Fig. 4.8a) and were probably short-lived. Conversely, the larger channels of the mid-fan region appear to have been longer lived, because of their size and substantial levees. No definitive explanation for the apparent change in behavior can be offered at present. However, the simplest explanation (i.e., one not involving speculation about climatically induced changes in the types of debris flows delivered to the fan and the magnitudes of stream-flow discharges) is that the deep fan-head trench now allows the debris flows to overwhelm, override, and bypass the frontal boulder wedges that once controlled their runout and deposition patterns, thereby greatly reducing the frequency of channel avulsions. This mechanism probably acts in concert with the rheologic influence on the frequency and magnitude of overbank deposition and the hydrologic influence on the likelihood of channel avulsion to produce the distinctive "raised" channels of the lower Rock Creek fan.

Frequency Distribution of Debris-Flow Rheologies

The frequency distribution of rheologies of the debris flows generated in lithologically similar basins in different climatic regimes should reflect: (1) differences in debris-flow initiation (mechanisms, volumes, and hydrologic conditions at time of failure) and (2) differences in weathering environment. The former directly affects both the volume and water content of the debris flows. The latter indirectly affects debris-flow rheology through its influence on debris fines content and has already been discussed. Unfortunately, likely differences in factors (1) and (2) above between the glaciated basins of the Sierra Nevada and the granitic fans of the White Mountains could have similar morphologic consequences. Therefore, a definitive statement as to whether the morphological differences between glaciated and unglaciated granitic-source fans described above are due to rheological differences associated with the observed difference in debris grain-size distributions (Fig. 4.11), a difference in typical debris-flow water contents, or a difference in the likelihood of avulsion (as discussed above), cannot be made at present.

CONCLUSIONS

Debris-flow fan morphology is controlled by a complex interaction of both climatic and lithologic factors. Within the range of climatic and lithologic conditions found in Owens Valley, however, lithology is found to be the dominant control. The importance of source lithology is due primarily to the sensitivity of debris-flow rheology and the channel avulsion process to the granulometry of the source regolith. Source lithology largely determines both the boulder abundance and the fines content of the regolith. Granitic sources produce bouldery, granular debris with about half the silt-and-clay content of mixed-source (metasedimentary, metavolcanic, and granitic) debris. Both boulder and fines contents have demonstrably powerful influences on debris-flow rheology and fan sedimentation processes. A critical factor in the morphological development of the mixed-source fans is the greater viscosity of fines-rich debris flows: channel conveyance capacity is severely limited and massive overbank deposition and steepening of the fan surface results. Different characteristic debris-flow hydrographs, related to climatic differences, may also play a role, but no data are available. However, comparisons between granitic-source fans on either side of the valley indicates that any such climatic control is of secondary importance to the lithologic effect. A second lithologically-controlled variable is the abundance of boulders transported by the debris flows. Two effects are anticipated: (1) the presence of boulders in debris-flow snouts reduces the erodibility of channel plugs and therefore increases the likelihood of channel avulsions; and (2) massive accumulations of boulders at the flow front can limit the mobility of debris flows, causing frequent in-channel deposition on the upper fan and leading to reduced channel longevity and steepening of the fan head.

ACKNOWLEDGMENTS

This research was supported by the National Science Foundation, Grant EAR-9004843, awarded to the author and T. Dunne. The author is grateful to Professors K. Okunishi and H. Suwa of Kyoto University, Japan, for their open sharing of data and video footage obtained at Kamikamihori Valley and for assistance in the field. Galen Whipple and Jason Paur are owed thanks for many hours of surveying in Owens Valley. Thanks also to the White Mountain Research Station, Bishop Laboratory, for accomodation.

CHAPTER 5

Interpreting Debris-Flow Hazard from Study of Fan Morphology

Chapter 5 develops practical, qualitative applications of the results of the study to the identification and interpretation of debris-flow hazards. The paper draws heavily on the conceptual model developed in Chapters 2 and 4. This chapter has already been published in a proceedings volume of the American Society of Civil Engineers under the title: "Interpreting debris-flow hazard from study of fan morphology" by K. Whipple in Hydraulic Engineering '93, p. 1302-1307.

CHAPTER SUMMARY

The deposits, stratigraphy, and surface morphology of debris-flow fans are a record of past debris-flow activity, and as such can provide useful information about debris-flow hazards. The morphology of the fan surfaces reflects both characteristic debris-flow inundation patterns and the frequency of channel avulsions; surface morphology is a sensitive indicator of the type of debris-flow hazard. A conceptual model describing the linkages between depositional processes and surface form on debris-flow fans, developed in earlier work, is applied to fans in three field sites to illustrate the use of fan morphologic characteristics in the analysis of debris-flow hazards. This approach should be taken as a first step in any debris-flow hazard mitigation project, particularly where extensive historical records do not exist.

INTRODUCTION

Debris flows are important agents of sediment transport and geomorphic change in mountainous regions throughout the world and have excited a great deal of attention, particularly because of their hazard potential. For this reason most research on debris flows has focused on either the process of debris-flow initiation or the fluid-mechanical description of the flow in an effort to predict flow occurrence and run-out distance (Takahashi, 1981; Costa, 1984). Successful prediction and mitigation of the hazard posed by debris flows, however, requires an understanding of the entire suite of processes active on fans, including the interaction of debris flows with fluvial processes and the channel system. This interaction is important because it governs both short-term and long-term patterns of inundation and deposition: without at least a qualitative understanding of the controls on characteristic inundation patterns and the frequency of sudden channel avulsions, responsible predictions of the potential debris-flow hazard can not be made. Fortunately, we have, in the deposits and morphology of the debris-flow fan itself, a record of past debris-flow events. A rapid assessment of the type of debris-flow hazard most prevalent on a fan can be made from observations of the morphological characteristics of the fan surface. The purpose of this paper is to illustrate how analysis of the deposits and landforms of debris-flow fans can be used to improve hazards recognition and, therefore, the development of mitigation strategies.

APPROACH: PROCESS AND FORM

Whipple and Dunne (1992) have developed a conceptual model of debris-flow fan construction that provides a framework within which the linkages between the physical properties of the debris flows (volume, hydrograph shape, sediment concentration, flow recurrence interval) and the morphology of the fan can be evaluated. According to them, the surface morphology of a debris-flow fan reflects: the nature of the fluvial system, the frequency of debris-flow occurrences, typical debris-flow volumes, typical inundation and depositional patterns, and the frequency of sudden lateral shifts of the active channel(s). These last two important factors are set, for a given fluvial system, by the frequency distributions of debris-flow rheologies, volumes, and hydrographs delivered to the fan. Taken together, inundation patterns and channel shifting behavior generally describe the nature of the debris-flow hazard. Morphological characteristics that can be related to different associations of debris-flow and channel behavior (i.e., different types of hazard) include: the number and spacing of abandoned channels, the heights of channel-margin levees, the texture of interfluve surfaces, and the irregularity and convexity of cross-fan topographic profiles (Whipple and Dunne, 1992).

Debris-flow properties are largely determined by source area conditions that set flow initiation mechanisms and debris granulometry. Consequently, great variations in both debris-flow fan morphology and the nature of the debris-flow hazard exist between fans derived from different lithologic assemblages and under different climates. Specifically, inter-fan differences can be ascribed to: (1) differences in debris-flow rheology related to differing debris-flow grain-size distributions (e.g., O'Brien and Julien, 1988; Phillips and Davies, 1991); (2) differences in characteristic debris-flow hydrographs, related to both differing initiation mechanisms and differing grain-size distributions (Dunne and Fairchild, 1984; Fairchild, 1987); (3) differences in debris-flow snout erodibility related to differing concentrations of boulders in the debris flows;

and (4) different hydrological conditions associated with the occurrence of debris flows.

FIELD SITE DESCRIPTIONS

This paper illustrates the application of the Whipple and Dunne (1992) conceptual model to fans in three field settings: two sites in Owens Valley, California, and one in the Xiaoxiang River valley in China. The three field sites cover a range of geologic and climatic conditions (Table 5.1) and illustrate a range of debris-flow depositional modes (from well-channelized to essentially unconfined) which result in distinct fan morphological characteristics and are associated with distinct hazards (Table 5.2).

Fans on the western slope of Owens Valley have surfaces characterized by many well-preserved abandoned channels with little relief on narrow, sharply-defined levees, smooth interfluves, narrow, bouldery debris-flow snouts, and gently convex to flat cross-fan profiles (Fig.s 5.1a and 5.2a). Fans on the east side of Owens Valley, in contrast, have surfaces characterized by fewer well-preserved abandoned channels, substantial relief on broad levees, uneven, tiered interfluves (with tiers defined by the margins of wide debris-flow lobes), and more pronounced cross-fan convexity (Fig.s 5.1b and 5.2b). The debris-flow fans studied in the Xiaoxiang River Valley lack well-preserved abandoned channels and well-defined levees. They have smooth interfluves textured with on-lapping, thin, areally extensive debris-flow lobes, and only subtle cross-fan convexity (Fig. 5.1c; see also Fig. 5 of Li et al, 1983).

GEOLOGIC CONDITIONS, FAN MORPHOLOGY, AND DEBRIS-FLOW HAZARD

This section aims to (1) explain the morphological differences between fans in the three field areas, and (2) demonstrate the use of morphological interpretations to gauge differences in the debris-flow hazard.

Western slope, Owens Valley, California

These fans were built under glacial climatic conditions, with debris flows originating as failures of morainal or supra-glacial debris or, possibly, as a consequence of glacial outburst floods (Table 5.1). The debris flows were generally well channelized on the fans owing to vigorous erosion and efficient channel maintenance by sustained meltwater discharges between debris-flows. Debris flows in this area tend to segregate into a dense, bouldery, relatively immobile frontal snout and a more fluid, dilute tail,

Figure 5.1. Oblique aerial views of debris-flow fans: A. Owens Valley, west, B. Owens Valley, east. C. Ciaqing Gully, China.

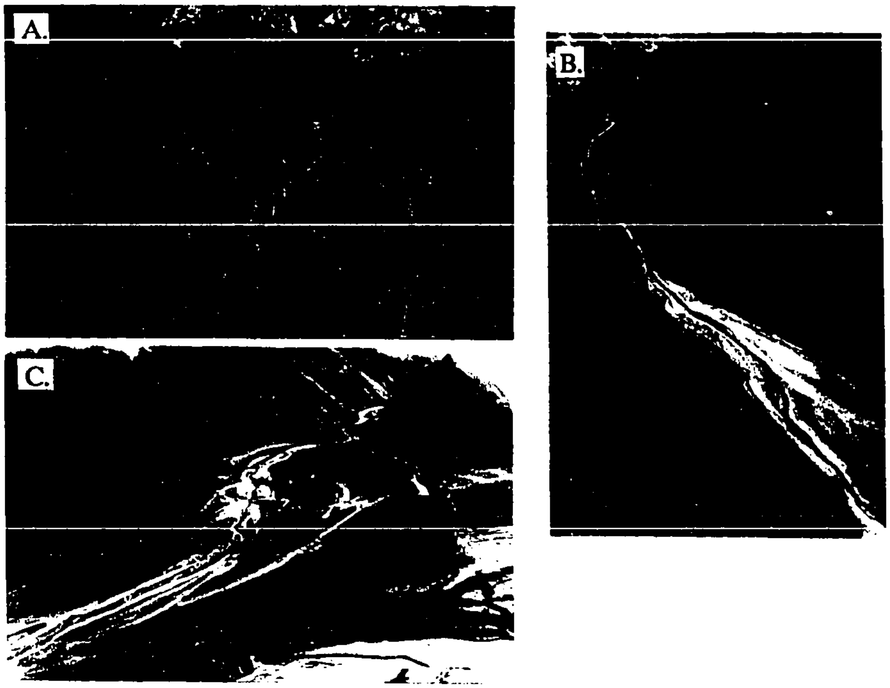
A.
B.
C.

Table 5.1. Field Conditions

Field Site	Lithology	Climate	Initiation Mechanism
Owens Valley, west	granodiorite	glacial	failure of saturated morainal and supra-glacial debris
Owens Valley, east	meta-sedimentary and meta-volcanic	arid	failure of debris in talus cones or bedrock chutes during brief, intense thunderstorm activity
Xiaoxiang River	sedimentary and meta-sedimentary	humid-monsoonal	massive failure of unstable gully sideslopes during sustained monsoonal rains

Table 5.2. Debris-Flow Hazards

Field Site	Effective Channelization	Channel Longevity	Type of Hazard
Owens west	strong	short (10's - 100's yr)	channel blockage by bouldery debris-flow snouts and sudden avulsion, narrow corridor of inundation
Owens east	moderate	long (100's - 1000s yr)	overbank flooding by thick, viscous, slow-moving debris flows, extensive near fan-head
Xiaoxiang River Valley	weak	v. short (1 - 10 yr)	massive overbank flooding by large volumes of low-viscosity debris flows, fan-wide inundation

perhaps as a consequence of the physical properties of the debris itself. Although a correlation with grain-size distribution is unproven, I suggest that the degree of spatial inhomogeneity is set by a combination of: (1) the initiation mechanism(s); (2) the availability and source of additional water inputs; and (3) the mobility of water within the debris flow, which is a function of grain-size distribution. The idea is that the sand- and granule-rich granitic debris is more susceptible to both draining of the steep frontal bore and dilution of the body by stream water. Certainly dense frontal snouts are common on fans draining granitic source rocks in Owens Valley, and either much less so or absent on the other fans studied.

Although dense frontal snouts were common, they apparently constituted a small proportion of the total sediment delivered to the fan: large-scale overbank deposition of thick, bouldery flows was rare. However, these relatively immobile flows often plugged channels, causing sudden avulsions (Whipple and Dunne, 1992). Frequent channel avulsions have important consequences to both hazards and fan morphology (Fig. 5.1a). The relatively fluid body and tail of the debris flows constitute the larger share of the sediment flux, have low apparent viscosities, can be effectively channelized, are carried far down-fan, and spread thinly on smooth, low-relief interfluves (see Fig. 5.1a).

Generally, deposition on this type of fan is limited to a narrow corridor along the active channel: fan-wide deposition rarely, if ever, occurs. However, because of the prevalence of dense, bouldery frontal debris-flow snouts, sudden channel avulsion is a major threat (Table 5.2). Morphological attributes indicative of fans with this hazard include: (1) many closely-spaced well-preserved abandoned channels with abrupt headward terminations on the fan; (2) channels with narrow, bouldery levees of limited height; and (3) subdued cross-fan convexity (see Fig.s 5.1a and 5.2a).

Eastern slope, Owens Valley, California

Debris flows on these fans are generally less-well channelized than on the fans described above. Fan-wide deposition is rare, but debris-flows commonly spread over large portions of the upper fan. This is largely a consequence of marked contrasts in typical debris-flow hydrographs generated in the unglaciated, meta-sedimentary and meta-volcanic source terrain. The debris flows initiate as barely-saturated landslides during intense thunderstorms. The debris is silt- and clay-rich and the low saturated hydraulic conductivity is thought to preclude much interaction with stream waters and to limit the segregation process so important in more granular debris flows.

Figure 5.2. Transverse topographic profiles, scales in meters. A1. Owens west, upper fan (middle ground, Fig. 1a). A2. Owens west, mid-fan (foreground, Fig. 5.1a). B1. Owens east, upper fan (middle ground, Fig. 5.1b). B2. Owens east, mid fan (foreground, Fig. 5.1b).

A1.

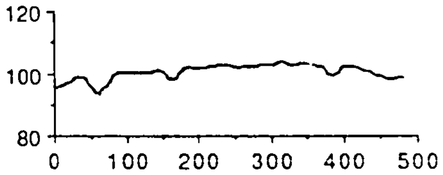
120
100
80
0
100
200
300
400
500

B1.

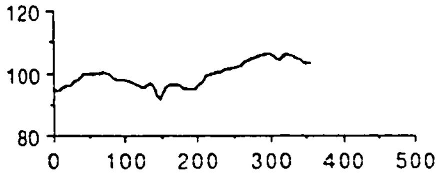
120
100
80
0
100
200
300
400
500

A2.

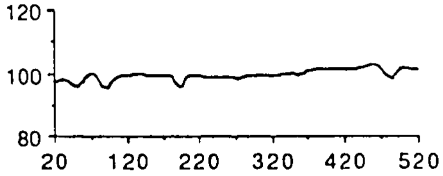
120
100
80
20
120
220
320
420
520

B2.

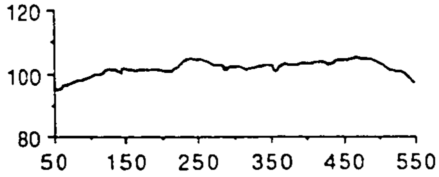
120
100
80
50
150
250
350
450
550

Consequently, the bulk of sediment delivered to the fans comes in the form of relatively viscous debris flows which can not be effectively channelized (Whipple and Dunne, 1992; see Fig. 5.1b). Broad levees and uneven, tiered interfluves and steeper fan profiles result.

Wide spread debris-flow inundation is a greater hazard on these fans. Sudden channel avulsion is not a frequent occurrence, however, because dense, bouldery frontal debris-flow snouts are uncommon and because the dilute flood-water discharges that commonly follow desert debris flows (Hooke, 1967) effectively scour freshly deposited debris-flow sediments and re-establish channel courses. The morphological consequences of the reduced frequency of channel avulsions are: (1) fewer well-preserved abandoned channels (Fig. 5.1b); (2) significant heights on broad channel-margin levees (Fig. 5.2b); and (3) pronounced cross-fan convexity (see Fig. 5.2b).

Jiangjia and Ciaqing Gullies, Xiaoxiang River Valley, China

The geologic and climatic conditions that prevail in the Jiangjia and Ciaqing gullies lead to the formation of frequent, massive, fluid debris flows. Deeply incised gullies have cut steep, unstable hillslopes into the weak bedrock, forest cover has been almost entirely removed, and heavy monsoonal rains cause massive failure and mobilization of debris as often as 20 times a year (Li et al, 1983). The high fines content of the regolith and the great volumes of water available combine to produce huge volumes of mobile, low-strength debris. In general, owing to the vast amounts of sediment deposited annually, channels can not be maintained on these fans (see Li et al, 1983). For example, an extensive, five-meter-deep fan-head trench canyon on upper Ciaqing fan was almost entirely obliterated in just two years (observation communicated by T. Davies, Lincoln College, N.Z., 1992). Channels are not blocked by bouldery, immobile flows; they are simply obliterated by massive deposition. As a result, inundation patterns are largely unconstrained by channels and fan-wide deposition is the norm, rather than the exception. Entire fan surfaces are resurfaced as often as every seven years (Kang Z., Chengdu Acad. Sin., 1992). The debris-flow hazard is severe on these fans. Distinctive morphological characteristics include: (1) no abandoned channels preserved on the fan surface; (2) smooth interfluves, with little relief on the margins of individual debris-flow lobes; (3) a lack of debris-flow levees; and (4) minimal cross-fan convexity (see Fig. 5.1c).

CONCLUSIONS

A rapid assessment of the type of debris-flow hazard most prevalent on a fan can be made from observations of the morphological characteristics of the fan surface. Critical observations include: the number and spacing of abandoned channels, the texture and irregularity of interfluves, the form of channel-margin levees, and the degree of cross-fan convexity. These features can be readily identified and measured on the ground or from remotely sensed imagery with sufficient spatial resolution (e.g., aerial photographs, TMS, SPOT, AVIRIS) and are useful indicators of the patterns of debris-flow inundation and channel shifts characteristic of the fan, as outlined briefly here and covered in more detail by Whipple and Dunne (1992). Analysis of fan morphology is a simple and inexpensive approach which can yield important, and otherwise potentially overlooked, information about debris-flow hazards. This type of assessment should always be made first, before initiating any expensive computational analyses. In addition, given time and resources, a detailed study of debris-flow deposits and fan stratigraphy should be conducted to help guide computational analyses, if any are deemed necessary.

ACKNOWLEDGMENTS

This research was supported by NSF Grant EAR-9004843, awarded to the author and T. Dunne. The author is grateful to the Chengdu Institute of Mountain Disasters for their hospitality at the Dongchuan Debris-Flow Observation station, and to Chris Phillips for providing the photo in Figure 5.1c.

BIBLIOGRAPHY

Bagnold, R. A., 1954, Experiments on a gravity-free dispersion of large solid spheres in a Newtonian fluid under shear: Proceedings of the Royal Society of London, Series A, v. 225, p. 49-63.

Barnes, H. A., and Walters, K., 1985, The yield stress myth?: Rheology Acta, v. 24, p. 323-326.

Batchelor, G. K., 1967, An Introduction to Fluid Dynamics: Cambridge, Cambridge University Press, 615 p.

Bay, R. S., and Tucker, C. L., 1992, Fiber Orientation in Simple Injection Moldings. Part I: Theory and Numerical Methods, *in* eds., Polymer Composites: August ?, p. 317-331.

Beaty, C. B., 1963, Origin of alluvial fans, White Mountains, California and Nevada: Association of American Geographers Annals, v. 53, p. 516-535.

Beaty, C. B., 1970, Age and estimated rate of accumulation of an alluvial fan, White Mountains, California, USA: American Journal of Sciences, v. 268, p. 50-77.

Beaty, C. B., 1974, Debris flows, alluvial fans, and a revitalized catastrophism: Zeitschrift fur Geomorphologie Supplementband, v. 21, p. 39-51.

Beaty, C. B., 1990, Anatomy of a White Mountains debris-flow --The making of an alluvial fan, *in* Rachocki, A. H., and Church, M., eds., Alluvial Fans: A Field Approach: New York, Wiley & Sons, p. 69-90.

Bercovier, M., and Engleman, M., 1980, A finite element method for incompressible non-Newtonian flows: Journal of Computational Physics, v. 36, p. 313-326.

Beris, A. N., Tsamopoulos, J. A., Armstraong, R. C., and Brown, R. A., 1985, Creeping motion of a sphere through a Bingham plastic: Journal of Fluid Mechanics, v. 158, p. 219-244.

Beverly, C. R., and Tanner, R. I., 1992, Numerical analysis of three-dimensional Bingham plastic flow: Journal of Non-Newtonian Fluid Mechanics, v. 42, p. 85-115.

Bierman, P. R., Gillespie, A. R., Whipple, K. X., and Clark, D., 1991, Quaternary geomorphology and geochronology of Owens Valley, California, *in* Walawender, M. J., and Hanan, B. B., eds., Geological Excursions in Southern California and Mexico: San Diego, Geological Society of America, p. 199-223.

Bird, R. B., Dai, G. C., and Yarusso, B. J., 1982, The rheology and flow of viscoplastic materials: Reviews of Chemical Engineering, v. 1, p. 1-70.

Blackwelder, E., 1928, Mudflow as a geologic agent in semi-arid mountains: Geological Society of America Bulletin, v. 39, p. 465-484.

Bull, W. B., 1964, Geomorphology of segmented alluvial fans in western Fresno County, California: U. S. Geological Survey Professional Paper, v. 352-E, p. 89-129.

Bull, W. B., 1972, Recognition of alluvial-fan deposits in the stratigraphic record, *in* Rigby, J. K., and Hamblin, W. K., eds., Recognition of Ancient Sedimentary Environments: Society of Economic Paleontologists and Mineralogists, Special Publication 16, p. 63-83.

Bull, W. B., 1977, The alluvial fan environment: Progress in Physical Geography, v. 1, p. 222-270.

Carson, M. A., and Kirkby, M. J., 1972, Hillslope Form and Process: Cambridge, Cambridge University Press, 475 p.

Chapman, R. H., Healey, D. L., and Troxel, B. W., 1973, Bouguer Gravity Map of California, Death Valley Sheet: California Division of Mines and Geology, scale 1:250,000.

Church, M., Kellerhals, R., and Terry, J. D., 1988, Regional clastic sediment yield in British Columbia: Canadian Journal of Earth Sciences, v. 26, p. 31-45.

Coleman, P. F., 1993, A new explanation of the debris flow phenomenon: EOS, Transactions of the American Geophysical Union, v. 74(16), p. 154.

Costa, J. E., 1984, Physical geomorphology of debris flows, *in* Costa, J. E., and Fleisher, P. J., eds., Developments and Applications of Geomorphology: Berlin, Springer-Verlag, p. 269-315.

Costa, J. E., and Williams, G. P., 1984, Debris-flow dynamics (videotape): U.S. Geological Survey Open File Report, v. 84-606, p. 22.5 min.

Coussot, P., 1992, Debris flow rheology - Study of concentrated suspensions [Ph.D. thesis]: Grenoble, France, L'Institute National Polytechnique, Grenoble, 420 p.

Coussot, P., and Piau, J.-M., in press, On the behavior of fine mud suspensions: Rheologica Acta.

Crowder, D. F., Robinson, P. F., and Harris, D. L., 1972, Geologic map of the Benton Quadrangle, Mono County, California and Esmeralda and Mineral Counties, Nevada: U.S. Geological Survey Map, GQ-1013, scale 1:62,500.

Crowder, D. F., and Sheridan, M. F., 1972, Geologic map of the White Mountain Peak Quadrangle, Mono County, California: U.S. Geological Survey Map, GQ-1012, scale 1:62,500.

Dahlen, F. A., 1984, Noncohesive critical coulomb wedges: an exact solution: Journal of Geophysical Research, v. 89(B12), p. 10,125-10,133.

Denny, C. S., 1965, Alluvial fans in the Death Valley Region, California and Nevada: U. S. Geological Survey Professional Paper, v. 466, p. 1-62.

Engleman, M. S., 1980, FIDAP Theoretical and User's Manuals: Boulder, CIRES, University of Colorado.

Fairchild, L. H., 1985, Lahars at Mount St. Helens [Ph.D. thesis]: Seattle, Washington, University of Washington, 374 p.

Fink, J. H., Malin, M. C., D'Alli, R. E., and Greeley, R., 1981, Rheological properties of mudflows associated with the spring 1980 eruptions of Mount St. Helens Volcano, Washington: Geophysical Research Letters, v. 8, p. 43-46.

Gartling, D. K., and Phan-Thien, N., 1984, A numerical simulation of a plastic fluid in a parallel-plate palstometer: Journal of Non-Newtonian Fluid Mechanics, v. 14, p. 347-360.

Gillespie, A. R., 1982, Quaternary glaciation and tectonism in the southeastern Sierra Nevada, Inyo County, California [Ph.D. thesis]: Pasadena, California, California Institute of Technology, 695 p.

Harbor, J., and Warburton, J., 1993, Relative rates of glacial and nonglacial erosion in alpine environments: Artic and Alpine Research, v. 25, p. 1-7.

Harvey, A. M., 1984, Debris flows and fluvial deposits in Spanish Quaternary alluvial fans: implications for fan morphology, *in* Koster, E. H., and Steel, R. J., eds., Sedimentology of Gravels and Conglomerates: Canadian Society of Petroleum Geologists, p. 123-132.

Hicks, D. M., McSaveney, M. J., and Chinn, T. J. H., 1990, Sedimentation in proglacial Ivory Lake, southern Alps, New Zealand: Artic and Alpine Research, v. 22, p. 26-42.

Hollett, K. J., Dinskin, W. R., McCaffrey, W. H., and Walti, C. L., 1989, Geology and water resources of Owens Valley, California: U.S. Geological Survey Open File Report, v. 88-715, p. 1-118.

Hooke, R., LeB., and Rohrer, W. L., 1977, Relative erodibility of source-area rock types, as determined from second-order variations in alluvial-fan size: Geological Society of America Bulletin, v. 88, p. 1177-1182.

Hooke, R. L., 1967, Processes on arid-region alluvial fans: Journal of Geology, v. 75, p. 438-460.

Hooke, R. L., 1968, Steady-state relationships on arid-region aluvial fans in closed basins: American Journal of Science, v. 266, p. 609-629.

Hooke, R. L., 1972, Geomorphic evidence for Late-Wisconsin and Holocene tectonic deformation in Death Valley, California: Geological Society of America Bulletin, v. 83, p. 2073-2098.

Hooke, R. L., 1987, Mass Movement in Semi-Arid Environments and the Morphology of Alluvial Fans, *in* Anderson, M. G., and Richards, K. S., eds., Slope Stability: New York, John Wiley & Sons Ltd., p. 505-529.

Hooke, R. L., and Rohrer, W. L., 1979, Geometry of alluvial fans: effect of discharge and sediment size: Earth Surface Processes, v. 4, p. 147-166.

Hubert, J. F., and Filipov, A. J., 1989, Debris-flow deposits in alluvial fans on the western flank of Owens Valley, California, USA: Sedimentary Geology, v. 61, p. 177-205.

Hunt, C. B., and Mabey, D. R., 1966, Stratigraphy and structure, Death Valley, California: U.S. Geological Survey Professional Paper, v. 494-A, p. 1-162.

Iverson, R. M., 1985, A constitutive equation for mass-movement behavior: Journal of Geology, v. 93, p. 143-160.

Iverson, R. M., 1993, Differential equations governing slip-induced pore-pressure fluctuations in a water-saturated granular medium: Mathematical Geology, v. 25, p. 1027-1048.

Iverson, R. M., and Denlinger, R. P., 1987, The physics of debris flows -- a conceptual assessment, *in* Beschta, R. L., Blinn, T., Grant, G. E., Ice, G. G., and Swanson, F. J., eds., Erosion and Sedimentation in the Pacific Rim: Corvallis, Oregon, International Association of Hydrological Science, Publication no. 165, p. 155-165.

Iverson, R. M., and LaHusen, R. G., 1989, Dynamic pore pressure fluctuations in rapidly shearing granular materials: Science, v. 246, p. 796-799.

Iverson, R. M., and LaHusen, R. G., 1993, Friction in debris flows: Inferences from large-scale flume experiments, *in* Shen, H. W., Su, S. T., and Wen, F., eds., Hydraulic Engineering '93: Proceedings of the 1993 Conference, San Francisco, California, July 25 - 30: New York, American Society of Civil Engineers, p. 1604-1609.

Jackson, L. E., Kostaschuk, R. A., and MacDonald, G. M., 1987, Identification of debris flow hazard on alluvial fans in the Canadian Rocky Mountains: Geological Society of America Reviews in Engineering Geology, v. 7, p. 115-124.

Jansson, P., Jacobson, D., and Hooke, R. L., 1993, Fan and playa areas in southern California and adjacent parts of Nevada: Earth Surface Processes and Landforms, v. 18, p. 109-119.

Jeyapalan, J. K., Duncan, J. M., and Seed, H. B., 1983, Analysis of flow failures of mines tailings dams: Journal of Geotechnical Engineering, American Society of Civil Engineers, v. 109(2), p. 150-171.

Johnson, A. M., 1965, A model for debris flow [Ph.D. thesis]: Pennsylvannia State University, p.

Johnson, A. M., 1970, Physical Processes in Geology: San Francisco, California, Freeman, Cooper & Co., 577 p.

Johnson, A. M., and Rahn, P. H., 1970, Mobilization of debris flows: Zeitschrift fur Geomorphologie Supplementband, v. 9, p. 168-186.

Johnson, A. M., and Rodine, J. D., 1984, Debris flow, *in* Brunsden, D., and Prior, D. B., eds., Slope Instability: Chichester, England, John Wiley & Sons, Ltd., p. 257-361.

Keener, C., Serpa, L., and Pavlis, T. L., 1993, Faulting at Mormon Point, Death Valley, California: A low-angle normal fault cut by high-angle faults: Geology, v. 21, p. 327-330.

Lawson, D. E., 1982, Mobilization, movement, and deposition of active subaerial sediment flows, Matanuska Glacier, Alaska: Journal of Geology, v. 90, p. 279-300.

Lecce, S. A., 1990, The alluvial fan problem, *in* Rachocki, A. H., and Church, M., eds., Alluvial Fans: A Field Approach: New York, John Wiley & Sons Ltd., p. 3-24.

Lecce, S. A., 1991, Influence of lithologic erodibility on alluvial fan area, western white mountains, California and Nevada: Earth Surface Processes and Landforms, v. 16, p. 11-18.

Lee, C., and Tucker, C. L., 1987, Flow and Heat Transfer in Compression Mold Filling: Journal of Non-Newtonian Fluid Mechanics, v. 24, p. 245-264.

Li, J., Yuan, J., Bi, C., and Luo, D., 1983, The main features of the mudflow in Jiang-Jia Ravine: Zeitschrift fur Geomorphologie, v. 27(3), p. 325-341.

MacArthur, R. C., and Schamber, D. R., 1986, Numerical methods for simulating mudflows, *in* Wang, S. Y., Shen, H. W., and Ding, L. Z., eds., River

Sedimentation: proceedings of the Third International Symposium on River Sedimentation: Jackson, Mississippi, University of Mississippi, p. 1615-1623.

Macedonio, G., and Pareschi, M. T., 1992, Numerical simulation of some lahars from Mount St. Helens: Journal of Volcanology and Geothermal Research, v. 54, p. 65-80.

Major, J. J., 1993, Rheometry of natural sediment slurries, *in* Shen, H. W., Su, S. T., and Wen, F., eds., Hydraulic Engineering '93: Proceedings of the 1993 Conference, San Francisco, California, July 25 - 30: New York, American Society of Civil Engineers, p. 1415-1421.

Major, J. J., and Iverson, R. M., 1993, Is the dynamic behavior of a debris flow recorded by its deposit?: EOS, Transactions of the American Geophysical Union, v. 74(43), p. 315.

Major, J. J., and Pierson, T. C., 1992, Debris flow rheology: Experimental analysis of fine-grained slurries: Water Resources Research, v. 28(3), p. 841-857.

Matthews, R. A., and Burnett, J. C., 1965, Geologic Map of California, Fresno Sheet: California Division of Mines and Geology, scale 1:250,000.

Melton, M. A., 1965, The geomorphic and paleoclimatic significance of alluvial deposits in southern Arizona: Journal of Geology, v. 73(1), p. 1-38.

Mizuyama, T., Yazawa, A., and Ido, K., 1987, Computer simulation of debris flow depositional processes, *in* Beschta, R. L., Blinn, T., Grant, G. E., Ice, G. G., and Swanson, F. J., eds., Erosion and Sedimentation in the Pacific Rim: Corvallis, Oregon, International Association of Hydrological Sciences, Publication no. 165, p. 179-190.

Nelson, C. A., 1966a, Geologic Map of the Blanco Mountain Quadrangle, Inyo and Mono Counties, California: U. S. Geological Survey Map, GQ-529, scale 1:62,500.

Nelson, C. A., 1966b, Geologic Map of the Waucoba Mountain Quadrangle, Inyo County, California: U. S. Geological Survey Map, GQ-528, scale 1:62,500.

Nilsen, T. H., and Moore, T. E., 1984, Bibliography of Alluvial-Fan Deposits: Norwich, Geo Books, 96 p.

O'Brien, J. S., 1993, Hydraulic modeling and mapping of mud and debris flows, *in* Shen, H. W., Su, S. T., and Wen, F., eds., Hydraulic Engineering '93: Proceedings of the 1993 Conference, San Francisco, California, July 25 - 30: New York, American Society of Civil Engineers, p. 1762-1767.

O'Brien, J. S., and Julien, P. Y., 1988, Laboratory analysis of mudflow properties: Journal of Hydraulic Engineering, v. 114, p. 877-887.

Okuda, S., Suwa, H., Okunishi, K., Yokoyama, K., and Nakano, M., 1980, Observations on the motion of a debris flow and its geomorphological effects: Zeitschrift fur Geomorphologie Supplementband, v. 35, p. 142-163.

Oldroyd, J. G., 1947, Two-dimensional flow of a Bingham solid: Proceedings of the Cambridge Philosophical Society, v. 43, p. 383-395.

Oliver, H. W., and Robbins, S. L., 1978, Bouguer Gravity Map of California, Mariposa Sheet: California Division of Mines and Geology, scale 1:250,000.

Oliver, H. W., and Robbins, S. L., 1982, Bouguer Gravity Map of California, Fresno Sheet: California Division of Mines and Geology, scale 1:250,000.

Oreskes, N., Shrader-Frechette, K., and Belitz, K., 1994, Verification, validation, and confirmation of numerical models in the earth sciences: Science, v. 263, p. 641-646.

Pakiser, L. C., Kane, M. F., and Jackson, W. H., 1964, Structural geology and volcanism of Owens Valley region, California -- A geophysical study: U.S. Geological Survey Professional Paper, v. 438, p. 1-68.

Phillips, C. J., and Davies, T. R., 1991, Determining rheological parameters of debris flow material: Geomorphology, v. 4, p. 101-110.

Pierson, T. C., 1980, Erosion and deposition by debris flows at Mount Thomas, North Canterbury, New Zealand: Earth Surface Processes, v. 5, p. 227-247.

Pierson, T. C., 1984, Effects of slurry composition on debris flow dynamics, Rudd Canyon, Utah, *in* Bowles, D. S., eds., Delineation of Landslide, Flash Flood, and Debris Flow Hazards in Utah: Logan, Utah, p. 132-152.

Pierson, T. C., 1985, Initiation and flow behavior of the 1980 Pine Creek and Muddy River lahars, Mount St. Helens, Washington: Geological Society of America Bulletin, v. 96, p. 1056-1069.

Pierson, T. C., 1986, Flow behavior of channelized debris flows, Mount St. Helens, Washington, *in* Abrahams, A. D., eds., Hillslope Processes: Boston, Allen and Unwin, p. 269-296.

Pierson, T. C., and Costa, J. E., 1987, A rheologic classification of subaerial sediment-water flows: Geological Society of America Reviews in Engineering Geology, v. 7, p. 1-12.

Pierson, T. C., Janda, R. J., Thouret, J., and Borrer, C. A., 1990, Perturbation and melting of snow and ice by the 13 November eruption of Nevado Del Ruiz, Columbia, and consequent mobilization, flow, and deposition of lahars: Journal of Volcanology and Geothermal Research, v. 41, p. 17-67.

Prager, W., 1961, Introduction to the Mechanics of Continua: New York, Ginn & Co., 230 p.

Rantz, S. E., 1969, Mean Annual Precipitation in the California Region: U.S. Geological Survey, Water Resources Division Map, scale 1:750,000.

Reneau, S. L., and Dietrich, W. E., 1991, Erosion rates in the Southern Oregon Coast Range: Evidence for an equilibrium between hillslope erosion and sediment yield: Earth Surface Processes and Landforms, v. 16, p. 307-322.

Savage, S. B., 1993, Mechanics of debris flows, *in* Shen, H. W., Su, S. T., and Wen, F., eds., Hydraulic Engineering '93: Proceedings of the 1993 Conference, San Francisco, California, July 25 - 30: New York, American Society of Civil Engineers, p. 1402-1407.

Savage, S. B., and Hutter, K., 1989, The motion of a finite mass of granular material down a rough incline: Journal of Fluid Mechanics, v. 199, p. 177-215.

Scott, K. M., 1988, Origins, behavior, and sedimentology of lahars and lahar-runout flows in the Tuttle-Cowlitz River system: U.S. Geological Survey Professional Paper, v. 1447-A, p. 1 - 74.

Seidl, M. A., and Dietrich, W. E., 1992, The problem of channel erosion into bedrock: Catena Supplement, v. 23, p. 101-124.

Serpa, L., de Voogd, B., Wright, L., Willemin, J., Oliver, J., Hauser, E., and Troxel, B., 1988, Structure of the central Death Valley pull-apart basin and vicinity from COCORP profiles in the southern Great Basin: Geological Society of America Bulletin, v. 100(9), p. 1437-1450.

Strand, R. G., 1967, Geologic Map of California, Mariposa Sheet: California Division of Mines and Geology, scale 1:250,000.

Streitz, R., and Stinson, M. C., 1977, Geologic Map of California, Death Valley Sheet: California Division of Mines and Geology, scale 1:250,000.

Suwa, H., 1988, Focusing mechanism of large boulders to a debris-flow front: Transactions of the Japanese Geomorphological Union, v. 9, p. 151-178.

Suwa, H., and Okuda, S., 1983, Deposition of debris flows on a fan surface, Mt. Yakedake, Japan: Zeitschrift fur Geomorphologie Supplementband, v. 46, p. 79-101.

Szabo, P., and Hassager, O., 1992, Flow of viscoplastic fluids in eccentric annular geometries: Journal of Non-Newtonian Fluid Mechanics, v. 45, p. 149-169.

Takahashi, T., 1978, Mechanical characteristics of debris flow: Journal of the Hydraulics Division, American Society of Civil Engineers, v. 104, p. 1153-1169.

Takahashi, T., 1980, Debris flow on open prismatic channel: Journal of the Hydraulics Division, American Society of Civil Engineers, v. 106, p. 381-386.

Takahashi, T., 1981, Debris flow: Annual Reviews of Fluid Mechanics, v. 13, p. 57-77.

Takahashi, T., 1991, Debris Flow: Rotterdam, Netherlands, A.A. Balkema, 165 p.

Takahashi, T., and Tsujimoto, H., 1985, Delineation of the debris flow hazardous zone by a numerical simulation method, *in* Takei, A., eds., Proceedings of the International Symposium on Erosion, Debris Flow and Disaster Prevention: Tsukuba, Japan, p. 457-462.

Walton, I. C., and Bittleston, S. H., 1991, The axial flow of a Bingham plastic in a narrow eccentric annulus: Journal of Fluid Mechanics, v. 222, p. 39-60.

Wasson, R. J., 1977, Late-glacial alluvial fan sedimentation in the lower Derwent Valley, Tasmania: Sedimentology, v. 24, p. 781-799.

Wells, S. G., and Harvey, A. M., 1987, Sedimentologic and geomorphic variations in storm-generated alluvial fans, Howgill Fells, northwest England: Geological Society of America Bulletin, v. 98, p. 182-198.

Whipple, K. X., 1991, Lithologic and climatic controls on debris-flow fan surface morphology, Owens Valley, California: Geological Society of America Abstracts with Programs, v. 23(5), p. A89.

Whipple, K. X., 1992, Predicting debris-flow runout and deposition on fans: the importance of the flow hydrograph, *in* Walling, D., Davies, T., and Hasholt, B., eds., Erosion, Debris Flow and Environment in Mountainous Regions: Chengdu, China, International Association of Hydrological Sciences, Publication no. 209, p. 337-345.

Whipple, K. X., 1993, Interpreting debris-flow hazard from study of fan morphology, *in* Shen, H. W., Su, S. T., and Wen, F., eds., Hydraulic Engineering '93: Proceedings of the 1993 Conference, San Francisco, California, July 25 - 30: New York, NY, American Society of Civil Engineers, p. 1302-1307.

Whipple, K. X., and Dunne, T., 1992, The influence of debris-flow rheology on fan morphology, Owens Valley, California: Geological Society of America Bulletin, v. 104, p. 887-900.

Wigmosta, M. S., 1983, Rheology and flow dynamics of the Toutle debris flows from Mount St. Helens [M.S. thesis]: Seattle, Washington, University of Washington, 184 p.

Wilson, S. D. R., 1993, Squeezing flow of a yield-stress fluid in a wedge of slowly-varying angle: Journal of Non-Newtonian Fluid Mechanics, v. 50, p. 45-63.

Zienkiewicz, O. C., and Taylor, R. L., 1991, The Finite Element Method. Volume 2: Solid and Fluid Mechanics, Dynamics and Non-linearity: New York, McGraw-Hill Book Company, 807 p.

VITA

Kelin X. Whipple
Born: June 17, 1963 in Midland, MI USA

EDUCATION B.A. 1985 University of California, Berkeley (Geology)
M.S. 1989 University of Washington (Geological Sciences)
Ph.D. 1994 University of Washington (Geological Sciences)

HONORS Mackin Grant, Geological Society of America, 1990
Scholarships for academic achievement (U.W. Geological Sciences Department): 1987; 1988; 1989; 1990; 1992

PUBLICATIONS

Refereed Articles:

Whipple, K.X., and Dunne, T., 1992, The influence of debris-flow rheology on fan morphology, Owens Valley, California: Geological Society of America, Bulletin, v. 104, p. 887-900.

Whipple, K.X., 1992, Predicting debris-flow runout and deposition on fans: the importance of the flow hydrograph, *in* Walling, D., Davies, T., Hasholt, B., eds., Erosion, debris-flow and environment in mountain regions: Proceedings of the International Association of Hydrological Sciences Symposium, Chengdu, China, July 5-9, IAHS Publication # 209, p. 337-345.

Whipple, K.X., 1993, Interpreting debris-flow hazard from study of fan morphology, *in* Shen, H.W., Su, S. T., and Wen, F., eds., Hydraulic Engineering '93: Proceedings of the 1993 Conference Sponsored by the Hydraulics Division/ASCE, July 25-30, San Francisco, California, p. 1302-1307.

Guidebooks:

Bierman, P.R., Gillespie, A.R. , Whipple, K.X., and Clark, D., 1991, Quaternary geomorphology and geochronology of Owens Valley, California, *in* Walawender, M.J., and Hanan, B.B., eds., Geological excursions in southern California and Mexico: Geological Society of America, 1991 Annual Meeting, San Diego, California, Guidebook, p. 199-223.

Booth, D.B., Bell, K., Whipple, K.X., 1991, Sediment transport along the south fork and mainstem of the Snoqualmie River, Washington: King County Surface Water Management Division, Basin Planning Techincal Report.

In Rewiew:

Juteau, T., Bideau, D., Dauteuil, O., Manac'h, G., Naidoo, D., Nehlig, P., Ondreas, H., Tivey, M., and Whipple, K., The Western Blanco Depression and Parks Plateau: a submersible study in the Blanco Fracture Zone: submitted to Marine Geophysical Research.